ISABELA RAMOS

CARACTERIZAÇÃO DE ACIDOCALCISSOMOS EM SISTEMAS DE VITELO DE OVOS DE DIFERENTES MODELOS

TESE SUBMETIDA À UNIVERSIDADE FEDERAL DO RIO DE JANEIRO VISANDO A OBTENÇÃO DO GRAU DE DOUTOR EM CIÊNCIAS

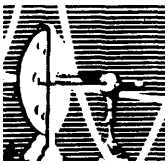

Universidade Federal do Rio de Janeiro
Centro de Ciências da Saúde
Instituto de Biofísica Carlos Chagas Filho
2 0 10

Livros Grátis

http://www.livrosgratis.com.br

Milhares de livros grátis para download.

UNIVERSIDADE FEDERAL DO RIO DE JANEIRO

ISABELA RAMOS

CARACTERIZAÇÃO DE ACIDOCALCISSOMOS EM SISTEMAS DE VITELO DE OVOS DE DIFERENTES MODELOS

RIO DE JANEIRO

2010

ISABELA RAMOS

CARACTERIZAÇÃO DE ACIDOCALCISSOMOS EM SISTEMAS DE VITELO DE OVOS DE DIFERENTES MODELOS

Tese de Doutorado apresentada ao programa de Pós-Graduação em Ciências Biológicas (Biofísica), Instituto de Biofísica Carlos Chagas Filho, Universidade Federal do Rio de Janeiro, como parte dos requisitos necessários para a obtenção do título de Doutor em Ciências.

Orientadores:
Ednildo de Alcantara Machado
Wanderley de Souza

Rio de Janeiro
2010

CARACTERIZAÇÃO DE ACIDOCALCISSOMOS EM SISTEMAS DE VITELO DE OVOS DE DIFERENTES MODELOS

Isabela Ramos

Orientadores: Prof. Dr. Ednildo de Alcantara Machado/ Prof. Dr.Wanderley de Souza

Tese de doutorado submetida ao Instituto de Biofísica Carlos Chagas Filho da Universidade Federal do Rio de Janeiro, como parte dos requisitos necessários para a obtenção do grau de mestre em Ciências Biológicas (Biofísica).

Banca Examinadora:

Prof. Dr. Ednildo de Alcantara Machado
Professor Adjunto, Instituto de Biofísica Carlos Chagas Filho, CCS – UFRJ
Orientador

Prof. Dr. Wanderley de Souza
Professor Titular, Instituto de Biofísica Carlos Chagas Filho, CCS – UFRJ
Orientador

Prof. Dr. Marcelo Einicker Lamas
Professor Adjunto, Instituto de Biofísica Carlos Chagas Filho, CCS – UFRJ
Presidente da banca

Prof. Dr. Hatisaburo Masuda
Professor TItular, Instituto de Bioquímica Médica, CCS – UFRJ
Membro da banca

Prof. Dr .José Garcia Abreu
Professor Adjunto, Departamento de Anatomia, ICB, CCS – UFRJ
Membro da banca

Prof. Dr .Jenifer Lowe
Professor Adjunto, Instituto de Biofísica Carlos Chagas Filho, CCS – UFRJ
Suplente interno

Prof. Dr. Ulisses Lins
Professor Adjunto, Instituto de Microbiologia e Imunologia Paulo de Góes, CCS – UFRJ
Suplente externo

Prof. Dr. Kátia Calp Gondim
Professor Adjunto, Instituto de Bioquímica Médica, CCS – UFRJ
Revisor

Rio de Janeiro
Julho de 2010

Ramos, Isabela
Caracterização de acidocalcissomos em sistemas de vitelo de ovos de diferentes modelos. – 2010
125 f.: il.

Tese (Doutorado em Ciências) – Universidade Federal do Rio de Janeiro, Instituto de Biofísica Carlos Chagas Filho, Rio de Janeiro, 2010.

Orientadores: Ednildo de Alcantara Machado
Wanderley de Souza

1. Ovos. 2. Acidocalcisomo. 3. *Rhodnius prolixus*. 4. *Periplaneta americana.* 5. *Lytechinus variegatus*. 6. *Gallus gallus.* 7. Vitelo. – Teses.
I. Machado, Ednildo de Alcantara (orient.). II Universidade Federal do Rio de Janeiro. Instituto de Biofísica Carlos Chagas Filho. III. Título.

O presente trabalho foi realizado nos Laboratórios de Entomologia Médica e Ultraestrutura Celular Hertha Meyer, Programa de Biologia Celular e Parasitologia, Instituto de Biofísica Carlos Chagas Filho, Universidade Federal do Rio de Janeiro, em colaboração com o Laboratório de Bioquímica de Insetos (IBqM, UFRJ), Laboratório de Bioquímica de Artrópodos Hematófagos (IBqM, UFRJ) e *Center of Tropical and emerging global diseases (University of Georgia, USA)* sob a orientação dos professores Dr. Ednildo A. Machado e Dr. Wanderley de Souza, na vigência de auxílios concedidos pelo Conselho Nacional de Desenvolvimento Científico e Tecnológico (CNPq), Coordenadoria de Aperfeiçoamento de Pessoal de Ensino Superior (CAPES), Financiadora de Estudos e Projetos (FINEP) e Fundação Carlos Chagas Filho de Amparo à Pesquisa do Estado do Rio de Janeiro (FAPERJ).

Agradecimentos:

A minha família.

Aos amigos do Laboratório de Entomologia e aos meus orientadores, por tantas coisas, que fica inviável escrever em um ou dois parágrafos nesta seção. De fato, no que diz respeito às pessoas com quem eu tive a oportunidade de trabalhar nesse tempo, eu tive muita sorte.

A todos do laboratório de Ultraestrutura Celular Hertha Meyer, por tudo que foi preciso e pela boa vontade sempre.

A todo o grupo do Prof. Roberto Docampo, na Universidade da Georgia, por terem me recebido da melhor forma possível.

A todos que de alguma forma contribuíram ao longo desses quatro anos...Obrigada.

RAMOS, Isabela. **Caracterização de acidocalcissomos em sistemas de vitelo de ovos de diferentes modelos.** Rio de Janeiro, 2010. Tese (Doutorado em Ciências Biológicas – Biofísica) – Instituto de Biofísica Carlos Chagas Filho, Universidade Federal do Rio de Janeiro.

Em animais ovíparos, os ovos armazenam todos os componentes necessários para a divisão e diferenciação das células embrionárias. Os componentes de reserva, comumente chamados de vitelo, são estocados durante a ovogênese majoritáriamente em organelas chamadas grânulos de vitelo. Assim, após a formação dos ovos, o citoplasma se encontra preenchido por grânulos, e o seu conteúdo fornecerá moléculas fundamentais para o metabolismo das células embrionárias durante a embriogênese. Acidocalcissomos são organelas originalmente descritas em protozoários, sendo recentemente encontradas em diferentes modelos de microrganismos. Neste trabalho, organelas similares a acidocalcissomos foram caracterizadas em sistemas de vitelo de ovos de diferentes modelos de estudo: dois insetos (*P. americana* e *R. prolixus*), dois equinodermos (*A. punctulata* e *L. variegatus*) e uma ave (*Gallus gallus*). Estas organelas são caracterizadas por seram acídicas, altamente eletrondensas, apresentarem um H^+-PPase vacuolar e acumularem grandes quantidades de elementos como fósforo (na forma de fosfato inorgânico, Pi, pirofosfato, PPi e polifosfato, PoliP), cálcio, potássio, sódio e magnésio. Nos sistemas de vitelo, organelas similares aos acidocalcsiomos, i.e. vesículas eletrondensas, ácidas, acumulando fósfosro, cálcio, magnésio, potássio e sódio, foram detectadas a partir de técnicas de microanálise de raios-X acoplada à microscopia eletrônica. Os níveis de PoliP foram determinados nos ovos, a partir de ensaios enzimáticos usando uma exopolifosfatase recombinante, e este polímero foi localizado nos acidocalcissomos, usando DAPI como sonda. Em insetos, a presença de atividadade PPásica foi detectada nas membranas dos acidocalcissomos, e estas organelas se mostraram imunoreativas a anticorpos anti-VH^+-PPase de plantas, assim como os acidocalcissomos de protozoários. Em equinodermos, a participação dos acidocalcissomos em eventos de liberação de Ca^{2+} e a presença de trocadores Ca^{2+}/H^+ e Na^+/H^+ foram investigadas. Em ovos de galinha, os acidocalcissomos foram localizados no interior de vesículas maiores, em grupos, e o perfil de PoliP foi investigado durante a embriogênese inicial. As possíveis funções dos acidocalcissomos em modelos de embriogênese e suas diferenças entre os modelos estudados são discutidas.

RAMOS, Isabela. **Characterization of acidocalcisomes in yolk systems of eggs from different models.** Rio de Janeiro, 2010. Tese (Doutorado em Ciências Biológicas – Biofísica) – Instituto de Biofísica Carlos Chagas Filho, Universidade Federal do Rio de Janeiro.

In oviparous animals, the eggs store all components required for growth and differentiation of embryonic cells. The storage components, usually called yolk, are stored during oogenesis, mainly in organelles named yolk granules. This way, in the end of oogenesis the egg cytoplasm is filled with granules, and their contents will provide fundamental molecules for the metabolism of embryonic cells during embryogenesis. Acidocalcisomes are organelles originally described in protozoa, being recently found in different microorganisms. In this work, organelles similar to acidocalcisomes were characterized in the yolk system of different study models: two insects (*P. americana* e *R. prolixus*), two echinoderms (*A. punctulata* e *L. variegatus*) and one bird (*Gallus gallus*). These organelles are characterized by their acidic and high electron density nature, the presence of a vacuolar H^+-PPase and the storage of high concentrations of phosphorus (in the form of inorganic phosphate, Pi, pyrophosphate, PPi, and polyphosphate, PolyP), calcium, potassium, sodium and magnesium. In the yolk systems, acidocalcisome-like organelles i.e. acidic and electrondense vesicles presenting high concentrations of phosphorus, calcium, potassium, sodium and magnesium, were detected using X-ray microanalysis coupled with electron microscopy. PolyP levels were determined in the eggs, by enzymatic assays using a recombinant exopolyphosphatase, and this polymer was localized in the acidocalcisomes, using DAPI as probe. In insects, PPase activity was detected associated with membrane fractions of acidocalcisomes and these organelles were immunoreactive to antibodies against plant VH^+-PPase, as it happens with acidocalcisomes from protozoa. In echinoderms, the involvement of acidocalcisomes with Ca^{2+} releasing events and the presence of Ca^{2+}/H^+ e Na^+/H^+ exchangers were investigated. In chicken egg yolk, the acidocalcisomes were localized inside larger vesicles, in groups, and the profile of PolyP was investigated during embryogenesis. The possible functions of acidocalcisomes in embryogenesis systems and the differences between the models are discussed.

Lista de Ilustrações:

Lista de abreviaturas:

AMDP = aminometilenodifosfonato
AQP1 = aquaporina 1
BCECF = 2, 7 bis-carboxietil, 5, 6 carboxifluoresceína
β-NAD+ = β-Nicotinamida 1, 6 dinucleotídeo de etanoadenina
Ca^{2+}-ATPases = enzimas bombeadoras de cálcio através da hidrólise de ATP
cADPr = difosfato de adenosina ribose cíclica
CICR = *calcium-induced calcium release*
DAPI = 4,6 diaminofenilindole
FN = fagócitos nutridores
H^{+}-ATPases = enzimas bombeadoras de prótons através da hidrólise de ATP
H^{+}-PPases = enzimas bombeadoras de prótons através da hidrólise de PPi
$InsP_3$ = inositol trifosfato
$InsP_3R$ = receptor de inositol-tri-fosfato
MYP = *major yolk protein*
NAADP = ácido nicotínico de adenina dinucleotídeo fosfato
Pi = fosfato inorgânico
PMCA = *plasma membrane calcium ATPase*
PoliP = polifosfato
PPBD – domínio da exopolifosfatase que se liga a PoliP marcado com o epítopo *X-press*
PPi = pirofosfato inorgânico
PPase = pirofosfatase
PPásica = pirofosfatásica
RE = retículo endoplasmático
RMN = ressonância magnética nuclear
RNA = ácido ribonucléico
RyR = receptor de rianodina
SERCA = *sarcoplasmic/endoplasmic reticulum calcium ATPase*
TPC = *Two pore channels*

Sumário:

1- Introdução:

1- Ovos:

Ovos são células altamente especializadas que podem, uma vez ativadas, dar a origem a um novo indivíduo em questão de semanas ou até mesmo horas. Em geral, os ovos são células grandes que estocam todo o material necessário para programar as primeiras etapas do desenvolvimento (envolvendo sinalização molecular e síntese protéica a partir de mRNAs maternos) e nutrir o embrião até o o fim da embriogênese. O citoplasma dos ovos é rico em proteínas, lipídeos e polissacarídeos, que constituem a reserva de nutrientes para o crescimento embrionário, normalmente chamado de vitelo. Em ovíparos, que se desenvolvem totalmente desconectados do organismo materno, o vitelo pode representar mais de 95 % do volume dos ovos. Ovos de mamíferos são uma exceção a essa regra, já que são majoritariamente nutridos pela mãe, através da placenta. Por isso, ovos de mamíferos, apesar de serem células grandes, não precisam ser tão grandes como ovos de insetos, anfibios ou aves. Em mamíferos, a concentração de vitelo nos ovos é bem pequena, ou até mesmo inexistente. Ovócitos humanos têm aproximadamente 0,05 mm, em equinodermos medem cerca de 0,1 mm, em insetos podem variar de 0,2 a 5 cm e em anfíbios, aves e répteis os ovos podem chegar a vários centímetros (Gilbert, 2000).

2- Ovogênese – Formação dos ovos:

Ovogênese, por definição, é o processo completo de diferenciação de uma célula germinativa feminina em um ovócito maduro, ou seja, competente para ser fertilizado. A ovogênese é um processo particularmente complexo, quando comparado com a espermatogênese, por exemplo, pois não consiste apenas em formar um núcleo haplóide a partir de um ciclo meiótico completo. No geral, os ovócitos maduros contêm em seu citoplasma todo o material necessário para o controle do desenvolvimento inicial. Assim, a ovogênese é um processo que, além de gerar um gameta haplóide, por meiose, também constrói um estoque de enzimas, RNA, organelas e substratos metabólicos, gerando um citoplasma complexo (Gilbert, 2000). Como mencionado anteriormente, essa

característica é especialmente marcante em ovíparos em geral, já que nestes casos os embriões se desenvolvem completamente desconectados do organismo materno.

2.1. Maturação do ovócito:

O processo de maturação do ovócito começa quando uma determinada célula germinativa entra na primeira divisão meiótica e termina ao final do crescimento do ovócito, quando este se encontra pronto para ser fertilizado (Whitaker, 2006). Em várias espécies, o ciclo meiótico pode ser parado e retomado durante seu desenvolvimento. Assim, o sistema é capaz de coordenar o fim do ciclo com o fim da ovogênese (Sagata, 1996; Page e Orr-Weaver, 1997). Os ovócitos da maioria dos animais tem seu ciclo meiótico parado em 2 estágios diferentes (*arrest* 1 e *arrest* 2), sendo que o estágio de *arrest* 2 parece ser específico para cada espécie (Page e Orr-Weaver, 1997b). Um ovócito em *arrest* 2 é dito um ovócito maduro, pois se encontra competente para ser ativado/ fertilizado (Whitaker, 2006)

2.2. Vitelogênese:

Uma das etapas mais marcantes da ovogênese, que acontece durante o processo de maturação (com os ovócitos ainda em *arrest* 1), é a vitelogênese. Durante esta etapa, os ovócitos captam do líquido extracelular (sangue para aves, hemolinfa para insetos, fluido celômico para equinodermos, etc) uma grande quantidade de macromoléculas extra-ovarianas, incluindo lipídeos e proteínas. A incorporação de proteínas, em sua grande maioria proteínas de vitelo, é bastante conhecida em diversos modelos. As proteínas de vitelo são produzidas em sua maioria pelo fígado ou corpo gorduroso (órgão biossintético dos insetos com função semelhante ao fígado de vertebrados), sendo então exportadas para o líquido intracorpóreo, de onde serão incorporadas, através de endocitose mediada por receptores específicos, pelos ovócitos vitelogênicos (Raikhel e Dadhialla, 1992, Alberts, 2002). O final deste processo resulta no acúmulo de uma organela envolta por membrana e repleta de proteínas de vitelo, chamada grânulo de vitelo. Após a vitelogênese, os ovócitos se encontram repletos de grânulos de vitelo, além de gotículas de lipídeo. Depois desta etapa, segue-se então a continuação dos ciclos meióticos (até o *arrest* 2), ovulação, ativação e fertilização interna ou externa, dependendo do modelo.

2.3. Ativação/ Fertilização:

Ativação do ovócito, por definição, é o conjunto de eventos que levam à liberação do *arrest* 2 (Whitaker, 2006). Um ovócito em *arrest* 2 é dito maduro, pois a essa altura já acumulou todo o estoque de macromoléculas necessárias para o desenvolvimento inicial e, por isso, já pode ser fertilizado. A ativação do ovócito pode ser vista como o conjunto de eventos que reorganizam geneticamente o ovócito para que este seja competente para programar a embriogênese inicial. O evento de ativação tem como objetivos gerais ativar a síntese de macromoléculas, permitindo assim, a retomada e término do ciclo meiótico, a tradução de mRNAs maternos específicos (agora necessários para a embriogênese inicial) e a degradação de mRNAs que não são mais necessários (normalmente envolvidos no *arrest* da meiose e na maturação do ovócito) (Schier, 2007). No geral, nos modelos mais estudados como equinodermos e mamíferos, o processo de ativação do ovócito é disparado pela fertilização, apesar das bases moleculares dessa cascata ainda não serem conhecidas (Whitaker, 2006).

3- Classificação – Estrutura geral dos ovos nos diferentes modelos:

Em animais ovíparos, a quantidade de vitelo acumulada e sua disposição no citoplasma dos ovos influenciam diretamente os tipos de clivagens embrionárias iniciais em cada modelo. Ovos que acumulam muito vitelo (como os da maioria dos insetos e aves) no geral fazem clivagem do tipo meroblástica, onde as células embrionárias se dividem apenas em uma pequena parte do ovo, geralmente adjacente ao vitelo. Em ovos que acumulam pouco vitelo (como os de equinodermos) a clivagem embrionária é do tipo holoblástica, o que significa que toda a extensão dos ovos é dividida em duas partes iguais, e assim sucessivamente (Slack, 2006). Nesta tese, serão utilizados ovócitos e ovos de cinco modelos de estudo, os equinodermos *Arbacia punctulata* e *Lytechinus variegatus*, os insetos *Periplaneta americana* e *Rhodnius prolixus* e a ave *Gallus gallus*. Por isso, para maior compreensão do leitor, cada modelo será abordado separadamente nas próximas seções.

3.1. *Arbacia punctulata* e *Lytechinus variegatus*:

O filo echinodermata é contituído por invertebrados marinhos com cerca de 7.000 espécies distribuídas em seis classes distintas. A classe echinoidea inclui os chamados ouriços-do-mar ou ouriços regulares. Estes animais têm forma hemiesférica com projeções em formas de espinhos. Possuem reprodução sexuada e fecundação externa. Estes invertebrados apresentam cinco gônadas e de cada uma delas estende-se um gonoducto, que conduz os gametas para fora do seu corpo quando expelidos através do gonoporo. Uma fêmea típica expulsa cerca de três a seis milhões de ovócitos (pois nesse caso a fertlização é externa) em uma ovulação (Barnes e Rupert, 1996).

Ovócitos e ovos destes organismos têm sido bastante utilizados como modelos em estudos de embriologia experimental e sinalização por cálcio, e vários dos mecanismos descritos nestes animais se mostraram presentes em células de mamíferos (Whitaker, 2006). *Arbacia puntulata* e *Lytechinus variagatus* (Figura 1) são espécies comumente utilizadas como modelos em vários estudos envolvendo os mecanismos de exocitose de grânulos corticais e formação das ondas de cálcio após a fertilização (como será abordado a seguir).

Em ouriços, a ovogênese é um processo associado ao crescimento de outras células dos ovários (gônadas femininas). Os ovários crescem em tamanho não só porque a ovogênese aumenta o tamanho dos ovócitos, mas também porque algumas células somáticas (principalmente os chamados fagócitos nutridores, FN) no epitélio do ovário acumulam nutrientes de reserva antes da ovogênese começar (Walker e cols., 2001). Uma glicoproteína chamada MYP (do inglês, major yolk protein) é o principal nutriente estocado nos FN (Brooks e Wessel, 2002; Unuma e cols., 2003), e esta proteína é posteriormante encontrada nos ovos como a principal componente dos grânulos de vitelo (Yokota e Sappington, 2002). Assim, a MYP é estocada pelos FN antes da ovogênese e posteriormente transportada (por um mecanismo ainda não conhecido) para os grânulos de vitelo dos ovócitos em formação. Esta proteína será então a principal fonte de macromoléculas para construção de novas proteínas durante a embriogênese inicial (Unuma e cols., 2003). Após a ovogênese, os ovócitos maduros (medindo aproximadamente 0,1 mm) são estocados no lúmen dos ovários por dias ou até semanas até sua liberação na água do mar e posterior fertilização.

Por não acumularem uma grande quantidade de vitelo, se comparados com os ovos de insetos ou aves, os ovos de ouriço não crescem muito durante a etapa de vitelogênese (um ovócito de ouriço tem tamanho semelhante a um ovócito de mamífero). Por isso, fazem parte do grupo de ovos com clivagem holoblástica e poucos estudos são direcionados para a dinâmica das organelas e proteínas de vitelo neste modelo. Os ovócitos de ouriço contêm várias vesículas intracelulares identificadas por microscopia eletrônica. Dentre elas, as mais comuns são os grânulos corticais, que se localizam no córtex dos ovos e exocitam seu conteúdo durante a fertilização; os grânulos de vitelo, que compõem um grupo abundante de organelas com eletrondensidade uniforme que podem ocupar até 50% do volume do ovo; e os grânulos vazios, que são distribuídos pelo citoplasma e se caracterizam por uma aparência vazia quando observados por microscopia eletrônica de transmissão. Os grânulos corticais e os grânulos vazios são ácidos, enquanto os grânulos de vitelo são neutros, sendo levemente acidificados após a fertilização (Lee e Epel, 1983; Sardet, 1984).

Em equinodermos, o processo de ativação do ovócito é disparado pela fertilização, apesar das bases moleculares desta cascata ainda não serem conhecidas. O principal evento inicial observado após a ativação são as oscilações repetitivas nos níveis de Ca^{2+} do ooplasma, que levam à exocitose dos grânulos corticais, estabelecendo o primeiro bloqueio à polispermia (Whitaker, 2006). Os eventos mais tardios na cascata da ativação incluem o término da meiose, aumento do pH do ooplasma, elevação da tradução dos RNAs estocados pela mãe, formação do pró-núcleo, início de síntese de DNA e início das mitoses embrionárias (Steinhardt e cols., 1977). Em *A. punctulata e L. variegatus,* o desenvolvimento dos ovos até a fase de larva leva em torno de 18 horas.

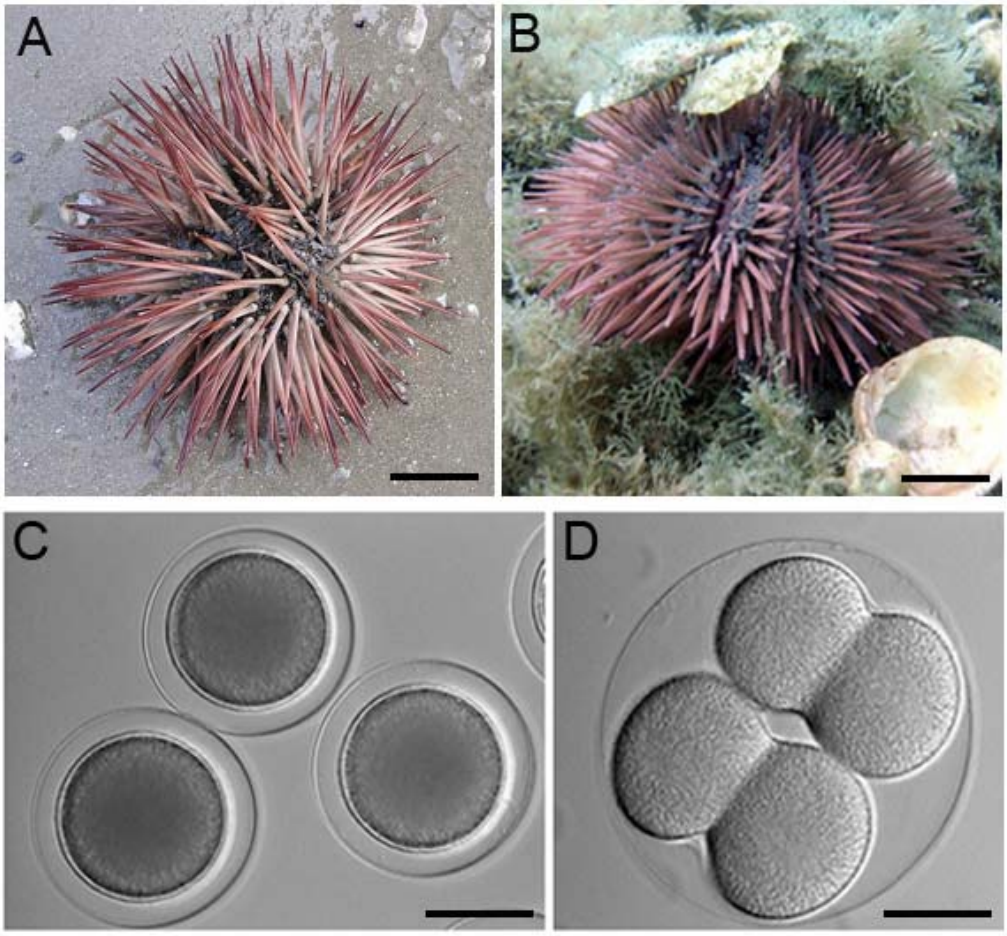

Figura 1: **(A)** *Arbacia punctulata*. **(B)** *Lytechinus variegatus*. Barras: 1 cm. **(C)** Ovos de *L. variegatus*. Barra: 80 µm. **(D)** Estágio de quatro células de um embrião de *L. variegatus*. Clivagem do tipo holoblástica. Barra: 30 µm.

Adaptado de *http://www.molbiolcell.org.*

3.2. *Periplaneta americana* e *Rhodnius prolixus*:

O grande sucesso da classe Insecta (Hexapoda) como o mais diverso e numeroso grupo do reino animal se deve principalmente à sua eficiente estratégia reprodutiva (Büning, 1994). Este grupo inclui espécies que são vetores de parasitoses humanas, pestes agrícolas e urbanas. Nesse contexto, a interferência nos processos reprodutivos pode ser utilizada como alvo no controle populacional de insetos, e daí surge a necessidade do conhecimento dos processos associados ao desenvolvimento destes animais.

A *Periplaneta americana* (Figura 2 A), vulgarmente conhecida como barata americana, é a maior das baratas encontradas em ambientes peridomésticos. Pertence à ordem *Blattodea* (família Blattidae) e é uma das espécies de barata mais conhecidas pelo homem. Atualmente, estima-se que uma única barata pode carregar um total de 13.470 espécies de bactérias (Rust e cols., 1991), sendo assim caracterizada como um eficiente vetor mecânico. Baratas estão comumente associadas a lixo, esgoto e doenças, além de serem extremamente ofensivas ao nosso senso de estética. Além disso, sua ampla distribuição geográfica e sua alta adaptabilidade a variados ambientes tornam este inseto uma das pragas urbanas mais comuns do mundo (Rust e cols., 1991). Nesse contexto, a *P. americana* pode se tornar um problema de saúde pública. Por exemplo, só o estado da Georgia (EUA) gasta US$ 420 milhões por ano no controle de pestes urbanas (Urban Pest Management Control, University of Georgia).

A tripanossomíase americana ou Doença de Chagas é a primeira causa de lesões cardíacas em adultos de idade economicamente ativa na América Latina (Moncayo, 2003). A Doença de Chagas é causada pelo protozoário parasito flagelado *Trypanosoma cruzi*, que é transmitido para o hospedeiro humano por insetos hematófagos pertencentes à ordem Hemiptera (família Reduviidae), conhecidos popularmente no Brasil como barbeiros. Um dos modelos experimentais a ser utilizado nesta tese é o inseto *Rhodnius prolixus* (Figura 2 B), principal vetor biológico do *T. cruzi* na Venezuela, Colômbia e Honduras, e o vetor secundário em El Salvador, Guatemala e Nicarágua (WHO, 2008).

O sistema reprodutivo feminino em insetos é basicamente constituído de dois hemi-ovários localizados na cavidade abdominal de adultos. Cada um deles é composto por unidades independentes denominadas ovaríolos, sendo estas as unidades produtoras

de ovos. No geral, o ovaríolo é constituído de um *cluster* de células germinativas na sua região apical, seguido de uma seqüência de ovócitos em crescimento. Nestas unidades, os ovócitos em formação vão crescendo a partir da captação de macromoléculas provindas da hemolinfa e do epitélio folicular (vitelogênese) (Buning, 1994).

Em insetos, ao fim da vitelogênese, o ovócito se encontra repleto de grânulos de vitelo e as moléculas incorporadas que estão estocadas nos grânulos constituirão a principal fonte de aminoácidos para o desenvolvimento embrionário (Gilbert, 2000). Sabe-se que a ativação do ovócito nos insetos começa antes da fertilização, logo após a ovulação (passagem do oviduto lateral para o oviduto comum), e continua acontecendo até a chegada do ovócito ao fim do oviduto comum, onde será fertilizado (Heifetz e cols., 2001). Porém, os eventos resultantes da cascata de sinalizaçao são desconhecidos (Mahowald e cols., 1983; Page e Orr-Weaver, 1997). Em geral, os ovos de insetos acumulam grandes quantidades de vitelo, fazendo então clivagem embrionária do tipo meroblástica, e têm um tamanho maior (quando comparados com os de ouriço), com mais de 90 % do seu conteúdo preenchido por grânulos de vitelo. Por isso, investigações bioquímicas sobre os mecanismos de hidrólise das proteínas de vitelo nestes modelos são um pouco mais explorados, como descrito a seguir. Após a vitelogênese, segue-se então a formação do córion (casca do ovo) e a fecundação. A partir deste momento, o ovo é colocado no ambiente.

Além das proteínas de vitelo, várias hidrolases já foram descritas em ovócitos e ovos de insetos. A origem destas enzimas nos ovos ainda não é bem conhecida, mas algumas delas já foram identificadas como componentes da hemolinfa que são incorporadas pelo ovócito e estocadas nos grânulos de vitelo, assim como as proteínas de vitelo. Em *Bombyx mori* já foi caracterizada a *Bombyx* cisteíno protease, que é sintetizada pelo corpo gorduroso, captada pelo ovócito e estocada em grânulos de vitelo na forma inativa (Yamamoto e cols., 2000). A carboxipeptidase vitelínica de *Aedes aegypti* também é uma protease sintetizada extraovarianamente e captada pelos ovócitos em vitelogênese (Snigirevskaya e cols., 1997). Algumas catepsinas também são estocadas nos grânulos de vitelo em forma inativa, como a catepsina B de *Musca domestica* (Ribolla e cols., 2001) e a catepsina D de *Rhodnius prolixus* (Nusseinzveig e cols., 1992). Além de proteinases, outras classes de enzimas lisossomais têm sido descritas nos

grânulos de vitelo de diversos insetos, como fosfatases ácidas em *Drosophila melanogaster* (Sawicki e MacIntyre, 1977), *R. prolixus* (Nusseizveig e cols., 1992), *P. americana* (Oliveira e cols., 2007) e *M. domestica* (Ribolla e cols., 1993). Muitas destas enzimas encontradas nos grânulos de vitelo, por exemplo, catepsinas (Takahashi e cols., 1996; Cho e cols., 1999; Ribolla e cols., 2001), fosfatases (Nussenzveig e cols., 1992; Ribolla e cols., 1993; Fialho e cols., 2002; Fialho e cols., 2005) e glicosidases (Purcell e cols., 1988) são ativadas somente em valores baixos de pH (pH ácido). Além disso, várias destas enzimas têm sua atividade aumentada durante a embrigênese inicial (Takahashi e cols., 1996; Cho e cols., 1999; Oliveira e cols., 2007) e postula-se que esta ativação esteja relacionada com a degradação das proteínas de vitelo, que acontece em intervalos de tempo específicos durante a embrigênese. Em *P. americana*, os ovos são colocados agrupados em estruturas chamadas ootecas, e os primeiros produtos de degradação das vitelinas aparecem no quinto dia de embriogênese, em um total de 31 dias. Em *R. prolixus* os primeiros produtos de degradação do vitelo começam a ser visíveis a partir do dia 3, em um total de 13 dias de embriogênese (Fialho e cols., 2005).

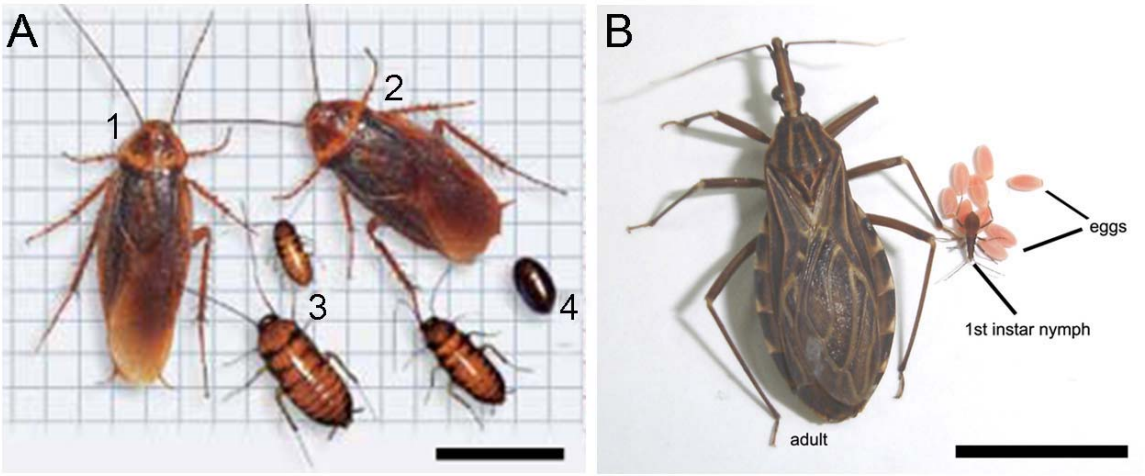

Figura 2: **(A)** *Periplaneta americana.* **1:** Macho adulto, **2:** Fêmea adulta, **3:** Ninfas, **4:** Ooteca. Barra: 2 cm. **(B)** *Rhodnius prolixus.* Adulto, ninfa de primeiro estádio e ovos estão indicados na imagem. Barra: 1 cm.

3.3. *Gallus gallus*:

A galinha é a fêmea da espécie *Gallus gallus domesticus* de aves da ordem Galiformes e classe Fasianídeas. A galinha tem uma enorme importância econômica para o homem, sendo o animal doméstico mais difundido e abundante do planeta. Estas aves representam uma das principais fontes de alimento para os homens, que consomem primariamente sua carne e ovos (Burley e Vadehra, 1989) (Figura 3). O trato reprodutivo das aves é basicamente formado por dois ovários, onde os ovócitos acumulam macromoléculas provindas do sangue, do epitélio folicular e das células nutridoras (*nurse cells*). Assim como nos insetos, os grânulos de vitelo também são formados a partir de endocitose de macromóleculas provindas do sangue (previamente produzidas pelo fígado) durante a vitelogênese (Slack e cols., 2006). Após a vitelogênese, segue-se a formação do albúmen (clara dos ovos), que é basicamente constituído de água e proteínas secretadas por células do ovário, e a secreção dos constituintes do córion (casca do ovo), que é formado por 95 % de cristais de carbonato de cálcio estabilizados por ligações cruzadas com proteínas. Os ovócitos são então fertilizados e colocados no ambiente e, por acumular grandes quantidades de vitelo, ovos de aves fazem clivagem embrionária do tipo meroblástica. Neste modelo, devido a existência de vários de estudos nutricionais, a composição química do ovo é bem definida, sendo constituído aproximadamente por 12% de lipídeos, 12 % de proteínas e 1 % de carboidratos do total do peso úmido da estrutura (Lovell Badge e cols., 1985). Aves são classicamente modelos mais estudados para padrões mais tardios de desenvolvimento embrionário (Bancroft e cols., 1976; Bellairs e cols., 1980; Bellairs e cols., 1998). Porém, estudos que investigaram os eventos inicias da embriogênese e as estruturas do vitelo identificaram diferentes tipos de partículas e vesículas nos ovos de galinha: as esferas de vitelo (vesículas de aproximadamente 100 μm e chamadas de solúveis), glóbulos de vitelo (partículas de aproximadamente 100 μm e chamdas de insolúveis) e os grânulos de vitelo. Os últimos são os mais abundantes (representam um quarto do peso seco do vitelo), são menores do que as esferas e os glóbulos (10 - 40 μm) e contêm a maior parte das lipovitelinas (principal lipoproteína de vitelo) e fosvitinas (principal fosfoproteína do vitelo) dos ovos (Willems and Stockx, 1973a; Veini e cols.,1991). Os ovos fertilizados levam um total de

21 dias de desenvolvimento (a 37ºC e 55 % umidade relativa), e podem manter os primeiros estágios de clivagem embrionária quando incubados a 4ºC por semanas ou até meses.

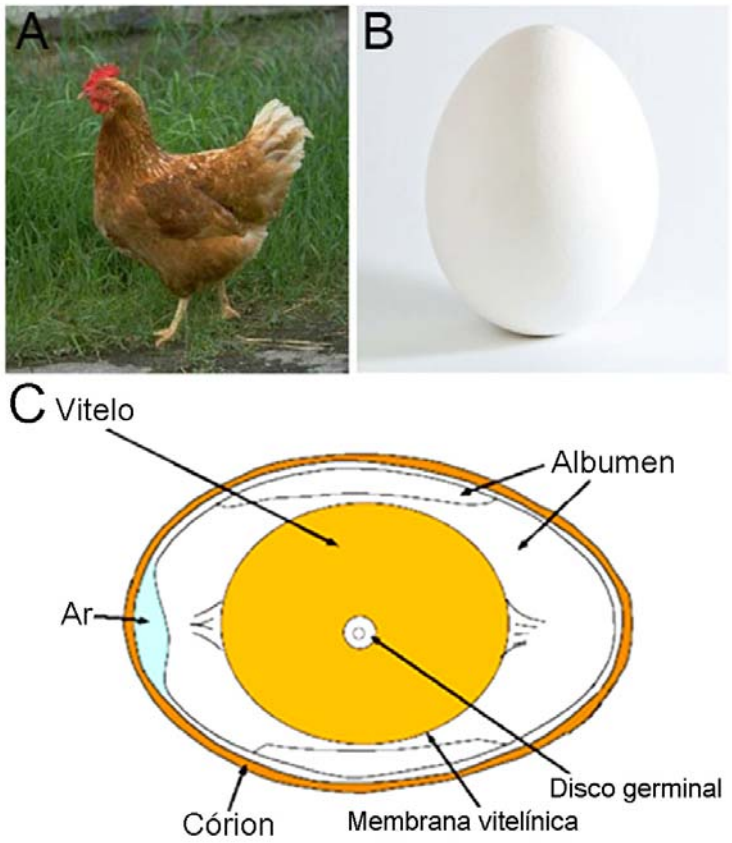

Figura 3: **(A)** *Gallus gallus domesticus*, adulto. **(B)** Ovo. **(C)** Esquema das principais estruturas do ovo de *Gallus gallus*. O vitelo é central, envolvido por uma membrana vitelínica, uma camada de albúmen e pelo córion.

Adaptado de Burley e Vadehra, 1989. The avian egg. In: yolk structures. p 213.

4- O sistema de vitelo nos ovos:

Para que as macromoléculas de vitelo sirvam como fonte de nutrientes para a construção dos tecidos embrionários é necessário que, durante a embriogênese, estas sejam degradadas e mobilizadas do interior do grânulo para o embrião. A degradação destas macromoléculas fornecerá moléculas primordiais (monossacarídeos, aminoácidos, etc) para que o desenvolvimento embrionário inicial ocorra. Este processo ocorre a partir da ativação das hidrolases, que também são estocadas nos grânulos de vitelo. Para que estas sejam ativadas é necessário que o ambiente luminal dos grânulos seja acidificado. A acidificação dos grânulos de vitelo ocorre a partir da ação de enzimas bombeadoras de prótons como V-H^+-ATPases (Fagotto, 1990; Fagotto, 1995) e V-H^+-PPases (Motta e cols., 2004), levando à maturação das pró-enzimas que degradam as proteínas de vitelo (Figura 4). Em geral, a maquinaria necessária para a que a proteólise ocorra é incorporada ao ovócito durante a ovogênese (Fagotto, 1991; Fagotto, 1995; Takahashi e cols., 1996; Cho e cols., 1999; Ribolla e cols., 2001). Dessa forma, o ovo recém-posto possui todas as ferramentas para que o processo de proteólise ocorra. No entanto, de uma maneira geral, a proteólise não começa logo após a ovoposição, e sim após algum tempo da embriogênese inicial. O intervalo para o início da degradação do vitelo varia entre as espécies e o mecanismo que modula o momento de início desse processo ainda é desconhecido.

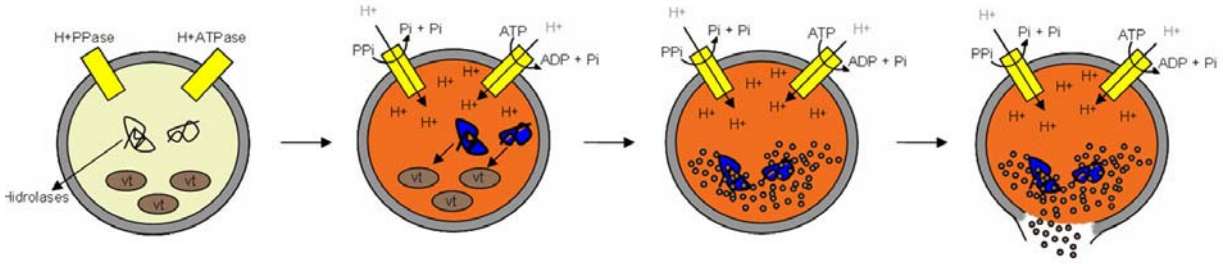

Figura 4: Esquema do modelo de ativação da degradação do vitelo. A ativação das bombas de prótons leva à acidificação do interior das organelas e ativação das hidrolases ácidas, que degradam as proteínas de vitelo. H^+PPase: Próton pirofosfatase vacuolar, PPi: pirofosfato, Pi: Fosfato inorgânico, H^+: prótons

Em muitos modelos estudados, a formação dos grânulos de vitelo durante a ovogênese passa por diferentes rotas de empacotamento de proteínas, gerando um ovócito maduro com uma população hetereogênea de organelas (Figura 5). Apesar do acúmulo de proteínas e presença de grânulos de vitelo ser uma característica ubíqua em ovos de diferentes espécies, pouco se sabe sobre a organização celular desse sistema. No geral, se chama grânulo de vitelo qualquer vesícula extraída de sistemas de vitelo, porém, é comumente observado na literatura que a população de vesículas presente nos ovos é bastante variada. Em vários modelos, incluindo equinodermos, insetos, anfíbios e aves, as vesículas podem ser fracionadas de acordo com suas diferenças de tamanho e densidade (Fagotto, 1991; Chestkov e cols., 1998; McNeil e cols., 2000; Yamahama e cols., 2003, Burley e Vadehra, 2001; Churchill e cols., 2002). Sabe-se também que as diferentes vesículas podem passar por eventos de fusão durante a embriogênese inicial, e que esses processos são importantes para a degradação das proteínas de vitelo em insetos (Ramos e cols., 2006, Ramos e cols., 2007) ou para o bloqueio inicial da poliespermia em equinodermos (Whitaker, 2006).

No bicho-da-seda *Bombyx mori*, as hidrolases estão presentes apenas nos grânulos pequenos e as proteínas de vitelo só foram localizadas em grânulos de tamanho grande (Yamahama e cols., 2003). No bicho-pau *Carausius morosus* observou-se a acidificação diferencial de grânulos ao longo da embriogênese. Foi mostrado que os grânulos pequenos são observados ácidos com mais freqüência e podem ser comumente encontrados rodeando os grânulos grandes (Fausto e cols., 2001). No carrapato *Boophilus microplus* a atividade proteolítica foi correlacionada com a acidificação diferencial de vesículas na periferia do ovo (Abreu e cols., 2004). Em ovos de equinodermos, a principal proteína de vitelo (MYP) se encontra estocada apenas nos grânulos de vitelo, e esta organela (ao lado do retículo endoplasmático, RE) pode também ser utilizada como fonte de cálcio para sinalização intracelular nos primeiros eventos de ativação (Churchill e cols., 2002; Morgan e Galione, 2007). Além disso, os grânulos vazios também são abundantes no citoplasma dos ovos mas, apesar de serem reconhecidamente acídicos, sua função ainda é desconhecida. Em aves, a atividade de diferentes enzimas já foi correlacionada com frações diferentes de vesículas do vitelo. Lipoproteínas e fosfoproteínas estão associadas apenas a uma população restrita de organelas, os

denominados grânulos de vitelo (e não às esferas ou glóbulos), e esta população pode ser fracionada, por centrifugação diferencial, em duas subpopulações. A subpopulação mais densa apresenta mais de 85 % da atividade fosfatase ácida detectada no vitelo, e a menos densa mais de 70 % da atividade ribonuclease do sistema (Willems and Stockx, 1973b).

Porém, apesar dos relatos sobre as variações na população de vesículas dos ovos serem comuns, a origem e o papel dessas diferenças ainda não são bem conhecidos. Pouco se sabe sobre como as diferentes organelas do sistema de vitelo se organizam no interior dos ovos, ou como essas estruturas são reguladas e capazes de coordenar processos celulares complexos, como a regulação da degradação do vitelo, a iniciação dos eventos de ativação e a disponibilização de macromoléculas fundamentais para o embrião.

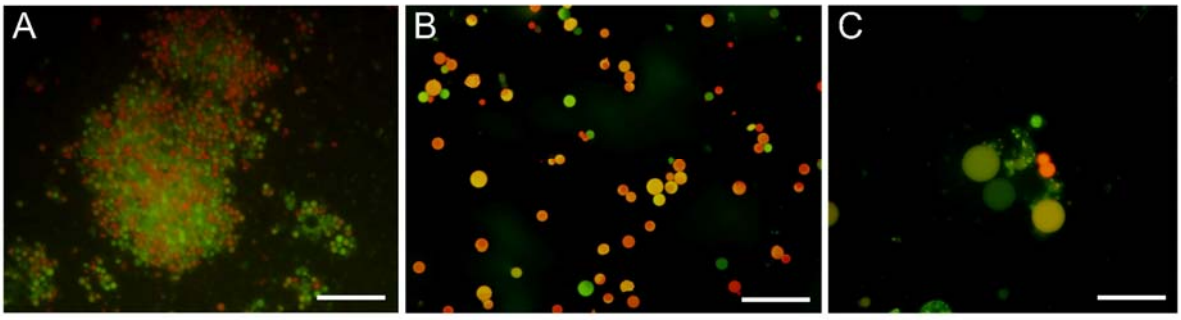

Figura 5: Microscopia de fluorescência de grânulos de vitelo extraídos de ovos de diferentes espécies incubados com o marcador de ambientes ácidos Laranja de Acridina. Fluorescência na faixa do laranja-vermelho indica o grau de acidificação dos diferentes compartimentos. Fluorescência na faixa do verde indica ambientes neutros. **(A)** *Lytechinus variegatus*, barra: 10 μm. **(B)** *Gallus gallus*, barra: 100 μm. **(C)** *Rhodnius prolixus*, barra: 10 μm.

5- Cálcio e sinalização intracelular:

O íon Ca^{2+} é uma molécula de sinalização intracelular ubíqua, capaz de controlar uma enorme variedade de processos celulares (Berridge e cols., 1993; Carafoli e cols., 2001). O RE é considerado o principal compartimento intracelular de estoque de Ca^{2+} em células eucarióticas. Suas funções de captação e liberação de Ca^{2+} para o citoplasma são controladas por proteínas que funcionam no transporte ativo (utilizadas para captar o Ca^{2+} para dentro da organela), proteínas ligadoras de Ca^{2+} (utilizadas para acumular este íon no lúmen) e os canais ativados por ligantes (utilizados para liberação passiva de Ca^{2+} para o citoplasma). Os sinais para liberação de compartimentos internos são principalmente controlados por duas famílias de canais: os receptores de Rianodina (RyR, que receberam esse nome não por seu ligante, mas por seu antagonista) e os receptores de Inositol-trifosfato ($InsP_3R$). Estes se encontram nas membranas do RE, e seus ligantes são a ADP ribose cíclica (cADPr) e o $InsP_3$ respectivamente. Além disso, foi descoberto um novo mensageiro para liberação intracelular de Ca^{2+}, o ácido nicotínico de adenina dinucleotídeo fosfato (NAADP). Este é produzido pela mesma enzima que gera a cADPr, a partir de β-Nicotinamida 1, 6 dinucleotídeo de etanoadenina (β-NAD+) (Aarhus e cols., 1995). Uma característica marcante deste novo mensageiro é que as liberações de Ca^{2+} induzidas por NAADP não são provenientes do RE. Há indicações que seu alvo é um canal na membrana de organelas com características lisossomais. Estas organelas têm um trocador Ca^{2+}/H^{+} dirigido pelo seu caráter acídico e, além disso, são capazes de reter Ca^{2+} por longos períodos, mesmo que o trocador esteja inibido (Churchil et al, 2002; Morgan e Galione, 2007). Recentemente, os TPCs (do inglês *two pore channels*) foram identificados como os receptores para liberação de calcio via NAADP (Calcraft e cols., 2009).

As liberações de Ca^{2+} no citoplasma são quase sempre transientes, deixando o íon Ca^{2+} disponível para sinalização por um curto período de tempo em uma determinada região. Assim, após um sinal elementar de liberação de Ca^{2+}, a partir dos canais descritos acima, a célula utiliza uma outra maquinaria para recapturar rapidamente o Ca^{2+} liberado para o compartimento interno ou transportar o Ca^{2+} para fora da célula pela membrana plasmática. Neste caso, o tipo de transporte a ser realizado é ativo, e normalmente é feito pelo trocador Ca^{2+}/Na^{+} e pelas chamadas Ca^{2+}-ATPases (Carafoli e cols., 2001). Na

membrana plasmática, o primeiro é o principal responsável pelas baixas concentrações de Ca^{2+} no citoplasma, e permite o transporte ativo de Ca^{2+} para fora da célula dirigido pela energia da entrada de Na^{+} para o citosol, de acordo com seu gradiente eletroquímico, que é ativamente mantido pela bomba Na^{+}/K^{+}. A Ca^{2+}-ATPase de membrana plasmática (PMCA, do inglês *plasma membrane* Ca^{2+}-ATPase) é também uma importante via de saída de Ca^{2+} pela membrana, e mesmo em células em que o trocador é predominante, esta se encontra presente e ativa, funcionando como um regulador fino da concentração de Ca^{2+} no citosol (Carafoli e cols., 2001). Esta enzima acopla a hidrólise do ATP ao transporte de íons Ca^{2+} por membranas, dirigindo ativamente a saída de Ca^{2+} das células. No RE, uma outra Ca^{2+}-ATPase atua da mesma forma, rapidamente recapturando o Ca^{2+} liberado para dentro do compartimento. A Ca^{2+}-ATPase de retículo (SERCA, do inglês *sarcoplasmic/endoplasmic reticulum* Ca^{2+}-ATPase) representa cerca de ~70 % das proteínas de membrana de retículo, reforçando o papel dessa organela no estoque e homeostase de Ca^{2+} na célula (Carafoli e cols., 2001).

6- Acidocalcissomos:

Ao contrário do que acontece na maioria das células eucarióticas, em diferentes protozoários, a maior parte do cálcio intracelular é estocada em organelas acídicas chamadas acidocalcissomos. A partir de experimentos realizados em diferentes parasitos permeabilizados com digitonina, um *pool* de cálcio não mitocondrial sensível à nigericina (trocador K^{+}/H^{+}) foi detectado em *T. brucei* (Vercesi e cols., 1994), e incubações com diferentes indicadores de cálcio (como FURA-2 e Arsenazo III) demonstraram que a maior parte do cálcio dessas células está presente nesta organela (Vercesi e cols., 1994; Docampo e cols., 1995; Vercesi e Docampo, 1996). A partir deste conjunto de trabalhos iniciais, diferentes técnicas bioquímicas, de análises fisiológicas e analíticas, demonstraram a presença de acidocalcissomos em vários membros da família Trypanosomatidae como *Trypanosoma cruzi*, *Trypanosoma brucei* (Vercesi e cols., 1994; Docampo e cols., 1995; Vercesi e Docampo, 1996), *Leishmania spp* (Lu e cols., 1997; Rodrigues e cols., 1999; Miranda e cols., 2004), *Phytomonas francai* (Miranda e cols., 2004) e parasitos do grupo apicomplexa como *Toxoplasma gondii* (Moreno e Zhong, 1996; Rodrigues e cols., 2002) e *Plasmodium spp* (Marchesini e cols., 2000; Ruiz e cols.,

2004). Uma bateria de estudos de transporte iônico, utilizando diferentes indicadores para cálcio (Fura, Arsenazo III) e pH (laranja de acridna, BCECF) demonstraram a presença de várias bombas e trocadores na membrana dos acidocalcissomos. A organela é acidificada por duas bombas de prótons, uma H^+-ATPase vacuolar, sensível a bafilomicina A1 (Vercesi e cols., 1994; Docampo e cols., 1995), e uma H^+-PPase vacuolar, sensível a aminometilenodifosfonato (AMDP) (Scott e cols., 1998; Rodrigues e cols., 1999a; 1999b). A captação de cálcio para o lúmen da organela é promovida por uma Ca^{2+}/H^+-ATPase, sensível a altas concentrações de ortovanadato de sódio (Vercesi e cols., 1994; Docampo e cols., 1995; Luo e cols., 2004) e um trocador Ca^{2+}/nH^+ dirigido pelo caráter acídico da organela, mantido pelas bombas (Vercesi e cols., 1994). Além disso, um trocador Na^+/nH^+ (Vercesi e Docampo, 1996; Vercesi e cols., 1997; Vercesi e cols., 2000) que pode atuar na liberação de cálcio acoplado ao trocador Ca^{2+}/nH^+, e uma aquaporina (AQP1) (Montaveltti e cols., 2004) também foram descritos na membrana de acidocalcissomos (Figura 6 B).

Posteriormente, técnicas de fracionamento subcelular associadas à microscopia eletrônica analítica (principalmente espectroscopia por perda de energia de elétrons e microanálise de raios-X) permitiram associar os acidocalcissomos como correspondentes aos grânulos eletrodensos já descritos anteriormente em vários parasitos como *T. cruzi* e *L. major* (Vickerman e Tetley, 1977; Dvorak e cols., 1988; Le Furgey e cols., 1990). Em 1997, Scott e colaboradores, também utilizando a técnica de microanálise de raios-X, encontraram altos níveis de fósforo, oxigênio, sódio, magnésio, potássio, cálcio e zinco nos grânulos eletrondensos de *T. cruzi*. Por isso, foi sugerido pelos autores que, por apresentarem grandes acúmulos de cálcio, os grânulos eletrodensos corresponderiam aos acidocalcissomos (Scott e cols., 1997; Rodrigues e cols., 1999a). Esse dado foi confirmado por experimentos de fracionamento subcelular, onde os grânulos densos isolados exibiam os mesmos padrões de transporte de prótons e cálcio apresentrados pelos vacúolos observados anteriormente em parasitos permeabilizados com digitonina (Vercesi e cols., 1994; Docampo e cols., 1995; Vercesi e Docampo, 1996), e eram imunoreativos a anticorpos anti-VH^+-PPase de plantas e VH^+-ATPase de diferentes organismos (Scott e cols., 1998b; Rodrigues e cols., 1999; Scott e Docampo, 2000; Miranda e cols., 2004b) (Figura 6). VH^+-PPases identificadas em acidocalcissomos de

protozoários têm sua atividade estimulada por íons K^+ e inibida por Na^+ e análogos de PPi. Frações de acidocalcissomos isolados de diferentes parasitos apresentaram atividade PPásica altamente enriquecida, e reação positiva para marcação com anticorpos anti-VH^+-PPase de plantas. Assim, por estarem concentradas nos acidocalcissomos, a H^+-PPase vacuoloar é considerada um marcador para esta organela (Rodrigues e cols., 1999; Ruiz e cols., 2001; Lemercier e cols., 2002).

Além do típico conteúdo eletrondenso e acúmulo de elementos como fósforo, cálcio, potássio, magnésio e sódio, uma outra característica comum aos acidocalcissomos é o estoque de fósforo na forma de polifosfatos inorgânicos. Polifosfatos (PoliP) são polímeros de cadeia linear constituídos de poucas unidades ou até centenas de resídos de fosfato, unidos por ligações fosfoanidro (Kornberg, 1999). PoliP podem ser encontrados tanto em bactérias como em mamíferos e podem participar de várias funcões celulares como armazenamento de fósforo, sequestro e armazenamento de cátions (como Ca^{2+}, por exemplo), controle de processos de transcrição, entre outras (Kulaev e Kulakovskaya, 2000). Recentemente, vem se mostrando que os acidocalcissomos de protozoários acumulam gandes quantidades de PoliP (Urbina e cols., 1999; Scott e cols., 2000; Ruiz e cols., 2004) e que o níveis desses polímeros na organela podem ser rapidamente alterados mediante diferentes estímulos extracelulares (Ruiz e cols., 2001) e silenciamento de diferentes enzimas (Fang e cols., 2007; de Jesus e cols., 2010), sugerindo uma participação importante em diferentes processos fisiólogicos nestas células.

Em protozoários, os acidocalcissomos têm sido associados a diversas funções celulares (Docampo e cols., 1999, 2001, 2005, 2008, 2010; Miranda e cols., 2008). Em várias espécies, estas organelas representam o principal compartimento de estoque de cálcio, sódio, magnésio, potássio e fósforo (na forma de PoliP, PPi e Pi), podendo por isso fazer parte da homeostase iônica da célula. O controle de pH também é uma função atribuída aos acidocalcissomos, visto que alterações na expressão de bombas de prótons (como a VH^+-PPase) induz a falhas na homeosatse de pH em células submetidas a pHs levemente alcalinos ou acídicos (Lemercier e cols., 2002). Além disso, o papel dos acidocalcissomos na osmoregulação em parasitos também foi demonstrado. Foi observado que os níveis de PoliP são aumentados em células submetidas a estresse hiperosmótico, enquanto que o fenômeno inverso pode ser observado sob estresse

hiposmótico (Ruiz e cols., 2001). Acredita-se que esse metabolismo tem função importante na sobrevivência do parasito frente aos desafios osmóticos lançados pelo hospedeiro vertebrado e invertebrado, já que a degradação de PoliP em Pi dentro dos acidocalcissomos resulta no turgor da organela (Rohloff e cols., 2004; Docampo e cols., 2010).

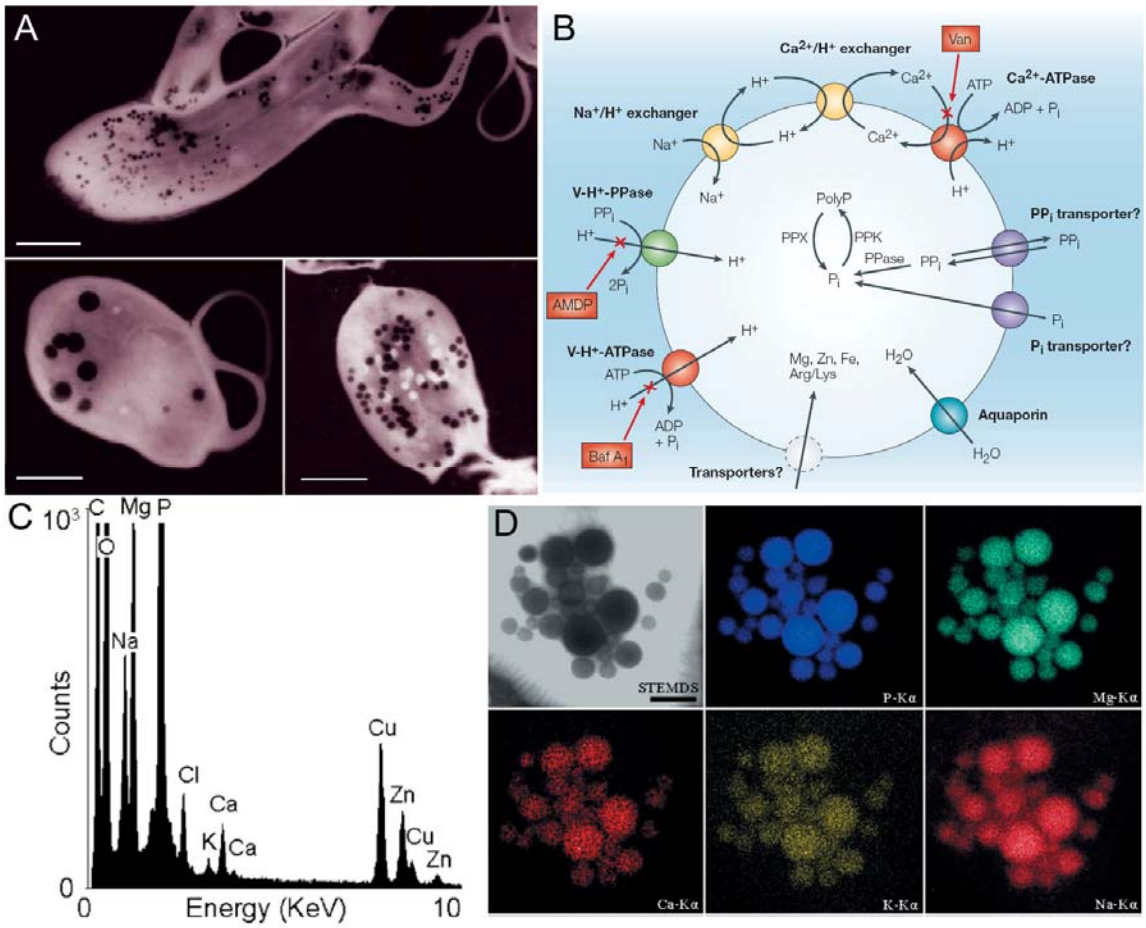

Figura 6: Acidocalcissomos. **(A)** Imagens espectroscópicas de parasitos inteiros (*Crithidia deanei* e *T. cruzi*) evidenciando a presença dos acidocalcissomos eletrondensos distribuídos no citoplasma. Barra: 5 µm. **(B)** Esquema das bombas, trocadores e canais já identificados na membrana dos acidocalcissomos. **(C)** Espectro de microanálise de raios-X e **(D)** mapeamento de elementos de acidocalcissomos em uma espécie de *Leishmania*. Barra: 1 µm.

Imagens adaptadas de Docampo et al., 2005; Miranda et al., 2004.

Nos últimos anos, a presença de organelas similares aos acidocalcissomos vem sido descrita em diferentes microrganismos, além dos protozoários (Figura 7). Organelas similares a acidocalcissomos foram também encontradas em bactérias (Seufferheld e cols., 2003, 2004), na alga biflagelada *Chlamydomonas reinhardtii* (Ruiz e cols., 2001b) e na ameba social *Dictyostelium discoideum* (Marchesini et al, 2002). Recentemente, uma organela similar aos acidocalcissomos foi descrita pela primeira vez em um modelo animal superior, em plaquetas humanas. Esta organela apresenta características morfológicas típicas de acidocalcissomos, e seu conteúdo de PoliP foi sugerido como um modulador da cascata de coagulação sanguínea (Ruiz e cols., 2004b). A ampla distribuição de acidocalcissomos em diferentes tipos celulares, sua morfologia e diferentes funções foram revisadas por Docampo e colaboradores em 2005.

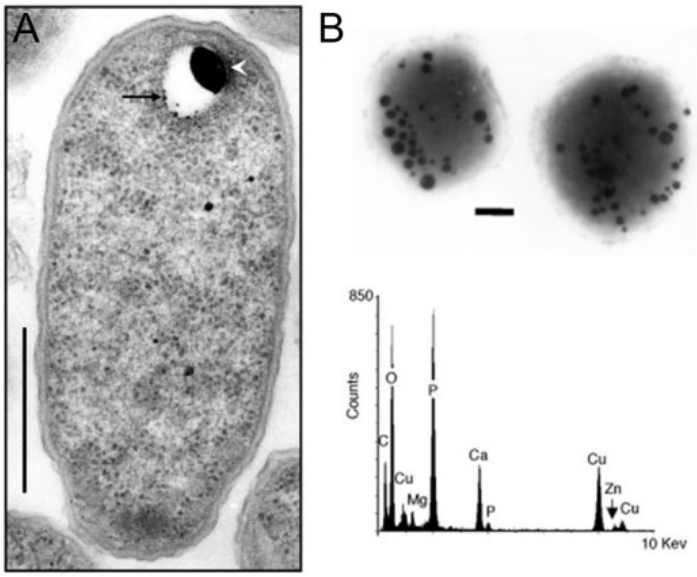

Figura 7: Acidocalcissomos em modelos de microrganismos não protozoários. **(A)** Preparação para microscopia eletrônica de transmissão da bactéria *R. rubrum*. A seta aponta um acidocalcissomo, a cabeça de seta aponta o remanescente de conteúdo eletrondenso após a preparação para microscopia eletrônica de trasnmissão. Barra: 0,1 μm. **(B)** Organelas eletrondensas com acúmulo de fósforo e cálcio observadas em células inteiras de *Chalydomonas* e espectro de microanálise de raios-X evidenciando o acúmulo de fósforo e cálcio nestes compartimentos. Barra: 1 μm.
Imagens adaptadas de Seuferheld et al., 2003; Ruiz et al., 2004.

2- Objetivos:

O objetivo geral desta tese é caracterizar organelas similares a acidocalcissomos em ovos de diferentes espécies, e investigar as possíveis funções deste compartimento nos processos de embriogênese inicial em diferentes modelos biológicos.

Objetivos específicos:

→ Investigar a presença de acidocalcissomos nos ovos;

→ Investigar o conteúdo de elementos destas organelas;

→ Isolar ou enriquecer os acidocalcissomos;

→ Investigar o conteúdo de PoliP nestas organelas;

→ Localizar estas organelas nos ovos;

→ Investigar sua possível função em eventos de liberação de cálcio no ovos;

3- Material e Metodologias:

3.1. *Periplaneta americana*

O material e as metodologias empregadas na obtenção dos resultados utilizando o modelo *Periplaneta americana* estão descritos no tópico "Material and Methods" do artigo intitulado "Proton-pyrophosphatase and polyphosphate in acidocalcisome like vesicles from oocytes and eggs of *periplaneta americana*" (anexo I, página 26), oriundo dos resultados experimentais obtidos durante o desenvolvimento desta tese. Neste trabalho as organelas extraídas dos ovos foram submetidas a diferentes técnicas de microscopia eletrônica e de fluorescência. Além disso, os níveis de PoliP foram detectados (a partir de ensaios enzimáticos uilizando uma exopolifosfatase recombinante), e este polímero foi localizado utilizando DAPI como sonda para microscopia de fluorescência.

3.2. *Rhodnius prolixus*

O material e as metodologias empregadas nos resultados obtidos utilizando o modelo *Rhodnius prolixus* estão descritos no tópico "Material and Methods" do manuscrito submetido intitulado "Acidocalcisomes are important calcium-storage compartments in eggs of the insect *Rhodnius prolixus* Stahl", anexado à página 36 (Anexo II). Neste modelo, as organelas extraídas dos ovos foram submetidas a diferentes técnicas de microscopia eletrônica (rotina e microanálise de raios-X) e de fluorescência. Técnicas de fracionamento subcelular foram utilizadas para isolar as organelas similares aos acidocalcissomos dos ovos. Técnicas de quantificação de elementos (espectrometria de emissão óptica e microanálise de raios-X semi-quantitativa) foram utilizadas para estimar a contribuição dos acidocalcissomos no estoque de elementos inorgânicos dos ovos. Por último, os níveis de PoliP foram detectados em ovos ao longo da embriogênese inicial.

3.3. *Arbacia punctulata e Lytechinus variegatus*

O material e as metodologias empregadas nos resultados obtidos utilizando os modelos *Arbacia punctulata e Lytechinus variegatus* estão descritos no tópico "Material and Methods" do artigo intitulado "Calcium and polyphosphate-containing acidic granules of sea urchin eggs are similar to acidocalcisomes but are not the targets for NAADP", anexado à página 71 (Anexo III). Em ovos de ouriços, a presença dos acidocalcissomos foi detectada a partir de experimentos similares aos citados anteriormente para os insetos (microscopia eletrônica analítica, técnicas de fluorescência, fracionamento subcelular, etc). Porém, a presença e localização de PoliP foram detectadas utilizando alguns ensaios adicionais: ressonância magnética e localização com um domínio recombinante específico da exopolifosfatase de levedura. Técnicas de fluorimetria, utilizando marcadores fluorescentes sensíveis a Ca^{2+}, também foram utilizadas na investigação da participação dos acidocalcissomos em eventos de liberação de Ca^{2+} sinalizados por NAADP.

3.4. *Gallus gallus*

O material e as metodologias empregadas nos resultados obtidos utilizando o modelo *Gallus gallus* estão descritos no tópico "Material and Methods" do artigo intitulado "Calcium and polyphosphate-containing acidocalcisomes in chicken egg yolk" anexado à página 86 (Anexo IV). Os acidocalcissomos foram novamente detectados a partir de técnicas de microscopia, e os níveis (medidos em ensaios com a exopolifosfatase) e padrões de tamanho (em géis de agarose corados por DAPI ou azul de toluidina) de PoliP foram investigados durante a embriogênese inicial.

4- Resultados:

4.1. *Periplaneta americana*

Os resultados referentes aos experimentos realizados utilizando como modelo a *P. americana* estão mostrados no artigo a seguir (página 26, anexo I), oriundo dos resultados experimentais obtidos durante o desenvolvimento desta tese.

Nesta primeira parte do trabalho, nós descrevemos a presença de organelas eletrondensas, com marcação imunoreativa para anticorpos contra a H^+-PPase vacuolar, atividade PPásica associada a preparações de membranas e acúmulo de PoliP. Por isso, estes compartimentos foram sugeridos como organelas sismilares aos acidocalcissomos em ovos deste inseto.

4.2. *Rhodnius prolixus*

Os resultados obtidos utilizando o modelo *Rhodnius prolixus* estão mostrados no manuscrito a ser submetido, anexado à página 36 (Anexo II), oriundo dos resultados experimentais obtidos durante o desenvolvimento desta tese.

Neste modelo, organelas eletrondensas similares às decritas acima para a *P. americana* também foram encontradas. A partir de fracionamento subcelular, uma fração enriquecida em acidocalcissomos foi obtida. Quantificações de elementos evidenciaram que aproximadamente 25 % do cálcio detectado nos ovos se encontra na fração dos acidocalcissomos. Durante a embriogênese inicial, foi visto que os acidocalcissomos são acidificados no dia 3 (coincidente com o início da degradação de proteínas de vitelo), e os níveis de PoliP nestas organelas são diminuídos. A possível participação dos acidocalcissomos na homeostase de cálcio e fósforo neste sistema é discutida.

4.3. *Arbacia punctulata e Lytechinus variegatus*

Os resultados obtidos utilizando os modelos *Arbacia punctulata e Lytechinus variegatus* estão mostrados no artigo anexado à página 71 (Anexo III), oriundo dos resultados experimentais obtidos durante o desenvolvimento desta tese.

Neste modelo, organelas eletrondensas similares às decritas para os insetos também foram encontradas. Porém, a presença de PoliP foi detectada pela primeira vez, e esse polímero foi localizado nos acidocalcissomos. A participação dos acidocalcissomos em eventos de liberação de Ca^{2+} via NAADP foi investigada, e os possíveis papéis destas organelas em ovos destes modelos são discutidos.

4.4. *Gallus gallus*

Os resultados obtidos utilizando o modelo *Gallus gallus domesticus* estão mostrados no artigo, anexado à página 86 (Anexo IV), oriundo dos resultados experimentais obtidos durante o desenvolvimento desta tese.

A presença de acidocalcissomos foi novamente detectada, a partir do uso das mesmas técnicas citadas acima, mas estas organelas foram encontradas em grupos de vesículas dentro de um compartimento único (organelas compostas). Foi observado também que os níveis de PoliP ao longo da embriogênese não são alterados, mas o comprimento das cadeias deste polímero é diminuído no primeiro dia de embriogênese.

5- Anexo I:

Insect Biochemistry and Molecular Biology 39 (2009) 198–206

Contents lists available at ScienceDirect

Insect Biochemistry and Molecular Biology

journal homepage: www.elsevier.com/locate/ibmb

Proton-pyrophosphatase and polyphosphate in acidocalcisome-like vesicles from oocytes and eggs of *Periplaneta americana*

Lucimar S. Motta [a,b,c,1], Isabela B. Ramos [a,d,1], Fabio M. Gomes [a], Wanderley de Souza [d], Donald E. Champagne [b,c], Marcelo F. Santiago [e], Roberto Docampo [b,c], Kildare Miranda [d,**], Ednildo A. Machado [a,*]

[a] *Laboratório de Entomologia Médica, Programa de Parasitologia e Biologia Celular, Instituto de Biofísica Carlos Chagas Filho (UFRJ), Brazil*
[b] *Center for Tropical and Emerging Global Diseases, Department of Entomology, University of Georgia, Athens, GA 30602, USA*
[c] *Center for Tropical and Emerging Global Diseases, Department of Cellular Biology, University of Georgia, Athens, GA 30602, USA*
[d] *Laboratório de Ultraestrutura Celular Hertha Meyer, Programa de Parasitologia e Biologia Celular, Instituto de Biofísica Carlos Chagas Filho (UFRJ), Brazil*
[e] *Laboratório de Neurobiologia Celular e Molecular, Programa de Terapia Celular e Bioengenharia, Instituto de Biofísica Carlos Chagas Filho (UFRJ), Brazil*

ARTICLE INFO

Article history:
Received 10 October 2008
Received in revised form
27 November 2008
Accepted 29 November 2008

Keywords:
Acidocalcisomes
Eggs
Oocytes
Proton-pyrophosphatase
Polyphosphate

ABSTRACT

Acidocalcisomes are acidic organelles containing large amounts of polyphosphate (poly P), a number of cations, and a variety of cation pumps in their limiting membrane. The vacuolar proton-pyrophosphatase (V-H^+-PPase), a unique electrogenic proton-pump that couples pyrophosphate (PPi) hydrolysis to the active transport of protons across membranes, is commonly present in membranes of acidocalcisomes. In the course of insect oogenesis, a large amount of yolk protein is incorporated by the oocytes and stored in organelles called yolk granules (YGs). During embryogenesis, the content of these granules is degraded by acid hydrolases. These enzymes are activated by the acidification of the YG by a mechanism that is mediated by proton-pumps present in their membranes. In this work, we describe an H^+-PPase activity in membrane fractions of oocytes and eggs of the domestic cockroach *Periplaneta americana*. The enzyme activity was optimum at pH around 7.0, and was dependent on Mg^{2+} and inhibited by NaF, as well as by IDP and Ca^{2+}. Immunolocalization of the yolk preparation using antibodies against a conserved sequence of V-H^+-PPases showed labeling of small vesicles, which also showed the presence of high concentrations of phosphorus, calcium and other elements, as revealed by electron probe X-ray microanalysis. In addition, poly P content was detected in ovaries and eggs and localized inside the yolk granules and the small vesicles. Altogether, our results provide evidence that numerous small vesicles of the eggs of *P. americana* present acidocalcisome-like characteristics. In addition, the possible role of these organelles during embryogenesis of this insect is discussed.

© 2008 Elsevier Ltd. All rights reserved.

1. Introduction

Periplaneta americana, the domestic cockroach, is among the largest of the peridomestic cockroaches found in urban environments. It has worldwide distribution, is a potential carrier of a wide variety of pathogenic organisms, and is considered for this reason a public health problem (Rust et al., 1991). The understanding of the mechanisms underlying the reproductive processes of this insect could provide useful information for their population control and reduction of pathogen dissemination.

Oogenesis in insects, as in all oviparous animals, occurs by incorporation of yolk protein through receptor-mediated endocytosis (Raikhel and Dhadialla, 1992). Once inside the oocytes, the yolk proteins are stored in organelles known as yolk granules (YGs) (Kunkel and Nordin, 1985; Purcell et al., 1988). At the end of vitellogenesis (the period of massive uptake of yolk proteins during oogenesis) the YGs fill almost the entire volume of the oocytes and later, during embryogenesis, the stored yolk proteins are mobilized and for this reason are considered as the main amino acid source for embryo development.

Yolk mobilization starts when the yolk proteins undergo a process of degradation, which occurs by activation of acid hydrolases also stored within YGs. To activate hydrolases, YGs undergo a process of acidification mediated by proton-pumps such as the proton ATPase (H^+-ATPase) (Fagotto, 1991; Nordin et al., 1991; Mallya et al., 1992; Fagotto, 1995) and a proton-pyrophosphatase

* Corresponding author. Tel.: +55 21 2562 6589; fax: +55 21 2280 8193.
** Corresponding author. Tel.: +55 21 2562 6593; fax: +55 21 2260 2364.
E-mail addresses: kmiranda@biof.ufrj.br (K. Miranda), ednildo@biof.ufrj.br (E.A. Machado).
[1] These authors contributed equally to this work.

0965-1748/$ – see front matter © 2008 Elsevier Ltd. All rights reserved.
doi:10.1016/j.ibmb.2008.11.003

(H^+-PPase) (Motta et al., 2004). In insects, several hydrolytic enzymes found in YGs such as cathepsins (Takahashi et al., 1996; Cho et al., 1999) and acid phosphatases (Ribolla et al., 1993; Fialho et al., 2002, 2005; Oliveira and Machado, 2006) were shown to be activated by low pH. In addition, it has recently been reported that calcium-modulated fusion of different YGs might also be important for yolk degradation (Ramos et al., 2006, 2007). Acidification of YGs, therefore, results in activation of hydrolases and subsequent degradation of the yolk proteins. This process is widely conserved within oviparous animals, being essential for yolk mobilization during embryo development.

It is generally accepted that the vesicle population inside the eggs is not homogeneous. In several species YGs can be fractionated according to their different size and density (Fagotto, 1991; Chestkov et al., 1998; McNeil et al., 2000; Yamahama et al., 2003). In the stick insect *Carausius morosus*, the pro-proteases are restricted to an YG population different from the one that contains the active enzyme (Fausto et al., 2001). In the silk moth *Bombyx mori*, the acid hydrolases are only present in the small YGs whereas the yolk storage proteins are localized in the large ones (Yamahama et al., 2003). It has also been shown, for different species, that small granules are mainly distributed in the peripheral cytoplasm of the mature egg. In this region the vesicles are preferentially acidified, and this process is involved in yolk mobilization (Reimer and Crawford, 1995; Abreu et al., 2004). However, the origin or possible roles of these differences remain unknown.

H^+-PPases are electrogenic proton-pumps distributed among land plants, algae, protists, bacteria, and archaea. These enzymes couple pyrophosphate (PPi) hydrolysis to active proton transport across membranes, being commonly described as taking part in acidification of intracellular stores, as an alternative to ATP driven proton transport (Maeshima, 2000). The H^+-PPases were recently divided into two main types, based on their kinetic parameters of activity. Type I H^+-PPases are strongly dependent on K^+ and moderately sensitive to inhibition by Ca^{2+}. In contrast, type II H^+-PPases are independent of K^+ and highly sensitive to Ca^{2+}. Both types are inhibited by aminomethylenediphosphonate, imidodiphosphate (IDP), and high concentrations of fluoride (NaF), and are active only in the presence of Mg^{2+} (McIntosh et al., 2001). H^+-PPases have been found in acidocalcisomes of parasites such as *Trypanosoma cruzi* (Scott et al., 1998), *Leishmania* spp. (Miranda et al., 2004) and *Plasmodium falciparum* (Ruiz et al., 2004). An apparently vacuolar-type H^+-PPase was detected in rat liver Golgi fractions (Brightman et al., 1992) although there is no evidence that the enzyme is similar to the plant, algal, protists or bacterial enzymes since no homologous genes are present in animals. In addition, a K^+-insensitive H^+-PPase activity (type II) was recently described in eggs of the insect *Rhodnius prolixus* (Motta et al., 2004), although the gene encoding this enzyme has not yet been identified.

Acidocalcisomes are acidic organelles found in several microorganisms. They are characterized by their acidic nature, high electron density and high content of polyphosphate (poly P) and several cations. They are involved in several functions, including storage of cations, calcium homeostasis, osmoregulation and poly P metabolism (Docampo and Moreno, 2001; Docampo et al., 2005). Acidocalcisomes have a variety of cation pumps such as Ca^{2+}/H^+ ATPase, H^+ pumps such as the vacuolar H^+-ATPase and H^+-PPase, and a number of exchangers in their limiting membrane. They contain large amounts of cellular magnesium, sodium, phosphorus, potassium, calcium, iron and zinc. In several species, the H^+-PPase has been considered a marker for this organelle (Ruiz et al., 2001; Docampo et al., 2005). Although better described in protist species, acidocalcisomes have also been found in several other organisms and cell types, including bacteria (Seufferheld et al., 2003), the green algae *Chlamydomonas reinhardtii* (Ruiz et al., 2001), the slime mold *Dictyostelium discoideum* (Marchesini et al., 2002) and human platelets (Ruiz et al., 2004), having been conserved during evolution, as recently reviewed by Docampo et al. (2005).

In this work we report the biochemical characterization of a PPi-dependent proton uptake and a PPase activity in membrane fractions from ovaries and eggs of the insect *P. americana*. The PPi-dependent proton uptake activity was found in small vesicles and shown to be involved in their acidification. Immunofluorescence using antibodies against a conserved sequence of *Arabidopsis thaliana* H^+-PPase, showed labeling in small vesicles. X-ray microanalysis showed that several of these small vesicles have an elemental composition similar to that previously described for acidocalcisomes. In addition, enzymatic assays and 4′,6-diamidino-2-phenylindole (DAPI) staining suggested that they might be involved in poly P storage. Together, the results reveal new aspects of early embryogenesis in *P. americana*, and the potential involvement of a novel organelle in yolk mobilization.

2. Material and methods

2.1. Insects

Insects were taken from a colony of *P. americana* maintained at room temperature and 65 ± 5% relative humidity. Animals were fed with dog chow and water *ad libitum*. To obtain the ovaries, adult mated females were dissected under a stereoscopic microscope. Oothecae were collected from polypropylene plates or Styrofoam sheets present inside the jars where adults were kept. Day 0 oothecae were collect up to 24 h after its deposition.

2.2. Membrane fractions and pyrophosphatase (PPase) activity

Membrane associated PPase activity was detected using chorionated oocytes dissected from ovarian tissues. Membrane fractions were prepared by differential centrifugation, as previously described by Motta et al. (2004), and the protein concentration was determined by the method of Lowry et al. (1951). PPase activity, was measured by detecting Pi release from PPi by the method of Fiske and Subbarow (1925), using a microplate reader. The reaction medium contained 100 mM KCl, 0.3 mM PPi, 0.6 mM $MgCl_2$ and 50 mM MOPS–Tris pH 7.5. Reactions were started by the addition of membrane fractions (40 μg protein/ml final concentration) and stopped by the addition of 50% w/v trichloroacetic acid after 1 h at 28 °C. Blank reactions were performed using inactivated (boiled) membrane fractions, to assure that contaminant Pi from added PPi or membrane preparations was excluded from activity measurements and to monitor possible spontaneous hydrolysis of PPi. The enzyme was not a general phosphatase since *p*-nitrophenylphosphate (pNPP) was not significantly hydrolyzed (data not shown). To determine the optimum pH, the activities were assayed in media containing 50 mM buffer, 0.6 mM $MgCl_2$, 0.3 mM PPi and 100 mM KCl. For pH 5.0–7.5, MOPS–Tris was utilized as buffer. At pH 8.0 MOPS–Tris was replaced by glycylglycine. To determine the magnesium dependence, activities were assayed in a medium containing 50 mM MOPS–Tris (pH 7.5), 0.3 mM PPi, 100 mM KCl and different concentrations of $MgCl_2$. The effects of $CaCl_2$ and NaF were measured in the presence of 50 mM MOPS–Tris (pH 7.5), 0.3 mM PPi, 100 mM KCl and 0.6 mM $MgCl_2$. The effects of IDP were measured in the presence of 50 mM MOPS–Tris (pH 7.5), 0.3 mM PPi, 100 mM KCl and 0.6 mM $MgCl_2$.

2.3. Preparation of yolk granule fractions (YGFs)

Day 0 oothecae were gently disrupted, using a plastic pestle, in a modified cockroach saline solution (Blagburn and Sattelle, 1987). The sample was homogenized, allowed to rest for 30 s and

a protease inhibitor cocktail (2 mM AEBSF, 130 μM bestatin, 14 μM E64, 1 mM leupeptin, 0.3 μM aprotinin) was added to the supernatant. This mixture was used as YGF.

2.4. Proton uptake

PPi-driven H^+ uptake by the egg vesicles was assayed by measuring changes in the absorbance of acridine orange (AO) (A_{493}–A_{530}) in an Olis-modified SLM–Aminco DW 2000 dual wavelength spectrophotometer (Palmgren, 1991; Scott and Docampo, 1998). YGFs extracted from 3-day-old oothecae were resuspended in a reaction medium containing 130 mM KCl, 2 mM $MgCl_2$, 50 μM EGTA and 10 mM HEPES pH 7.2. AO (3 μM), 0.2 ml of YGF, 0.3 mM PPi and 10 mM NH_4Cl were added where indicated.

2.5. Western blot analysis and immunolocalization of H^+-PPase

Anti-H^+-PPase polyclonal antibodies were raised against KLH-conjugated synthetic peptides corresponding to the hydrophilic loops IV and XII of plant H^+-PPase (Motta et al., 2004). Membrane fractions were prepared and protein concentrations were determined by the method of Lowry et al. (1951). Twenty micrograms of protein was submitted to 10% SDS-PAGE (Laemmli, 1970) and the gel was electro-transferred to a nitrocellulose membrane. The membrane was incubated in blocking buffer containing 10 mM Tris, 150 mM NaCl, 3% bovine serum albumin (BSA) (w/v), and 0.1% tween (v/v) for 2 h. The sample was then incubated for 3 h with the primary antibody diluted 1:1000, followed by incubations with goat anti-rabbit antibody conjugated with alkaline phosphatase (1:1000). For immunolocalization, YGFs were fixed in 4% paraformaldehyde for 30 min and washed twice at room temperature. The sample was allowed to adhere to ethylenimine-coated coverslips and incubated for 30 min in blocking buffer (1.5% BSA, 0.5% fish gelatin and 0.02% tween diluted in TBS). The material was then incubated for 1 h with the primary antibody diluted 1:500, followed by incubations with goat anti-rabbit antibody associated with fluorescein (1:150). Immunofluorescence images were obtained using a Zeiss Axioplan epifluorescence microscope.

2.6. Imaging of vesicle acidification

Day 0 YGF was incubated in the presence of 5 μg/ml acridine orange (AO) for 10 min. PPi was added at a final concentrations of 0.3 mM directly to the glass slides right before sample observation. Fluoride (NaF) treatments were done by pre-incubation in the presence of 1 mM of this compound prior to incubations with AO. Samples were observed in a Zeiss LSM310 Confocal Microscope equipped with an argon laser.

2.7. X-ray microanalysis

Fresh oothecae were squeezed in a microtube, washed and resuspended in 0.25 M sucrose. Droplets were applied to formvar-coated copper grids and blotted dry with a filter paper. For *Leishmania amazonensis*, whole unfixed cells were dried onto formvar-coated grids. Samples were examined in a JEOL 1200 EX transmission electron microscope. X-rays were collected for 300 s using a Si (Li) detector with Norvar window on a 0–10-KeV energy range with a resolution of 10 eV/channel. Analyses were performed using a Noran/Voyager III analyzer.

2.8. Polyphosphate (poly P) content

Long and short chain poly Ps were extracted using the content of a single ovary or a fresh ootheca. Long chain and short chain poly P extractions were performed as described by Ault-Riche et al. (1998) and Ruiz et al. (2001), respectively. The principal differential extractions are that long chain poly P is first extracted by lysis and then bound to powdered glass (Glassmilk from Bio 101 Inc, La Jolla, CA) by addition of ethanol. Poly P is eluted from the glass with hot water. Under these conditions, smaller poly P polymers do not bind to Glassmilk. To obtain short chain poly P, samples are extracted with $HClO_4$ followed by neutralization using KOH and $KHCO_3$. After centrifugation, shorter chain poly Ps remain in the supernatant. Poly P levels were determined from the amount of Pi released upon treatment with an excess recombinant exopolyphosphatase (rPPX) as described by Ruiz et al. (2001).

2.9. Localization of poly P

YGF was incubated at room temperature with 50 μg/ml of the fluorescent dye DAPI for 20 min. Samples were mounted on glass slides and observed in a Zeiss LSM510 Confocal Microscope META at an excitation wavelength of 458 nm and emission filtered lower than 475 nm.

3. Results

3.1. Biochemical characterization of membrane-bound PPase

Membrane fractions of chorionated oocytes of *P. americana* were obtained and tested for PPase activity. Fig. 1A shows that PPi hydrolysis was sensitive to variations in pH. Although considerable activity could be detected in slightly acid and alkaline pH, PPi hydrolysis was optimal in the pH range of 7.0–7.5. Fig. 1B shows Mg^{2+} dependence of the PPase activity. No PPi hydrolysis was detected in the absence of this cation and its maximum activity was obtained in the presence of 5 mM Mg^{2+}. PPase activity was significantly inhibited by Ca^{2+} (Fig. 1C), and by NaF (Fig. 1D). PPase activity was also shown to be K^+-insensitive (data not shown). In addition, Fig. 1E shows the effect of IDP (a nonhydrolyzable analog of PPi) on PPase activity. To investigate the pattern of inhibition of this compound, PPase activity was measured in three different PPi concentrations. When PPi concentration in the medium was adjusted to 0.05 mM, the enzyme was totally inhibited by 0.5 mM IDP. On the other hand, the same concentration of IDP only decreased the enzyme activity by 70% and 50% when PPi concentration in the medium was increased to 0.15 mM and 0.3 mM, respectively.

3.2. PPi-driven proton uptake

PPi-driven H^+ transport in YGFs was detected in a dual wavelength spectrophotometer using acridine orange (AO) as a probe. A decrease in absorbance indicates compartment acidification. Addition of AO to the cuvette was followed by a decrease in absorbance, indicative of an endogenous acidity of the egg vesicles (Fig. 2). Addition of 0.3 mM PPi induced a further decrease in absorbance, indicative of PPi-dependent acidification of YG, and 10 mM NH_4Cl completely collapsed the H^+ gradient formed across YG membrane (black trace). In the control groups (without PPi additions), no changes in the AO absorbance values were observed (gray trace).

3.3. Visualization of acidic compartments

Day 0 YGF was incubated with AO in the presence or absence of PPi and observed by fluorescence microscopy. This compound has been proved to be a reliable probe, both for spectrophotometric measurements and microscopic visualization of intracellular acidic

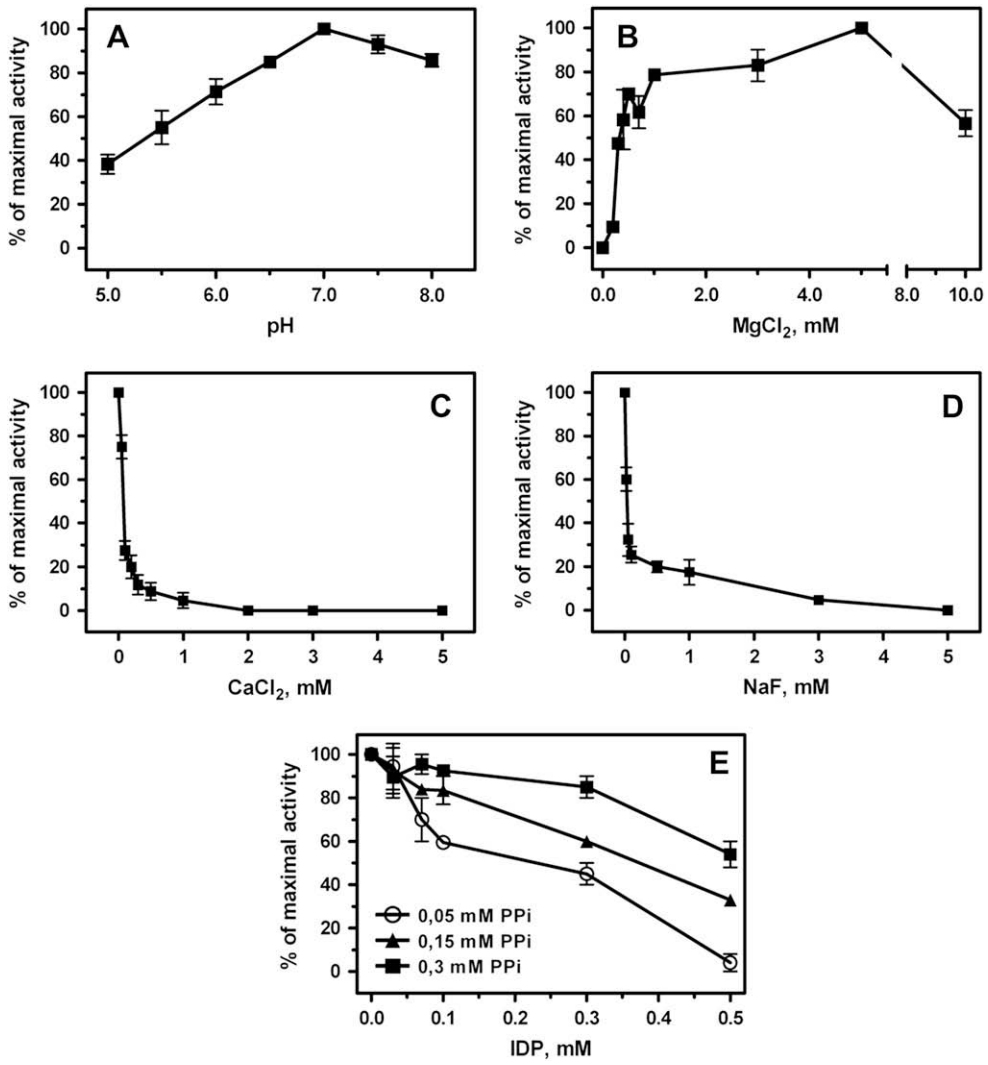

Fig. 1. Membrane-bound pyrophosphatase activity of oocytes. Preparations of membrane fractions were obtained from chorionated oocytes and aliquots were assayed for pyrophosphatase (PPase) activity at different pH values (A), and in medium containing different concentrations of $MgCl_2$ (B), $CaCl_2$ (C), NaF (D), or IDP, in three different PPi concentrations: 0.05 mM (*open circles*), 0.15 mM (*closed triangles*) and 0.3 mM (*closed squares*) (E).

compartments, including early endosomes, late endosomes and lysosomes (Anderson and Orci, 1988). Incubation of YGF in the absence of PPi showed no accumulation of AO (Fig. 3A–C) whereas the material incubated in the presence of 0.3 mM PPi showed red–orange staining in several small vesicles with a diameter <1 μM (4 ± 3 labeled vesicles/field, ~6.8% of total small vesicles, from 10 observed fields for each experiment) (Fig. 3D–F, arrows). Pre-incubation of YGF with 10 mM NaF prevented the acidification of the vesicles, as shown in Fig. 3G–I.

3.4. Western blot analysis and immunolocalization of H^+-PPase

To investigate whether the activity detected in the previous experiments was preferentially located in the small vesicles, polyclonal antibodies raised against a peptide sequence of *A. thaliana* H^+-PPase, which was previously shown to cross-react with the H^+-PPase of several trypanosomatids (Scott and Docampo, 1998; Miranda et al., 2004; Soares Medeiros et al., 2005; Moraes Moreira et al., 2005) and with YGs of the insect *R. prolixus* (Motta et al., 2004), were used and the material was tested by western blot analysis and immunofluorescence microscopy. Fig. 4A shows that

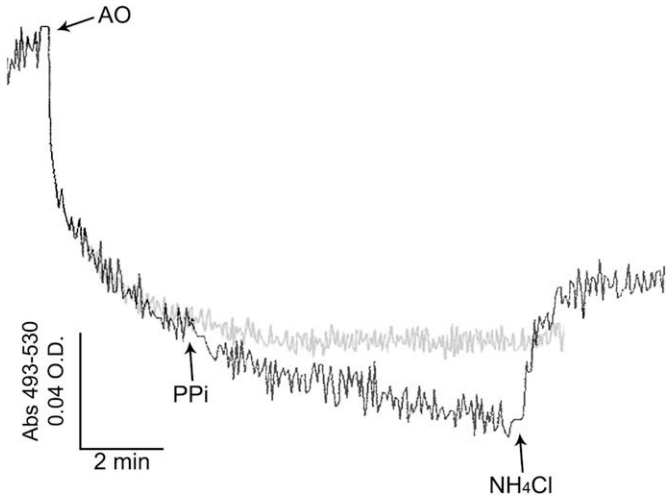

Fig. 2. PPi-driven proton uptake in YGs. Aliquots of YGF were obtained and incubated with 3 μM AO. PPi (0.3 mM) and 10 mM NH_4Cl were added where indicated (arrows). Control, without any further addition, is shown as the gray tracing. Traces are representative of four different experiments.

the anti-H^+-PPase antibody recognizes a single protein of approximately 65 kDa in the oocyte membranes, and results of immunofluorescence experiments showed a positive reaction in small vesicles ($\leq$5 μM) (Fig. 4B–G, arrows) whereas no labeling could be observed in large YGs (Fig. 4B–G, arrowheads).

3.5. Elemental composition of small vesicles

To study the elemental composition of the small vesicles previously shown to contain the H^+-PPase activity, YGF dried onto formvar-coated grids was observed and submitted to electron probe X-ray microanalysis. Several small vesicles (approximately 500 nm in diameter) showed an electron density similar to what has been previously observed for acidocalcisomes in trypanosomatids and apicomplexan parasites (Fig. 5A). Analysis of these vesicles showed considerable amounts of oxygen, sodium, magnesium, phosphorus and calcium concentrated in their matrix (Fig. 5B). Low signals of sulfur, chloride, potassium and iron were recorded. Higher concentrations of sulfur were found when the electron beam was focused onto large YGs (data not shown). All spectra taken from different samples were qualitatively equivalent to those described for acidocalcisomes of several organisms, as exemplified by *L. amazonensis* in Fig. 5C and D.

3.6. Poly P content

To investigate whether the phosphorus content previously detected by X-ray microanalysis was stored in the form of poly P, as occurs in acidocalcisomes of several microorganisms (Docampo et al., 2005), ovaries and eggs were submitted to poly P extraction and poly P was quantified by treatment with an excess of a recombinant exopolyphosphatase. Fig. 6 shows the detection of long and short chain poly Ps in both ovaries and oothecae of *P. americana*. It was observed that there was approximately six times more short chain than long chain poly P stored in both ovaries and eggs of *P. americana*. Poly P content was also localized by fluorescence microscopy in DAPI stained samples according to the procedure described by Tijssen et al. (1982) and Ruiz et al. (2001). Fluorescence emission of DAPI shifts to a longer wavelength (to 525 nm) when it binds to poly P, giving a green–yellow emission color in poly P-containing structures. As seen on Fig. 7, poly P was present in the small vesicles observed (Fig. 7A and arrows in the inset) and not in YGs larger than 5 μM.

4. Discussion

It is generally accepted that, in insects, yolk mobilization inside the eggs occurs during early embryogenesis. In this process the yolk proteins undergo proteolysis triggered by activation of latent pro-

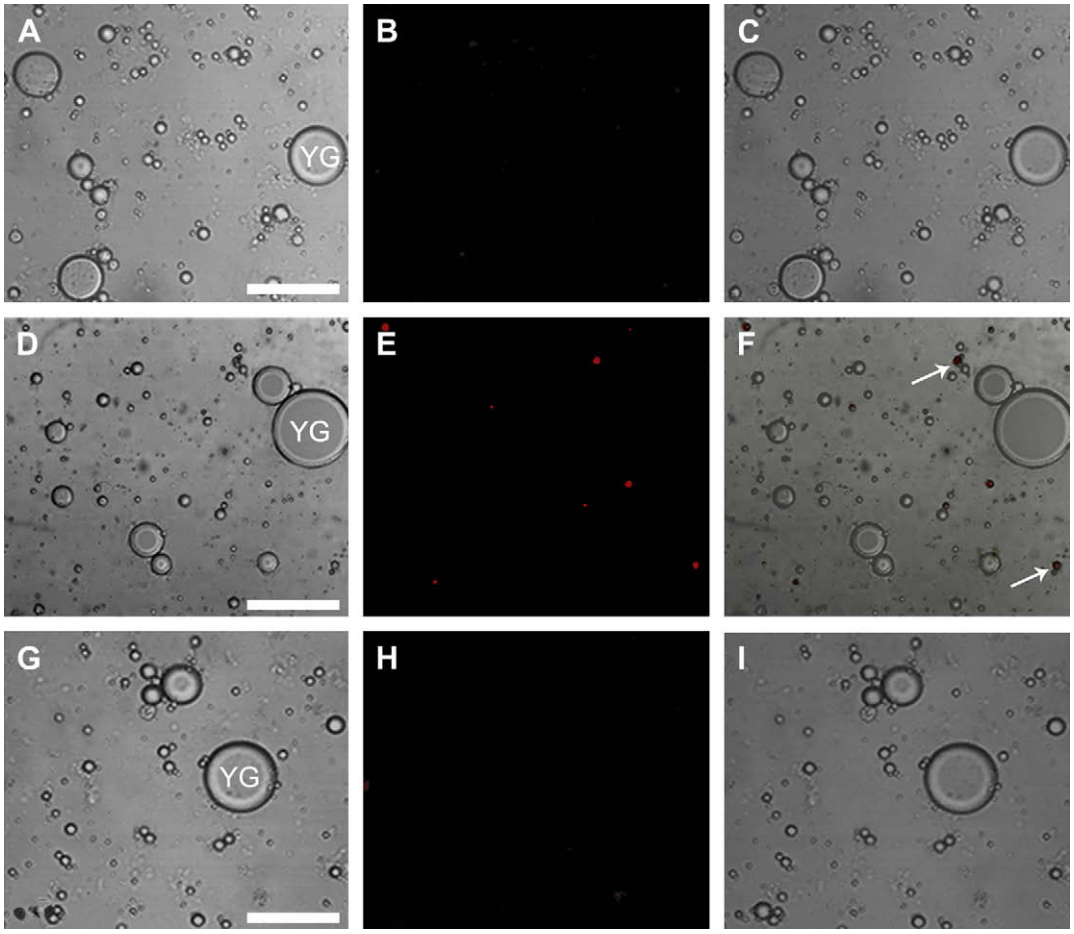

Fig. 3. PPi-driven acidification of small vesicles. Day 0 YGF was prepared and incubated with 5 μg/ml AO in the presence or absence of PPi. (A–C): Samples were incubated with AO only, without PPi. (D–F): Samples incubated with AO and PPi (0.3 mM). (G–I): Samples pre-incubated with 10 mM NaF and subsequently incubated with AO and PPi (0.3 mM). (A), (D) and (G) are phase contrast micrographs. (B), (E) and (H), corresponding fluorescence images of the left panel. (C), (F) and (I), overlay between phase contrast and fluorescence images. Arrows indicate acid small vesicles. The results are representative of three different experiments. YG: yolk granule. Bars: 15 μM.

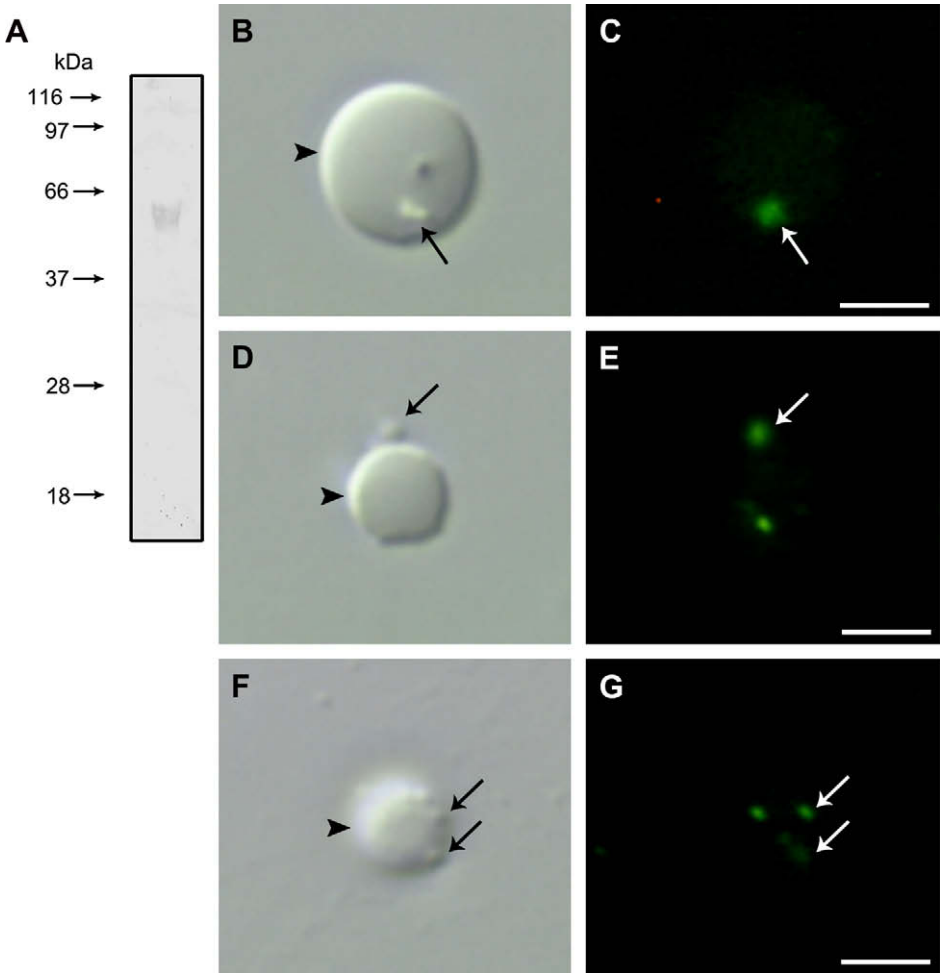

Fig. 4. Western blot analysis and immunolocalization of H^+-PPase in small vesicles. Membrane fractions and YGF were prepared for western blot analysis and immunolocalization, respectively, with polyclonal antibodies raised against a peptide sequence of H^+-PPase of *A. thaliana*. (A): Western blot analysis of H^+-PPase in membrane fractions of oocytes. (B), (D) and (F): Differential interference contrast of YGF and (C), (E) and (G) their corresponding fluorescence images. Arrows indicate labeled small vesicles, and arrowheads indicate larger YG. The images are representatives of three different experiments. Bars: 5 μM.

proteases (Fagotto, 1990; Nordin et al., 1991). Activation of these enzymes is achieved by luminal acidification of YGs, a process that is mediated by proton-pumps (Fagotto, 1991; Nordin et al., 1991; Mallya et al., 1992; Fagotto, 1995). Acidification of YGs was exclusively attributed to H^+-ATPases and H^+ exchangers (Fagotto and Maxfield, 1994), until the characterization of an H^+-PPase activity present in YGs of the insect *R. prolixus* by Motta et al. (2004). In the present work we showed that oocytes and eggs of the cockroach *P. americana* also posses an H^+-PPase activity and that this enzyme is differentially localized in small vesicles present in the egg cytoplasm.

Our results demonstrated that the membrane-bound PPase activity from chorionated oocytes has several characteristics similar to those of H^+-PPases from plants, bacteria, protists, and the insect *R. prolixus* (Maeshima, 2000; Motta et al., 2004). Nevertheless, some differences in the biochemical properties of H^+-PPases from the insects *P. americana* and *R. prolixus* were observed (Motta et al., 2004). The activity from *Periplaneta* is less sensitive to pH shifts when compared to the enzyme from *Rhodnius*, but is more affected by NaF and IDP. Differences in kinetic properties of H^+-PPases from different organisms have been already observed for trypanosomatids. It is possible that those differences might be associated to species-specific characteristics (Rodrigues et al., 1999a, b; Soares Medeiros et al., 2005; Moraes Moreira et al., 2005). The idea that H^+-PPases represent alternative ways to generate proton electrochemical gradients across the membrane of organelles during germination in plant models has been extensively discussed (Maeshima, 2000). In this system, during the massive anabolic activity in the course of germination, ATP is utilized in different reactions, whereas PPi is being produced in a subset of these reactions (Rea et al., 1992). It is possible that similar reactions could occur during insect embryo development, since this is a process that involves massive synthesis and degradation of macromolecules, including nucleic acids and proteins. In particular, acidification of specific compartments in the egg yolk system is especially important to allow activation of hydrolases and yolk mobilization. Acidification of the egg compartments is therefore indispensable for proper development of the embryo and the existence of an alternative proton-pump such as the H^+-PPase in this context seems to be functionally significant.

Our findings indicate that the H^+-PPase of *P. americana* eggs is preferentially located in small vesicles, and is capable of accomplishing the acidification of these compartments. Several groups have suggested that differential acidification is the signal that triggers yolk mobilization, and that differential activation of proton-pumps in different egg compartments might be an effective form of regulating the time course of yolk degradation during early embryogenesis. It is important to note that the H^+-PPase from day

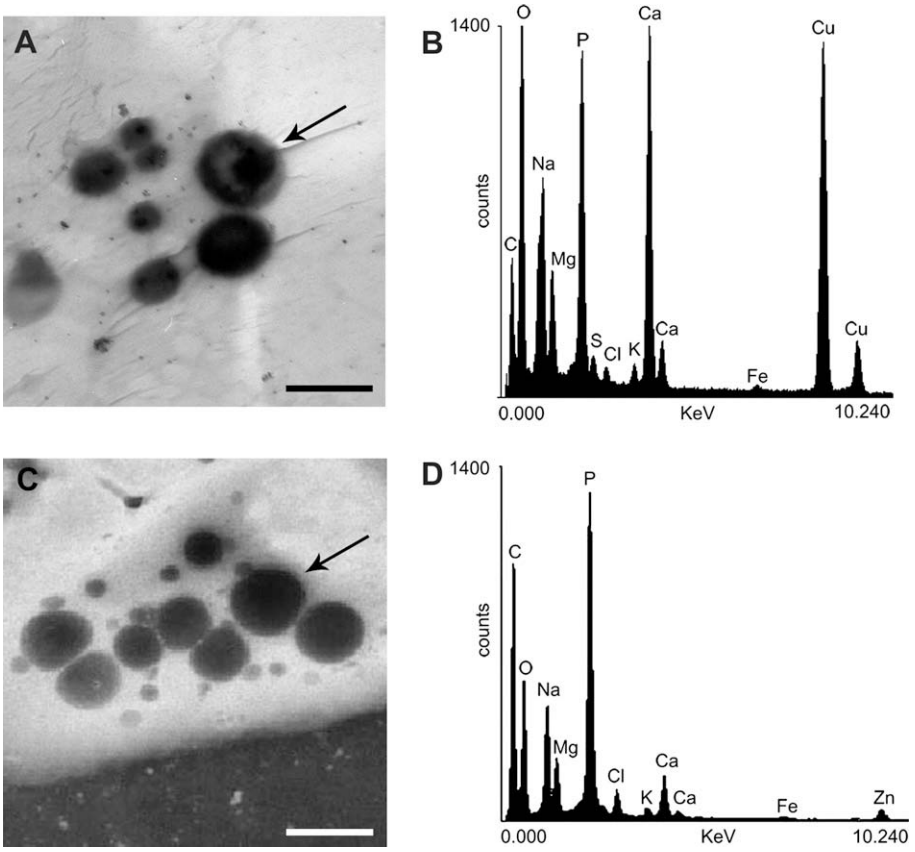

Fig. 5. TEM and X-ray microanalysis of small vesicles and acidocalcisomes. YGF was mounted on copper grids and submitted to elemental X-ray microanalysis. (A): Transmission electron micrograph of whole mount small vesicles adhered to formvar-coated grids. (B): X-ray microanalysis spectrum of the vesicle pointed in (A, black arrow). Cu peaks came from the grid. Spectrum is representative of three different experiments where at least 10 spectra were taken. (C): Transmission electron micrograph of whole unfixed *Leishmania amazonensis* promastigotes adhered to formvar-coated grids. (D): X-ray microanalysis spectrum of the acidocalcisome pointed in (C, black arrow). Bars: 500 nm.

0 eggs of *R. prolixus* is also localized in large YG (Motta et al., 2004), in contrast to what was observed here in *P. americana*. In these insects, a calcium-regulated process of membrane fusion of egg vesicles during early embryogenesis has been described and the transfer of H^+-PPase from small vesicles to large YGs has been suggested (Ramos et al., 2006, 2007). Total developmental periods for the two insects are different (12 days for *R. prolixus* compared to 31 days for *P. americana*), and day 0 eggs for each model are not in the same period of embryogenesis. Thus, different patterns of H^+-PPase localization in both insects may reflect different stages and rates of embryonic development.

In addition, the presence of compartments specialized in the storage of cations points to another interesting mechanism to modulate the H^+-PPase activity during early embryogenesis. A viable possibility is that the balance between free Ca^{2+} and free Mg^{2+} in the egg cytoplasm might control the H^+-PPase activity, indirectly influencing the acidification of compartments. In plants, Mg^{2+} has been proposed as a possible fine regulator of the H^+-PPase activity during embryogenesis (Leigh et al., 1992).

The elemental composition of the small vesicles was very similar to that of acidocalcisomes of several organisms (reviewed in Docampo et al., 2005). Because all egg vesicles are conventionally described as YGs, and YGs are defined as compartments that store yolk proteins, we expected to detect high traces of sulfur (a protein marker) in our samples. However, in a variety of small vesicles analyzed, high amounts of cations were found and sulfur was absent or detected in very low concentrations, indicating that these compartments might have functions other than protein storage. On the other hand, X-ray analyses of larger YGs detected high concentrations of sulfur, as expected. These data further support the idea that the vesicle population inside the egg is not homogeneous and might have different roles in yolk mobilization during embryogenesis. The egg is an isolated system, which, once laid by the female, is able to accomplish embryo development using only the elements that were previously stored during oogenesis. Much is

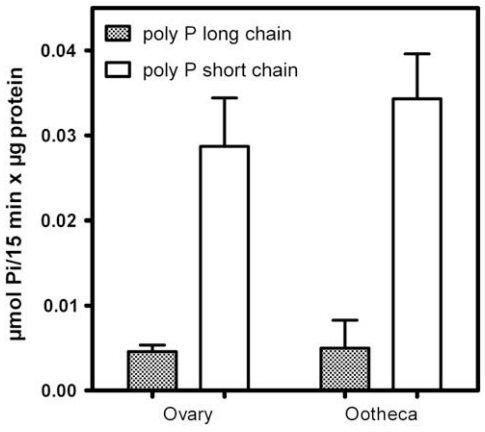

Fig. 6. Poly P quantification in ovaries and eggs. The whole contents of ovaries and oothecae were submitted to different extractions to obtain long and short chain poly P. *Closed columns* show the amount of Pi released after 15 min of incubation of long chain poly P preparations with rPPX. *Open columns* represent these same values obtained from short chain poly P preparations. The figure is shown with the mean ± SD of four different experiments.

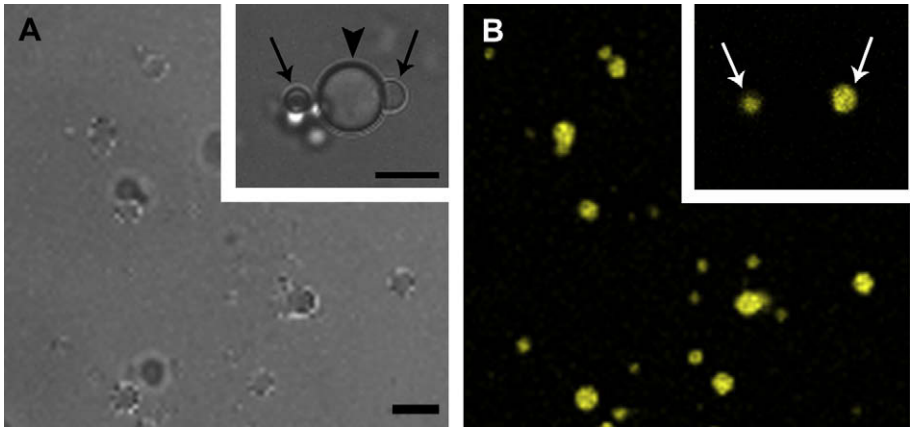

Fig. 7. Localization of poly P in yolk granules and small vesicles. To localize poly P, YGF was prepared and incubated with DAPI. Image (A) shows the phase contrast micrograph corresponding to the fluorescence image (B). The inset shows DAPI labeling preferentially in small vesicles (arrows), and not in large YGs (arrowhead). The results are representative of three experiments and at least five fields per experiment were observed. Bars: 10 μM.

known about the storage of yolk proteins and lipids in the egg cytoplasm (Raikhel and Dhadialla, 1992; Ziegler and Van Antwerpen, 2006), but little is known about the storage of elements such as calcium, magnesium or phosphorus, which are also indispensable for development. Our finding that the insect eggs also contain vesicles apparently specialized in the storage of these elements is the first evidence of their storage inside eggs. In addition, the fact that the H^+-PPase activity could be detected in oocytes suggests that the small vesicles might be formed and stored inside the egg during oogenesis, as occur with the YGs and lipid droplets. Whether or not these organelles have a specific location inside the egg is still uncertain.

The demonstration of the existence of polymers involved with phosphorus storage inside insect eggs opens new perspectives for the understanding of the metabolism and homeostasis of this essential element. Up to now, the source of Pi in insect eggs has been attributed to phosphorylated proteins, such as vitellin, the major yolk protein present in YGs in vertebrates and invertebrates (Goulas et al., 1996; Salerno et al., 2002). Acidocalcisomes or acidocalcisome-like organelles are known to be implicated in several cellular functions (Docampo and Moreno, 2001; Docampo et al., 2005). The accumulation of poly P in acidocalcisomes has been shown to be dependent on proton transport to the organelle (Ruiz et al., 2001). Calcium uptake and storage were also shown to occur as a function of the acidic intraorganellar environment, in part because of pumping systems and exchangers and because of the calcium chelating properties of poly P present in the matrix. Thus, it is possible that the acidification of the organelle could lead to poly P synthesis and calcium uptake/storage, suggesting an interesting alternative to control Pi and Ca^{2+} homeostasis in the egg cytoplasm.

Together our results show that several small vesicles present in the eggs of *P. americana* have acidocalcisome-like characteristics, with structure, composition and biochemical properties different from that described for YGs. These vesicles might be involved in pH and phosphate homeostasis in the egg, taking active part in the early embryogenesis of this insect and a functional role in yolk mobilization and embryo development.

Acknowledgments

We thank Dr Marcelo medeiros for research suggestions and critical reading of the manuscript. We also thank to Dra Suzete Bressan nascimento for cockroaches disposed to our work. This work was supported by grants from Conselho Nacional de Desenvolvimento Cientifico e Tecnológico (CNPq/Brazil), Programa Jovens Pesquisadores/CNPq-Brazil (to K.M.), Fundação Carlos Chagas Filho de Amparo à Pesquisa no Estado do Rio de Janeiro (FAPERJ), Programa de Apoio ao Desenvolvimento Cientifico e Tecnológico (PADCT), FINEP/PRONEX/FUJB no. 76.97.1000.000 (to E.A.M.), and by the Barbara and Sanford Orkin/Georgia Research Alliance Fund to R.D. L.S.M. was supported in part by a grant from the Ellison Medical Foundation to the Center for Tropical and Emerging Global Diseases and by a fellowship from the Coordenação de Aperfeiçoamento de Pessoal de Nivel Superior (CAPES, Brazil).

References

Abreu, L.A., Valle, D., Manso, P.P., Facanha, A.R., Pelajo-Machado, M., Masuda, H., Masuda, A., Vaz Jr., I., Lenzi, H., Oliveira, P.L., et al., 2004. Proteolytic activity of *Boophilus microplus* yolk pro-cathepsin D (BYC) is coincident with cortical acidification during embryogenesis. Insect Biochem. Mol. Biol. 34, 443–449.

Anderson, R.G., Orci, L., 1988. A view of acidic intracellular compartments. J. Cell Biol. 106, 539–543.

Ault-Riche, D., Fraley, C.D., Tzeng, C.M., Kornberg, A., 1998. Novel assay reveals multiple pathways regulating stress-induced accumulations of inorganic poly phosphate in *Escherichia coli*. J. Bacteriol. 180, 1841–1847.

Blagburn, J.M., Sattelle, D.B., 1987. Nicotinic acetylcholine receptors on a cholinergic nerve terminal in the cockroach, *Periplaneta americana*. J. Comp. Physiol. 161, 215–225.

Brightman, A.O., Navas, P., Minnifield, M.N., Morre, D.J., 1992. Pyrophosphate-induced acidification of *trans* cisternal elements of rat liver Golgi apparatus. Biochim. Biophys. Acta 1104, 188–194.

Chestkov, V.V., Radko, S.P., Cho, M.S., Chrambach, A., Vogel, S.S., 1998. Reconstitution of calcium-triggered membrane fusion using "reserve" granules. J. Biol. Chem. 273, 2445–2451.

Cho, W.L., Tsao, S.M., Hays, A.R., Walter, R., Chen, J.S., Snigirevskaya, E.S., Raikhel, A.S., 1999. Mosquito cathepsin B-like protease involved in embryonic degradation of vitellin is produced as a latent extraovarian precursor. J. Biol. Chem. 274, 13311–13321.

Docampo, R., de Souza, W., Miranda, K., Rohloff, P., Moreno, S.N., 2005. Acidocalcisomes – conserved from bacteria to man. Nat. Rev. Microbiol. 3, 251–261.

Docampo, R., Moreno, S.N., 2001. The acidocalcisome. Mol. Biochem. Parasitol. 114, 151–159.

Fagotto, F., 1990. Yolk degradation in tick eggs: I. Occurrence of a cathepsin L-like acid proteinase in yolk spheres. Arch. Insect Biochem. Physiol. 14, 217–235.

Fagotto, F., 1991. Yolk degradation in tick eggs: III. Developmentally regulated acidification of yolk spheres. Dev. Growth Differ. 33, 57–66.

Fagotto, F., 1995. Regulation of yolk degradation, or how to make sleepy lysosomes. J. Cell Sci. 108, 3645–3647.

Fagotto, F., Maxfield, F.R., 1994. Changes in yolk platelet pH during Xenopus laevis development correlate with yolk utilization: A quantitative confocal microscopy study. J. Cell Sci. 107, 3325–3337.

Fausto, A.M., Gambellini, G., Mazzini, M., Cecchettini, A., Masetti, M., Giorgi, F., 2001. Yolk granules are differentially acidified during embryo development in the stick insect *Carausius morosus*. Cell Tissue Res. 305, 433–443.

Fialho, E., Nakamura, A., Juliano, L., Masuda, H., Silva-Neto, M.A., 2005. Cathepsin D-mediated yolk protein degradation is blocked by acid phosphatase inhibitors. Arch. Biochem. Biophys. 436, 246–253.

Fialho, E., Silveira, A.B., Masuda, H., Silva-Neto, M.A., 2002. Oocyte fertilization triggers acid phosphatase activity during *Rhodnius prolixus* embryogenesis. Insect Biochem. Mol. Biol. 32, 871–880.

Fiske, C.F., Subbarow, Y., 1925. The colorimetric determination of phosphorus. J. Biol. Chem. 66, 375–400.

Goulas, A., Triplett, E.L., Taborsky, G., 1996. Oligophosphopeptides of varied structural complexity derived from the egg phosphoprotein, phosvitin. J. Protein Chem. 15, 1–9.

Kunkel, J.G., Nordin, J.H., 1985. Yolk proteins. In: Kerkut, G.A., Gilbert, L.I. (Eds.), Comprehensive Insect Physiology, Biochemistry, and Pharmacology, vol. 1. Pergamon Press, Oxford, UK, pp. 83–111.

Laemmli, U.K., 1970. Cleavage of structural proteins during assembly of the head of bacteriophage T4. Nature 227, 680–685.

Leigh, R.A., Pope, A.J., Jennings, I.R., Sanders, D., 1992. Kinetics of the vacuolar H^+-pyrophosphatase: the roles of magnesium, pyrophosphate, and their complexes as substrates, activators, and inhibitors. Plant Physiol. 100, 1698–1705.

Lowry, O.H., Rosebrough, N.J., Farr, A.L., Randall, R.J., 1951. Protein measurement with the Folin phenol reagent. J. Biol. Chem. 193, 265–275.

Maeshima, M., 2000. Vacuolar $H(^+)$-pyrophosphatase. Biochim. Biophys. Acta 1465, 37–51.

Mallya, S.K., Partin, J.S., Valdizan, M.C., Lennarz, W.J., 1992. Proteolysis of the major yolk glycoproteins is regulated by acidification of the yolk platelets in sea urchin embryos. J. Cell Biol. 117, 1211–1221.

Marchesini, N., Ruiz, F.A., Vieira, M., Docampo, R., 2002. Acidocalcisomes are functionally linked to the contractile vacuole of *Dictyostelium discoideum*. J. Biol. Chem. 277, 8146–8153.

McIntosh, M.T., Drozdowicz, Y.M., Laroiya, K., Rea, P.A., Vaidya, A.B., 2001. Two classes of plant-like vacuolar-type $H(^+)$-pyrophosphatases in malaria parasites. Mol. Biochem. Parasitol. 114, 183–195.

McNeil, P.L., Vogel, S.S., Miyake, K., Terasaki, M., 2000. Patching plasma membrane disruptions with cytoplasmic membrane. J. Cell Sci. 113, 1891–1902.

Miranda, K., Docampo, R., Grillo, O., Franzen, A., Attias, M., Vercesi, A., Plattner, H., Hentschel, J., de Souza, W., 2004. Dynamics of polymorphism of acidocalcisomes in *Leishmania* parasites. Histochem. Cell Biol. 121, 407–418.

Moraes Moreira, B.L., Soares Medeiros, L.C., Miranda, K., de Souza, W., Hentschel, J., Plattner, H., Barrabin, H., 2005. Kinetics of pyrophosphate-driven proton uptake by acidocalcisomes of *Leptomonas wallacei*. Biochem. Biophys. Res. Commun. 334, 1206–1213.

Motta, L.S., da Silva, W.S., Oliveira, D.M., de Souza, W., Machado, E.A., 2004. A new model for proton pumping in animal cells: the role of pyrophosphate. Insect Biochem. Mol. Biol. 34, 19–27.

Nordin, J.H., Beaudoin, E.L., Lin, X., 1991. Acidification of yolk granules in *Blatella germanica* eggs coincides with proteolytic processing of vitellin. Insect Biochem. 18, 177–192.

Oliveira, D.M., Machado, E.A., 2006. Characterization of a tyrosine phosphatase activity in the oogenesis of *Periplaneta americana*. Arch. Insect Biochem. Physiol. 63, 24–35.

Palmgren, M.G., 1991. Acridine orange as a probe for measuring pH gradients across membranes: mechanism and limitations. Anal. Biochem. 192, 316–321.

Purcell, J.P., Quinn, T.M., Kunkel, J.G., Nordin, J.H., 1988. Correlation of yolk phosphatase expression with the programmed proteolysis of vitellin in Blattella germanica during embryonic development. Arch. Insect Biochem. Physiol. 9 (3), 237–250.

Raikhel, A.S., Dhadialla, T.S., 1992. Accumulation of yolk proteins in insect oocytes. Annu. Rev. Entomol. 37, 217–251.

Ramos, I.B., Miranda, K., De Souza, W., Machado, E.A., 2006. Calcium-regulated fusion of yolk granules during early embryogenesis of *Periplaneta americana*. Mol. Reprod. Dev. 73, 1247–1254.

Ramos, I.B., Miranda, K., De Sousa, W., Oliveira, D.M.P., Lima, A.P.C.A., Sorgine, M.H.F., Machado, E.A., 2007. Calcium-regulated fusion of yolk granules is important for yolk degradation during early embryogenesis of *Rhodnius prolixus*. J. Exp. Biol. 210, 138–148.

Rea, P.A., Kim, Y., Sarafian, V., Poole, R.J., Davies, J.M., Sanders, D., 1992. Vacuolar $H(^+)$-translocating pyrophosphatases: a new category of ion translocase. Trends Biochem. Sci. 17, 348–353.

Reimer, C.L., Crawford, B.J., 1995. Identification and partial characterization of yolk and cortical granule proteins in eggs and embryos of the starfish, *Pisaster ochraceus*. Dev. Biol. 167, 439–457.

Ribolla, P.E.M., Dafre, S., de Bianchi, A.G., 1993. Cathepsin B and acid phosphatase activities during *Musca domestica* embryogenesis. Insect Biochem. Mol. Biol. 23, 217–223.

Rodrigues, C.O., Scott, D.A., Docampo, R., 1999a. Characterization of a vacuolar pyrophosphatase in *Trypanosoma brucei* and its localization to acidocalcisomes. Mol. Cell Biol. 19, 7712–7723.

Rodrigues, C.O., Scott, D.A., Docampo, R., 1999b. Presence of a vacuolar H^+-pyrophosphatase in promastigotes of *Leishmania donovani* and its localization to a different compartment from the vacuolar H^+-ATPase. Biochem. J. 340 (Pt 3), 759–766.

Ruiz, F.A., Lea, C.R., Oldfield, E., Docampo, R., 2004. Human platelet dense granules contain polyphosphate and are similar to acidocalcisomes of bacteria and unicellular eukaryotes. J. Biol. Chem. 279, 44250–44257.

Ruiz, F.A., Marchesini, N., Seufferheld, M., Govindjee, Docampo, R., 2001. The polyphosphate bodies of Chlamydomonas reinhardtii possess a proton-pumping pyrophosphatase and are similar to acidocalcisomes. J. Biol. Chem. 276, 46196–46203.

Rust, M.K., Reierson, D.A., Hansgen, K.H., 1991. Control of American cockroaches (*Dictyoptera: Blattidae*) in sewers. J. Med. Entomol. 28, 210–213.

Salerno, A.P., Dansa-Petretski, M., Silva-Neto, M.A., Coelho, H.S., Masuda, H., 2002. *Rhodnius prolixus* vitellin is composed of three different populations: comparison with vitellogenin. Insect Biochem. Mol. Biol. 32, 709–717.

Scott, D.A., de Souza, W., Benchimol, M., Zhong, L., Lu, H.G., Moreno, S.N., Docampo, R., 1998. Presence of a plant-like proton-pumping pyrophosphatase in acidocalcisomes of *Trypanosoma cruzi*. J. Biol. Chem. 273, 22151–22158.

Scott, D.A., Docampo, R., 1998. Two types of H^+-ATPase are involved in the acidification of internal compartments in *Trypanosoma cruzi*. Biochem. J. 331, 583–589.

Seufferheld, M., Vieira, M.C., Ruiz, F.A., Rodrigues, C.O., Moreno, S.N., Docampo, R., 2003. Identification of organelles in bacteria similar to acidocalcisomes of unicellular eukaryotes. J. Biol. Chem. 278, 29971–29978.

Soares Medeiros, L.C., Moreira, B.L., Miranda, K., de Souza, W., Plattner, H., Hentschel, J., Barrabin, H., 2005. A proton pumping pyrophosphatase in acidocalcisomes of *Herpetomonas* sp. Mol. Biochem. Parasitol. 140, 175–182.

Takahashi, S.Y., Yamamoto, Y., Zhao, X., Watabe, S., 1996. *Bombyx* acid cysteine proteinase. Int. J. Inver. Rep. Dev. 30, 265–281.

Tijssen, J.P., Beekes, H.W., Van Steveninck, J., 1982. Localization of polyphosphates in *Saccharomyces fragilis*, as revealed by 4′,6-diamidino-2-phenylindole fluorescence. Biochim. Biophys. Acta 721, 394–398.

Yamahama, Y., Uto, N., Tamotsu, S., Miyata, T., Yamamoto, Y., Watabe, S., Takahashi, S.Y., 2003. In vivo activation of pro-form *Bombyx* cysteine protease (BCP) in silkmoth eggs: localization of yolk proteins and BCP, and acidification of yolk granules. J. Insect Physiol. 49, 131–140.

Ziegler, R., Van Antwerpen, R., 2006. Lipid uptake by insect oocytes. Insect Biochem. Mol. Biol. 36, 264–272.

6- Anexo II:

Acidocalcisomes are important calcium-storage compartments in yolk systems of the insect *Rhodnius prolixus* Stahl

Ramos, I.B. [†‡]; Koeler, C. [†]; Gomes, F. [†‡]; W, Souza. [‡]; Docampo, R[†]; Miranda, K[‡]; Machado, E. A.[†]

[†]Laboratório de Entomologia Médica, Programa de Parasitologia e Biologia Celular, Instituto de Biofísica Carlos Chagas Filho (UFRJ) – Brasil.

[‡]Laboratório de Ultraestrutura Celular Hertha Meyer, Programa de Parasitologia e Biologia Celular, Instituto de Biofísica Carlos Chagas Filho (UFRJ) – Brasil.

Abstract:

Here we report the presence and characterization of elemental composition of acidocalcisome-like organelles in eggs of the insect *Rhodnius prolixus*. X-ray microanalysis revealed the presence of small electron-dense vesicles with elemental composition similar to that previously described for acidocalcisomes. Immunolocalization assays, using antibodies against a conserved sequence of *A. thaliana* VH^+-PPase (which is considered a marker for the acidocalcisomes), localized this enzyme in the small electron-dense vesicles, mainly in the egg cortex. A highly enriched fraction of acidocalcisomes was obtained and VH^+-PPase and polyphosphate polymers (PolyP) co-localized to the vesicles. PolyP quantification showed that the accs contain a significant amount of the whole long- and short-chain PolyP detected in day-0 eggs and elemental quantifications of the egg content showed that a considerable amount of the egg calcium (24.5 ± 0.65 %) is also stored in the acidocalcisomes. During embryogenesis, incubations with acridine orange showed that the acidocalciomes are acidified at day-3 (coincident with the yolk mobilization), appearing as neutral organelles before this point of development. PolyP quantification showed that the levels of long and short chain PolyP tend to decrease starting at day-2, being approximately 30 % lower at day-3 compared to day-0 eggs. Lastly, semi-quantitative elemental X-ray microanalysis showed that the relative amounts of the elements in the acidoclcisomes are not altered during early embryogenesis, being qualitatively similar at the first 4 days of development. Together, the results reveal new aspects of early embryogenesis in *R. prolixus*, and the potential involvement of a novel organelle in the storage and mobilization of inorganic elements to the embryonic cells.

Introduction:

Chagas disease is one of the main causes of cardiac lesions in Latin America, and the blood sucking insect *Rhodnius prolixus* is an important vector of this disease (WHO, 2008). The ability of insects to inhabit a variety of niches is partially due to their high reproductive outputs. Some insects are able to lay a mass of eggs equivalent to half of their body mass, and usually more than 95 % of the eggs produced are viable (Papaj, 2000). Therefore, studies regarding egg's organelles and cell biology could reveal an innovative approach to population control of several disease vectors and agriculture pests.

In insects, the process of embryogenesis occurs totally disconnected from the maternal body, thus requiring that all the nutritional reserve necessary for the growing embryo to be previously stored in the egg, during oogenesis. The aminoacid reserve in the eggs is mainly represented by the yolk proteins, which usually are lipoglicophosphoproteins that are stored in organelles called yolk granules (YG). Yolk consumption starts when the yolk proteins undergo a process of degradation, which occurs by activation of acid hydrolases also stored within YG. To activate hydrolases, YG are acidified via proton-pumps, such as a vacuolar proton ATPase (VH^+-ATPase) (Fagotto, 1991; Nordin et al., 1991; Fagotto, 1995) and a vacuolar proton pyrophosphatase (VH^+-PPase) (Motta et al., 2004). In this process (commonly known as yolk mobilization), fundamental molecules, such as aminoacids and monosacarides, are made accessible for the growing embryo, being, therefore, indispensable for embryonic development. In general, yolk degradation occurs in a regulated manner, starting after a certain period of early embryogenesis, depending on the species. In *R. prolixus*, yolk mobilization starts in the third day of embryogenesis, in a total embryonic development of 12-13 days (Fialho et al., 2002).

Although the basic components involved in yolk mobilization are generally understood (acidification of YG, leading to activation of hydrolases and consequent degradation of yolk proteins), little is known about how this process is controlled, i.e. how the different organelles from the yolk system couple their activities to perform highly regulated processes, such as the yolk mobilization. In general, all vesicles extracted from yolk systems are called YG. However, it is accepted that the vesicle

population inside the eggs is not homogeneous. In several species, YG can be fractionated according to their different size and density (Fagotto, 1991; Chestkov et al., 1998; Mcneil et al., 2000; Yamahama et al., 2003). It has also been shown, for different species, that small vesicles can comprise different types of hydrolases (Fausto et al.,2001; Yamahama et al., 2003), and are mainly distributed in the peripheral cytoplasm (cortex) of the mature egg. In this region, the vesicles are preferentially acidified, and this process is somehow involved in yolk mobilization (Reimer and Crawford, 1995; Abreu et al., 2004). However, the presence and functional roles of different organelles in these systems are poorly investigated, and the mechanisms underlying the connection between the hydrolyzed yolk content and the embryo cells are still unknown.

Acidocalcisomes are lysosome-related organelles widely distributed in several microrganisms. They are characterized by an acidic nature, high electron density and high content of polyphosphate (poly P) bound to several cations. They possess a typical elemental composition, containing accumulated magnesium, sodium, phosphorus, potassium, calcium, iron and zinc (Docampo and Moreno, 2001; Docampo et al., 2005). These organelles have a variety of cation and proton pumps, such as the vacuolar H^+-ATPase and H^+-PPase, and a number of exchangers such as Na^+/H^+ and Ca^{2+}/H^+ in their membrane. Although first and better described in Trypanosomatids, acidocalcisomes have also been found in several other microrganisms, including Apicomplexan parasites (Garcia et al., 1998, Marchesini et al., 2000, Luo et al., 2001), bacteria (Seufferheld et al., 2003; 2004), the green algae *Chlamydomonas reinharditi* (Ruiz et al., 2001) and the slime mold *Dictyostelium discoideum* (Marchesini et al., 2002). They have been implicated in several functions, including storage of cations, ion homeostasis, osmoregulation and poly P metabolism (Docampo et al., 2010). In the recent past, the presence of acidocalcisome-related organelles has been described in different cell types from higher eukariotes, including human platelets, in which polyP from acidocalcisomes was suggested as a modulator of blood clotting (Ruiz et al., 2004), and eggs of different animals including the insect *P. americana* (Motta et al., 2009), sea urchins (Ramos et al., 2010) and chicken (Ramos et al., 2010). However, the functional roles of acidocalcisomes in the later animals, as integral part of the egg yolk systems, are still unknown.

In this study, we characterized the presence of acidocalcisome-related organelles in the eggs of *Rhodnius prolixus*. Using transmission electron microscopy coupled with X-ray microanalysis, electron dense organelles presenting the typical elemental composition of acidocalcisomes were found in the eggs. Those organelles were localized in the egg cortex and presented other typical acidocalcisome characteristics, such as the presence of a VH^+-PPase and PolyP. Quantifications of inorganic elements showed that at least ~24 % of the total calcium in the egg is present in the acidocalcisomes at day-0, thus suggesting that these organelles are important calcium storage compartments in the eggs. Taken together, the results reveal new aspects of early embryogenesis in *R. prolixus*, and the potential involvement of a novel organelle participating in the storage and mobilization of inorganic components in oviparous animals.

Methodology:

Insects and eggs:

R. prolixus were reared in a colony maintained at 28ºC and 70 - 80% relative humidity. The insects were fed with rabbit blood in an artificial apparatus according to Garcia et al. (1975). Non-fertilized eggs were laid by non-mated adult females and collected 1 h after oviposition. Fertilized eggs were collected and used immediately or allowed to develop to the required embryogenesis stage.

Preparation of egg homogenates and acidocalcisome-enriched fractions (accs fraction):

Total egg homogenates were prepared by disrupting the eggs, using a plastic pestle, on ice cold buffer containing 10 mM Hepes, pH 7.2, 4 mM $MgCl_2$, 50 mM KCl, supplied with a protease inhibitors cocktail (Sigma, P834). For the preparation of acidocalcisome-enriched fractions, approximately 30 mg of day-0 eggs were disrupted in 5 mM HEPES, pH 7.2 supplied with protease inhibitors (Sigma, P8340). The egg homogenate was centrifuged twice at 10.000 x g for 1 min at 4ºC in the same buffer, and once in 5 mM HEPES plus 8.5% sucrose. The final pellet was used as acidocalcisome-enriched fraction (accs-fraction) and was chemically fixed, quickly frozen or resuspended in appropriate buffer for the different assays as described in the following sections. The remainder of the acidocalcisomes fractionation (supernatant of the first centrifugation) was also utilized in some experiments, and will be referred to from now on as yolk-fraction.

Transmission Electron Microscopy (TEM) and X-ray Microanalysis:

For conventional transmission electron microscopy samples were fixed in 4% paraformaldehyde, 2.5% glutaraldehyde diluted in 0.1 M sodium cacodylate buffer (pH 7.3) at $4^{\circ}C$ for 24 h, and then embedded in epoxy resin, sectioned and stained using standard methods. For X-ray microanalysis, the samples were applied to Formvar-coated copper grids and blotted dry with a filter paper. Samples were examined in a JEOL 1200 EX transmission electron microscope operating at 80 kV. X-rays were collected for 100 s

using a Si (Li) detector with Norvar window on a 0 to 10 KeV energy range with a resolution of 10eV/channel. Analyses were performed using a Noran/Voyager III analyzer.

Semi-quantitative elemental X-ray microanalysis of acidocalcisomes:

Semi-quantitative elemental analysis was peformed using the well stabilished Cliff-Lorimer method, as previously described by Miranda et al.,2004. Briefly, the atomic % was calculated from the measured weight % values (wt. %/ atomic wt.). The sum of the atomic weights of the selected elements was then normalized to 100%. Results are expressed as the percentage of the elements in the spectra. Cations signals were also normalized and represented as the percentage of the phosphorous signal.

Freeze-fracture:

Acidocalcisome-fractions were fixed in 2.5 % glutaraldehyde and 4 % freshly prepared formaldehyde in 0.1 M cacodylate buffer, pH 7.4, for 60 min at room temperature, washed in 0.1 M phosphate buffer, pH 7.2, and infiltrated in 30% glycerol. The material was then mounted on aluminum support disks and slammed onto liquid nitrogen-cooled gold block of a quick freezing device (Leica). Fracture was carried out at -115 °C in a Balzers-Leica freeze fracture apparatus. Platinum was evaporated onto the specimen at an angle of 15° and carbon was evaporated at an angle of 90°. Replicas were cleaned to remove the remaining organic material by digestion with sodium hypochloride, rinsed with distilled water, mounted on 300-mesh nickel grids and observed in a Zeiss EM 900 transmission electron microscope operating at 80 kV.

Staining with acridine orange:

Accs-fraction obtained from eggs of different days during early embryogenesis were stained with acridine orange for 5-20 min at room temperature in the dark at final concentrations of 6 μM. Images were obtained using a Zeiss Axioplan fluorescence microscope coupled with a CCD (charge-coupled device) camera using appropriate filter sets (λex = 450-490 nm, λem > 500 nm).

Preparation of anti-VH^+-PPase polyclonal antibodies:

One hundred micrograms of KLH-conjugated synthetic peptides corresponding to the hydrophilic loop IV of plant VH^+-PPase (KIATYANARTTLEARKGVGKAFIVAFR) were used to immunize New Zealand White female rabbits using complete Freund´s adjuvant for the initial injection and incomplete Freund´s for booster injections. Pre-immune serum was tested to monitor the absence cross-reactivity with the antigenic peptide. Anti-VH^+-PPase antiserum from bleed 3 was used for *western blotting* and immunolocalization assays as described in the following sections.

Western Blotting:

Sixty micrograms of protein (Lowry et al., 1951) from different fractions (yolk-fraction or accs-fraction) of day-0 eggs were submitted to 10% SDS-PAGE (Laemmli, 1970) and the gels were electro-transferred to a nitrocellulose membrane. The membranes were incubated in blocking buffer containing 10 mM Tris, 150 mM NaCl, 3% bovine serum albumin (BSA) (w/v) and 0.1% tween (v/v) for 2 h. The samples were then incubated for 3 h with the primary antibody (anti-VH^+-PPase polyclonal antibodies) diluted 1:1000, followed by incubations with goat anti-rabbit antibody associated with alkaline phosphatase (1:5000).

Immunogold electron microscopy (IEM):

Day-0 eggs were fixed in 0.2% glutaraldehyde, 4% freshly prepared formaldehyde and 0.5 % picric acid in 0.1 M cacodylate buffer, pH 7.4, at 4^oC for 24 h. Following fixation, the samples were washed, dehydrated in acetone series (25 minutes each), and embedded in LR-White resin at 4^oC. Polymerization was carried out at -20^oC under UV radiation for 96 h. Thin sections of LR-White embedded material were collected on nickel grids, incubated in 100 mM NH_4Cl in TBS for 30 min, and transferred to blocking buffer for 30 min at room temperature. Grids were incubated in the primary anti-H^+-PPase antibodies diluted 1:500 in the same buffer for 1 h. After washing, grids were incubated with 15 nm gold-labeled goat anti-rabbit IgG, diluted 1:100. The sections were washed, stained in uranyl acetate and lead citrate, and observed in JEOL 1200 EX transmission electron

microscope. Quantifications of gold particles were performed in random fileds from five different sections obtained from three experiments.

Immunofluorescence against H^+-PPase and PolyP binding domain:

For co-localization of VH^+-PPase and PolyP, anti-VH^+-PPase antibodies were used together with the recombinant polyP binding domain of *Escherichia coli* exopolyphosphatase linked to an *Xpress* epitope tag (PPBD), as previously described (Saito et al., 2005). Acidocalcisome-fractions were incubated for 20 min in blocking buffer and for additional 30 min with 12 µg/ ml of recombinant PPBD. After washing, the samples were fixed in 4% paraformaldehyde for 30 min and washed twice at room temperature. The samples were allowed to adhere to Poly-L-lysine-coated coverslips and incubated for 30 min in 100 mM NH_4Cl and for 30 min in blocking buffer. The samples were then incubated for 1 h with primary anti-H^+-PPase antibodies diluted 1:300 and 5 µg/ ml of Anti Xpress epitope tag (Invitrogen). Secondary antibodies (Alexa Fluor^{tm} 488 goat anti mouse IgG and Alexa Fluor^{tm} 568 goat anti rabbit IgG, Invitrogen) diluted 1:400 were incubated with the amples for 1 h. Immunofluorescence Images were obtained using a Zeiss Axioplan fluorescence microscope coupled with a CCD (charge-coupled device) camera using appropriate filter sets (λex = 450-490 nm, λem = 510-560 nm and λex = 510-425 nm, λem = 560-600).

Extraction and quantification of Long and Short Chain poly P:

Total egg homogenates, yolk-fractions and accs-fractions were obtained and treated with methods to extract either long chain or short chain poly P. Long chain (LC) poly P extraction was performed as described by Ault-Riché et al. (2002). Short chain (SC) poly P extraction was done as described by Ruiz et al. (2001). Protein measurements were performed using the method of Lowry et al. (1951). Poly P levels were determined from the amount of phosphate (P_i) released upon treatment with an excess of recombinant *S. cerevisiae* exopolyphosphatase 1 (rScPPX1). The recombinant enzyme was prepared as described before (Ruiz et al., 2001). Aliquots of poly P extracts (always less than 1.5 nmol, monomeric P_i) were incubated for 15 min at 35^{o}C with 60 mM Tris-HCl, pH 7.5, 6.0 mM $MgCl_2$, and 3,000-5,000 units of purified rScPPX1 in a final volume of 100 µl.

One unit corresponds to the release of 1 pmol of P_i/min at 35°C. Release of P_i was monitored by the method of Lanzetta et al. (Lanzetta et al., 1979). A sodium phosphate standard curve was included on every assay microplate, and activity controls (polyP_{75+}, Sigma) at a final concentration of 300 nM (in terms of polymer) was included as a control for yield.

Poly P detection in agarose gels and DAPI staining:

Poly P extraction was performed as described before by Gomes et al. (2008). Briefly, accs-fractions were resuspended in water, and sonicated. After treatment with DNAse (10 μg/ml) and RNAse (10 μg/ml) for 30 min at 37°C, one volume of chloroform was added, and the samples were vortexed for 5 min. The samples were centrifuged at 10,000 *g* for 5 min at 4°C to separate the phases. The water-soluble fraction was collected, dried in a speed vac, and resuspended in 60 mM Tris-HCl, pH 7.5, 6.0 mM $MgCl_2$. Poly P samples were then mixed with DNA loading buffer (10 mM Tris-HCl, pH 7.5, 10 mM EDTA, 0.25 % Orange-G and 0.65 % sucrose) and loaded into 1-2% agarose gels. The gels were run at 200 V in Tris-acetate pH, 8.2, 1 mM EDTA (TAE buffer) until the dye (Orange-G) reached the middle of the gel. Staining was performed as described before by Smith and Morrissey (2007) with minor modifications. Gels were incubated for 30 min in the dark with 2 μg/ml DAPI, 10 mM EDTA and 0.3 % Fluoromount-G. The gels were washed twice for an hour in the same solution without DAPI. Images of DAPI fluorescence were acquired with Alpha Imager gel imaging system (AlphaInotech, San Leandro, CA) using an excitation wavelength of 365 nm.

Preparation of membrane fractions and PPase activity (PPi hydrolysis):

PPase activity was detected using yolk-fractions and accs-fractions from day-0 eggs. Membrane fractions were prepared by differential centrifugation, as previously described by Motta et al. (2004), and the protein concentration was determined by the method of Lowry et al. (1951). PPase activity, was measured by detecting Pi release from PPi by the method of Fiske and Subbarow (1925), using a microplate reader. The reaction medium contained 100 mM KCl, 0.3 mM PPi, 0.6 mM $MgCl_2$ and 50 mM MOPS-Tris pH 7.5. When used, aminomethylenediphosphonate (AMDP) concentration was of 40 μM.

Reactions were started by the addition of membrane fractions (40 µg protein/ml final concentration) and stopped by the addition of 50% w/v trichloroacetic acid after 1 h at 28°C.

Quantification of elements, inductively coupled plasma optical emission spectroscopy (ICP-OES):

165 mg of eggs (wet weight) were disrupted and fractionated into accs-fraction and yolk-fraction. The samples were dried on speed-vac and digested in sub-distilled HNO_3 at 80ºC for 30 min. The samples were then diluted in ultra-pure water and read in an inductively coupled plasma optical emission spectrometer (Optima 4300 DV, Perkin Elmer Instruments, Norwalk, CT, USA). The analytical lines used were 213.618 nm for phosphorus (Limit of detection, LOD = 0.030 mg/L, axial view), 393.366 nm for calcium (LOD = 0.0001 mg/L, radial view), 279.553 nm for magnesium (LOD = 0.0002 mg/L, radial view) and 589.592 nm for sodium (LOD = 0.002 mg/L, axial view). The values were obtained by comparing the readings with a calibration curve for each element.

Results:

Electron dense organelles in the eggs

Day-0 eggs (at cleavage stage, before the beginning of blastoderm, Heming and Huebner, 1994) were disrupted in appropriate buffer and the suspension of the egg organelles was placed in formvar-coated grids and directly observed in transmission electron microscope. Results showed the presence of organelles differing in size and electron density (Figure 1 A). X-ray elemental analysis of the larger (>3 μm) and less electron dense vesicles (Figure 1 A, white arrow) only presented accumulated sulfur (Figure 1 C), which suggests the presence of high amounts of protein in these organelles. Additionally, several smaller (0.57 ± 0.21 μm) and highly electron dense vesicles were also observed (Figure 1 A, black arrows and B). Their elemental profile were qualitatively similar (for at least 10 X-ray spectra taken), showing accumulated phosphorus, calcium, magnesium, sodium, chlorine and potassium (Figure 1 D), being therefore similar to accs of unicellular eukaryotes (Docampo et al., 2005). To further investigate the ultrastructural aspects of these organelles, whole eggs were processed for transmission electron microscopy. Standard procedures revealed the presence of several empty vesicles in the egg cortex (0.63 ± 0.19 μm) (Figure 1 E and F), which is the typical morphology of accs after the washings with organic solvents during the procedure (Docampo et al., 2005).

Localization of vacuolar-H^+-PPase

Motta et al. (2004) described the presence of a VH^+-PPase activity in eggs of *Rhodnius prolixus*, and this enzyme has been previously considered a marker for accs in several microorganisms (Docampo et al., 2005). For this reason, we decided to investigate the localization of this enzyme in the eggs of *R. prolixus*. The polyclonal antibodies raised in this study (against the conserved loop IV of the V-H^+PPase from *A. thaliana)* were already shown to cross-react with a ~70 kDa fragment in oocytes of *R. prolixus* (Motta et al., 2004), and to cross-react with the VH^+-PPase of *T. cruzi* (Scott et al., 1998), *Leishmania spp*. (Miranda et al., 2004), *Plasmodium spp.* (Marchesini et al., 2000) and others. *Western blotting* using day-0 eggs of *R. prolixus*, *T. cruzi* epimastigotes as positive control and human macrophages as negative control, revealed a positive cross-

reaction fragment of ~69 kDa in *Rhodnius* eggs. *Western blotting* and immunofluorescence (not shown) in *T. cruzi* epimastigotes confirmed the labeling pattern expected for accs. Immunofluorescence using a suspension of the eggs organelles showed that only small vesicles are labeled (and not large YG) (Figure 2 B-E) and immunogold electron microscopy showed that the periphery of empty vesicles are specifically labeled by the VH^+-PPase antibodies (Figure 2 F and G). Immunolocalization assays in thick longitudinal sections of day-0 eggs, using confocal laser scanning microscopy, showed that the vacuolar H^+-PPase is mainly localized in the egg cortex (Figure 2 H and I, supplementary movie 1), coincident with the localization of the empty vesicles described before (Figure 1 E and F). Control experiments (omitting the primary antibodies), did not show labeling in the cortex, although auto fluorescence is seen in the chorion (supplementary movie 1).

Isolation of acidocalcisome-like organelles

Differential centrifugation protocols using hypotonic buffers allowed us to selectively disrupt the larger yolk granules and to obtain a highly enriched fraction of acidocalcisomes-like organelles (accs-fraction) (Figure 3 A and B). Morphometric analysis showed that the average diameter of the recovered organelles (0.55 ± 0.26 μm) is similar to the diameter of acidocalcisomes in the suspensions of egg organelles and in thin sections of standard TEM. X-ray microanalysis of the isolated organelles showed that the ion content of the acidocalcisomes in the recovered fraction is retained (Figure 3 C). Standard TEM (Figure 3 D) and freeze-fracture (Figure 3 E) of isolated acidocalcisomes confirmed that the membranes of the organelles are intact after the fractionation procedure.

Vacuolar-H^+-PPase and PolyP co-localize to the acidocalcisomes-like organelles

Western blotting analysis using the accs-fraction showed that immunolabeling for the V-H^+-PPase is increased in the fraction, when compared to same amount of loaded protein from yolk fractions (Figure 4 A). Activity of PPi hydrolysis was tested in membrane preparations of the same fractions. Results showed that accs-fractions have 50 % more PPase activity then the yolk components (yolk-fractions) (Figure 4 B). PolyP

quantifications in the accs-fraction showed that a reasonable amount of the short- and long-chain PolyP, respectively, in the eggs is found in the acidocalcisomes (Figure 4 C). To investigate the localization of PolyP and the V-H^+-PPase in the acidocalcisomes, the PolyP binding domain (PPDB) of *S. cerevisiae* exopolyphosphatase (PPX) was used together with antibodies against the V-H^+-PPase. Results show that both PolyP and the V-H^+-PPase co-localize in the vesicles present in the accs-fraction (Figure 4 D-G).

PPi hydrolysis activity in the acidocalcisomes

To further investigate the profile of PPi hydrolysis activity detected in the accs-fraction, membrane preparations of accs and yolk were obtained and tested for PPase activity in the presence of known inhibitors and co-factors of the VH^+-PPase. Results showed that AMDP (a non-hydrolysable analog of PPi which is considered a specific inhibitor of V-H^+-PPase) was able to inhibit approximately 35 % of the enzyme specific activity in acidocalcisomes. In addition, as expected, no activity was detected in the absence of Mg^{2+} (co-factor of the enzyme) or PPi (substrate) (Figure 5 A). To confirm that the VH^+-PPase is associated with the membrane (insoluble) fraction of the organelles, accs-fractions were frozen and thawed, and soluble and insoluble components were separated by ultra-centrifugation. *Western blotting* showed that the immunodetection of the enzyme is indeed associated with the insoluble components of the acidocalcisomes (Figure 5B), thus confirming that the VH^+-PPase is associated to the organelle membranes.

Quantification of inorganic elements in the eggs and accs-fraction

Total egg homogenates, yolk- fractions and accs-fractions were obtained, dried on speed-vac and the contents of phosphorus, calcium, magnesium and sodium were quantified by means of inductively coupled plasma optical emission spectroscopy. Results showed that the egg contains approximately seven times more phosphorus than calcium and magnesium, and high amounts of sodium (Table 1). Additionally, the total amounts of calcium in the eggs (18 ± 0.6 μg), at least 24 ± 0.9 % (4.2 ± 0.6) is present in the acidocalcisomes, suggesting that this compartment is one of the main calcium storage compartments in the egg.

Acidocalcisomes during early embryogenesis: acidification, polyP content and elemental quantifications

Observation of the accs-fractions obtained from eggs of different days of development in the presence of acridine orange (AO) allowed us to investigate the acidity of these organelles during early embryogenesis. This compound has been proved to be a reliable probe, both for spectrophotometric measurements and microscopic visualization of intracellular acidic compartments, including endosomes, lysosomes (Anderson and Orci, 1988) and acidocalcisomes from different microorganisms (Miranda et al., 2008) and eggs (Motta et al., 2004, Motta et al., 2009). Incubation of acidocalcisomes with AO showed that they appear as neutral organelles from day-0 to day-2 of embryogenesis, and that, at day-3, they become acidified (Figure 6), coincident with the beginning of the yolk proteins mobilization. PolyP in the acidocalcisomes during embryogenesis was detected by DAPI staining in agarose gels (Figure 7 A). Additionally, quantifications of PolyP levels in the acidocalcisomes reveled that long-chain PolyP contents in these organelles tend to decrease starting at day 2, and that short-chain PolyP decreases starting at day-1 (Figure 7 B). Semi-quantitative elemental analysis (Cliff-Lorimer ratios method) of the acidocalcisomal contents, during the first 5 days of embryogenesis, showed that the relative amounts of the elements in the organelles are not significantly altered (Table 2), being, therefore, qualitatively similar in elemental composition.

Discussion:

The yolk system of meroblastic eggs is a highly regulated and compartmentalized cellular structure. It enables the yolk proteins, which are comprised within individual and varied stores, to be hydrolyzed in a programmed time course, and nourishes the embryo with fundamental molecules for cellular metabolism and growth. However, the presence and functional roles of the different organelles in these systems are poorly investigated, and the coupling activities of the intracellular yolk compartments and their interchange with the embryo cells are still to be elucidated. In this context, we report here the presence and characterization of the elemental content of acidocalcisome-related organelles in the yolk system of the insect *R. prolixus*. The existence of this organelle in the eggs was attested by observations that some small vesicles in the yolk share many characteristics with acidocalcisomes: 1) high electron density; 2) storage of extremely high amounts of calcium and other cations such as magnesium, sodium and potassium 3) storage of large amounts of phosphorus in the form of PolyP; 4) an empty appearance with an enclosing membrane when thin sections are examined by standard transmission electron microscopy; 5) the presence of a VH^+-PPase in their enclosing membrane; and 5) Ability to undergo acidification, being able to accumulate acidophilic dyes such as AO.

The presence of a vacuolar H^+-PPase in acidocalcisomes has been widely described (Docampo et al., 2005), and detection of a membrane bound PPase activity in yolk vesicles was already described for the insects *R. prolixus* (Motta et al.,2004) and *Periplaneta americana*. In the later, the enzyme was also localized in small vesicles similar to acidocalcisomes (Motta et al., 2009). In *Rhodnius* acidocalcisomes, PPase activity showed similar kinetic properties to those previously described for the yolk vesicles (Motta et al., 2004), plants, bacteria and protists (Maeshima, 2000). Additionally, the enzyme was shown to be associated with the acidocalcisome membranes and to be moderately inhibited by AMDP (an inhibitor of vacuolar H^+-PPases, Maeshima, 2000). The idea that H^+-PPases represent an alternative way to generate proton electrochemical gradients across the membrane of organelles during germination in plant models has been extensively discussed (Maeshima, 2000). In such a system, with massive anabolic

activity, ATP is largely utilized, whereas PPi is produced in a subset of these reactions (Rea et al., 1992). The same assumption fits the systems of embryo development, since they also involve massive synthesis and degradation of macromolecules necessary for rapid embryo growth (Schier, 2007). Because acidification of the egg compartments is indispensable for proper development, the existence of such an alternative for proton-pumping seems to be a convenient attribute to insect yolk breakdown systems.

The egg cortex is a large assemblage of the plasma membrane to which a characteristic set of cytoskeletal elements, organelles and macromolecules adhere. It is possible to isolate the egg cortex of equinoderms, molluscs, mouse and *Xenopus laevis* (Terasaki et al., 1991; Elinson et al., 1993; Walker et al., 1994; Alarcon and Elinson, 2001), but the present knowledge is relatively limited considering published works in structure and function of the cortex, compared to the extensive data available concerning plasma membrane permeability, calcium release and cytoskeleton (Sardet et al., 2002). In addition, most of the knowledge regarding structure of the cortex is the result of studies in echinoderms, molluscs and annelids, whereas little is known about the structure and function of the cortex in *Caenorhabditis elegans, Drosophila* (the two genetically tractable species) or any other insect (Sardet et al., 2002). The localization of the acidocalcisomes in the egg cortex in *R. prolixus* suggests that, in insects, the egg periphery is also a particular important region of the cell and might contain important organelles and macromolecules necessary for patterning formation and regulation of yolk mobilization. Therefore, further investigations on the molecular machinery present in the acidocalcisome membranes, or the characterization of novel organelles in this region will certainly provide new insights to the functional role of the egg cortex and the cellular organization of the yolk system in insects.

Inorganic elements are fundamental for eukaryotic cell metabolism and comprise bulk biological elements (present in greater amounts in the cell, e.g. calcium and phosphorus) and trace elements (e.g. magnesium, zinc and manganese) (Williams, 2006). They are known to be essential as co-factors for many enzymes that play important roles as tissue growth (Schwartz et al., 1994), electron-transfer processes (Hsu, 1980) and protein synthesis (Marin Briano et al., 1995; Singla et al., 1998). In this regard, these components must be taken into account in the yolk storage reserve, especially in a system

of intense biosynthetic reactions as a growing embryo. Most of the efforts in studies about the yolk components were directed to unveiling the role and isolation of specific macromolecules, mainly the yolk proteins (Oliveira et al., 1986; Oliveira et al., 1989). It is widely described in the literature that vitellins from insects are phosphorylated, and can bind cations such as Ca^{2+} and Mg^{2+} (Kerkut and Gilbert, 1985). However, it is still uncertain if the products of vitellins hydrolysis would provide sufficient amounts of the inorganic elements required by the growing embryo, mostly for bulk biological elements that are needed in greater amounts by the cells. In this context, the acidocalcisome might be a new compartment in the yolk, which could work as an additional source of inorganic elements for the embryo. Isolation of acidocalcisomes coupled with proteomics analyses are likely to identify ion-pumps, channels and exchangers in those organelles membranes, and will certainly help in the investigations of the functional role of acidocalcisomes in the yolk system.

PolyP is known to be a Pi store in different models (Kornberg, 1999; Kulaev et al., 1999; Kulaev and Kulakovskaya, 2000). The presence of PolyP stored in acidocalcisomes has been extensively reported (Docampo et al., 2005, Docampo et al., 2010), and changes in its levels according to varied extracellular stimuli were also observed (Ruiz et al., 2001). Interestingly, the levels of polyP in *Rhodnius* acidocalcisomes tend to decrease slightly before the beginning of yolk mobilization, and a decrease in the levels of this polymer was already observed in eggs of the cattle tick *Boophilus microplus* (Campos et al., 2007) and the cockroach *Periplaneta americana* (Gomes et al., 2008). These data suggest that PolyP might be widely used as Pi source for growing embryos, mainly in invertebrates, that do not store massively phosphorylated yolk proteins as phosvitins (Colman et al., 1976).

The fact that the acidocalcisomes store at least ~24 % of the total calcium detected in *R. prolixus* eggs indicates that this organelle is an important calcium storage compartment for the system. Calcium plays essential roles during embryonic development as second messenger for several signaling pathways (Webb and Miller, 2003), and global calcium release events are extensively described at fertilization and early steps of development (Whitaker, 2006). In insects, events of calcium-modulated fusion of yolk granules were described and shown to be important for yolk mobilization

(Ramos et al., 2006; Ramos et al., 2007). Thus, we cannot rule out the possibility that acidocalcisomes can participate in those events of calcium release and reuptake, perhaps combined with the peripheral endoplasmic reticulum via calcium induced calcium release (CICR). Another possibility is that most of the calcium present in the acidocalcisomes is not available for signaling, being bound to PolyP (which is an anionic polymer known to bind to several cations) or complexed with phosphorous in inorganic minerals as calcium phosphates. In this case, calcium from acidocalcisomes could be used as inorganic element supply for the embryo cells in later steps of embryogenesis, when the cell mass of the embryo is increased concomitantly with the consumption of fundamental molecules. Finally, in the ambiance of the yolk system, it is still uncertain if the calcium stored in the acidocalcisomes could be used as a supply for inorganic elements for the embryo, as second messenger available for calcium signaling, or both. Anyway, the fact that this element is stored in such high amounts in those organelles surely suggests an important function of the acidocalcisomes in this ion homeostasis during embryogenesis.

References:

Abreu LA, Valle D, Manso PP, Facanha AR, Pelajo-Machado M, et al. 2004. Proteolytic activity of Boophilus microplus Yolk pro-Cathepsin D (BYC) is coincident with cortical acidification during embryogenesis. *Insect Biochem Mol Biol* 34:443-9

Anderson RG, Orci L. 1988. A view of acidic intracellular compartments. *J Cell Biol* 106:539-43

Ault-Riche D, Fraley CD, Tzeng CM, Kornberg A. 1998. Novel assay reveals multiple pathways regulating stress-induced accumulations of inorganic polyphosphate in Escherichia coli. *J Bacteriol* 180:1841-7

Campos E, Facanha A, Moraes J, da Silva Vaz I, Jr., Masuda A, Logullo C. 2007. A mitochondrial exopolyphosphatase activity modulated by phosphate demand in Rhipicephalus (Boophilus) microplus embryo. *Insect Biochem Mol Biol* 37:1103-7

Chestkov VV, Radko SP, Cho MS, Chrambach A, Vogel SS. 1998. Reconstitution of calcium-triggered membrane fusion using "reserve" granules. *J Biol Chem* 273:2445-51

Colman A, Gadian DG. 1976. 31P nuclear-magnetic-resonance studies on the developing embryos of Xenopus laevis. *European journal of biochemistry / FEBS* 61:387-96

Docampo R, de Souza W, Miranda K, Rohloff P, Moreno SN. 2005. Acidocalcisomes - conserved from bacteria to man. *Nat Rev Microbiol* 3:251-61

Docampo R, Moreno SN. 2001. The acidocalcisome. *Mol Biochem Parasitol* 114:151-9

Docampo R, Ulrich P, Moreno SN. Evolution of acidocalcisomes and their role in polyphosphate storage and osmoregulation in eukaryotic microbes. *Philos Trans R Soc Lond B Biol Sci* 365:775-84

Fagotto F. 1991. Yolk degradation in tick eggs: III. Developmentally regulated acidification of yolk spheres. . *Develop. Growth and Differ.* 33:57-66

Fagotto F. 1995. Regulation of yolk degradation, or how to make sleepy lysosomes. *J Cell Sci* 108 (Pt 12):3645-7

Fausto AM, Gambellini G, Mazzini M, Cecchettini A, Masetti M, Giorgi F. 2001. Yolk granules are differentially acidified during embryo development in the stick insect Carausius morosus. *Cell Tissue Res* 305:433-43

Fialho E, Silveira AB, Masuda H, Silva-Neto MA. 2002. Oocyte fertilization triggers acid phosphatase activity during Rhodnius prolixus embryogenesis. *Insect Biochem Mol Biol* 32:871-80

Fiske CF, Subbarow Y. 1925. The colorimetric determination of phophorus. *Journal of Biological chemistry* 66:375-400

Garcia CR, Ann SE, Tavares ES, Dluzewski AR, Mason WT, Paiva FB. 1998. Acidic calcium pools in intraerythrocytic malaria parasites. *Eur J Cell Biol* 76:133-8

Garcia ES, Macarini JD, Garcia ML, Ubatuba FB. 1975. [Feeding of Rhodnius prolixus in the laboratory]. *Anais da Academia Brasileira de Ciencias* 47:537-45

Gomes FM, Ramos IB, Motta LM, Miranda K, Santiago MF, et al. 2008. Polyphosphate polymers during early embryogenesis of Periplaneta americana. *J Insect Physiol* 54:1459-66

Kornberg A. 1999. Inorganic polyphosphate: a molecule of many functions. *Prog Mol Subcell Biol* 23:1-18

Kulaev I, Kulakovskaya T. 2000. Polyphosphate and phosphate pump. *Annu Rev Microbiol* 54:709-34

Kulaev I, Vagabov V, Kulakovskaya T. 1999. New aspects of inorganic polyphosphate metabolism and function. *J Biosci Bioeng* 88:111-29

Lanzetta PA, Alvarez LJ, Reinach PS, Candia OA. 1979. An improved assay for nanomole amounts of inorganic phosphate. *Anal Biochem* 100:95-7

Leung PL, Li XL. 1996. Multielement analysis in serum of thyroid cancer patients before and after a surgical operation. *Biol Trace Elem Res* 51:259-66

Lowry OH, Rosebrough NJ, Farr AL, Randall RJ. 1951. Protein measurement with the Folin phenol reagent. *J Biol Chem* 193:265-75

Maeshima M. 2000. Vacuolar H(+)-pyrophosphatase. *Biochim Biophys Acta* 1465:37-51

Marchesini N, Luo S, Rodrigues CO, Moreno SN, Docampo R. 2000. Acidocalcisomes and a vacuolar H+-pyrophosphatase in malaria parasites. *Biochem J* 347 Pt 1:243-53

Marchesini N, Ruiz FA, Vieira M, Docampo R. 2002. Acidocalcisomes are functionally linked to the contractile vacuole of Dictyostelium discoideum. *J Biol Chem* 277:8146-53

Marin Briano MV, Castillo Duran C, Uauy Dagach R. 1995. [Mineral balance during nutritional recuperation of infants with protein deficiency]. *Arch Latinoam Nutr* 45:172-7

McNeil PL, Vogel SS, Miyake K, Terasaki M. 2000. Patching plasma membrane disruptions with cytoplasmic membrane. *J Cell Sci* 113 (Pt 11):1891-902

Miranda K, de Souza W, Plattner H, Hentschel J, Kawazoe U, et al. 2008. Acidocalcisomes in Apicomplexan parasites. *Experimental parasitology* 118:2-9

Miranda K, Docampo R, Grillo O, de Souza W. 2004a. Acidocalcisomes of trypanosomatids have species-specific elemental composition. *Protist* 155:395-405

Miranda K, Docampo R, Grillo O, Franzen A, Attias M, et al. 2004b. Dynamics of polymorphism of acidocalcisomes in Leishmania parasites. *Histochem Cell Biol* 121:407-18

Motta LS, da Silva WS, Oliveira DM, de Souza W, Machado EA. 2004. A new model for proton pumping in animal cells: the role of pyrophosphate. *Insect Biochem Mol Biol* 34:19-27

Motta LS, Ramos IB, Gomes FM, de Souza W, Champagne DE, et al. 2009. Proton-pyrophosphatase and polyphosphate in acidocalcisome-like vesicles from oocytes and eggs of Periplaneta americana. *Insect Biochem Mol Biol* 39:198-206

Nordin JH, Beaudoin, E. L., Lin, X. . 1991. Acidification of yolk granules in Blatella germanica eggs coincides with proteolytic processing of vitellin. . *Insect Biochem.* 18:177-92

Oliveira PL, Petretski MDA, Masuda H. 1989. Vitelling processing and degradation during embryogenesis of Rhodnius prolixus. *Insect Biochem*:489-98

Olivera PL, Gondim KC, Guedes d, Masuda H. 1986. Uptake of Yolk Protein in Rhodnius Prolixus. *J. Insect Physiol.*:859-66

Papaj DR. 2000. Ovarian dynamics and host use. *Annual review of entomology* 45:423-48

Ramos IB, Miranda K, de Souza W, Machado EA. 2006. Calcium-regulated fusion of yolk granules during early embryogenesis of Periplaneta americana. *Mol Reprod Dev* 73:1247-54

Ramos IB, Miranda K, de Souza W, Oliveira DM, Lima AP, et al. 2007. Calcium-regulated fusion of yolk granules is important for yolk degradation during early embryogenesis of Rhodnius prolixus Stahl. *J Exp Biol* 210:138-48

Ramos IB, Miranda K, Pace DA, Verbist KC, Lin FY, et al. Calcium and polyphosphate-containing acidic granules of sea urchin eggs are similar to acidocalcisomes but are not the targets for NAADP. *Biochem J*

Ramos IB, Miranda K, Ulrich P, Ingram P, LeFurgey A, et al. Calcium- and polyphosphate-containing acidocalcisomes in chicken egg yolk. *Biol Cell* 102:421-34

Rea PA, Kim Y, Sarafian V, Poole RJ, Davies JM, Sanders D. 1992. Vacuolar H(+)-translocating pyrophosphatases: a new category of ion translocase. *Trends Biochem Sci* 17:348-53

Reimer CL, Crawford BJ. 1995. Identification and partial characterization of yolk and cortical granule proteins in eggs and embryos of the starfish, Pisaster ochraceus. *Dev Biol* 167:439-57

Ruiz FA, Lea CR, Oldfield E, Docampo R. 2004. Human platelet dense granules contain polyphosphate and are similar to acidocalcisomes of bacteria and unicellular eukaryotes. *J Biol Chem* 279:44250-7

Ruiz FA, Marchesini N, Seufferheld M, Govindjee, Docampo R. 2001a. The polyphosphate bodies of Chlamydomonas reinhardtii possess a proton-pumping pyrophosphatase and are similar to acidocalcisomes. *J Biol Chem* 276:46196-203

Ruiz FA, Rodrigues CO, Docampo R. 2001b. Rapid changes in polyphosphate content within acidocalcisomes in response to cell growth, differentiation, and environmental stress in Trypanosoma cruzi. *J Biol Chem* 276:26114-21

Saito K, Ohtomo R, Kuga-Uetake Y, Aono T, Saito M. 2005. Direct labeling of polyphosphate at the ultrastructural level in Saccharomyces cerevisiae by using the affinity of the polyphosphate binding domain of Escherichia coli exopolyphosphatase. *Applied and environmental microbiology* 71:5692-701

Sardet C, Prodon F, Dumollard R, Chang P, Chenevert J. 2002. Structure and function of the egg cortex from oogenesis through fertilization. *Dev Biol* 241:1-23

Schier AF. 2007. The maternal-zygotic transition: death and birth of RNAs. *Science* 316:406-7

Scott DA, de Souza W, Benchimol M, Zhong L, Lu HG, et al. 1998. Presence of a plant-like proton-pumping pyrophosphatase in acidocalcisomes of Trypanosoma cruzi. *J Biol Chem* 273:22151-8

Seufferheld M, Lea CR, Vieira M, Oldfield E, Docampo R. 2004. The H(+)-pyrophosphatase of Rhodospirillum rubrum is predominantly located in polyphosphate-rich acidocalcisomes. *J Biol Chem* 279:51193-202

Seufferheld M, Vieira MC, Ruiz FA, Rodrigues CO, Moreno SN, Docampo R. 2003. Identification of organelles in bacteria similar to acidocalcisomes of unicellular eukaryotes. *J Biol Chem* 278:29971-8

Singla PN, Chand P, Kumar A, Kachhawaha JS. 1998. Serum magnesium levels in protein-energy malnutrition. *J Trop Pediatr* 44:117-9

Smith SA, Morrissey JH. 2007. Sensitive fluorescence detection of polyphosphate in polyacrylamide gels using 4',6-diamidino-2-phenylindol. *Electrophoresis* 28:3461-5

Terasaki M, Henson J, Begg D, Kaminer B, Sardet C. 1991. Characterization of sea urchin egg endoplasmic reticulum in cortical preparations. *Dev Biol* 148:398-401

Webb SE, Miller AL. 2003. Calcium signalling during embryonic development. *Nat Rev Mol Cell Biol* 4:539-51

Whitaker M. 2006. Calcium at fertilization and in early development. *Physiol Rev* 86:25-88

WHO. 2008. Report of the expert committee on the control of Chagas disease

Yamahama Y, Uto N, Tamotsu S, Miyata T, Yamamoto Y, et al. 2003. In vivo activation of pro-form Bombyx cysteine protease (BCP) in silkmoth eggs: localization of yolk proteins and BCP, and acidification of yolk granules. *J Insect Physiol* 49:131-40

Table 1: Elemental quantification in the eggs using optical emission spectroscopy

	Phosphorus	Calcium	Sodium	Magnesium
Egg	141 ± 2.8	18 ± 0.6	97 ± 2.1	20 ± 0.6
Yolk	138 ± 4.6	13 ± 0.6	95 ± 5.2	18 ± 0.6
Accs	3.8 ± 1.0	4.2 ± 0.9	0.11 ± 0.01	0.31 ± 0.1

Table 1: Relative elemental quantification in the acidocalcisomes during early embryogenesis (Cliff-Lorimer method)

Days of development	Magnesium	Phosphorus	Chloride	Potassium	Calcium
0	3.4 ± 0.5	44.3 ± 2.4	2.4 ± 1.2	14.7 ± 0.8	35.1 ± 0.7
1	4.4 ± 0.3	46.6 ± 2.2	1.3 ± 0.8	12.9 ± 2.2	34.7 ± 2.6
2	5.6 ± 1.2	45.6 ± 1.2	1.7 ± 1.1	14.9 ± 2.0	32.1 ± 3.3
3	4.9 ± 0.6	46.2 ± 1.3	1.4 ± 0.6	6.3 ± 1.1	41.1 ± 1.1
4	4.7 ± 0.6	45.8 ± 1.6	0.9 ± 0.5	6.2 ± 2.7	42.3 ± 2.0
5	4.4 ± 0.9	42.4 ± 1.2	1.9 ± 0.5	14.2 ± 3.7	36.9 ± 3.6
Non fertilized	4.5 ± 0.7	46.81 ± 1.6	1.2 ± 0.4	9.1 ± 2.4	44.3 ± 3.2

Figure legends:

Figure 1: Electron-dense small vesicles in the eggs have the typical elemental composition of acidocalcisomes. A, B, Suspensions of the eggs organelles were applied to formvar-coated grids and directly observed in the transmission electron microscope. YG: yolk granule. Black arrows: small electron-dense vesicles. Bars: A, 10 μm. B, 1 μm. **C,** X-ray spectrum of the yolk granule shown in A (white arrow). **D,** X-ray spectrum of the electron-dense vesicle pointed in B (arrowhead). **E, F** Standard transmission electron micrographs of the egg cortex showing the presence of empty vesicles. Ac: acidocalcisome. Vm: vitelline membrane. Oo: egg cytoplasm. Bars: 1 μm; 200 nm.

Figure 2: Localization of the vacuolar H^+-PPase in small vesicles in the egg cortex. A, *Western blotting* using anti-VH^+-PPase polyclonal antibodies. *Lane cruzi: T. Cruzi* epimastigotes. *Lane MØ:* human macrophages. *Lane egg:* total egg homogenates. Arrows indicate molecular weighs in kDa. **B, C, D, E,** Immunofluorescence of the VH^+-PPase in the egg organelles adhered to glass slides. Arrows indicate labeled small vesicles. YG: yolk granule. Bars: 10 μm. **F,** Immunogold electron microscopy of LR-White embedded samples showing the localization of the VH^+-PPase (gold particles) in the periphery of empty vesicles. Bar: 500 nm. **G,** quantification of gold particles in the different organelles of the egg cortex. (*) indicate significant difference (One Way ANOVA, $p < 0.05$). **H, I,** Confocal laser scanning image (optical section) of the VH^+-PPase localization in a thick longitudinal section of the egg. (See also supplementary movie 1). Bars: 200 μm.

Figure 3: Isolation of acidocalcisome-like organelles. A, B, Fraction of enriched acidocalcisomes (accs fraction) observed in formvar-coated grids. Bars: 3 μm. **C,** X-ray microanalysis spectrum of the acidocalcisome pointed in B. **D,** Standard transmission electron microscopy of the fixed acidocalcisomes in the fraction, evidencing the integrity of the organelle membranes. Ac: acidocalcisome. Bar: 1 μm. **E, F,** Freeze-fracture of the fixed acidocalcisomes in the fraction showing E- and P- faces of fractured membranes, respectively. Bars: 500 nm.

Figure 4: Vacuolar H^+-PPase and PolyP co-localize to the acidocalcisomes. VH^+-PPase and PolyP were detected in the accs-fractions and yolk-fractions. **A,** *Western blotting* using anti-VH^+-PPase polyclonal antibodies in the yolk-fraction (*lane yolk*) and accs-fraction (*lane accs*), showing enrichment of the enzyme in the acidocalcisomes. Samples with *T. cruzi* epimastigotes (*lane cruzi*) were loaded as a positive control. All lanes were loaded with 60 μg of protein. **B,** Membrane preparations of yolk-fractions and accs-fractions were obtained and tested for PPi hydrolysis activity. Data are from 3 experiments, and show means ± S.E.M. (*) indicates significant differences (t-test, $p<0.05$). **C,** Short- and long-chain PolyP were extracted and quantified in the yolk and accs fraction. Data are from 4 experiments, and show means ± S.E.M. (*) indicates significant differences (One way ANOVA, $p<0.05$). **D, E, F, G,** co-localization of poly P, using the recombinant poly P binding domain of *E. coli* exopolyphosphatase (PPBD) linked with an Xpress epitope tag, and VH^+-PPase, using anti-VH^+-PPase polyclonal antibodies. Bars: 10 μm.

Figure 5: PPi hydrolysis in acidocalcisomes is sensitive to specicific inhibitors and immunodetection is associated with membrane fractions. A, PPi hydrolysis activity was measured in membrane fractions of the yolk-fractions and accs-fractions. AMDP (40 μM) was added where indicated. Data are from 4 experiments, and show means ± S.E.M. (*) indicates significant differences (One way ANOVA, $p<0.05$). **B,** accs-fractions were separated into soluble and insoluble components by differential ultra centrifugation and tested in *Western blotting* for VH^+-PPase. *Lane MØ:* human macrophages (negative control). *Lane accs:* accs-fraction, before membrane preparations. *Lane soluble:* soluble (supernatant) fraction of the acidocalcisomes membrane preparation. *Lane insoluble:* insoluble (pellet) fraction of the acidocalcisomes membrane preparation.

Figure 6: Incubation of acidocalcisomes with acridine orange (AO) in different days of embryogenesis. Accs fractions were obtained from eggs of different days of embryogenesis and incubated in the presence of 6 μM AO. **A,** acidocalcisomes from day-

0 eggs. **B,** acidocalcisomes from day-1 eggs. **C,** acidocalcisomes from day -2 eggs. **D,** acidocalcisomes from day-3 eggs. Bars: 15 μm.

Figure 7: PolyP quantifications in the acidocalcisomes in different days of embryogenesis. A, agarose gel electrophoresis of poly P stained with DAPI. *Lane P75*: 5 μg of commercial $polyP_{75+}$; *Lanes 0, 1, 2* and *3* indicate the days of development in which polyP was extracted from accs and loaded in the gel. **B**, short- and long-chain poly P were quantified in the accs-fractions using the recombinant exopolyphosphatase of *Saccharomyces cerevisiae*, as described under "Materials and Methods". Data are from 4 experiments, and show means ± S.E.M. (*) indicates significant differences (One way ANOVA, $p<0.05$).

Table 1: Elemental quantification in the eggs using optical emission spectroscopy. Results are expressed in micrograms, as mean ± SD of three independent quantifications, from 165 mg of eggs (wet weight) which corresponds to 23 ± 1.4 mg of dry weight or approximately 200 eggs.

Table 2: Relative elemental quantification in the acidocalcsisomes during early embryogenesis (Cliff-Lorimer method). Semi quantitative X-ray microanalyses of the acidocalcisomes in different days of embryogenesis in eggs of *Rhodnius prolixus*. Numbers are expressed as the atomic % of each element (mean ± SEM, $n_{accs} = 7$).

Figure 1

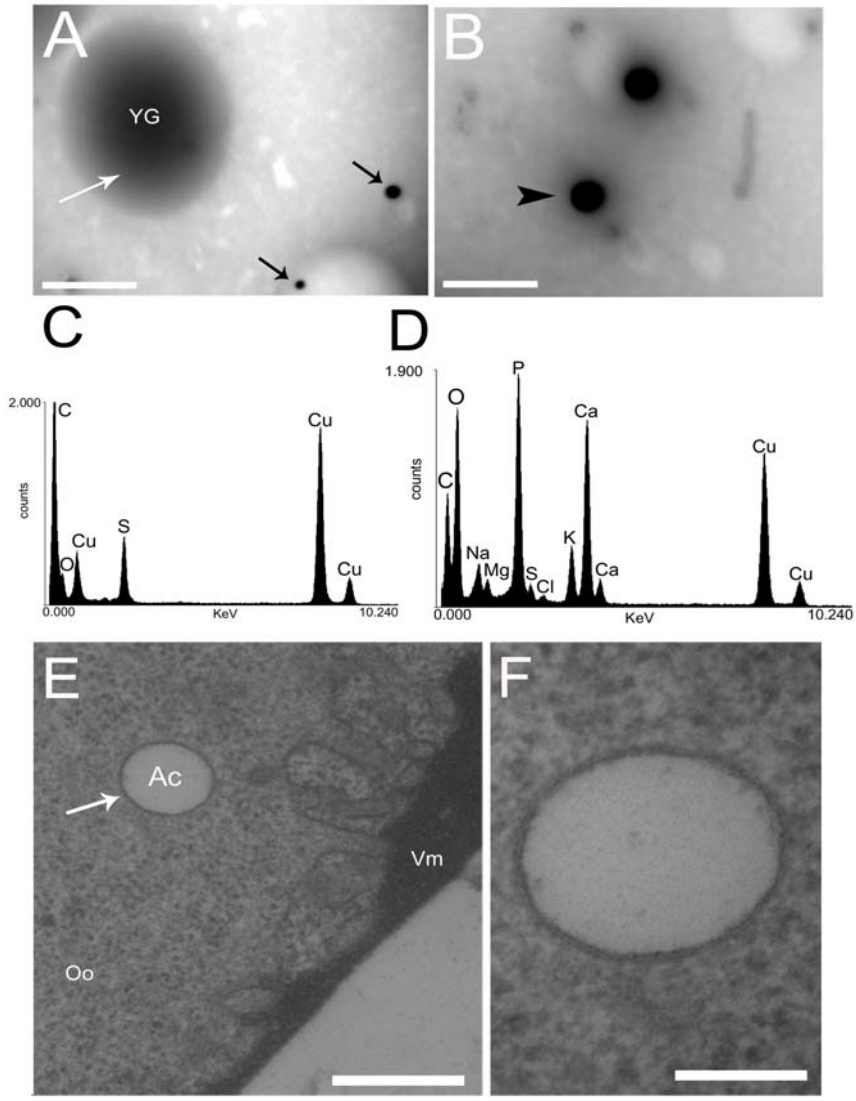
A
YG
B
C
2.000
C
Cu
S
Cu
O
Cu
counts
0.000
KeV
10.240
D
1.900
P
O
Ca
Cu
C
Na
Mg
S
Cl
K
Ca
Cu
counts
0.000
KeV
10.240
E
Ac
Vm
Oo
F

Figure 2

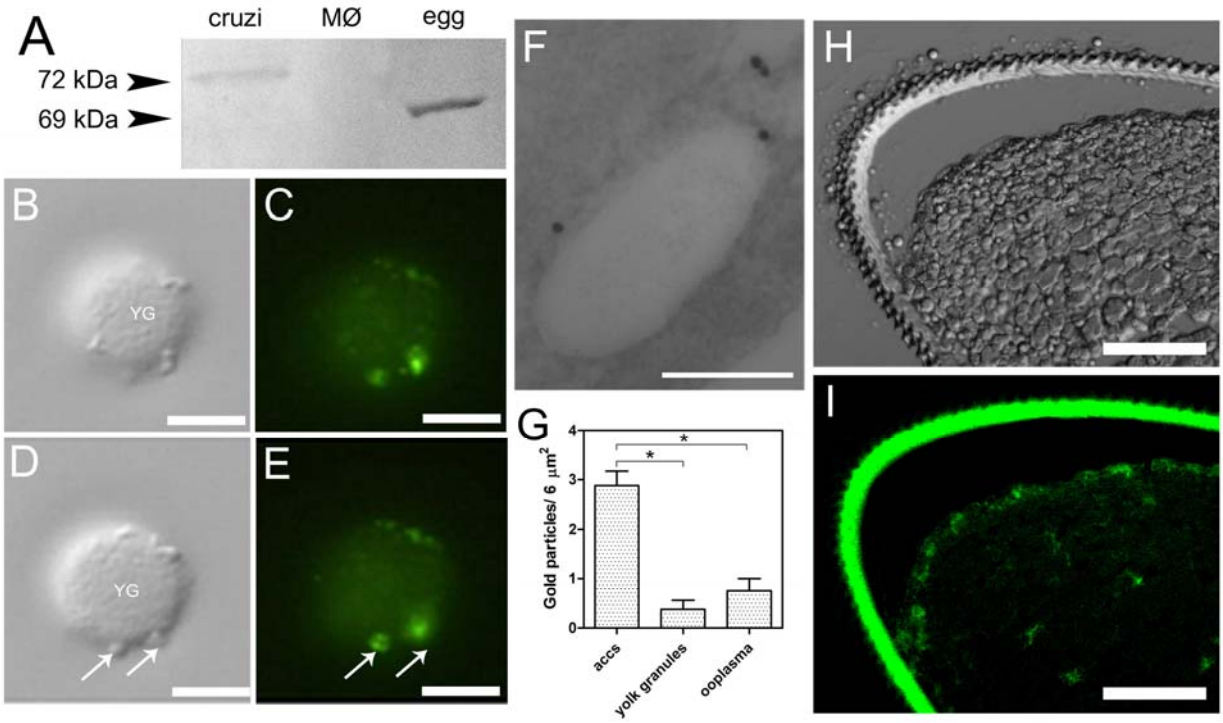
A
cruzi
MØ
egg
72 kDa
69 kDa
B
YG
C
D
YG
E
F
G
Gold particles/ 6 µm²
4
3
2
1
0
*
*
accs
yolk granules
ooplasma
H
I

Supplementary movie1

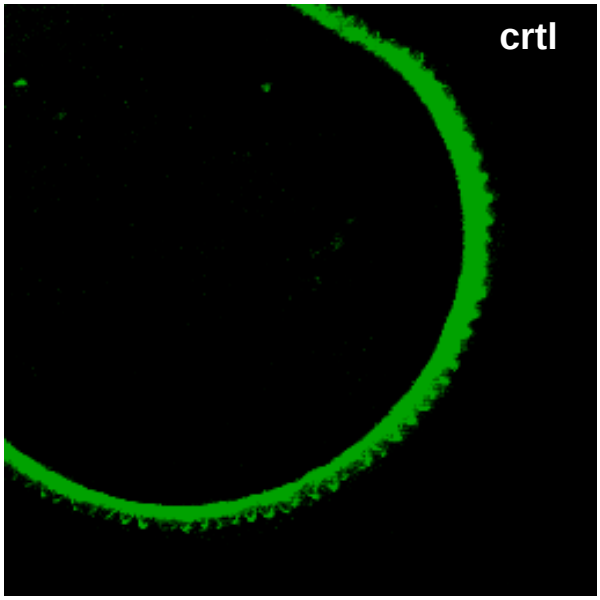

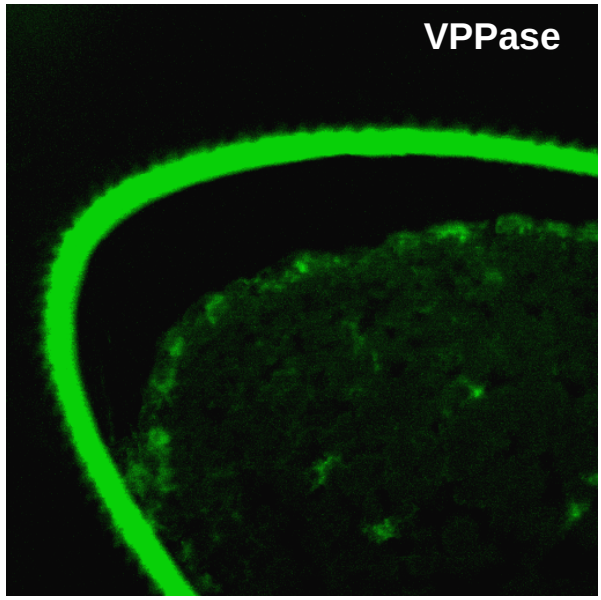

Figure 3

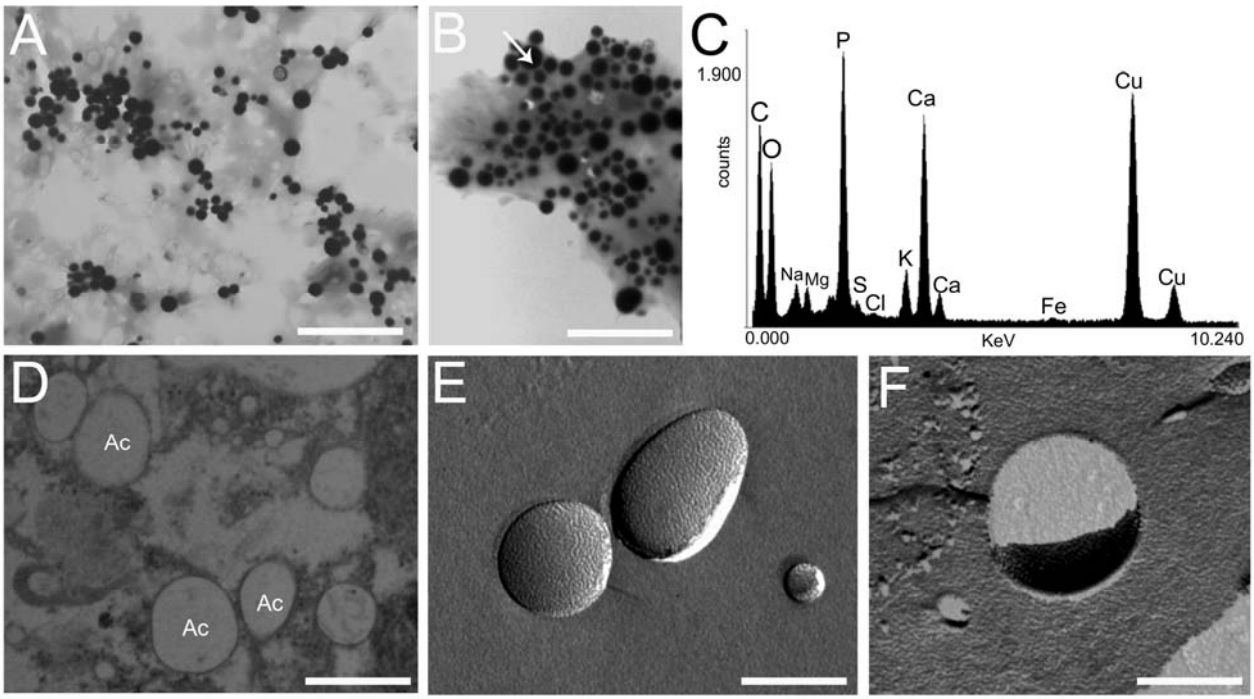
A
B
C
1.900
counts
C
O
P
Ca
Cu
Na
Mg
S
Cl
K
Ca
Fe
Cu
0.000
KeV
10.240
D
Ac
Ac
Ac
E
F

Figure 4

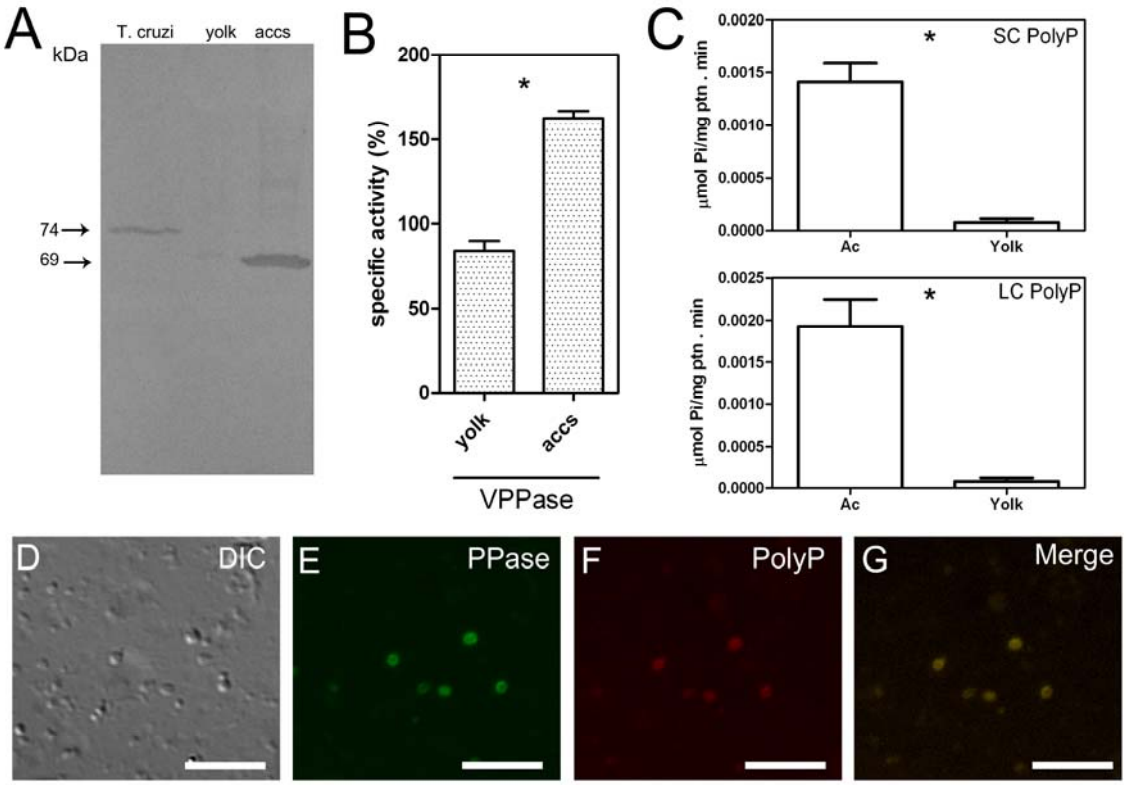
A
kDa
T. cruzi
yolk
accs
74
69
B
specific activity (%)
200
150
100
50
0
*
yolk
accs
VPPase
C
SC PolyP
µmol Pi/mg ptn . min
0.0020
0.0015
0.0010
0.0005
0.0000
*
Ac
Yolk
LC PolyP
µmol Pi/mg ptn . min
0.0025
0.0020
0.0015
0.0010
0.0005
0.0000
*
Ac
Yolk
D
DIC
E
PPase
F
PolyP
G
Merge

Figure 5

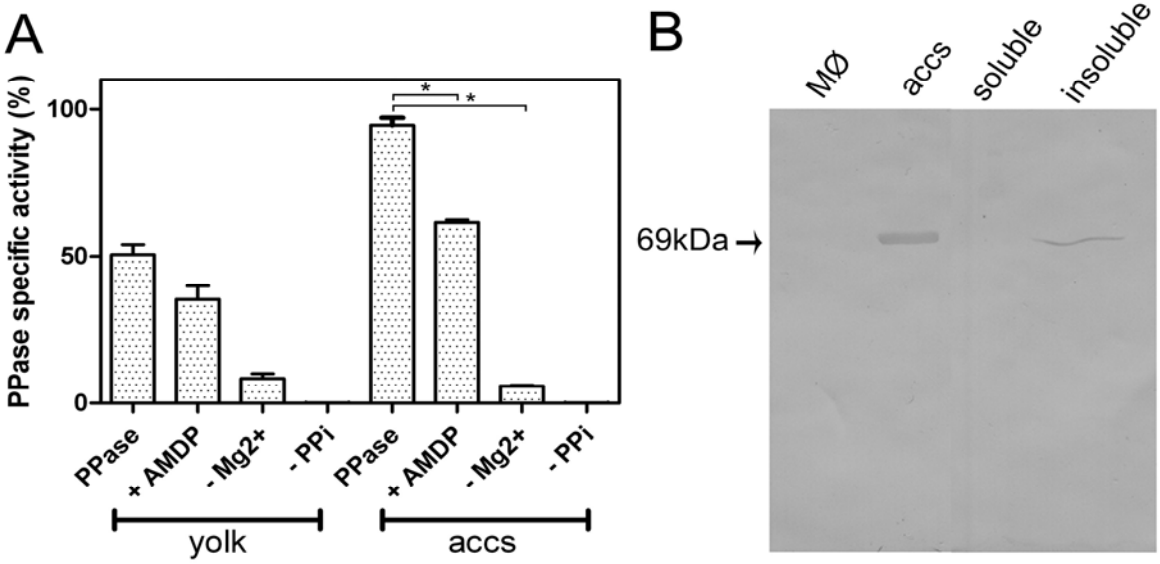
A
PPase specific activity (%)
100
50
0
*
*
PPase
+ AMDP
- Mg2+
- PPi
PPase
+ AMDP
- Mg2+
- PPi
yolk
accs
B
MØ
accs
soluble
insoluble
69kDa

Figure 6

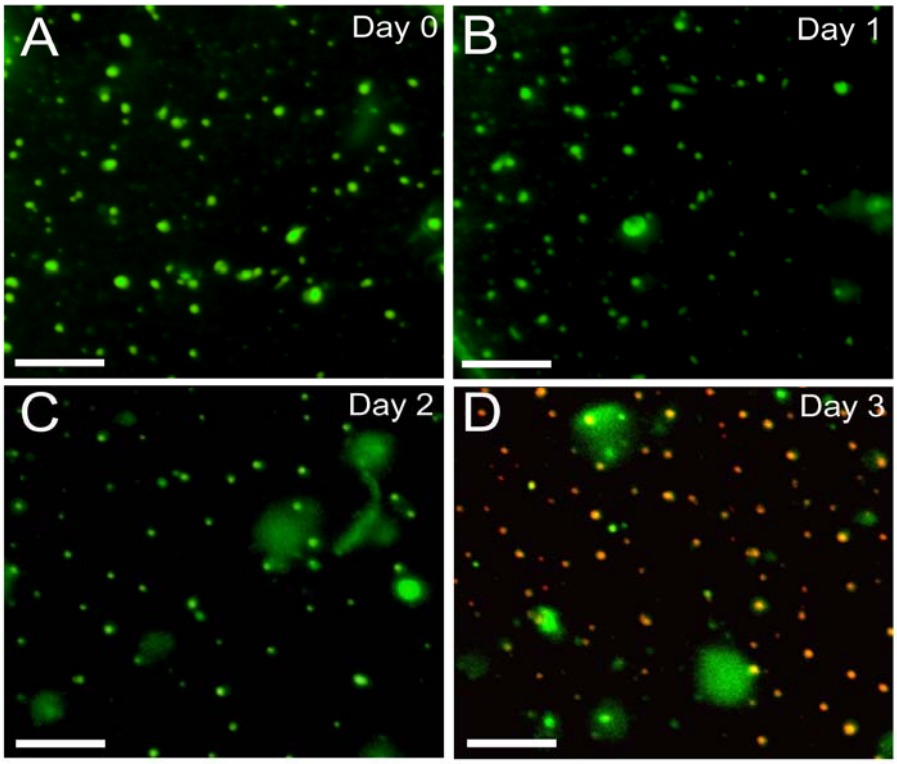

Figure 7

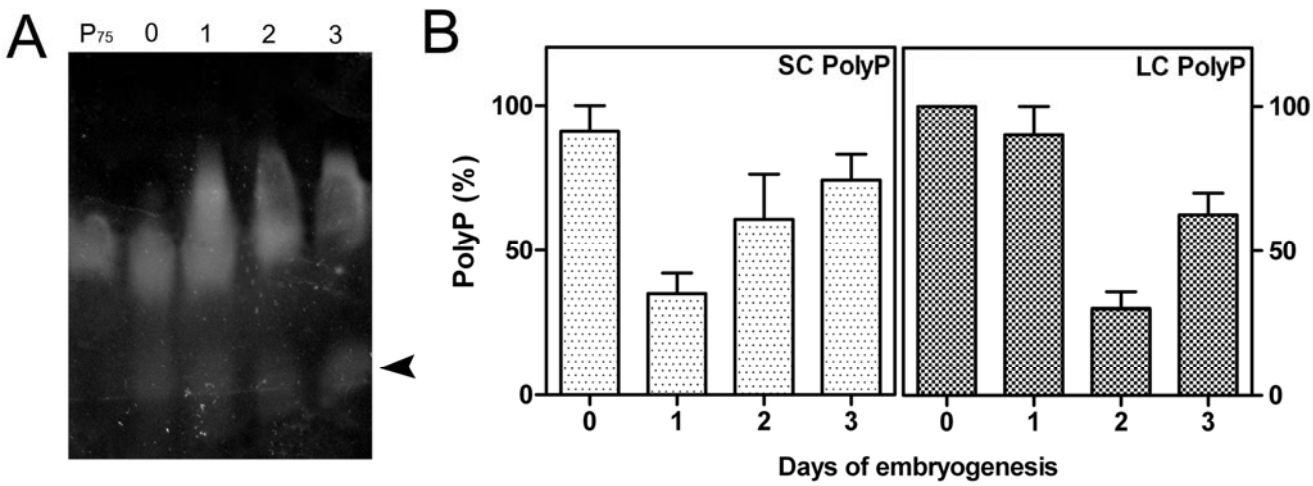
A
P75
0
1
2
3
B
SC PolyP
LC PolyP
PolyP (%)
100
50
0
0
1
2
3
0
1
2
3
Days of embryogenesis

7- Anexo III:

BJ www.biochemj.org

Biochem. J. (2010) **429**, 485–495 (Printed in Great Britain) doi:10.1042/BJ20091956

This is a data-enriched, interactive PDF that provides the gateway to a world of information when opened in Utopia Documents
Download FREE software now

BJ Cell

multimedia online data

Calcium- and polyphosphate-containing acidic granules of sea urchin eggs are similar to acidocalcisomes, but are not the targets for NAADP

Isabela B. RAMOS*†, Kildare MIRANDA†‡, Douglas A. PACE*, Katherine C. VERBIST*, Fu-Yang LIN§, Yonghui ZHANG‖, Eric OLDFIELD§‖, Ednildo A. MACHADO†‡, Wanderley DE SOUZA† and Roberto DOCAMPO*[1]

*Department of Cellular Biology and Center for Tropical and Emerging Global Diseases, University of Georgia, Athens, GA 30602, U.S.A., †Instituto de Biofísica Carlos Chagas Filho, and Instituto Nacional de Ciência e Tecnologia em Bioimagens e Biologia Estrutural, Universidade Federal do Rio de Janeiro, Rio de Janeiro, RJ 21941, Brazil, ‡Instituto Nacional de Metrologia Normalização e Qualidade Industrial, Diretoria de Programas, Xerém, Rio de Janeiro, RJ 25250, Brazil, §Center for Biophysics and Computational Biology, University of Illinois at Urbana-Champaign, Urbana, IL 61801, U.S.A., and ‖Department of Chemistry, University of Illinois at Urbana-Champaign, Urbana, IL 61801, U.S.A.

Acidocalcisomes are acidic calcium-storage compartments described from bacteria to humans and characterized by their high content in poly P (polyphosphate), a linear polymer of many tens to hundreds of P_i residues linked by high-energy phosphoanhydride bonds. In the present paper we report that millimolar levels of short-chain poly P (in terms of P_i residues) and inorganic PP_i are present in sea urchin extracts as detected using ^{31}P-NMR, enzymatic determinations and agarose gel electrophoresis. Poly P was localized to granules randomly distributed in the sea urchin eggs, as shown by labelling with the poly-P-binding domain of *Escherichia coli* exopolyphosphatase. These granules were enriched using iodixanol centrifugation and shown to be acidic and to contain poly P, as determined by Acridine Orange and DAPI (4′,6′-diamidino-2-phenylindole) staining respectively. These granules also contained large amounts of calcium, sodium, magnesium, potassium and zinc, as detected by X-ray microanalysis, and bafilomycin A_1-sensitive ATPase, pyrophosphatase and exopolyphosphatase activities, as well as Ca^{2+}/H^+ and Na^+/H^+ exchange activities, being therefore similar to acidocalcisomes described in other organisms. Calcium release from these granules induced by nigericin was associated with poly P hydrolysis. Although NAADP (nicotinic acid–adenine dinucleotide phosphate) released calcium from the granule fraction, this activity was not significantly enriched as compared with the NAADP-stimulated calcium release from homogenates and was not accompanied by poly P hydrolysis. GPN (glycyl-L-phenylalanine-naphthylamide) released calcium when added to sea urchin homogenates, but was unable to release calcium from acidocalcisome-enriched fractions, suggesting that these acidic stores are not the targets for NAADP.

Key words: acidocalcisome, calcium, glycyl-L-phenylalanine-naphthylamide (GPN), polyphosphate, sea urchin egg, vacuolar H^+-ATPase.

INTRODUCTION

The sea urchin egg has been an invaluable model for studying Ca^{2+} homoeostasis and signalling. Intracellular Ca^{2+} increases upon fertilization and is important for the generation of the fertilization envelope and for initiation of the biochemical events that serve to wake the egg from a state of dormancy [1].

A number of second messengers able to release Ca^{2+} from different intracellular stores were described for the first time in sea urchin eggs, such as cADPR (cyclic adenosine diphosphate ribose) [2] and NAADP (nicotinic acid–adenine dinucleotide phosphate) [3]. Whereas cADPR and IP_3 (inositol 1,4,5-trisphosphate) release Ca^{2+} from the ER (endoplasmic reticulum) of sea urchin eggs, NAADP does it from acidic vesicles that were proposed to be lysosome-like organelles [4], possibly the so-called yolk platelets [5]. NAADP was also shown to increase the pH of these acidic vesicles by a mechanism coupled to Ca^{2+} release via the NAADP receptor [6]. It was proposed that the fall in the luminal $[Ca^{2+}]$ allows H^+ to bind to vacated sites on a luminal polyanionic matrix, thus resulting in alkalinization of the store [6].

The findings that NAADP released Ca^{2+} from acidic organelles of sea urchin eggs [4] led to investigations as to whether NAADP was also able to mobilize Ca^{2+} from lysosomes of mammalian cells. NAADP was shown initially to release Ca^{2+} from acidic organelles of pancreatic acinar and β-cells [7,8], coronary artery myocytes [9] and the phaeochromocytoma cell line PC12 [10], but apparently not from T-lymphocyte cell lines [11,12]. It was found that NAADP-induced Ca^{2+} release was associated with endolysosomal function because the Ca^{2+}-release response was dependent on a proton gradient maintained by an ATP-dependent vacuolar-type proton pump that is primarily present in the endocytic pathway [13]. Accumulating evidence showed that this NAADP-sensitive Ca^{2+} store was unique and distinct from IP_3- and cADPR-sensitive Ca^{2+} stores [14,15], and results suggested that, at least in rat liver, it is the lysosome [13]. Two-pore channels have recently emerged as potential receptors for NAADP in the lysosomes of mammalian cells [16–18], and they have now been identified as NAADP targets for Ca^{2+} release in the sea urchin [19].

Sea urchin eggs have a number of intracellular vesicles and several types of granules in their cytoplasm, as identified by electron microscopy. Among them are the cortical granules, which are located close to the surface and are exocytosed upon fertilization and formation of the fertilization envelope, the yolk platelets, which are an abundant group of organelles of high

Abbreviations used: ASW, artificial sea water; cADPR, cyclic adenosine diphosphate ribose; DAPI, 4′,6′-diamidino-2-phenylindole; ER, endoplasmic reticulum; GluIM, gluconate intracellular-like medium; GPN, glycyl-L-phenylalanine-naphthylamide; IP_3, inositol 1,4,5-trisphosphate; LC, long-chain; NAADP, nicotinic acid–adenine dinucleotide phosphate; poly P, polyphosphate; PPase, pyrophosphatase; PPBD, poly-P-binding domain; PPX, exopolyphosphatase; rPPX1, recombinant *Saccharomyces cerevisiae* PPX1; SC, short-chain; TBS, Tris-buffered saline.

[1] To whom correspondence should be addressed (email rdocampo@uga.edu).

© 2010 The Author(s)

The author(s) has paid for this article to be freely available under the terms of the Creative Commons Attribution Non-Commercial Licence (http://creativecommons.org/licenses/by-nc/2.5/) which permits unrestricted non-commercial use, distribution and reproduction in any medium, provided the original work is properly cited.

Biochemical Journal

and uniform electron-density and that can occupy approximately half the volume of the egg [20], and the clear granules [21,22] characterized by their clear appearance, that are distributed at random in the unfertilized eggs [21]. Both the cortical granules [4] and the clear granules [21] are acidic, whereas the yolk platelets increase their acidity from pH 6.8 to pH 6.1 upon fertilization [23]. These changes in pH in yolk platelets (alkalinization on NAADP stimulation and acidification upon fertilization) reveals the multiphasic nature of this phenomenon, with the NAADP-induced response being a 'rapid' response and acidification upon fertilization being a 'slow' response.

Yolk platelets have been proposed to be the acidic organelles responsible for Ca^{2+} release upon NAADP stimulation [4,5]. This is in agreement with experiments using eggs stratified by centrifugation. Under these conditions, yolk platelets localize to the centrifugal pole, which is the site where the higher Ca^{2+} release occurs upon local photolysis of caged NAADP [24] and is opposite to the nucleus and lipid droplets. However, photolysis of NAADP at the centripetal pole, which is the region where clear granules localize, also results in a transient Ca^{2+} release [24]. Interestingly this region of clear granules is the one more intensely labelled with Acridine Orange [21], suggesting that clear granules are more acidic than yolk platelets. In contrast LysoTracker Red appears to preferentially label the yolk platelets [4] and this labelling disappears after treatment with GPN (glycyl-L-phenylalanine-naphthylamide), a substrate of the lysosomal cathepsin C that selectively disrupts these organelles via osmotic lysis [25]. Interestingly, although yolk platelets are distributed at random in the sea urchin egg, NAADP induces a peripheral vesicular alkalinization, even when injected into the middle of the egg, suggesting the presence of a subpopulation of NAADP-sensitive stores [6].

The clear granules of sea urchin eggs are morphologically very similar to acidocalcisomes, which are lysosome-related organelles characterized by their abundant content of the polyanion poly P (polyphosphate) bound to cations such as calcium, magnesium and zinc [26]. Acidocalcisomes are present in trypanosomatid and apicomplexan parasites [26], as well as in the green alga *Chlamydomonas reinhardtii* [27] and the slime mould *Dictyostelium discoideum* [28], and were also identified in bacteria [29,30], human platelets [31], and insect [32] and chicken [33] eggs. As acidocalcisomes are acidic, rich in Ca^{2+} and in the polyanion poly P, and it has been shown that Ca^{2+} can be released from them after their alkalinization with NH_4Cl or by the K^+/H^+ ionophore nigericin [34], we investigated whether some of the acidic granules of sea urchin eggs are equivalent to acidocalcisomes, and whether they are also targets for NAADP-stimulated Ca^{2+} release.

MATERIALS AND METHODS

Chemicals and reagents

ATP, nigericin, valinomycin, DAPI (4′,6-diamidino-2-phenylindole), IP_3, NAADP, PP_i, tripolyphosphate (poly P_3), poly P_{75+} and protease inhibitors (P8340) were purchased from Sigma Chemical. Coomassie Blue protein assay reagent was from Bio-Rad Laboratories. The anti-Xpress epitope monoclonal antibody and Fluo-3 were from Invitrogen. Bafilomycin A_1 was from Kamiya Biomedical. *Escherichia coli* strain CA38 pTrcPPX1 was kindly provided by Professor Arthur Kornberg (Stanford University School of Medicine, Stanford, CA, U.S.A.). *E. coli* DH5a harbouring pTrc-PPBD was provided by Dr Katsuharu Saito (Shinshu University, Nagano-Ken, Japan). LysoTracker Red DND-99 was from Invitrogen. All other reagents were of analytical grade.

Egg collection and homogenate preparation

Sea urchins were obtained from Gulf Specimen Marine Laboratories or from the Guanabara Bay (Rio de Janeiro, Brazil). Eggs from *Lytechinus variegatus* or *Arbacia punctulata* were harvested by intracoelomic injection of 0.5 M KCl and collected in ASW (artificial sea water; 435 mM NaCl, 40 mM $MgCl_2$, 15 mM $MgSO_4$, 11 mM $CaCl_2$, 10 mM KCl, 2.5 mM $NaHCO_3$ and 20 mM Tris base, pH 8.0). Egg homogenates were prepared as described previously [6]. Briefly, eggs were washed four times in Ca^{2+}-free ASW (the first two washes containing 1 mM EGTA) and then washed in GluIM (gluconate intracellular-like medium; 250 mM potassium gluconate, 250 mM *N*-methylglucamine, 20 mM Hepes and 1 mM $MgCl_2$, pH 7.2) without an ATP-generating system. Eggs were then homogenized in the same medium in the presence of protease inhibitors (P8340, Sigma). The homogenate (50 %, v/v) was centrifuged at 13000 ***g*** for 10 s at 4 °C, and the supernatant was sequentially diluted in equal volumes of GluIM over a period of 3 h, as described previously [6]. Microscopy experiments were performed with both species of sea urchin eggs with similar results. All other experiments were performed using *L. variegatus* eggs.

Isolation of dense granules

The egg homogenate (8 ml, $\sim 4 \times 10^5$ eggs/ml) was centrifuged at 5000 ***g*** for 10 min at 4 °C. The supernatant (4 ml) was then loaded on to the top of a 20 % iodixanol fractionation medium (OptiPrep™, Greiner Bio-One) diluted in GluIM buffer (20 ml). The preparation was centrifuged at 60000 ***g*** for 60 min at 4 °C. The pellet was resuspended in 100 μl of GluIM buffer, washed at least three times in GluIM, and used as the dense granule fraction.

Electron microscopy and X-ray microanalysis

For imaging, whole cells and dense granule fractions were washed first in 100 mM Hepes buffer (pH 7.4) and directly applied to Formvar-coated 200-mesh copper grids, allowed to adhere for 10 min at room temperature (22 °C), blotted dry and observed directly in an energy-filtering Zeiss 902 transmission electron microscope. This treatment avoided salt precipitation. Electron energy-filtered images were taken at an energy loss of 70 eV using a spectrometer slit width of 10 eV. For X-ray microanalysis, samples were examined in a JEOL 1200 EX transmission electron microscope. X-rays were collected for 150 s using a Si (Li) detector with a Norvar window on a 0–10 KeV energy range with a resolution of 10 eV/channel. Analysis was performed using a Noran Voyager III analyser with a standard analysis identification program. No changes in the size of the organelles were detected when the fractions were suspended in 100 mM Hepes (pH 7.4), plus 300 mM or 400 mM sucrose, instead of 100 mM Hepes alone.

For conventional electron microscopy, eggs and dense granule fractions were fixed in 4 % formaldehyde and 2.5 % glutaraldehyde diluted in 0.1 M sodium cacodylate buffer (pH 7.3) at 4 °C for 24 h, and then embedded in epoxy resin, sectioned and stained using standard methods. To verify that osmotic conditions did not change the size of organelles, the fixative was also diluted in ASW, but no changes in the morphology of different organelles were observed.

© 2010 The Author(s)
The author(s) has paid for this article to be freely available under the terms of the Creative Commons Attribution Non-Commercial Licence (http://creativecommons.org/licenses/by-nc/2.5/) which permits unrestricted non-commercial use, distribution and reproduction in any medium, provided the original work is properly cited.

Extraction of PP_i and long- and short-chain poly P

Egg homogenates were centrifuged at 16000 ***g*** for 30 min at 4 °C and the pellet was treated with methods to extract either LC (long-chain) or SC (short-chain) poly P and PP_i. Different samples were used for each method. Aliquots of known volumes from different steps of the dense granule fraction separation were also obtained and centrifuged at 14000 ***g*** for 30 min at 4 °C. The pellets were extracted and used for poly P and PP_i determinations. LC poly P extraction was performed as described by Ault-Riché et al. [35]. SC poly P and PP_i extraction was performed as described by Ruiz et al. [34]. Protein measurements were performed using the Bradford protein assay kit (Bio-Rad Laboratories).

Analysis of PP_i and poly P

Poly P levels were determined from the amount of P_i released upon treatment with an excess of rPPX1 [recombinant *Saccharomyces cerevisiae* PPX (exopolyphosphatase) 1]. The recombinant enzyme was prepared as described previously [34]. Aliquots of LC and SC poly P extracts (always less than 1.5 nmol) were incubated for 15 min at 37 °C with 60 mM Tris/HCl (pH 7.5), 6.0 mM $MgCl_2$ and 3000–5000 units of purified rPPX1 in a final volume of 100 μl. One unit corresponds to the release of 1 pmol of P_i/min at 35 °C. Release of P_i was monitored using the method of Lanzetta et al. [36]. For PP_i quantification, the procedure was essentially the same, but using an excess of soluble TiPPase [thermostable inorganic PPase (pyrophosphatase); New England Biolabs], 0.04 unit per reaction, in 50 mM Tris/HCl (pH 7.5) and 5 mM $MgCl_2$, for 30 min at 35 °C. To detect poly P degradation by dense granule fractions in the presence of 10 μM nigericin, aliquots were collected after 5, 10 and 15 min and centrifuged at 14000 ***g*** for 10 s, and the pellets were used for poly P extraction and determinations, as described above. The intracellular concentration of phosphate compounds was calculated taking into account a volume of 904 pl/egg.

NMR spectroscopy

For NMR analyses, EDTA was added to poly P extracts to a final concentration of 25 mM prior to adjusting to pH 7.0. All of the extracts contained 10 % (v/v) ^2H_2O to provide a field-frequency lock. Phosphorus NMR spectra were acquired at 242.8 MHz using a Varian INOVA NMR spectrometer equipped with a 14.1 T Oxford Instruments magnet. For perchloric acid extracts, 10784 transients were collected at room temperature using 25 μs (90°) pulse excitation, a 20-kHz spectral width, 32768 data points and a 5 s recycle time. Inverse gated proton decoupling was used to remove NOE (nuclear Overhauser effect) and J-coupling effects. The chemical shifts of all the ^{31}P spectra were referenced to 0 p.p.m. using an 85 % phosphoric acid external standard. The specific assignments of individual resonances were based on published chemical shifts and ^{31}P–^{31}P scalar couplings and, in some cases, co-addition of authentic compounds. NMR spectra were processed using the MacNuts 0.9.4 program (Acorn NMR) and included base-line correction, zero-filling and a 2-Hz exponential line broadening prior to Fourier transformation.

Fluorescence microscopy

For poly P localization in whole eggs, the recombinant PPBD (poly-P-binding domain) of *E. coli* PPX linked to an Xpress epitope tag was used, as described previously [37]. Briefly, eggs suspended in ASW were permeabilized with 0.1 % Triton X-100 for 2 min. After washing in TBS [Tris-buffered saline; 100 mM Tris/HCl (pH 7.2) and 150 mM NaCl], eggs were incubated in blocking buffer (3 % BSA in TBS, pH 7.2) for 30 min. PPBD (8 μg/ml) and 10 μg/ml anti-Xpress epitope monoclonal antibody were added, and the samples were incubated for 1 h under gentle agitation. The samples were washed with blocking buffer and TBS, and fixed in 4 % paraformaldehyde diluted in TBS for 30 min. After fixation the eggs were blocked for 15 min in 100 mM NH_4Cl in TBS, and for an additional 30 min in blocking buffer plus 0.1 % Tween 20. Secondary antibodies (Alexa Fluor® 488-conjugated goat anti-mouse IgG; Invitrogen) were diluted in the same buffer (1:1000) and incubated with the eggs for 1 h under gentle agitation. After washing in blocking buffer plus Tween 20, the samples were observed using an Olympus IX-71 fluorescence microscope with a Photometrix $CoolSnap_{HQ}$ CCD (charge-coupled device) camera driven by Delta Vision software (Applied Precision) using filters with excitation at 480–500 nm and emission at 510–550 nm. For the egg three-dimensional projection (Supplementary Movie S1 at http://www.BiochemJ.org/bj/429/bj4290485add.htm), *z*-stacks were acquired and reconstructed using the same software as described above.

For localization of Acridine Orange and DAPI, the dense granule fraction was incubated with 3 μM Acridine Orange or 10 μg/ml DAPI for 10 min at room temperature in the presence of protease inhibitor cocktail (Sigma, P8340), 2 μg/ml oligomycin and 2 μg/ ml antimycin, and observed in the microscope described above with excitation at 340–380 nm for DAPI and at 450–490 nm for Acridine Orange, and emission >500 nm for both dyes.

Egg stratification

Egg stratification was performed as reported previously [4,24]. PPBD and DAPI staining were performed as described above. For LysoTracker staining, eggs were incubated with 0.5 nM LysoTracker Red DND-99 for 30 min at room temperature before stratification [4], and then stained with PPBD as described above.

Fluorimetry

H^+ movements, and Ca^{2+} release were monitored using a fluorimeter (F4500, Hitachi Instruments). H^+ movements were monitored by following changes in Acridine Orange (6 μM) fluorescence (excitation at 495 nm, emission at 530 nm) after incubating dense granule fractions (50–80 μg of protein for bafilomycin experiments; 600–800 μg of protein for Na^+/H^+ and Ca^{2+}/H^+ experiments) in 2 ml of GluIM containing 2 μg/ml oligomycin and 2 μg/ml antimycin A. Acridine Orange was allowed to equilibrate for 2–5 min, whereas the dye partitioned into dense granules, and then valinomycin (10 μM), bafilomycin A_1 (1 μM) and/or nigericin (5 μM) were added as indicated. Ca^{2+} release was measured following changes in the fluorescence (excitation 506 nm, emission 526 nm) of Fluo-3 (3 μM). Total homogenates and dense granule fractions (310 μg of protein for NAADP experiments; 600–800 μg of protein for GPN experiments) were diluted in 2 ml of GluIM buffer. IP_3 (300 nM), NAADP (200 nM) and nigericin (5 μM) were added where indicated in the Figures.

Gel electrophoresis

Perchloric acid extracts were dried in a SpeedVac and resuspended in 60 mM Tris/HCl (pH 7.5) and 6.0 mM $MgCl_2$. For PPX-treated

© 2010 The Author(s)
The author(s) has paid for this article to be freely available under the terms of the Creative Commons Attribution Non-Commercial Licence (http://creativecommons.org/licenses/by-nc/2.5/) which permits unrestricted non-commercial use, distribution and reproduction in any medium, provided the original work is properly cited.

samples, rPPX1 [34] was added (3000–5000 units) in a final volume of 50 μl and incubated for 30 min at 35 °C. Poly P samples were then mixed with DNA-loading buffer [10 mM Tris/HCl (pH 7.5), 10 mM EDTA, 0.25 % Orange-G and 0.65 % sucrose] and loaded into 1–2 % agarose gels. The gels were run at 200 V in TAE buffer [40 mM Tris/acetate (pH 8.2) and 1 mM EDTA] until the dye (Orange-G) reached the middle of the gel. The gels were then stained with 0.1 % Toluidine Blue for 1 h, and then de-stained with several changes of deionized water for 4 h.

PPX and PPase activities in the dense granule fraction

Dense granule fractions were homogenized using a Teflon pestle tissue homogenizer in ice-cold reaction buffer for PPX [20 mM Tris/HCl, 5 mM magnesium acetate and 100 mM ammonium acetate (pH 7.5)], or PPase [50 mM Tris/HCl and 5 mM $MgCl_2$ (pH 7.5)] activities, and supplemented with protease inhibitor cocktail (P8340, Sigma). To these samples, 0.1 mM poly P_{75+} or 0.1 μM PP_i was added and aliquots were collected at 5, 10 and 15 min after substrate addition. The aliquots were centrifuged at 14 000 ***g*** for 10 s, and the pellets were processed for poly P and PP_i determinations as described before. Controls were performed with no sample, incubating the substrates in plain buffer under the same conditions.

Data analysis

All results are expressed as means $\pm$ S.D. or, when appropriate, S.E.M. for n different experiments. Statistical significance was determined using a Student's t test or by one-way ANOVA at $P<0.05$.

RESULTS

Ultrastructure and elemental analysis of sea urchin egg granules

Ultrastructural analysis of sea urchin eggs allowed the identification of several granules. The cortical granules (whose size varies from 0.39 ± 0.02 to 0.92 ± 0.05 μm diameter in different sea urchin species [38]) are located close to the surface and are identified by the presence of star-like dense material in their interior (Figure 1A, cg, thin arrow). An abundant group of organelles of approx. 1–2 μm diameter, oval form and high and uniform electron-density are known as yolk platelets (Figures 1B and 1C; YP) [20]. In addition, clear granules [21,22], characterized by their clear appearance and the presence in most of them of an electron-dense material in various states of condensation (Figures 1A and 1B, thick arrows), are distributed at random in the unfertilized eggs [20]. These clear granules, of an average diameter of 0.83 ± 0.29 μm, are very similar in their appearance to the acidocalcisomes described in different organisms [26]. A large number of other clear granules that are smaller (average diameter 0.19 ± 0.04 μm) than the granules described above, but which also have a similar appearance to acidocalcisomes (empty appearance with a thin-layer of dense material that sticks to the inner face of the membrane; Figures 1B and 1E, white arrowheads) and mitochondria (Figures 1B and 1D, black arrowheads) are also visible.

To investigate whether the clear granules correspond to acidocalcisomes, whole-cell mounts of sea urchin eggs or homogenates were analysed by energy-filtering transmission electron microscopy. Using this technique, the contrast of a given structure in the image solely arises from its mass density since these preparations are not stained. Many electron-dense vesicles

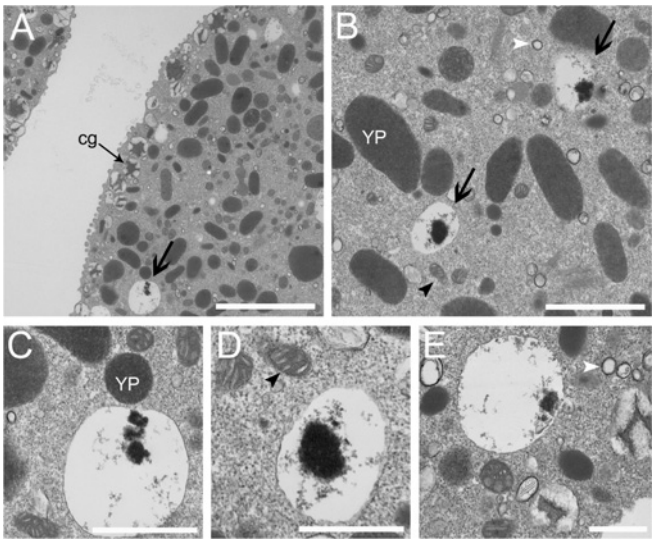

Figure 1 Transmission electron microscopy of *A. punctulata* eggs

The preparation was fixed and processed for standard electron microscopy. Cortical granules (cg, thin arrow), yolk platelets (YP) and 'clear granules' containing residual electron-dense material (thick arrow), smaller clear vesicles (white arrowheads) and mitochondria (black arrowheads) are indicated. Scale bars in (**A**) are 3 μm, (**B**) 1 μm and (**C**–**E**) 0.5 μm.

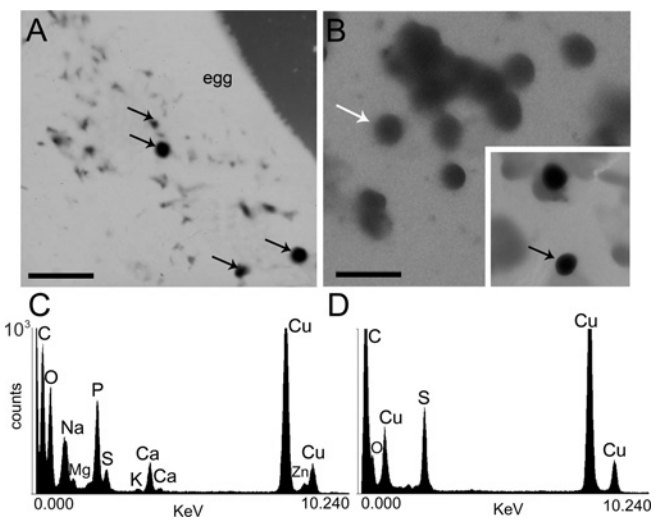

Figure 2 Electron microscopy and X-ray microanalysis of whole intact eggs and homogenates

(**A** and **B**) Electron energy-filtered transmission electron microscopy of an unfixed and unstained egg (**A**) or an egg homogenate (**B**) from *A. punctulata*. Dense granules are identified by black arrows. (**C**) Typical X-ray microanalysis spectrum of dense granules found in egg homogenates [black arrow in (**B**)]. (**D**) Typical X-ray microanalysis spectrum of a less-electron-dense vesicle (probably a yolk platelet) [white arrow in (**B**)] found in egg homogenates. Scale bars in (**A**) and (**B**) are 3 μm.

of various diameter (average 0.73 ± 0.09 μm) were seen in intact eggs (Figure 2A, black arrows) or homogenates (Figure 2B, black arrow). Other larger and less electron-dense vesicles (probably yolk platelets) were also observed (Figure 2B, white arrow). X-ray microanalysis of these vesicles was performed (Figures 2C and 2D). All ten spectra of the very-electron-dense vesicles taken from different homogenates were qualitatively similar showing considerable amounts of oxygen, sodium, magnesium, phosphorus, sulfur, calcium and zinc concentrated in their matrix

© 2010 The Author(s)
The author(s) has paid for this article to be freely available under the terms of the Creative Commons Attribution Non-Commercial Licence (http://creativecommons.org/licenses/by-nc/2.5/) which permits unrestricted non-commercial use, distribution and reproduction in any medium, provided the original work is properly cited.

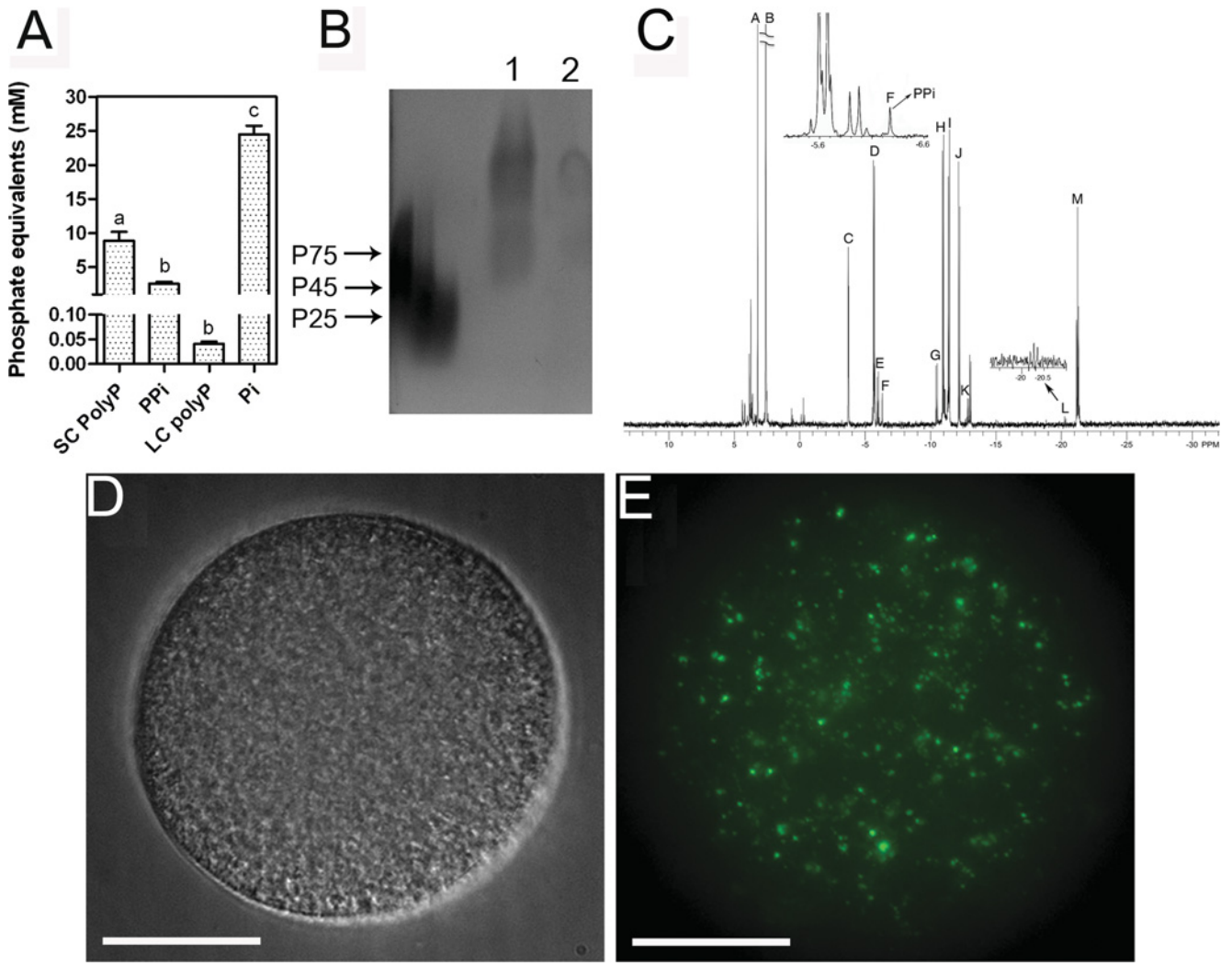

Figure 3 Detection of PP_i and poly P in sea urchin eggs

(**A**) PP_i, SC poly P and LC poly P were assayed as described in the Materials and methods section, and levels are expressed as mM poly P (in terms of P_i residues). Data are from four experiments, and show means ± S.E.M. Different letters indicate significant differences (one-way ANOVA, $P < 0.05$). (**B**) Agarose gel electrophoresis of poly P stained with Toluidine Blue. Lane 1, poly P extract; lane 2, poly P extract after rPPX1 treatment. P75, P45 and P24 are poly P standards of 75+, 45 and 25 phosphate units. (**C**) 242.8-MHz (^{1}H decoupled) ^{31}P-NMR spectra of a perchloric acid extract of sea urchins eggs. See assignments in Table 1. (**D**) Differential interferential microscopy of the sea urchin egg shown in (**E**). (**E**) Localization of poly P using the recombinant PPBD of *E. coli* PPX linked with an Xpress epitope tag. Images were deconvolved for 15 cycles using Softwarx deconvolution software. Other conditions are described in the Materials and methods. Scale bars in (**D**) and (**E**) are 15 μm.

(Figure 2C). X-ray microanalysis of the less electron-dense granules, probably corresponding to yolk platelets (Figure 2B, white arrow), revealed only the presence of sulfur (Figure 2D), suggesting that they are rich in proteins. Copper arose from the Formvar-coated grids in both cases and was also detected in spectra taken from the background (results not shown).

PP_i and poly P in sea urchin eggs

One of the characteristics of acidocalcisomes is that they contain large amounts of SC and LC poly P, and also PP_i [26]. As shown in Figure 3(A) egg homogenates contain ~220-fold more SC than LC poly P, whereas PP_i content was approximately half the amount of SC poly P (all expressed in terms of P_i residues for comparative purposes). Poly P was also detected by electrophoresis of extracts in 1 % agarose gels stained with Toluidine Blue (Figure 3B, lane 1), and pre-treatment of these samples with rPPX1 resulted in considerable decrease in staining (Figure 3B, lane 2).

Figure 3(C) shows a representative 242.8 MHz (^{1}H-decoupled) ^{31}P-NMR spectrum of perchloric acid extracts of sea urchin eggs. Resonance assignments for this spectrum are given in Table 1. The predominant peak in the spectrum is P_i (peak B). The inset region at ~ −6 p.p.m. (left-hand inset) contains the PP_i resonance, peak F. The region between −19 and −22 p.p.m. is shown in the right-hand inset and contains peaks for the β-phosphate of nucleoside triphosphates (M), in addition to the central phosphate of poly P (L). The spectrum shows considerable amounts of phosphorylcholine (A) and phosphoarginine (C).

Poly P, as detected using the PPBD of *S. cerevisiae* PPX [37], was localized in small vesicles randomly distributed in the egg (Figures 3D and 3E, and Supplementary Movie S1). There was no poly P signal in the negative controls (i.e. in the absence of PPBD).

© 2010 The Author(s)
The author(s) has paid for this article to be freely available under the terms of the Creative Commons Attribution Non-Commercial Licence (http://creativecommons.org/licenses/by-nc/2.5/) which permits unrestricted non-commercial use, distribution and reproduction in any medium, provided the original work is properly cited.

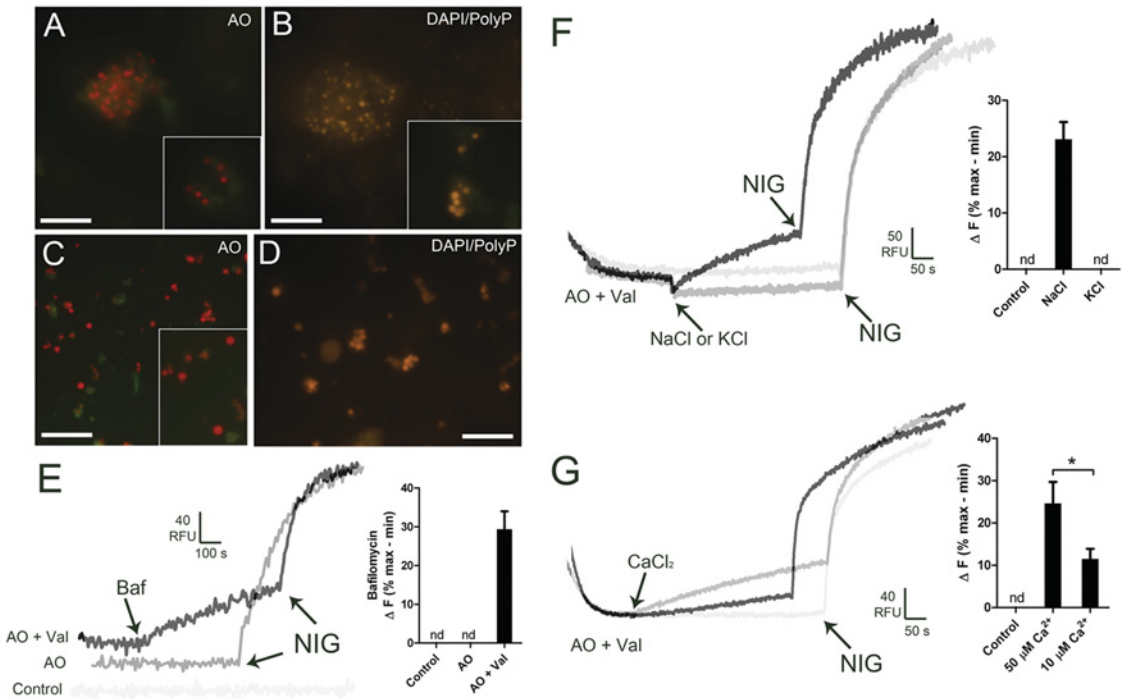

Figure 4 Fluorescence microscopy and Acridine Orange release from dense granule fractions

Dense granule fractions were incubated with 3 μM Acridine Orange [AO (**A** and **C**)] or 10 μg/ml DAPI (**B** and **D**) as described in the Materials and methods section. Note the accumulation of Acridine Orange [(**A** and **C**), orange] and DAPI [(**B** and **C**), yellow] in vesicles distributed in groups (**A** and **B**) or isolated (**C** and **D**). Scale bars in (**A**–**D**) are 5 μm. (**E**) The dense granule fraction was diluted in GluIM buffer in the presence of 6 μM Acridine Orange with and without 10 μM valinomycin (Val), and changes in fluorescence were monitored in a fluorimeter. Bafilomycin A_1 (Baf, 1 μM) and nigericin (NIG, 1 μM) were added where indicated. Grey trace (AO) is the control in the absence of valinomycin. Light grey trace (Control) is the control in the absence of additions. Tracings are representative of five experiments. The histogram summarizes the changes in fluorescence (ΔF) in (**E**), and is shown as the means $\pm$ S.D of five determinations expressed as a percentage of the maximal nigericin response. (**F** and **G**) The dense granule fraction was pre-incubated with 3 μM Acridine Orange and 10 μM valinomycin until it equilibrated. (**F**) NaCl (100 mM; black trace) or 100 mM KCl (dark grey trace) and 5 μM nigericin were added where indicated. (**G**) $CaCl_2$ at 10 μM (black trace) or 50 μM (dark grey trace) and 5 μM nigericin were added where indicated. Control tracings without NaCl or KCl (**F**) or without $CaCl_2$ (**G**) are shown in light grey. Traces in (**F**) and (**G**) are representative of at least three experiments The histograms summarize the changes in fluorescence (ΔF) in (**F**) and (**G**), and are shown as the means $\pm$ S.D of three determinations expressed as a percentage of the maximal nigericin response. Asterisks indicate significant differences (measured using a Student's *t* test, $P < 0.05$). Ordinates are scaled as RFU (relative fluorescence units) for (**E**–**G**).

Table 1 ^{31}P-NMR resonance assignments for perchloric acid extracts of sea urchin eggs

*NTP, nucleoside triphosphate; #NDP, nucleoside diphosphate.

Peak	Assignment	Chemical shift
A	Phosphorylcholine	3.22
B	P_i	2.60
C	Phosphoarginine	−3.71
D	γ-P of NTP*	−5.66
E	β-P of NDP#	−5.97
F	Inorganic PP_i	−6.29
G	α-P of NDP#	−10.45
H	α-P of NTP*	−10.94
I, J	NAD(H)	−11.39, −12.17
K	NDP-glucose	−12.84
L	Central P of LC poly P	−20.28
M	β-P of NTP*	−21.21

Isolation of dense granules and demonstration of their acidity and poly P content

To isolate the dense granules (Figure 2) and investigate their chemical and enzymatic content, we used iodixanol centrifugation as described in the Materials and methods section. The pellet fraction was applied to Formvar-coated grids, and direct observation showed the presence of multiple electron-dense granules of variable size (Supplementary Figure S1A at http://www.BiochemJ.org/bj/429/bj4290485add.htm). X-ray microanalysis (Supplementary Figures S1B and S1C) showed that most of these granules (15 out of 25) contained a similar elemental composition to that of dense granules in whole eggs or homogenates (Figure 2C). Standard transmission electron microscopy of this fraction revealed the presence of clear granules (corresponding to dense granules), which most of the time appeared empty or containing a residual electron-dense material, as previously observed in whole eggs (Figure 1), and some mitochondrial contamination (results not shown).

The presence of granules in the dense fraction was confirmed by incubation of the preparation in the presence of Acridine Orange. The Acridine Orange-stained granules appeared in groups (Figure 4A) or as isolated vesicles (Figure 4C). We also investigated the location of poly P using DAPI (Figures 4B and 4D). DAPI is known to shift its emission fluorescence to a maximum wavelength of 525 nm (yellow) in the presence of poly P, this change being specific for poly P and not produced by PP_i or other anions [31]. We detected the staining of numerous vesicles, either in groups (Figure 4B) or isolated (Figure 4D). No staining was detected when DAPI was omitted (results not shown).

Work by Morgan and Galione [6] has shown that acidification of granules in sea urchin eggs is maintained by a V-H^+-ATPase

© 2010 The Author(s)
The author(s) has paid for this article to be freely available under the terms of the Creative Commons Attribution Non-Commercial Licence (http://creativecommons.org/licenses/by-nc/2.5/) which permits unrestricted non-commercial use, distribution and reproduction in any medium, provided the original work is properly cited.

(vacuolar type H^+-ATPase), as happens with other acidic organelles, including the acidocalcisomes of *Trypanosoma cruzi* [39], *Trypanosoma brucei* [40], *D. discoideum* [28], *C. reinhardtii* [27] and human platelets [31]. Interestingly, the function of this proton pump could be demonstrated only by inhibition of acidification by bafilomycin A_1 after pre-incubation of the preparation with either valinomycin or FCCP (carbonyl cyanide *p*-trifluoromethoxyphenylhydrazone) [6]. In agreement with those results, bafilomycin A_1 released Acridine Orange after pre-incubation of the dense granule fractions with valinomycin (Figure 4E, black trace), but not in its absence (Figure 4E, grey trace), although this could be accomplished by nigericin (Figure 4E, grey trace). Addition of nigericin after bafilomycin A_1 completed the release of Acridine Orange from the vesicles (Figure 4E, black trace).

Evidence for Na^+/H^+ and Ca^{2+}/H^+ exchange activities in dense granules

Acidocalcisomes of *T. brucei* [40,41] and *Leishmania donovani* [42,43] have been reported to contain Na^+/H^+ and Ca^{2+}/H^+ exchangers and the coupled interaction of these exchangers was postulated to result in a mechanism of Ca^{2+} release upon alkalinization or Na^+ entry into acidocalcisomes [42]. Experiments on enriched dense granule fractions showed the presence of these ion-exchange mechanisms. For example, addition of 100 mM NaCl (Figure 4F, black trace), but not of 100 mM KCl (Figure 4F, light grey trace) resulted in Acridine Orange efflux, suggesting the activity of a Na^+/H^+ exchanger in the dense granule fraction. Addition of 10 and 50 μM $CaCl_2$ under similar conditions also resulted in Acridine Orange efflux (Figure 4G, black and dark grey traces respectively), suggesting the operation of a Ca^{2+}/H^+ exchanger, and the potential function of these exchangers as a mechanism of Ca^{2+} release upon alkalinization of dense granules [43]. Under physiological conditions, these exchangers could contribute to Na^+ and Ca^{2+} uptake into these acidic compartments, as occurs with the plant vacuole [44].

Association of Ca^{2+} release and poly P hydrolysis

It has been shown that Ca^{2+} release from acidocalcisomes of *T. cruzi* occurs in parallel with poly P hydrolysis [34]. We therefore investigated whether there was a correlation between Ca^{2+} release from the acidic compartment containing poly P in the sea urchin egg dense granule fraction and poly P hydrolysis. Addition of nigericin resulted in Ca^{2+} release from the dense granule fraction, as detected by changes in the fluorescence of Fluo-3 (Figure 5A) and this resulted in a significant decrease in the levels of SC poly P, but not in the levels of LC poly P (Figure 5C). Addition of nigericin also resulted in alkalinization of the vesicles (Figure 5B) confirming the link between alkalinization of acidocalcisomes and Ca^{2+} release.

Degradation of poly P and PP_i in dense granules

Acidocalcisomes are known to possess enzymes linked to PP_i and poly P metabolism [26]. The rapid hydrolysis of poly P that occurs when Ca^{2+} release is stimulated by nigericin (Figure 5) suggested the presence of an PPX activity in the dense granule fraction. To know whether this was the case, we investigated PP_i and poly P hydrolysis by dense granule fractions. Hydrolysis of poly P_3 (Figure 6A) or PP_i (Figure 6B) was approximately linear with time, whereas hydrolysis of poly P_{75+} stopped after 5 min. This probably indicates the hydrolysis of contaminating SC poly Ps in

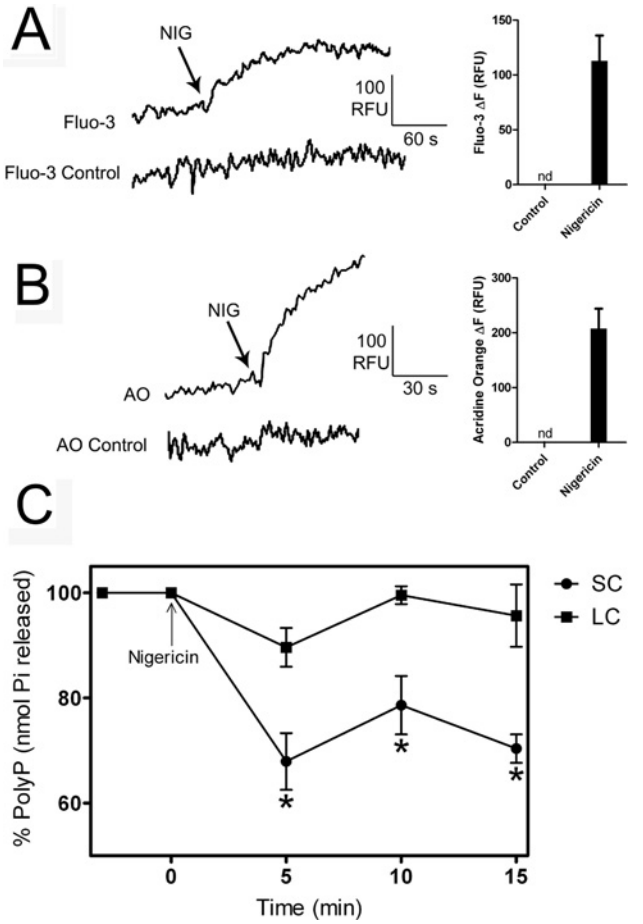

Figure 5 Effects of nigericin on calcium release, acidity and poly P content of dense granule fractions

(**A**) The dense granule fraction was incubated in GluIM in the presence of Fluo-3, and nigericin (5 μM) was added at the time indicated. (**B**) The dense granule fraction was pre-incubated with 3 μM Acridine Orange until it equilibrated, and nigericin (5 μM) was added at the time indicated. (**C**) SC and LC poly P levels were measured at different times after the addition of 10 μM nigericin. Tracings in (**A**) and (**B**) are representative of at least four experiments. Ordinates are scaled as RFU (relative fluorescence units). Controls without nigericin addition (**A** and **B**) are shown. The graph in (**C**) shows means $\pm$ S.E.M. for three experiments. Asterisks in (**C**) indicate significant differences (one-way ANOVA, $P < 0.05$).

the poly P_{75+} sample (which is a mixture of poly P molecules with a mean length of 84), and the inability of the polyphosphatase to cleave LC poly Ps.

NAADP-stimulated Ca^{2+} release from dense granules is not accompanied by hydrolysis of poly P and the fraction is not sensitive to GPN

NAADP has been shown to release Ca^{2+} from acidic granules of sea urchin eggs [4], whereas IP_3 releases Ca^{2+} from the ER [2]. Figures 7(A) and 7(D) show that both NAADP and IP_3 were able to release comparable amounts of Ca^{2+} from vesicular compartments in egg homogenates. A second addition of NAADP showed no response revealing desensitization (results not shown). NAADP (Figure 7B) or IP_3 (Figure 7E) were, however, less efficacious in the dense granule fraction. We next tested whether poly P hydrolysis occurred as a consequence of Ca^{2+} release by NAADP in dense granule fractions, but no significant changes were detected (Figure 7G). The lack of enrichment in NAADP-sensitive calcium stores, together with the lack of poly

© 2010 The Author(s)
The author(s) has paid for this article to be freely available under the terms of the Creative Commons Attribution Non-Commercial Licence (http://creativecommons.org/licenses/by-nc/2.5/) which permits unrestricted non-commercial use, distribution and reproduction in any medium, provided the original work is properly cited.

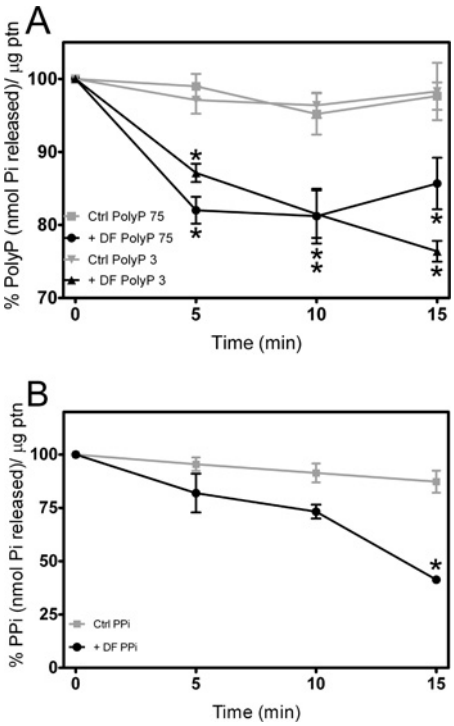

Figure 6 Poly P and PP_i hydrolysis in dense granule fractions

Dense granule fractions (DF) were homogenized in GluIM buffer and tested for PPX and PPase activities as described in the Materials and methods section. (**A**) Levels of poly P_3 and poly P_{75+} after different times of incubation with the dense granule fraction. (**B**) Levels of PP_i after different times of incubation with the dense granule fraction. Controls (Ctrl) are the substrates incubated in buffer, with no fraction added. Graphs show mean relative activities ± S.E.M. for four experiments. Asterisks indicate significant differences (one-way ANOVA, $P < 0.05$).

P hydrolysis accompanying calcium release by NAADP suggests that the acidocalcisome-related organelles of sea urchin eggs are not the calcium stores sensitive to NAADP.

The presence of releasable Ca^{2+} in lysosomes has been demonstrated based on experiments using GPN and it has been reported that NAADP-targeted stores are sensitive to GPN [4]. GPN is a lysosome-disrupting cathepsin-C substrate that was originally used to distinguish lysosomes, which contain cathepsin C, from pre-lysosomal endocytic vacuoles, which do not [25]. Hydrolysis of GPN by cathepsin C induces osmotic swelling of the lysosome and release of its content, including Ca^{2+}, into the cytoplasm. Treatment of sea urchin homogenates with GPN caused Ca^{2+} release, which was completed by nigericin (Figure 7H, trace TH). In contrast, addition of GPN to dense granule fractions did not cause Ca^{2+} release (Figure 7H, trace DF) suggesting that this fraction is not contaminated with lysosomes.

Use of stratified eggs reveals that dense granules localize to the centripetal pole of the egg

As discussed above, when eggs are stratified by centrifugation, yolk platelets localize to the centrifugal pole which is the site where higher Ca^{2+} release occurs upon local photolysis of caged NAADP and which is opposite to the nucleus and lipid droplets, where clear granules localize [24]. When eggs were stratified and stained with either PPBD (Supplementary Figures S2B and S2C at http://www.BiochemJ.org/bj/429/bj4290485add.htm) or DAPI (Supplementary Figures S2E and S2F), staining was detected in the centripetal pole in agreement with the reported localization of the clear granules [24] and with the results showing negligible NAADP-stimulated Ca^{2+} release by dense granule fractions. In contrast, staining with LysoTracker Red was in the centrifugal pole, where the yolk platelets localize and where higher NAADP-stimulated Ca^{2+} release has been detected [4] (Supplementary Figures S2G–S2J).

DISCUSSION

We report in the present paper that sea urchin eggs are rich in poly P. Poly P was detected by a biochemical method based on its specific hydrolysis by a PPX, by Toluidine Blue staining in agarose gels, by ^{31}P-NMR and by a recently developed method based on staining with the specific poly-P-binding region of *S. cerevisiae* PPX [37]. This was confirmed by visualization of poly P in the dense granule fraction using DAPI and by its hydrolysis when nigericin released Ca^{2+} from these fractions. We also found considerable amounts of phosphoarginine, a phosphagen present in many invertebrates although not previously reported in sea urchin eggs [45].

Our results also suggest that the dense granules of sea urchin eggs, which could correspond to the clear granules detected by transmission electron microscopy (both large and small; Figure 1) have many characteristics in common with acidocalcisomes [26]: (i) they are acidic due to the operation of a bafilomycin A_1-sensitive vacuolar ATPase and are able to accumulate acidophilic dyes such as Acridine Orange; (ii) they can store extremely large amounts of calcium and other cations such as magnesium, sodium and zinc, and can release Ca^{2+} in the presence of nigericin; (iii) they contain very large amounts of phosphorus in the form of phosphate, PP_i, and poly P; (iv) they have very high electron density, when examined by energy-filtering transmission electron microscopy, and have an empty appearance with condensed material in their interior, when examined by standard transmission electron microscopy; and (v) they possess activities commonly found in acidocalcisomes, such as PPase [46], PPX [47], and Ca^{2+}/H^+ and Na^+/H^+ exchangers [40–43].

Clear granules are distributed at random in unfertilized sea urchin eggs [21], in agreement with the distribution of poly P-labelled granules (Figure 3E, and Supplementary Movie S1). The function of these clear granules is unknown, but their composition, investigated in the present study, implies an important role in storage of phosphorus and cations needed for embryo development. Our results suggest that, although these granules are acidic and contain large amounts of calcium, they are not the targets for NAADP-stimulated Ca^{2+} release.

It has been reported that fertilization induces pH changes in acidic stores of sea urchin eggs [5], and we have demonstrated that alkalinization of dense granules leads to Ca^{2+} release and poly P hydrolysis. Alkalinization of acidic stores of the sea urchin egg could be either upon vesicle fusion with the plasma membrane, when the alkaline extracellular medium exchanges with the acidic lumen of cortical granules that are the primary egg exocytic vesicles, or upon Ca^{2+} release from yolk platelets stimulated by NAADP [5]. It has been reported that cortical alkalinization coincides with NAADP-induced Ca^{2+} release from intracellular stores [5], and that this alkalinization appears to occur at the individual vesicle level [5]. Alkalinization of yolk platelets is increased by NAADP by a mechanism coupled to Ca^{2+} release via the NAADP receptor [5]. It has been proposed that the fall in the luminal [Ca^{2+}] allows H^+ to bind to vacated sites on a luminal polyanionic matrix, thus resulting in alkalinization of the store [6].

In addition to acidic store alkalinization, it has been shown that fertilization of sea urchin eggs led to a change in cytosolic pH

© 2010 The Author(s)
The author(s) has paid for this article to be freely available under the terms of the Creative Commons Attribution Non-Commercial Licence (http://creativecommons.org/licenses/by-nc/2.5/) which permits unrestricted non-commercial use, distribution and reproduction in any medium, provided the original work is properly cited.

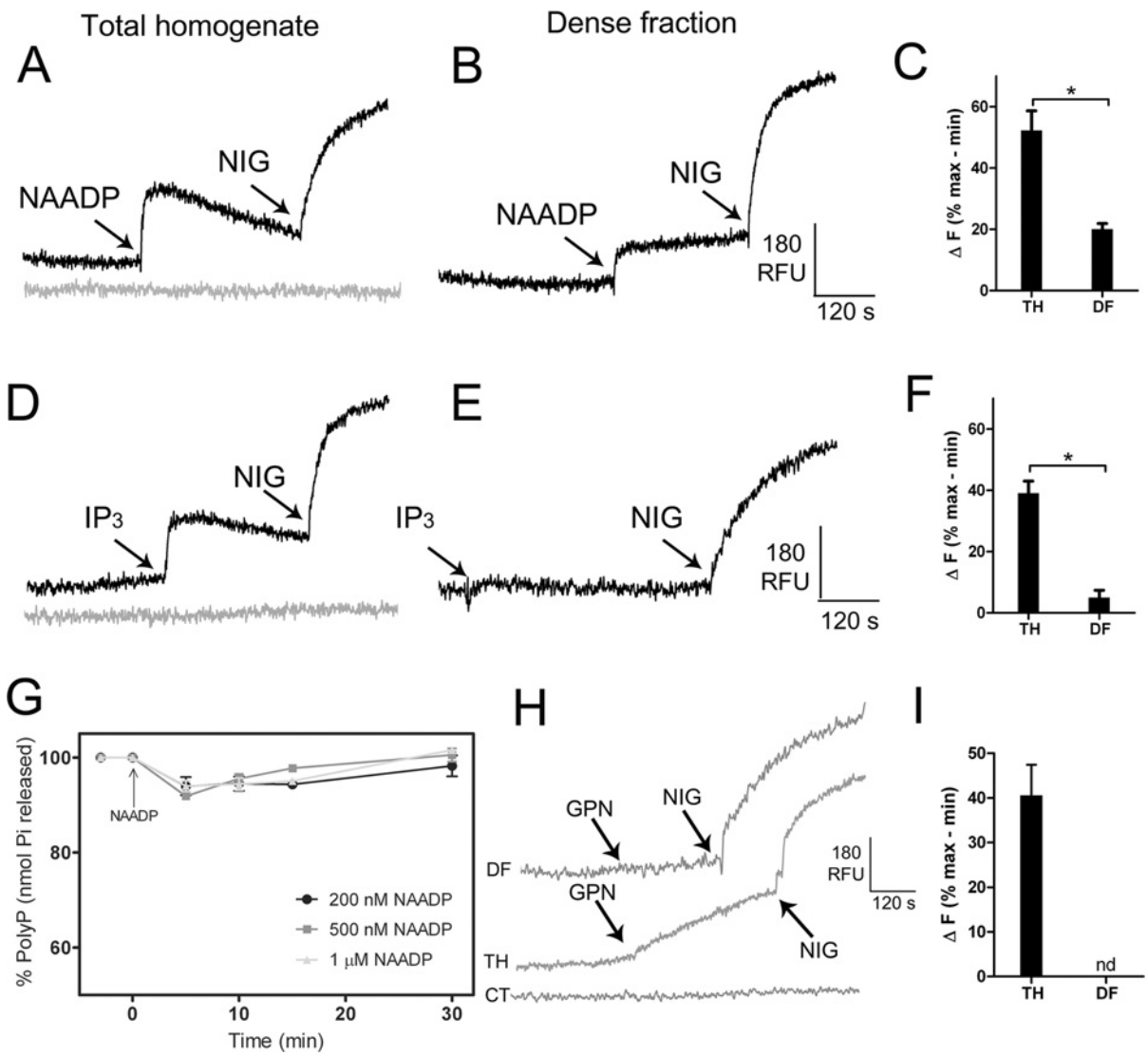

Figure 7 Effect of Ca^{2+}-releasing agents on poly P content of dense granule fractions

Total homogenates (**A** and **D**) and dense granule fractions (**B** and **E**) (310 μg of protein in each case) were tested for calcium release triggered by IP_3 and NAADP. Preparations were incubated in GluIM buffer in the presence of 3 μM Fluo-3 as described in the Materials and methods section. IP_3 (300 nM), NAADP (200 nM) and nigericin (5 μM) were added where indicated. Tracings are representative of at least four experiments. Controls without additions are shown in grey. Ordinates are scaled as RFU (relative fluorescence units). (**C** and **F**) The histograms summarize the changes in fluorescence (ΔF) in (**A** and **B**) and (**D** and **E**) respectively, and are shown as the means $\pm$ S.D. for three experiments expressed as a percentage of the maximal nigericin response. Asterisks indicate significant differences (measured using a Student's *t* test, $P < 0.05$). (**G**) SC poly P levels were measured at different times after the addition of increasing NAADP concentrations. Graph shows means $\pm$ S.E.M. for three experiments. (**H**) Dense granule fractions (trace 1) and total homogenate (trace 2) were incubated in GluIM in the presence of 3 μM Fluo-3. GPN (100 μM) and nigericin (5 μM) were added at the times indicated. The control with no additions is shown in trace 3. Ordinates are scaled as RFU (relative fluorescence units). (**I**) The histogram summarizes the changes in fluorescence (ΔF) in (**H**), and shows the means $\pm$ S.D of four determinations expressed as a percentage of the maximal nigericin response.

from 6.9 to 7.3 with a concomitant acidification of the sea water, and that the egg remains alkaline for approx. 60 min [48,49]. This change in cytosolic pH is driven by a plasma membrane Na^+/H^+ exchanger [48]. An increase in cytosolic sodium has been shown previously to increase the release of calcium from acidocalcisomes of *T. brucei* [40,41] and *L. donovani* [42,43], and this could potentially occur with the sea urchin egg dense granules. It has also been shown that suspension of sea urchin eggs in NH_4Cl (5 mM, pH 8.0), which could lead to alkalinization of all acidic granules, stimulates their metabolism and ability to undergo chromosome replication and condensation without triggering the cortical granule reaction [50]. Therefore we cannot rule out that alkalinization of dense granules could lead to an additional Ca^{2+} release.

Previous studies have indicated that the acidic compartments responsible for Ca^{2+} release induced by NAADP are lysosome-like organelles [4], possibly the yolk platelets [5]. This was based on experiments showing that GPN-mediated disruption of the organelles reduced the response to photoreleased or microinjected free NAADP, and on the response of yolk-platelet-enriched fractions to NAADP [4]. The lack of calcium detection in yolk platelets in our X-ray microanalyses (Figure 2D) does not indicate its absence, but simply that the amount of calcium present is below the limit of detection of this technique, which cannot discriminate between bound and free calcium. Yolk platelets would then be equivalent to the lysosomes of mammalian cells that are emerging as important calcium stores [51], whereas the clear (dense) granules would be,

© 2010 The Author(s)
The author(s) has paid for this article to be freely available under the terms of the Creative Commons Attribution Non-Commercial Licence (http://creativecommons.org/licenses/by-nc/2.5/) which permits unrestricted non-commercial use, distribution and reproduction in any medium, provided the original work is properly cited.

as acidocalcisomes, equivalent to lysosome-related organelles [51].

NAADP-induced Ca^{2+} signals are small and possibly localized, but can trigger ER Ca^{2+} mobilization through Ca^{2+}-induced Ca^{2+} release via IP_3 and ryanodine receptors [17], thus explaining the extensive Ca^{2+} waves detected after fertilization. Alkalinization of the cytosol and Ca^{2+} release from dense granules (acidocalcisomes) could also contribute to these Ca^{2+} waves. Supplementary Figure S3 (at http://www.BiochemJ.org/bj/429/bj4290485add.htm) shows a model of the Ca^{2+} mobilization pathways that could be involved in sea urchin eggs. NAADP would trigger Ca^{2+} release from yolk platelets that could then trigger ER Ca^{2+} mobilization through Ca^{2+}-induced Ca^{2+} release via IP_3 and ryanodine receptors. Alkalinization of the egg cytoplasm by Na^+ entry would release additional Ca^{2+} from dense granules (acidocalcisomes). Therefore acidocalcisomes, which are randomly distributed, could contribute to the NAADP-mediated two-phase Ca^{2+} release response. Alkalinization of these acidocalcisomes would lead to the hydrolysis of poly P, which would provide an important source of P_i for the anabolic reactions necessary for embryogenesis.

AUTHOR CONTRIBUTION

Isabela Ramos performed most of the experiments and participated in planning and writing of the paper; Douglas Pace assisted in sea urchin egg preparation and writing of the paper; Katherine Verbist prepared the recombinant PPBD of *E. coli* PPX; Fu-Yang Lin, Yonghui Zhang and Eric Oldfield carried out the NMR experiments and interpreted the results; Kildare Miranda, Ednildo Machado and Wanderley de Souza assisted in the design of the study, planning and manuscript preparation; and Roberto Docampo designed the study, and participated in planning and writing of the paper.

ACKNOWLEDGEMENTS

We thank the late Professor Arthur Kornberg for *E. coli* CA38 pTrcPPX1, and Dr Katsuharu Saito for *E. coli* DH5a pTrc-PPBD.

FUNDING

This work was supported by the Georgia Research Alliance/Barbara and Sanford Orkin Chair in Tropical and Emerging Global Diseases and Cellular Biology (to R.D.); I.B.R. was supported, in part, by a training grant from the Ellison Medical Foundation to the Center for Tropical and Emerging Global Diseases. D.A.P. was partially supported by the National Institutes of Health [NIH T32 training grant number AI-060546]. E.O., F.-Y.L and Y.Z. were supported, in part, by the National Institutes of Health [grant number GM-065307]. I.B.R., K.M., E.A.M. and W.S. were supported, in part, by the Fundação de Amparo a Pesquisa do Estado de Rio de Janeiro (FAPERJ) and the Conselho Nacional de Desenvolvimento Científico e Tecnológico (CNPq, Brazil).

REFERENCES

1 Parrington, J., Davis, L. C., Galione, A. and Wessel, G. (2007) Flipping the switch: how a sperm activates the egg at fertilization. Dev. Dyn. **236**, 2027–2038
2 Clapper, D. L., Walseth, T. F., Dargiem, P. J and Lee, H.C. (1987) Pyridine nucleotide metabolites stimulate calcium release from sea urchin egg microsomes desensitized to inositol trisphosphate. J. Biol. Chem. **262**, 9561–9568
3 Lee, H. C. and R., Aarhus (1995) A derivative of NADP mobilizes calcium stores insensitive to inositol trisphosphate and cyclic ADP-ribose. J. Biol. Chem. **270**, 2152–2157
4 Churchill, G. C., Okada, Y., Thomas, J. M., Genazzani, A. A., Patel, S. and Galione, A. (2002) NAADP mobilizes Ca^{2+} from reserve granules, lysosome-related organelles, in sea urchin eggs. Cell **111**, 703–708
5 Morgan, A. J. and Galione, A. (2007) Fertilization and nicotinic acid adenine dinucleotide phosphate induce pH changes in acidic Ca^{2+} stores in sea urchin eggs. J. Biol. Chem. **282**, 37730–37737
6 Morgan, A. J. and Galione, A. (2007) NAADP induces pH changes in the lumen of acidic Ca^{2+} stores. Biochem. J. **402**, 301–310
7 Yamasaki, M., Thomas, J. M., Churchill, G. C., Garnham, C., Lewis, A. M., Cancela, J. M., Patel, S. and Galione, A. (2005) Role of NAADP and cADPR in the induction and maintenance of agonist-evoked Ca^{2+} spiking in mouse pancreatic acinar cells. Curr. Biol. **15**, 874–878
8 Mitchell, K . J., Lai, F. A. and Rutter, G. A. (2003) Ryanodine receptor type I and nicotinic acid adenine dinucleotide phosphate receptors mediate Ca^{2+} release from insulin-containing vesicles in living pancreatic beta-cells (MIN6). J. Biol. Chem. **278**, 11057–11064
9 Zhang, F., Zhang, G., Zhang, A. Y., Koeberl, M. J., Wallander, E. and Li, P. L. (2006) Production of NAADP and its role in Ca^{2+} mobilization associated with lysosomes in coronary arterial myocytes. Am. J. Physiol. Heart Circ. Physiol. **291**, H274—H282
10 Brailoiu, E., Hoard, J. L., Filipeanu, C. M., Brailoiu, G. C., Dun, S L., Patel, S. and Dun, N. J. (2005) Nicotinic acid adenine dinucleotide phosphate potentiates neurite outgrowth. J. Biol. Chem. **280**, 5646–56450
11 Mándi, M., Tóth, B., Timár, G. and Bak, J. (2006) Ca^{2+} release triggered by NAADP in hepatocyte microsomes. Biochem. J. **395**, 233–238
12 Steen, M., Kirchberger, T. and Guse, A. H. (2007) NAADP mobilizes calcium from the endoplasmic reticular Ca^{2+} store in T-lymphocytes. J. Biol. Chem. **282**, 18864–18871
13 Zhang, F. and Li, P. L. (2007) Reconstitution and characterization of a nicotinic acid adenine dinucleotide phosphate (NAADP)-sensitive Ca^{2+} release channel from liver lysosomes of rats. J. Biol. Chem. **282**, 25259–25269
14 Cancela, J. M., Churchill, G. C. and Galione, A. (1999) Coordination of agonist-induced Ca^{2+}-signalling patterns by NAADP in pancreatic acinar cells. Nature **398**, 74–76
15 Churchill, G. C. and Galione, A. (2001) NAADP induces Ca^{2+} oscillations via a two-pool mechanism by priming IP_3- and cADPR-sensitive Ca^{2+} stores. EMBO J. **20**, 2666–2671
16 Calcraft, P. J., Ruas, M, Pan, Z., Cheng, X., Arredouani, A., Hao, X., Tang, J., Rietdorf, K., Teboul, L., Chuang, K. T. et al. (2009) NAADP mobilizes calcium from acidic organelles through two-pore channels. Nature **459**, 596–600
17 Brailoiu, E., Churamani, D., Cai, X., Schrlau, M. G., Brailoiu, G. C., Gao, X., Hooper, R., Boulware, M. J., Dun, N. J., Marchant, J. S. and Patel, S. (2009) Essential requirement for two-pore channel 1 in NAADP-mediated calcium signaling. J. Cell Biol. **186**, 201–209
18 Zong, X., Schieder, M., Cuny, H., Fenske, S., Gruner, C., Rötzer, K., Griesbeck, O., Harz, H., Biel, M. and Wahl-Schott, C. (2009) The two-pore channel TPCN2 mediates NAADP-dependent Ca^{2+}-release from lysosomal stores. Pflugers Arch. **458**, 891–899
19 Brailoiu, E., Hooper, R., Cai, X., Brialoiu, G. C., Keebler, M. V., Dun, N. J., Marchant, J. S. and Patel, S. (2010) J. Biol. Chem. **285**, 2897–2901
20 Terasaki, M. and Jaffe, L. A. (2004) Labeling of cell membranes and compartments for live cell fluorescence microscopy. Methods Cell Biol. **74**, 469–489
21 Lee, H. C. and Epel, D. (1983) Changes in intracellular acidic compartments in sea urchin eggs after activation. Dev. Biol. **98**, 446–454
22 Sardet, C. (1983) The ultrastructure of the sea urchin egg cortex isolated before and after fertilization. Dev. Biol. **105**, 196–210
23 Mallya, S. K., Partin, J. S., Valdizan, M. C. and Lennarz, W. J. (1992) Proteolysis of the major yolk glycoproteins is regulated by acidification of the yolk platelets in sea urchin embryos. J. Cell Biol. **117**, 1211–1221
24 Lee, H. C. and Aarhus, R. (2000) Functional visualization of the separate but interacting calcium stores sensitive to NAADP and cyclic ADP-ribose. J. Cell Sci. **113**, 4413–4420
25 Jadot, M., Colmant, C., Wattiaux-De Coninck, S. and Wattiaux, R. (1984) Intralysosomal hydrolysis of glycyl-L-phenylalanine 2-naphthylamide. Biochem. J. **219**, 965–970
26 Docampo, R., de Souza, W., Miranda, K., Rohloff, P. and Moreno, S. N. J. (2005) Acidocalcisomes: conserved from bacteria to man. Nat. Rev. Microbiol. **3**, 251–261
27 Ruiz, F. A., Marchesini, N., Seufferheld, M. and Govindjee, Docampo, R. (2001) The polyphosphate bodies of *Chlamydomonas reinhardtii* possess a proton-pumping pyrophosphatase and are similar to acidocalcisomes. J. Biol. Chem. **276**, 46196–46203
28 Marchesini, N., Ruiz, F. A., Vieira, M. and Docampo, R. (2002) Acidocalcisomes are functionally linked to the contractile vacuole of *Dictyostelium discoideum*. J. Biol. Chem. **277**, 8146–8153
29 Seufferheld, M., Vieira, M., Ruiz, F. A., Rodrigues, C. O., Moreno, S. N. J. and Docampo, R. (2003) Identification of organelles in bacteria similar to acidocalcisomes of unicellular eukaryotes. J. Biol. Chem. **278**, 29971–29978
30 Seufferheld, M., Lea, C. R., Vieira, M., Oldfield, E. and Docampo, R. (2004) The H^+-pyrophosphatase of *Rhodospirillum rubrum* is predominantly located in polyphosphate-rich acidocalcisomes. J. Biol. Chem. **279**, 51193–51202
31 Ruiz, F. A., Lea, C. R., Oldfield, E. and Docampo, R. (2004) Human platelet dense granules contain polyphosphate and are similar to acidocalcisomes of bacteria and unicellular eukaryotes. J. Biol. Chem. **279**, 44250–44257
32 Motta L.S., Ramos I. B., Gomes F.M., de Souza W., Champagne D.E., Santiago M. F., Docampo, R., Miranda, K. and Machado, E.A. (2009) Proton-pyrophosphatase and polyphosphate in acidocalcisome-like vesicles from oocytes and eggs of *Periplaneta americana*. Insect Biochem. Mol. Biol. **39**, 198–206

© 2010 The Author(s)
The author(s) has paid for this article to be freely available under the terms of the Creative Commons Attribution Non-Commercial Licence (http://creativecommons.org/licenses/by-nc/2.5/) which permits unrestricted non-commercial use, distribution and reproduction in any medium, provided the original work is properly cited.

33 Ramos, I. B., Miranda, K., Ulrich, P, Ingram, P, LeFurgey, A., Machado, E. A., de Souza, W. and Docampo, R. (2010) Calcium- and polyphosphate-containing acidocalcisomes in chicken egg yolk. Biol. Cell **102**, 421–434

34 Ruiz, F. A., Rodrigues, C. O. and Docampo, R. (2001) Rapid changes in polyphosphate content within acidocalcisomes in response to cell growth, differentiation, and environmental stress in *Trypanosoma cruzi*. J. Biol. Chem. **276**, 26114–26121

35 Ault-Riche, D., Fraley, C D., Tzeng, C M. and Kornberg, A. (1998) Novel assay reveals multiple pathways regulating stress-induced accumulations of inorganic polyphosphate in *Escherichia coli*. J. Bacteriol. **180**, 1841–1847

36 Lanzetta, P. A., Alvarez, L. J., Reinach, P. S. and Candia, O. A. (1979) An improved assay for nanomole amounts of inorganic phosphate. Anal. Biochem. **100**, 95–97

37 Saito, K., Ohtomo, R., Kuga-Uetake, Y., Aono, T. and Saito, M. (2005) Direct labeling of polyphosphate at the ultrastructural level in *Saccharomyces cerevisiae* by using the affinity of the polyphosphate binding domain of *Escherichia coli* exopolyphosphatase. Appl. Environ. Microbiol. **71**, 5692–5701

38 Afzelius, B. A. (1956) The ultrastructure of the cortical granules and their products in the sea urchin egg as studied with the electron microscope. Exp. Cell Res. **10**, 257–285

39 Lu, H. G., Zhong, L., de Souza, W., Benchimol, M., Moreno, S. N. J. and Docampo, R. (1998) Ca^{2+} content and expression of an acidocalcisomal calcium pump are elevated in intracellular forms of *Trypanosoma cruzi*. Mol. Cell. Biol. **18**, 2309–2323

40 Rodrigues, C. O., Scott, D. A. and Docampo, R. (1999) Characterization of a vacuolar pyrophosphatase in *Trypanosoma brucei* and its localization to acidocalcisomes. Mol. Cell. Biol. **19**, 7712–7723

41 Vercesi, A. and Docampo, R. (1996) Sodium-proton exchange stimulates Ca^{2+} release from acidocalcisomes of *Trypanosoma brucei*. Biochem. J. **315**, 265–270

42 Rodrigues, C. O., Scott, D. A. and Docampo, R. (1999) Presence of a vacuolar H^+-pyrophosphatase in promastigotes of *Leishmania donovani* and its localization to a different compartment from the vacuolar H^+-ATPase. Biochem. J. **340**, 759–766

43 Vercesi, A., Rodrigues, C. O., Catisti, R. and Docampo, R. (2000) Presence of a Na^+/H^+ exchanger in acidocalcisomes of *Leishmania donovani* and their alkalinization by anti-leishmanial drugs. FEBS Lett. **473**, 203–206

44 Maeshima, M. (2001) Tonoplast transporters: organization and function. Annu. Rev. Plant Physiol. Plant Mol. Biol. **52**, 469–497.

45 Ratto, A. and Christen, R. (1988) Purification and characterization of arginine kinase from sea-urchin eggs. Eur. J. Biochem. **173**, 667–674

46 Lemercier, G., Espiau, B., Ruiz, F. A., Vieira, M., Luo, S., Baltz, T., Docampo, R. and Bakalara, N. (2004) A pyrophosphatase regulating polyphosphate metabolism in acidocalcisomes is essential for *Trypanosoma brucei* virulence in mice. J. Biol. Chem. **279**, 3420–3425

47 Rodrigues, C. O., Ruiz, F. A., Vieira, M., Hill, J. E. and Docampo, R. (2002) An acidocalcisomal exopolyphosphatase from *Leishmania major* with high affinity for short chain polyphosphate. J. Biol. Chem. **277**, 50899–50906.

48 Johnson, J. D. and Epel, D. (1976) Intracellular pH and activation of sea urchin eggs after fertilisation. Nature **262**, 661–664

49 Shen, S. S. and Steinhardt, R. A. (1978) Direct measurement of intracellular pH during metabolic derepression of the sea urchin egg. Nature **272**, 253–254

50 Epel, D. and Carroll, Jr, E. J. (1975) Molecular mechanisms for prevention of polyspermy. Res. Reprod. **7**, 2–3

51 Patel, S. and Docampo, R. (2010) Acidic calcium stores open for business: expanding the potential for intracellular Ca^{2+} signaling. Trends Cell Biol. **20**, 277–286

Received 23 December 2009/6 May 2010; accepted 24 May 2010
Published as BJ Immediate Publication 24 May 2010, doi:10.1042/BJ20091956

© 2010 The Author(s)
The author(s) has paid for this article to be freely available under the terms of the Creative Commons Attribution Non-Commercial Licence (http://creativecommons.org/licenses/by-nc/2.5/) which permits unrestricted non-commercial use, distribution and reproduction in any medium, provided the original work is properly cited.

This is a data-enriched, interactive PDF that provides the gateway to a world of information when opened in Utopia Documents
Download FREE software now

Biochem. J. (2010) **429**, 485–495 (Printed in Great Britain) doi:10.1042/BJ20091956

multimedia online data

SUPPLEMENTARY ONLINE DATA

Calcium- and polyphosphate-containing acidic granules of sea urchin eggs are similar to acidocalcisomes, but are not the targets for NAADP

Isabela B. RAMOS*†, Kildare MIRANDA†‡, Douglas A. PACE*, Katherine C. VERBIST*, Fu-Yang LIN§, Yonghui ZHANG‖, Eric OLDFIELD§‖, Ednildo A. MACHADO†‡, Wanderley DE SOUZA† and Roberto DOCAMPO*[1]

*Department of Cellular Biology and Center for Tropical and Emerging Global Diseases, University of Georgia, Athens, GA 30602, U.S.A., †Instituto de Biofísica Carlos Chagas Filho, and Instituto Nacional de Ciência e Tecnologia em Bioimagens e Biologia Estrutural, Universidade Federal do Rio de Janeiro, Rio de Janeiro, RJ 21941, Brazil, ‡Instituto Nacional de Metrologia Normalização e Qualidade Industrial, Diretoria de Programas, Xerém, Rio de Janeiro, RJ 25250, Brazil, §Center for Biophysics and Computational Biology, University of Illinois at Urbana-Champaign, Urbana, IL 61801, U.S.A., and ‖Department of Chemistry, University of Illinois at Urbana-Champaign, Urbana, IL 61801, U.S.A.

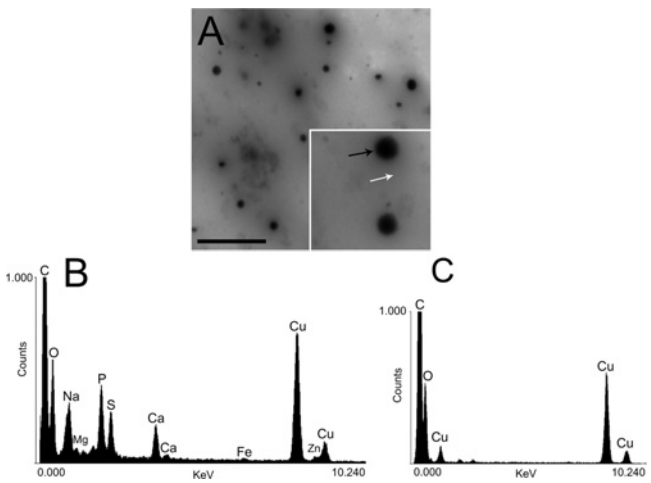

Figure S1 Electron microscopy and X-ray microanalysis of the dense granule fraction

(**A**) Direct observation of unfixed and unstained dense granules air-dried directly on to microscope grids. (**B**) Typical X-ray microanalysis spectrum of dense granules (black arrow). (**C**) Control spectrum of an adjacent area (white arrow). Scale bars in (**A**) are 0.5 μm.

[1] To whom correspondence should be addressed (email rdocampo@uga.edu).

© 2010 The Author(s)
The author(s) has paid for this article to be freely available under the terms of the Creative Commons Attribution Non-Commercial Licence (http://creativecommons.org/licenses/by-nc/2.5/) which permits unrestricted non-commercial use, distribution and reproduction in any medium, provided the original work is properly cited.

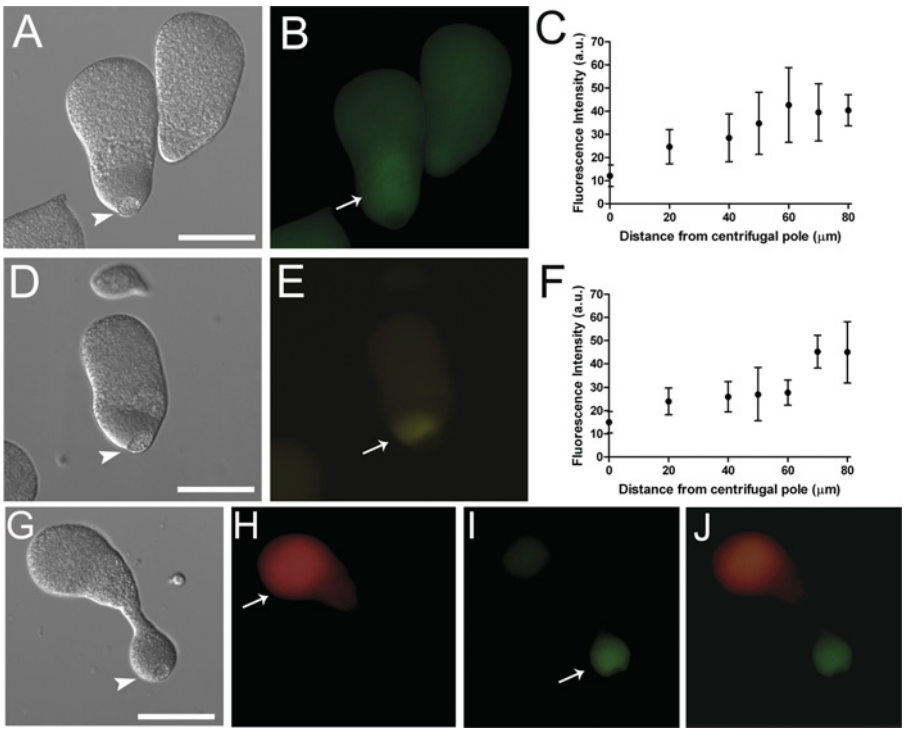

Figure S2 Segregation of poly P stores in stratified sea urchin eggs

(**A**, **B** and **C**) Sea urchin eggs were stratified and poly P stores were localized using the recombinant PPBD of *E. coli* PPX linked with an Xpress epitope tag. (**D, E** and **F**) Stratified eggs after DAPI incubation for poly P localization. (**C** and **F**) Fluorescence intensity profile plots of PPBD and DAPI staining respectively. Graphs show means ± S.D. for five eggs. (**G, H, I** and **J**) Sea urchin eggs were incubated with LysoTracker Red, stratified and then fixed and stained with PPBD as described in the Materials and methods section of the main text. (**G**) Differential interferential contrast microscopy image of one stratified egg. (**H, I** and **J**) LysoTracker, PPBD and merged corresponding images of (**G**) respectively. Arrows in (**B, E, H** and **I**) indicate staining near the centripetal pole, where the nucleus and lipid droplets (arrowheads in **A**, **D** and **G**) are also located. Images were not deconvolved. Scale bars are 50 μm.

© 2010 The Author(s)

The author(s) has paid for this article to be freely available under the terms of the Creative Commons Attribution Non-Commercial Licence (http://creativecommons.org/licenses/by-nc/2.5/) which permits unrestricted non-commercial use, distribution and reproduction in any medium, provided the original work is properly cited.

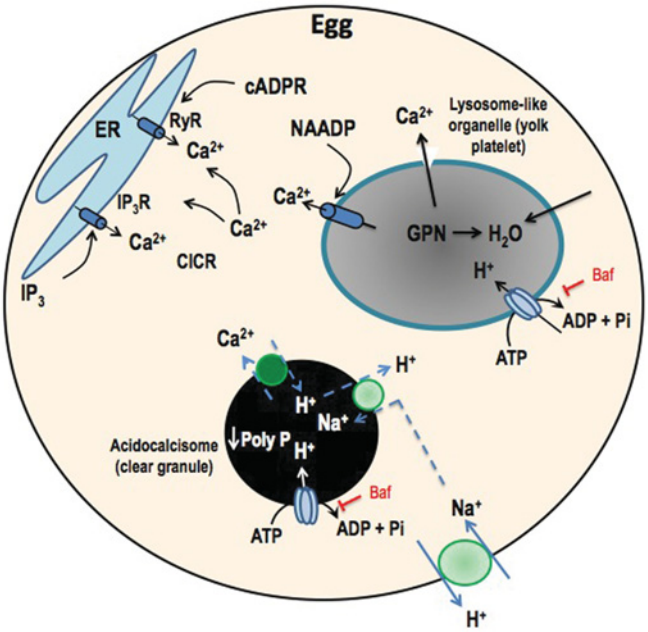

Figure S3 Proposed Ca^{2+} mobilization pathways in sea urchin eggs

ER, acidocalcisomes and yolk platelets are major Ca^{2+} storage organelles. IP_3 receptors (IP_3R) and ryanodine receptors (RyR) mediate Ca^{2+} release from the ER in response to increases in IP_3 and cADPR respectively. Both receptors types are, in addition, activated by Ca^{2+} via the so-called Ca^{2+}-induced Ca^{2+}-release mechanism (CICR). NAADP triggers Ca^{2+} release from yolk platelets and this in turn triggers ER Ca^{2+} mobilization through Ca^{2+}-induced Ca^{2+} release via IP_3R and RyR. Na^+ entry after fertilization leads to alkalinization of the cytosol and stimulates Ca^{2+} release from acidocalcisomes by coupling the activity of Na^+/H^+ and Ca^{2+}/H^+ exchangers. GPN is hydrolysed by cathepsin C increasing the osmolarity of yolk platelets, attracting water and leading to osmotic lysis and Ca^{2+} release. Both acidocalcisomes and yolk platelets possess bafilomycin A_1 (Baf)-sensitive vacuolar-type H^+-ATPases to acidify the organelles. Poly P is hydrolysed after alkalinization of acidocalcisomes.

Received 23 December 2009/6 May 2010; accepted 24 May 2010
Published as BJ Immediate Publication 24 May 2010, doi:10.1042/BJ20091956

© 2010 The Author(s)
The author(s) has paid for this article to be freely available under the terms of the Creative Commons Attribution Non-Commercial Licence (http://creativecommons.org/licenses/by-nc/2.5/) which permits unrestricted non-commercial use, distribution and reproduction in any medium, provided the original work is properly cited.

8- Anexo IV:

Biol. Cell (2010) **102**, 421–434 (Printed in Great Britain) doi:10.1042/BC20100011

Research article

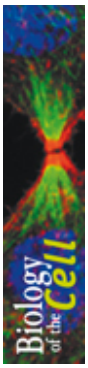

Calcium- and polyphosphate-containing acidocalcisomes in chicken egg yolk

Isabela B. Ramos*†, Kildare Miranda*†‡, Paul Ulrich*, Peter Ingram§‖, Ann LeFurgey§‖, Ednildo A. Machado†‡, Wanderley de Souza† and Roberto Docampo*[1]

*Department of Cellular Biology and Center for Tropical and Emerging Global Diseases, University of Georgia, Athens, GA 30602, U.S.A., †Instituto de Biofísica Carlos Chagas Filho, Universidade Federal do Rio de Janeiro, Rio de Janeiro, RJ 21941, Brazil, ‡Instituto Nacional de Metrologia Normalização e Qualidade Industrial-RJ, DIPRO - Diretoria de Programas, Xerém, RJ 25250020, Brazil, §Departments of Cell Biology and Pathology, Duke University Medical Center, Durham, NC 27710, U.S.A., and ‖Veterans Affairs Medical Center, Durham, NC 27705, U.S.A.

Background information. Poly P (inorganic polyphosphate) is a polymer formed by P_i residues linked by high-energy phosphoanhydride bonds. The presence of poly P in bacteria, fungi, algae and protists has been widely recognized, but the distribution of poly P in more complex eukaryotes has been poorly studied. Poly P accumulates, together with calcium, in acidic vesicles or acidocalcisomes in a number of organisms and possesses a diverse array of functions, including roles in stress response, blood clotting, inflammation, calcification, cell proliferation and apoptosis.

Results. We report here that a considerable amount of phosphorus in the yolk of chicken eggs is in the form of poly P. DAPI (4′,6-diamidino-2-phenylindole) staining showed that poly P is localized mainly in electron-dense vesicles located inside larger vacuoles (compound organelles) that are randomly distributed in the yolk. These internal vesicles were shown to contain calcium, potassium, sodium, magnesium, phosphorus, chlorine, iron and zinc, as detected by X-ray microanalysis and elemental mapping. These vesicles stain with the acidophilic dye Acridine Orange. The presence of poly P in organellar fractions of the egg yolk was evident in agarose gels stained with Toluidine Blue and DAPI. Of the total phosphate (P_i) of yolk organelles, 16% is present in the form of poly P. Total poly P content was not altered during the first 4 days of embryogenesis, but poly P chain length decreased after 1 day of development.

Conclusions. The results of the present study identify a novel organelle in chicken egg yolk comprising acidic vesicles with a morphology, physiology and composition similar to those of acidocalcisomes, within larger acidic vacuoles. The elemental composition of these acidocalcisomes is proportionally similar to the elemental composition of the yolk, suggesting that most of these elements are located in these organelles, which might be an important storage compartment in eggs.

Introduction

Poly P (inorganic polyphosphate) is a polymer formed by P_i residues linked by high-energy phosphoanhydride bonds. The presence of poly P in bacteria, fungi, algae and protists has been widely recognized, but the distribution of poly P in more complex eukaryotes has been poorly studied due to its lower abundance and lack of sensitive methods for its detection (Kornberg, 1995). Enzymatic assays allow quantitative detection of levels of 20–120 μM (in terms of P_i monomers) poly P in chains 50–800 residues long in tissues (brain, heart, kidneys, liver and lungs) and subcellular fractions (nuclei, mitochondria, plasma membrane and microsomes) (Kumble and Kornberg, 1995). Poly P possesses a diverse array of functions, including

[1]To whom correspondence should be addressed (email rdocampo@uga.edu).
Key words: acidocalcisome, calcium, chicken egg, polyphosphate, yolk.
Abbreviations used: DAPI, 4′,6-diamidino-2-phenylindole; DTT, dithiothreitol; DV, dense vesicle; FCCP, carbonyl cyanide *p*-trifluoromethoxyphenylhydrazone; GluIM, gluconate intracellular-like medium; IMP, intramembranous particle; poly P, inorganic polyphosphate; rScPPX, recombinant *Saccharomyces cerevisiae* exopolyphosphatase; V-H^+-ATPase, vacuolar H^+-ATPase; V-H^+-PPase, vacuolar proton pyrophosphatase.

Biology of the Cell www.biolcell.org

roles in blood clotting (Smith et al., 2006), inflammation (Müller et al., 2009), calcification (Kawazoe et al., 2004), cell proliferation (Shiba et al., 2003; Wang et al., 2003), apoptosis (Hernandez-Ruiz et al., 2006), angiogenesis (Han et al., 2007), ion channel modulation (Zakharian et al., 2009), regulation of mitochondrial function (Abramov et al., 2007), development, predation and sporulation in the slime mold *Dictyostelium discoideum* (Zhang et al., 2005), and osmoregulation in *Trypanosoma cruzi* (Ruiz et al., 2001a) and *Trypanosoma brucei* (Fang et al., 2007).

In a number of organisms, from bacteria to humans (Docampo et al., 2005), poly P accumulates in acidic organelles, which are known as acidocalcisomes, where it can reach millimolar or molar levels (in terms of P_i monomers). Acidocalcisomes can be easily identified by electron microscopy due to their very high-electron density, and their high content of calcium and other cations can be detected by X-ray microanalysis (Docampo et al., 2005; LeFurgey et al., 2005).

Eggs from sea urchins (I.B. Ramos and R. Docampo, unpublished data) and insects (Gomes et al., 2008; Motta et al., 2009) are rich in phosphorus and calcium and possess poly-P-rich acidocalcisomes. Chicken eggs are also rich in phosphorus and calcium, and chicken egg yolk contains different types of vesicles, some of which are electron-dense and contain calcium (Komazaki et al., 1993).

In the present study, we report the isolation and biochemical characterization of electron-dense vesicles containing poly P, calcium and other cations from the yolk of chicken eggs. These vesicles are acidic and reside within larger vacuoles that we named compound organelles. We identified poly P in the vesicles by enzymatic assays and staining with DAPI (4′,6-diamidino-2-phenylindole). Additionally, we showed the presence of different elements using X-ray microanalysis and elemental mapping. The compound organelles and the vesicles inside them are acidic and the vesicles are similar to acidocalcisomes of other organisms.

Results

Ultrastructure and elemental analysis of the DVs (dense vesicles) inside compound organelles

To investigate the presence of acidic organelles in the egg yolk, yolk organelles were labelled with Acridine Orange (Figure 1A). A population of organelles (mean diameter ± S.D., 42.4 ± 14.1 μm) labelled green/yellow with Acridine Orange and contained smaller orange vesicles (arrows in Figure 1A, and see Figures 1B and 1C). These compound organelles were analysed by energy-filtering transmission electron microscopy. Using this technique the contrast of a given structure in the image solely arises from its mass density, as the preparations are not stained. Many electron-dense vesicles

Figure 1 | Fluorescence and energy-filtered transmission electron microscopy of compound organelles

(**A**) An enriched compound organelle fraction was obtained by differential centrifugation and stained with 6 μM Acridine Orange. The lumina of the organelles have yellow fluorescence, whereas the internal vesicles have orange/red fluorescence (arrows). Other organelles are labelled green and probably represent less acidic organelles or compound organelles that did not take up enough Acridine Orange during the incubation period. Scale bar, 200 μm. DIC (differential interference contrast) (**B**) and Acridine Orange staining (**C**) of a compound organelle. Scale bars, 20 μm. (**D**) Compound organelles observed by energy-filtering transmission electron microscopy. The internal vesicles are electron dense. Scale bar, 5 μm.

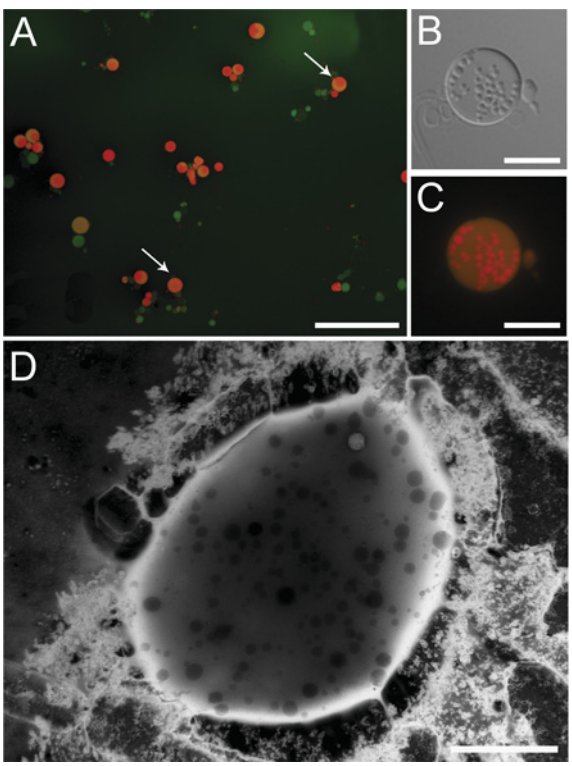

© The Authors Journal compilation © 2010 Portland Press Limited

(DVs, mean diameter ± S.D., 1.31 ± 0.11 μm), which correspond to the acidic vesicles seen inside the Acridine Orange-stained material, were observed inside the compound organelles (Figure 1D). X-ray microanalysis was performed on these DVs to investigate their elemental composition. The spectrum shown in Figure 2(B) is the one that yielded more counts in 100 s (of ten spectra obtained), but all spectra taken from DVs were qualitatively similar, showing considerable amounts of phosphorus, calcium, potassium, sodium, iron and chloride (Figures 2A and 2B). X-ray elemental mapping established that these elements are mainly stored in the DVs, rather than the extra-vesicular space in the lumen of the compound organelles (Figures 2C–2L). DVs are thus similar to acidocalcisomes in acidity (able to accumulate acidophilic dyes), electron density and large accumulations of phosphorus, calcium and other cations.

Poly P detection and localization in the DVs

As acidocalcisomes accumulate large amounts of poly P (Docampo et al., 2005), we investigated whether the phosphorus detected in DVs by X-ray microanalysis and elemental mapping corresponded to the presence of this polymer. Poly P was detected by electrophoresis of yolk organelle extracts in agarose gels stained with Toluidine Blue. Figure 3(A, lane 3) shows a large amount of high-molecular-mass poly P (black arrow) and a lower amount of shorter-chain poly P (diffuse staining indicated by white arrow) above the region where poly P_{75+} (synthetic poly P with a mean chain length of 84) migrates. Pre-treatment of these samples with rScPPX (recombinant *Saccharomyces cerevisiae* exopolyphosphatase) resulted in disappearance of the shorter-chain poly P, in agreement with the higher specificity of rScPPX for short-chain poly P (Wurst et al., 1995) and a considerable decrease [44.5 ± 2.6% decrease in pixel intensity (mean ± S.D.), $n = 3$] in staining of the high-molecular-mass band (Figure 3A, lane 4).

We also investigated poly P distribution within organelles using DAPI (Figures 3B and 3C). The emission fluorescence of DAPI shifts to a maximum wavelength of 525 nm (yellow) in the presence of poly P. This shift in emission wavelength is specific to poly P and is not produced by pyrophosphate (PP_i) or other anions (Smith et al., 2006; Ruiz et al., 2001a). DAPI staining localized to the DVs, rather than the lumen of the compound organelles (Figure 3C, and see Supplementary Movie 1 at http://www.biolcell.org/boc/102/boc1020421add.htm). Taken together, these results demonstrate that the DVs present in some organelles of the egg yolk are, indeed, similar to acidocalcisomes.

Separation of the acidocalcisome-like DVs

Differential centrifugation protocols using hypo-osmotic buffers allowed us to disrupt the compound organelles and obtain a clear fraction containing the acidocalcisome-like DVs free in suspension (Figure 4). Scanning (Figure 4A) and transmission (Figure 4B) electron microscopy of this fraction, dried on Formvar-coated grids, showed the presence of multiple vesicles with high electron density (Figure 4B). The vesicles in the fraction were also acidic, as shown by Acridine Orange staining (Figure 4C) and stored high concentrations of phosphorus, calcium, sulfur and magnesium (Figures 4D–4I, X-ray microanalysis and elemental mapping). Interestingly, lower amounts of potassium and sodium and higher amounts of sulfur and magnesium were detected in the DV fractions compared with the compound-organelle preparations (Figure 2B). This probably occurs owing to changes during fractionation of the samples due to the absence of endogenous energy sources to maintain their acidity. Similar changes in elemental composition after centrifugation have been reported with acidocalcisomes from other species (Ruiz et al., 2001a, 2001b; Seufferheld et al., 2003). Poly P was also detected in the DV fraction when separated on agarose gels and stained with Toluidine Blue (Figure 5A) and DAPI (Figure 5B). The migration of poly P extracted from DVs in agarose gels was dramatically different from that observed with poly P extracted from the total yolk organelles (Figure 5A, lanes yolk organelles and DV), with a shorter-chain-length smear in the lower part of the gel and a major spot with a slightly slower mobility than the poly P_{75+} standard. Pre-treatment of the DV poly P extracts with rScPPX1 resulted in a decrease in Toluidine Blue labelling [Figure 5A, lane DV + PPX, 23.2 ± 9.2% (means ± S.D.) decrease in pixel intensity as compared with non-treated samples, $n = 3$]. Poly P was also detected using DAPI (Smith and Morrissey, 2007). Poly P staining with DAPI was similar to Toluidine Blue staining, and pre-treatment of DV poly P with rScPPX1 resulted in considerable decrease in labelling [Figure 5B, lane DV + PPX,

Figure 2 | X-ray microanalysis and elemental mapping of the compound organelles

Compound organelles were analysed by analytical electron microscopy. (**A**) Electron energy-filtered image of a whole unfixed compound organelle. (**B**) Corresponding X-ray spectrum of the DV indicated by the arrow in (**A**). Copper peaks in the spectrum came from the grid. (**C**–**L**) Elemental mapping of the organelle shown in (**A**) reveals the localization of phosphorus, calcium, potassium, sodium, magnesium, chlorine, iron, zinc and sulfur. Scale bars, 10 μm.

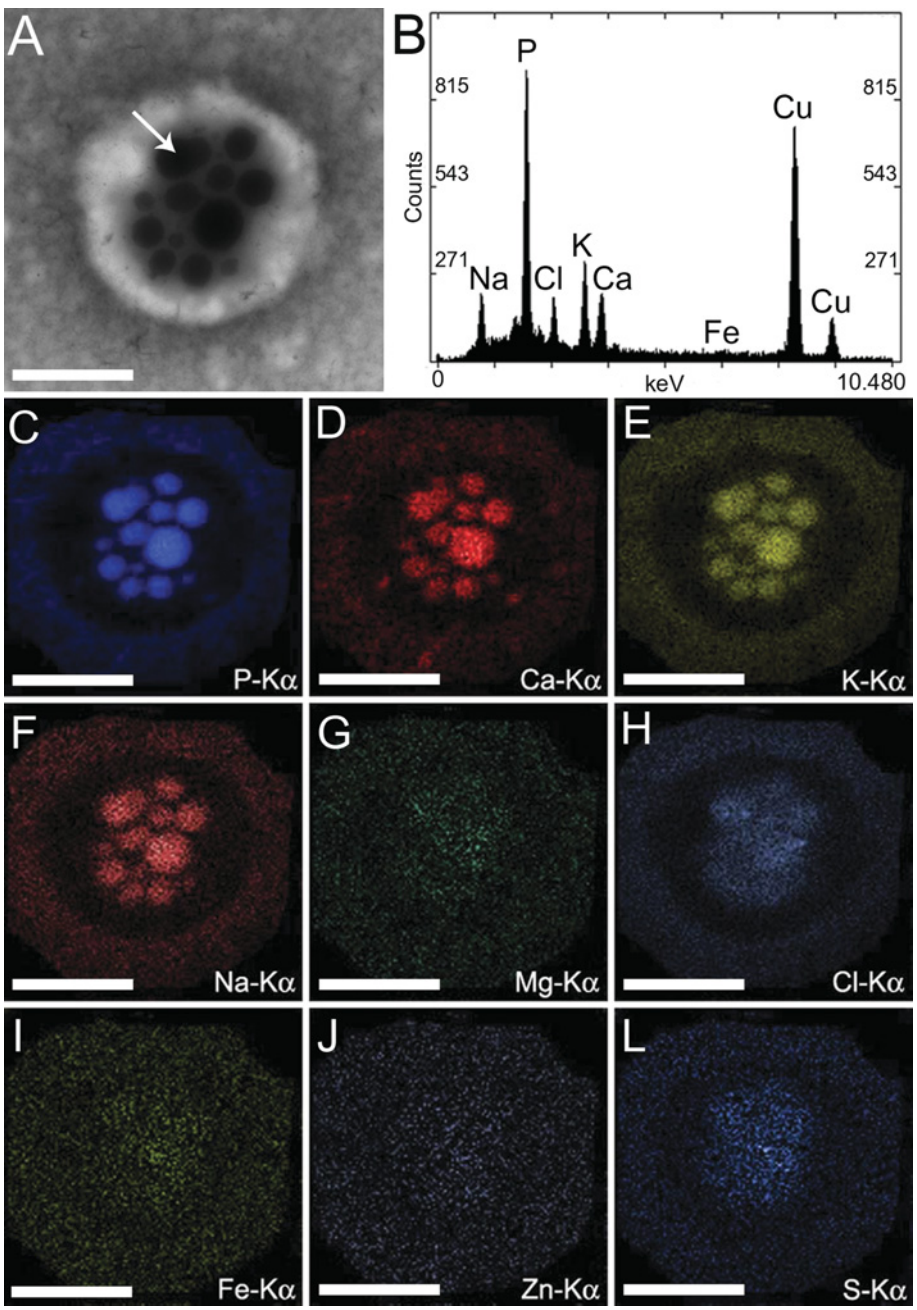

75 ± 4.5% (means ± S.D.) decrease in pixel intensity compared with non-rScPPX1-treated samples, lane DV, $n = 3$]. To rule out possible cross-reaction between DAPI and glycosaminoglycans, heparin was added to the gels, but was not detected after DAPI staining (Figure 5B, lane Heparin), further supporting DAPI specificity in binding to poly P. Additionally, poly P localization in DVs was confirmed by

© The Authors Journal compilation © 2010 Portland Press Limited

Figure 3 | Detection of poly P in the yolk organelles and its localization in DVs

(**A**) Poly P was extracted from the yolk organelles of one egg as described in the Materials and methods section, separated by agarose gel electrophoresis and stained with Toluidine Blue. Synthetic poly P (5 μg) with mean chain lengths of 25 (poly P_{25}), or 84 (poly P_{75+}) phosphate units were loaded on to lanes 1 and 2 as size standards (arrows). Lane 3: poly P from yolk organelles (the black arrow indicates high-molecular-mass poly P and the white arrow indicates shorter poly P). Lane 4, poly P from yolk organelles was incubated for 30 min with rScPPX prior to electrophoresis. (**B**, **C**) DIC (differential interference contrast) and DAPI staining of compound organelles demonstrate poly P localization in internal vesicles (see also Supplementary Movie 1 at http://www.biolcell.org/boc/102/boc1020421add.htm). Scale bars, 5 μm.

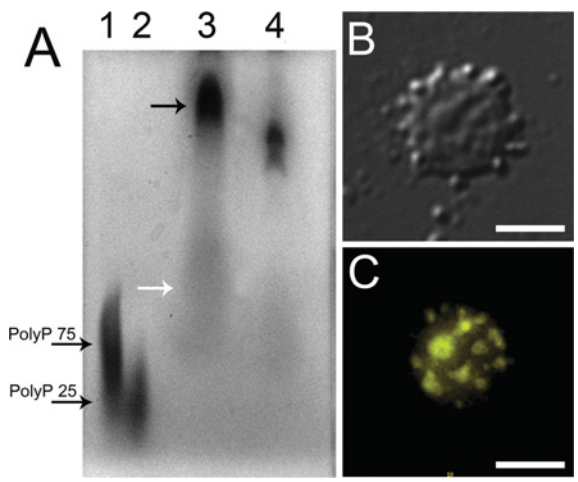

DAPI staining of fixed DV fractions (Figures 5C and 5D).

Poly P levels in the different fractions of egg yolk organelles

Total amounts of P_i and poly P were quantified in the different fractions of the egg yolk containing total yolk organelles, compound organelles or free DVs (Figures 6A–6C). Approx. 2% (146 ± 38 μM; means ± S.D.) of the free P_i detected in raw yolk (4.6 ± 0.8 mM, means ± S.D.; data not shown) is compartmentalized in the yolk organelles (Figure 6A). This suggests that at least part of the phosphorus found in the DVs (as detected by X-ray microanalysis, Figures 2B and 4D) might be stored within the vesicles in the form of free P_i. Poly P is present in the micromolar range in the yolk organelles (in terms of P_i residues; Figure 6B), supporting our findings that this polymer is mainly stored in organelles (Figure 3C). Compound organelles contain 64.2% of the poly P detected in the total yolk organelles, and 18.2% of the poly P from the compound organelles is found in the DVs (Figure 6B). When normalized by protein content for each fraction, the results confirm that this polymer is a major constituent of these compartments (Figure 6C).

Poly P levels and changes during early embryogenesis

Total poly P was quantified in the different fractions of the egg yolk organelles at different days of early embryogenesis. Figure 7(A) shows that the amount of poly P in the egg yolk organelle fractions was not significantly altered for the first 3 days of development (one-way ANOVA, $P > 0.05$). However, the apparent size of poly P, as visualized by Toluidine Blue and DAPI staining in agarose gels, was altered during the early events of embryogenesis, between days 0 and 1. The chain length of poly P extracted from the yolk organelles decreased at day 1 relative to the chain length of poly P from non-incubated eggs, and this pattern remained almost unaltered, at least until the third day of embryogenesis (Figure 7B, left-hand panels). Profiles of poly P extracted from the DVs exhibited a general chain-length decrease and the appearance of a population of shorter poly P chains beginning with day 1 (Figure 7B, arrow in upper right-hand gel). These differences cannot be attributed simply to poly P degradation into P_i, since the total levels of this polymer are the same during embryogenesis (Figure 7A). Changes in chain length are likely due to cleavage of high-molecular-mass polymers into smaller chains through the activity of endogenous polyphosphatases, thus maintaining total poly P levels while decreasing the average chain length of the poly P pool.

Nature of DV membranes

Although physiological data suggested the presence of an enclosing membrane in the DVs, analysis of thin sections of glutaraldehyde/osmium-fixed compound organelles by transmission electron microscopy did not reveal a typical lipid bilayer (probably due to the poor preservation of the preparations). To confirm

Figure 4 | Electron and fluorescence microscopy, X-ray microanalysis and elemental mapping of isolated DVs

(**A**, **B**) A fraction enriched in the interior vesicles of compound organelles (DVs) was obtained by hypo-osmotic lysis and centrifugation, and observed by scanning (**A**) and transmission (**B**) electron microscopy of whole unfixed mounts. Scale bars: 5 μm (**A**); 3 μm (**B**). (**C**) Isolated DVs were stained with 6 μM Acridine Orange. Scale bar, 60 μm. (**D**) X-ray microanalysis spectrum of the DV indicated by the arrow in (**E**). (**F–I**) Elemental mapping of the DV shown in (**E**) (boxed), revealing the co-localization of calcium, magnesium, sulfur and phosphorus. Scale bars, 2 μm.

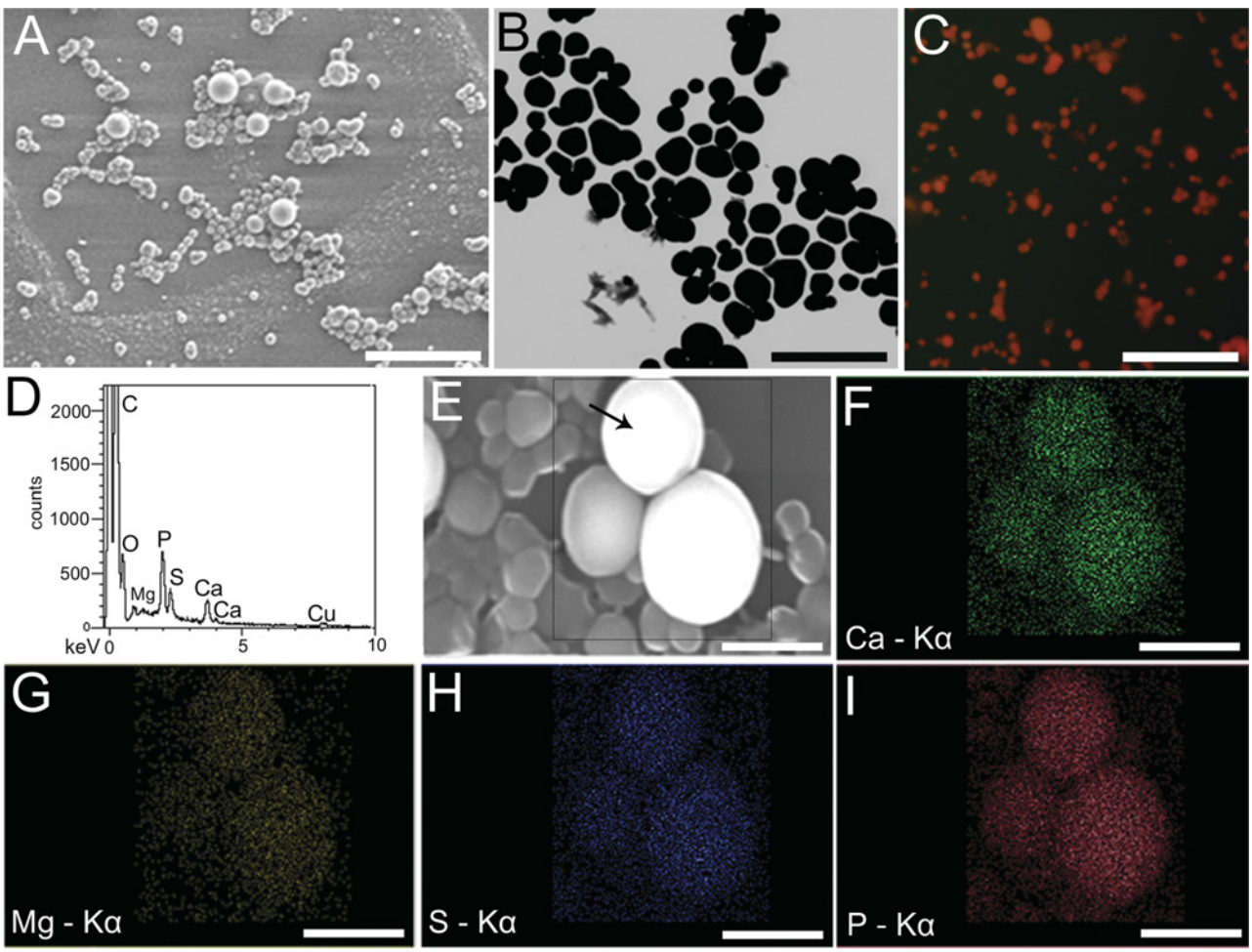

the presence of such structure and show the structural organization of DV membrane, samples were analysed by freeze–fracture (Figure 8). Using this technique, it was possible to observe the general smooth aspect of the fractured membranes (Figure 8A), presenting a low number of IMPs (intramembranous particles), distributed on the E (external face of the inner leaflet) (Figure 8C, black arrow) and the P (internal face of the outer leaflet) (Figure 8D, black arrow) faces of the membrane. The presence of a low number of IMPs indicates a low protein content, which may reflect in decreased sensitivity to glutaraldehyde fixation. This might explain why it was dificult to identify profiles of lipid bilayers in transmission electron microscopy images of thin sections (data not shown).

V-H^+-ATPase (vacuolar H^+-ATPase) activity in the isolated organelles

Bafilomycin-A_1-sensitive ATPase activity (measured by P_i release from ATP) was enriched in the compound organelles and DV fractions (Figure 9A, one-way ANOVA, $P < 0.05$), suggesting that the V-H^+-ATPase (Nelson et al., 2000) is present in these membranes. Although isolated DVs could take

© The Authors Journal compilation © 2010 Portland Press Limited

Figure 5 | Identification of poly P in the DVs

(**A**, **B**) Poly P was extracted from yolk organelles of one egg, as described in the Materials and methods section, separated by agarose gel electrophoresis and stained with Toluidine Blue (**A**) or DAPI (**B**). Synthetic poly P (5 μg) with mean chain lengths of 25 (poly P_{25}) or 84 (poly P_{75+}) phosphate units were loaded in (**A)** (arrows) and (**B**) (P25 and P75) as size standards. Poly P from yolk organelles or DV was loaded as indicated. The DV samples were also incubated for 30 min with rScPPX (PPX) prior to electrophoresis and loaded where indicated. Heparin (5 μg) was loaded in (**B**) as a control. (**C**, **D**) DIC (differential interference contrast) and DAPI staining of DV showing poly P localization. Scale bars, 10 μm.

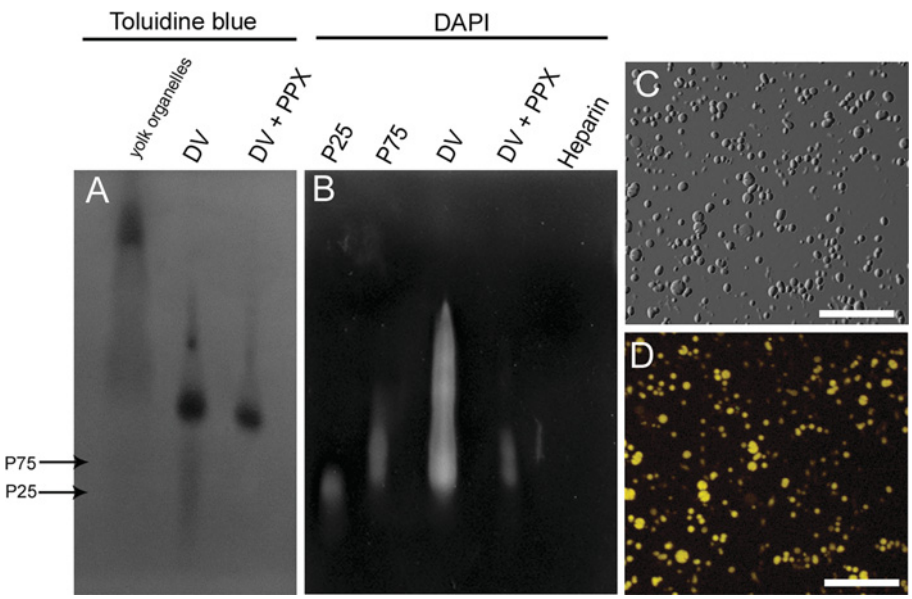

Figure 6 | Quantification of phosphate and poly P in the different fractions of the egg yolk

P_i and poly P were assayed in different fractions as described in the Materials and methods section. P_i (**A**) and poly P (**B**) concentrations in each fraction were calculated taking into account a yolk volume of 8.18 ml and expressed in terms of P_i residues. (**C**) Poly P levels per mg of protein (ptn) in the different fractions. Results are the means ± S.D. for at least five experiments. Asterisks in (**A**) and **B**) indicate significant differences between the fractions ($P < 0.05$, one-way ANOVA).

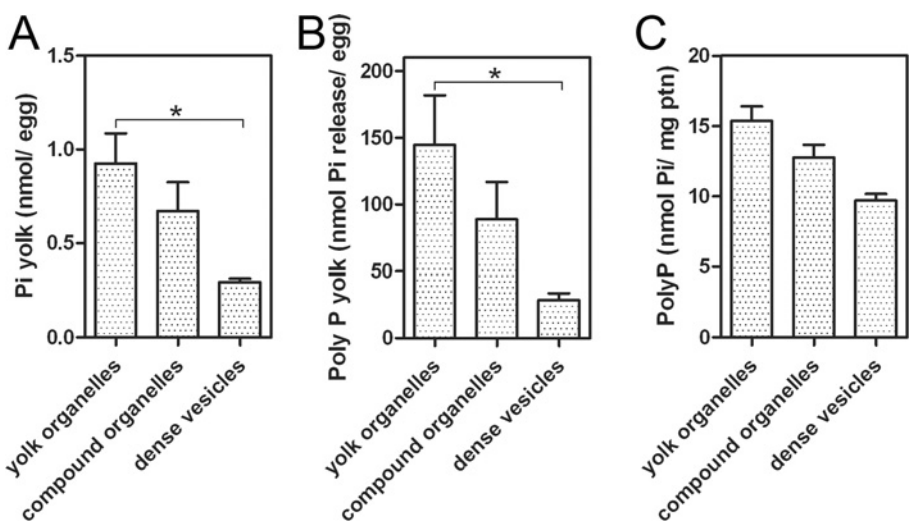

Figure 7 | Changes in poly P during early embryogenesis

(**A**) Poly P was extracted from different fractions of the egg yolk at different days of embryogenesis; results are expressed as the means ± S.D. for at least five experiments. (**B**) Poly P was extracted from yolk organelles and DV of one egg at day 0, 1, 2 and 3 of embryogenesis as described in the Materials and methods section, separated by agarose gel electrophoresis and stained with Toluidine Blue or DAPI, as indicated. Synthetic poly P (5 μg) with mean chain lengths of 25 (P25) or 84 (P75) phosphate units were loaded as size standards.

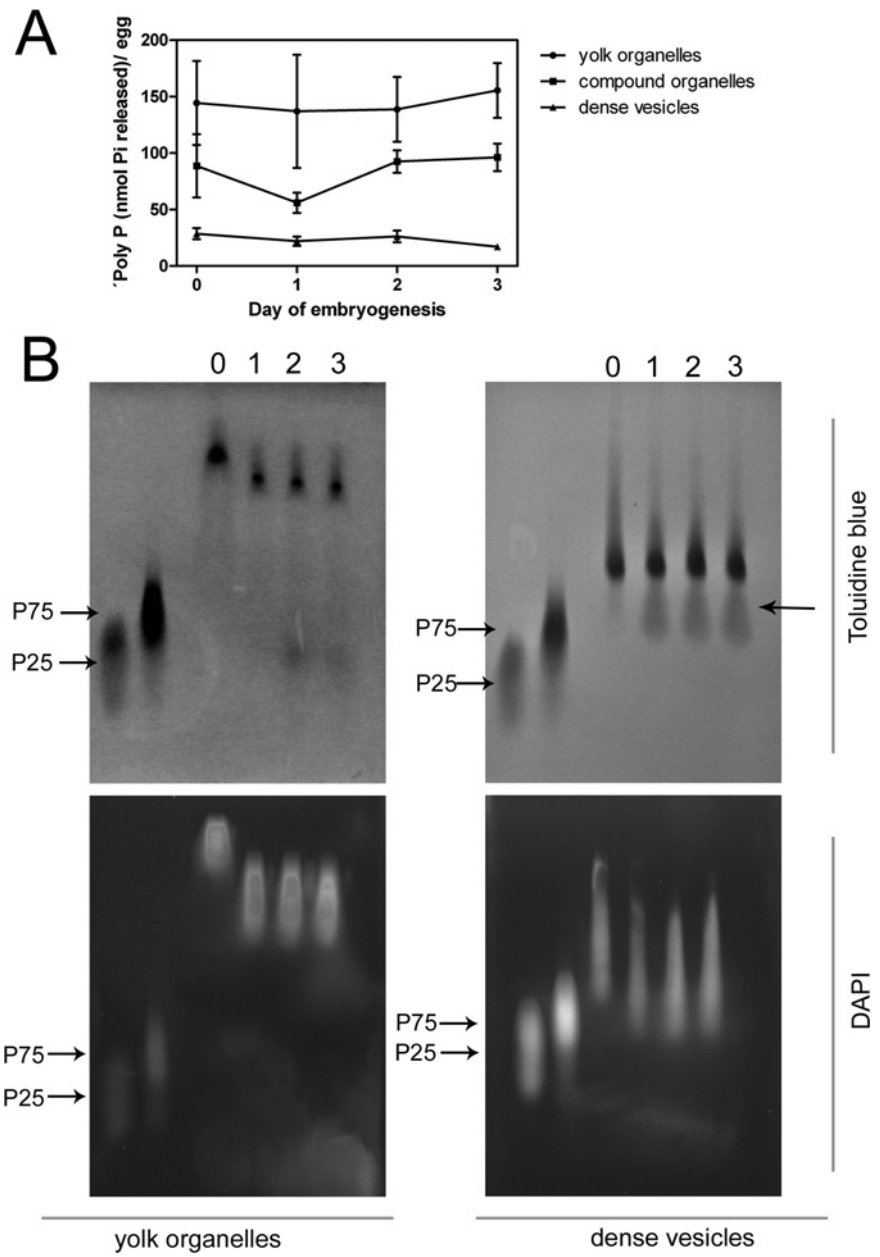

up Acridine Orange and thus remain intact and acidic, ATP did not stimulate this process (Figure 9B). Alkalinization of DVs by the addition of NH_4Cl resulted in the release of the Acridine Orange accumulated (Figures 9B and 9D, inset). Nigericin had no effect. Previous work with sea urchin eggs (Morgan and Galione, 2007) has shown that the function of the proton pump in yolk granules could be

© The Authors Journal compilation © 2010 Portland Press Limited

Figure 8 | Freeze–fracture analysis of DV fractions

(**A**, **B**) Freeze–fracture image of DVs showing the E (external face of the inner leaflet) and P (internal face of the outer leaflet) of fractured membranes (arrowheads and arrows respectively). Scale bars: 4 μm (**A**); 2 μm (**B**). (**C**, **D**) High-magnification images of freeze–fractured DVs, showing IMPs (black arrows) randomly distributed on the E and P of membranes. Scale bars, 2 μm.

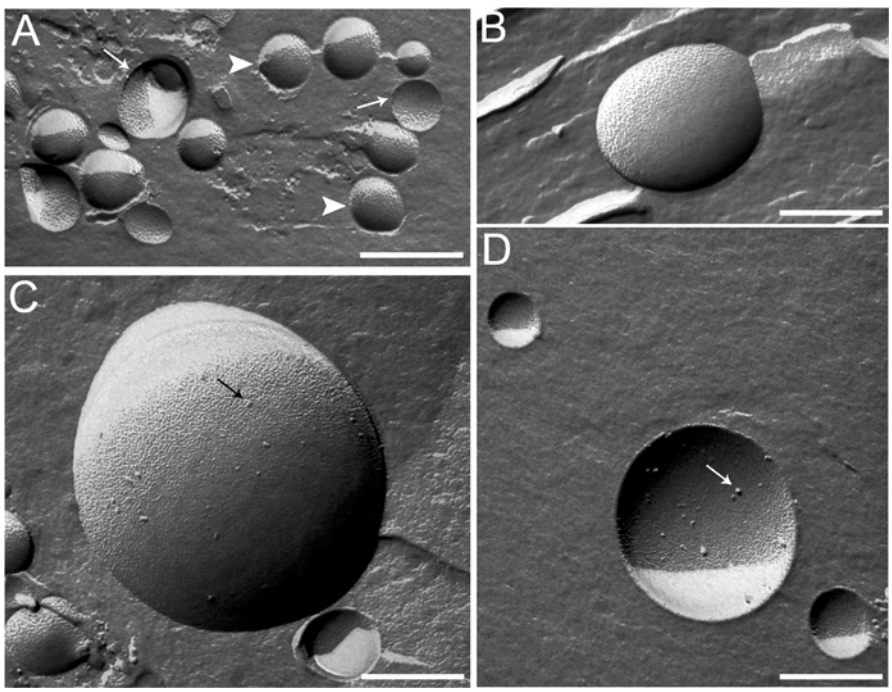

demonstrated only by inhibition of acidification by bafilomycin A_1 after pre-incubation of the preparation with either valinomycin or FCCP (carbonyl cyanide *p*-trifluoromethoxyphenylhydrazone), and this was attributed to the presence of negligible H^+ leak and 'tightness' of the vesicles. However, similar experiments using bafilomycin A_1, valinomycin or FCCP failed to demonstrate proton pumping in DVs of chicken egg yolk (data not shown). However, Figures 9(G) and 9(H) shows labelling of the membrane surrounding the acidic vesicles with monoclonal antibodies against the yeast V-H^+-ATPase A subunit, confirming the presence of this enzyme. These antibodies showed cross-reactivity with only one band of 73.2 kDa present in the fraction (Figure 9E).

Discussion

We report here that chicken egg yolk is rich in poly P as detected by a specific hydrolysis by an exopolyphosphatase and by Toluidine Blue and DAPI staining of poly P extracts separated on agarose gels. The length of the yolk poly P appears to change early during embryogenesis. We also identified a novel compound organelle that is acidic and possesses internal acidic and electron-dense vesicles rich in phosphorus, in the form of poly P and P_i, calcium and other cations. These vesicles are similar to acidocalcisomes present in other organisms, thus extending the phylogenetic distribution of these organelles to birds. On the basis of their electron density and elemental composition, and in their biochemical analyses, these organelles appear as rich in poly P and calcium as described for acidocalcisomes in other organisms.

Poly P is found in all organisms. Bacteria utilize poly P for energy storage, cation sequestration and storage, cell membrane formation and function, transcriptional control, regulation of enzymatic activities, response to stress and stationary phase, and the structure of channels and pumps (Kornberg et al., 1999; Kulaev and Kulakovskaya, 2000). Poly P has been implicated in stress responses in eukaryotic cells, such as yeast (Castro et al., 1995, 1999), fungi (Yang et al., 1993), algae (Pick and Weiss, 1991; Weiss et al.,

Figure 9 | Bafilomycin-A_1-sensitive ATPase activity in the different fractions of the egg yolk, Acridine Orange uptake by isolated DVs, and immunofluorescence and Western blot analyses with anti-V-H^+-ATPase antibodies

(**A**) Bafilomycin-A_1-sensitive ATPase activity is enriched in the compound organelles and DV fractions. Results are the means ± S.D. for two independent experiments. Asterisks indicate statistically significant difference ($P < 0.05$, one-way ANOVA). (**B**) The DV fraction was added to 2.0 ml of GluIM buffer in the presence of Acridine Orange (AO; 6 μM). ATP (1 mM), nigericin (NIG; 5 μM) and NH_4Cl (20 mM) were added where indicated. Changes in absorbance (Abs) were followed at 493–530 nm. The trace shown is representative of five experiments. (**C**, **D**) DIC (differential interference contrast) and fluorescence images of compound organelles incubated with ATP (1 mM) and NH_4Cl (20 mM, inset) in the presence of Acridine Orange (6 μM). Scale bars, 10 μm. (**E**) Detection of the H^+-ATPase by immunoblotting using a monoclonal antibody against the yeast A subunit. (**F**–**H**) Immunofluorescence of V-H^+-ATPase [anti-(yeast V-H^+-ATPase, A subunit) antibody], showing labelling in the internal vesicles. Scale bars, 5 μm. Images are representative of three experiments.

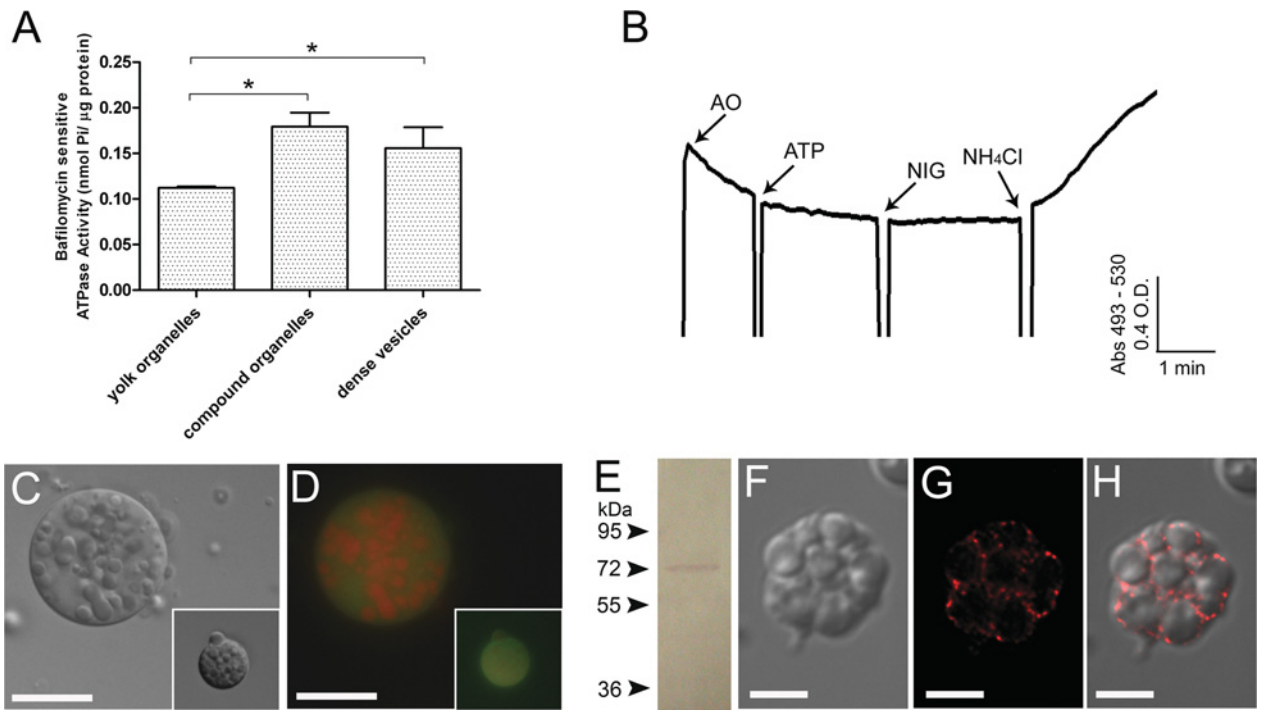

1991; Pick et al., 1991), and trypanosomatids and apicomplexan parasites (Docampo et al., 2005). The function of poly P in chicken egg yolk is unclear, but it is important to note that poly P has important emulsifying and pro-coagulant activities. Poly P is a safe additive to meats, enhancing water binding, emulsification and colour retention, while retarding oxidative rancidity. It is used in virtually all processed meat, poultry and fish products, and also serves as an antibacterial agent (Kornberg, 1995). Poly P is also an important modulator of plasma clotting, affecting the intrinsic pathway, the fibrinolytic system, Factor V activation and fibrin structure (Smith and Morrissey, 2008; Müller et al., 2009). Egg yolk is rich in coagulation factors such as Factor X, thrombin and thrombin-activatable fibrinolysis inhibitor (Mann and Mann, 2008). The emulsifying and coagulation properties of egg yolk are widely applied in food processing (Burley and Vadehra, 1989), and we cannot rule out an important role of yolk poly P in these processes.

When observed under an optical microscope, yolk preparations are seen to possess a number of small and large particles, including large 'yolk spheres' or 'globules' (yellow and white), 50–100 μm in diameter (Burley and Vadehra, 1989). Yolk spheres contain smaller particles inside, but their composition has not been studied in detail (Burley and Vadehra, 1989). Electron microscopy of yolk has also detected the presence of smaller 'yolk granules' and larger

© The Authors Journal compilation © 2010 Portland Press Limited

'insoluble yolk globules' (Burley and Vadehra, 1989), but our present work represents the first identification of compound organelles comprising large acidic vacuoles with internal electron-dense vesicles. Interestingly, the compound organelle itself is also acidic, although on the basis of its staining with Acridine Orange it appears as less acidic than the DVs inside. The mechanism used for its acidification is not known. Electron-dense vesicles within organelles have been described in other organisms, and they include organelles such as the hydrogenosomes of the parabasalid flagellates trichomonads and the plant protein storage vacuole (Docampo et al., 2005). Hydrogenosomes are double-membrane-bound organelles related to mitochondria (Dyall and Johnson, 2000) that contain a peripheral vesicle that, like the acidocalcisome, is electron-dense and contains large amounts of phosphorus, calcium, magnesium, iron and other elements (Consort Ribeiro et al., 2001). The protein storage vacuole is a single-membrane-bound organelle that contains a membrane-bound, acidic, electron-dense vesicle which is known as the globoid. The globoid, like the acidocalcisome, is characterized by the presence of a V-H^+-PPase (vacuolar proton pyrophosphatase) and an aquaporin [γ-TIP (tonoplast intrinsic protein)], and is rich in the phosphorus compound phytic acid (Jiang et al., 2001). V-H^+-PPases are only present in bacteria, plants and protists. However, several types of acidocalcisomes have been described as using a V-H^+-ATPase instead to maintain their acidity (Docampo et al., 2005). Although we measured bafilomycin-A_1-sensitive ATPase activity by P_i release from ATP, H^+ transport in isolated DVs could not be detected. This has been observed with acidocalcisomes known to possess a V-H^+-ATPase, and it has been proposed that the peripheral subunits of the V-H^+-ATPase dissociate or that the proton transport of the complex is inactivated during isolation, as has been observed in other cases (Ruiz et al., 2004). The presence of this pump was, however, confirmed by immunostaining with monoclonal antibodies against one of its membrane subunits.

In addition, the elemental composition of the DVs is proportionally similar to the elemental composition of the yolk (Burley and Vadehra, 1989), suggesting that most of these elements are located in these organelles and they might be an important storage compartment in eggs. Altogether, the results of the present study show that the internal vesicles (DVs) found in compound organelles from chicken egg yolk present structural, chemical and physiological properties similar to acidocalcisomes of bacteria and unicellular eukariotes, and this organelle might have a role in poly P mobilization and cation homoeostasis during early embryogenesis.

Materials and methods

Chemicals and reagents

DAPI, sodium tripolyphosphate (poly P_3), poly P_{25}, poly P_{75+}, protease inhibitors cocktail (catalogue no. P8340) and Toluidine Blue were purchased from Sigma Chemical Company. *Escherichia coli* strain CA38 pTrcPPX1 was provided by the late Professor Arthur Kornberg (Stanford University School of Medicine, Stanford, CA, U.S.A.). All other reagents were of analytical grade.

Fractionation of the yolk organelles

Fertilized SPF (specific pathogen-free) Leghorn chicken eggs were purchased through the Poultry Diagnostic Laboratory at the University of Georgia (Athens, GA, U.S.A.). Intact egg yolks were separated from the egg white manually and carefully rinsed with de-ionized water. The yolk membrane was punctured using a large pipette tip, and the yolk was removed by suction. The yolk was then diluted in 10 vol. of ice-cold GluIM (gluconate intracellular-like medium) containing 250 mM potassium gluconate, 250 mM *N*-methylglucamine, 20 mM Hepes and 1 mM $MgCl_2$, pH 7.2, containing protease inhibitor cocktail. Granules were separated by centrifugation at 1500 ***g*** for 10 min at 4°C and washed twice in the same buffer. The final pellet represents the total yolk organelles and was resuspended in GluIM buffer. To obtain enriched fractions of compound organelles, yolk organelles were pelleted for 1 min at 800 ***g*** and washed once in the same buffer. A fraction of DVs was obtained by lysing the compound organelles in a hypoosmotic buffer (10 mM Hepes, pH 7.2) at room temperature (22°C) for 10 min. The lysed vesicles were then centrifuged three times at 2000 ***g*** for 2 min. The upper white part of the pellet was carefully washed away, and the dark lower part of the pellet (DV fraction) was washed twice in the same buffer.

Enery-filtering electron microsocopy

Whole-mount DVs were prepared for microscopy and microanalysis by washing in 100 mM Hepes, pH 7.4, and then directly applied to Formvar-coated 200-mesh copper grids. The samples were allowed to adhere for 10 min at room temperature, blotted dry and observed directly in an energy-filtering 902 transmission electron microscope (Zeiss). Images were recorded at an energy loss of 70 eV using a spectrometer slit width of 10 eV.

X-ray microanalysis and elemental mapping

Energy-dispersive X-ray spectra and elemental mapping of compound organelles were recorded from samples dried on Formvar-coated grids. EPXMA (electron-probe X-ray microanalysis) analyses and STEM (scanning transmission electron microscopy) were performed on the specimens in a transmission electron microscope (1200EX TEMSCAN; JEOL, Peabody, MA, U.S.A.)

equipped with a low background rotation stage (Model # 925; Gatan, Pleasanton, CA, U.S.A.), a scanning device, an additional hard X-ray aperture, collimated 30 mm^2 Si(Li) energy-dispersive X-ray detector (Oxford Instruments America, Palo Alto, CA, U.S.A.) and pulse processor; the scanning and multichannel analyses were conducted with an X-ray pulse processor (4pi Analysis Spectral Engine; 4pi Analysis, Durham, NC; U.S.A.). Operating parameters and strategies for obtaining quantitative X-ray images were implemented as extensively described elsewhere (LeFurgey et al., 1992, 2001, 2005). Briefly, 128 pixel× 128 pixel spectral data sets were obtained at approx. 10 000 magnification (1 pixel = 0.2 μm^2) with a beam current of approx. 1 nA and dwell times of 4 s per pixel, with automation and any necessary quantification as described previously (LeFurgey et al., 2001).

For DV fractions, energy-dispersive X-ray microanalysis and elemental mapping were performed with a scanning electron microscope (1450EP; Zeiss). The microscope was operated at 15 kV using a tungsten filament and emission current of approx. 10 μA. Analyses were performed using Oxford INCA EDS system (Carl Zeiss MicroImaging, Thornwood, NY, U.S.A.; Oxford Instruments X-Ray Technology, Scotts Valley, CA, U.S.A.). Control spectra were collected from regions adjacent to the vesicles and from the Formvar film.

Freeze–fracture

The DV fraction was fixed in 2.5% glutaraldehyde and 4% freshly prepared formaldehyde in 0.1 M cacodylate buffer, pH 7.4, for 60 min at room temperature, washed in 0.1 M phosphate buffer, pH 7.2, and infiltrated with 30% glycerol. The material was then mounted on to aluminum support disks and slammed on to a liquid-nitrogen-cooled gold block of a quick-freezing device (Leica). Fracturing was carried out at −115°C in a freeze–fracture apparatus (Balzers-Leica). Platinum was evaporated on to the specimen at an angle of 15° and carbon was evaporated at an angle of 90°. Replicas were cleaned to remove the remaining organic material by digestion with sodium hypochlorite, rinsed with distilled water, mounted on 300-mesh nickel grids and observed in a EM 900 transmission electron microscope (Zeiss) operating at 80 kV.

Staining with Acridine Orange

Fractions of compound organelles or DVs were stained with Acridine Orange for 5–20 min at room temperature in the dark at final concentrations of 6 μM. We observed the organelles with an IX-71 fluorescence microscope (Olympus) coupled to a $CoolSnap_{HQ}$ CCD (charge-coupled device) camera (Photometrix) driven by Delta Vision software (Applied Precision) using appropriate filter sets ($\lambda_{excitation}$ = 450–490 nm; $\lambda_{emission}$ > 500 nm).

Poly P detection in agarose gels and Toluidine Blue staining

Poly P extraction was performed as described before by Gomes et al. (2008). Briefly, yolk organelles and DV were obtained, resuspended in water and sonicated [3 cycles of 10 s (with 10 s intervals) at 30% amplitude using a Branson digital sonifer and maintaining the tubes on ice]. After treatment with DNase (10 μg/ml) and RNase (10 μg/ml) for 30 min at 37°C, 1 vol. of chloroform was added, and the samples were vortex-mixed for 5 min. The samples were centrifuged at 10 000 *g* for 5 min at 4°C to separate the phases. The water-soluble fraction was collected, dried in a speed vacuum apparatus, and resuspended in 60 mM Tris/HCl, pH 7.5/6.0 mM $MgCl_2$. These samples were used as poly P extracts for all gel electrophoresis. For some samples, rScPPX1 was added (3000–5000 units) in a final volume of 50 μl and incubated for 30 min at 35°C. Poly P samples were then mixed with DNA loading buffer (10 mM Tris/HCl, pH 7.5, 10 mM EDTA, 0.25% Orange G and 0.65% sucrose) and loaded on to 1–2% agarose gels. The gels were run at 200 V in TAE buffer (Tris/acetate pH, 8.2, 1 mM EDTA) until the dye (Orange G) reached the middle of the gel. The gels were stained with 0.1% Toluidine Blue for 1 h and de-stained with several changes of de-ionized water for 4–8 h.

Poly P detection in agarose gels using DAPI staining

Staining was performed as described previously by Smith and Morrissey (2007) with minor modifications. Gels were incubated for 30 min in the dark with 2 μg/ml DAPI, 10 mM EDTA and 0.3% Fluoromount-G. The gels were washed twice for 1 h in the same solution without DAPI. Images of DAPI fluorescence were acquired with Alpha Imager gel imaging system (AlphaInotech, San Leandro, CA, U.S.A.) using an excitation wavelength of 365 nm.

Poly P localization in vesicles by DAPI staining

Fractions of DVs or compound organelles were fixed in 4% paraformaldehyde, washed in GluIM buffer and DAPI was added to the suspension to a final concentration of 2 μg/ml. The samples were incubated for 5 min at room temperature in the dark and observed using an IX-71 fluorescence microscope (Olympus) ($\lambda_{excitation}$ = 340–380 nm; $\lambda_{emission}$ > 500 nm) with a $CoolSnap_{HQ}$ CCD camera (Photometrix) driven by Delta Vision software (Applied Precision). For the three-dimensional projection of the compound organelles (Supplementary Movie 1 at http://www.biolcell.org/boc/102/boc1020421add.htm), *z*-stacks were acquired and reconstructed using the same software.

Quantification of poly P levels

Organellar fractions of the egg yolk were obtained as described above, and poly P was extracted using a perchloric acid protocol, as described previously by Ruiz et al. (2001a). Poly P levels were determined from the amount of phosphate (P_i) released upon treatment with an excess of rScPPX1. The recombinant enzyme was prepared as described previously (Ruiz et al., 2001a). Aliquots of poly P extracts (always less than 1.5 nmol, monomeric P_i) were incubated for 15 min at 35°C with 60 mM Tris/HCl, pH 7.5, 6.0 mM $MgCl_2$ and 3000–5000 units of purified rScPPX1 in a final volume of 100 μl. One unit corresponds to the release of 1 pmol of P_i/min at 35°C. Release of P_i was monitored by the method of Lanzetta et al. (1979). A sodium phosphate standard curve was included on every assay microplate, and activity controls (poly P_{75+}, Sigma) at a final concentration of 300 nM (in terms of polymer) was included as a control for yield. The intracellular concentration of poly P was calculated taking into account a yolk volume of 8.18 ml/yolk and is expressed in terms of P_i residues. All values reported are normalized to reaction yield.

© The Authors Journal compilation © 2010 Portland Press Limited

V-H$^+$-ATPase activity

We obtained membrane preparations from the different organellar fractions of the egg yolk. The samples were resuspended in equal volumes of ice-cold buffer containing [10% (v/v) glycerol, 0.13% (w/v) BSA, 5 mM EDTA, 150 mM KCl, 3.3 mM DTT (dithiothreitol), 1 mM PMSF and 100 mM Tris/HCl, pH 8.0]. The suspensions were homogenized with a glass Potter–Elvehjem homogenizer and centrifuged at 10 000 *g* for 10 min at 4°C. The supernatants were centrifuged at 100 000 *g* for 40 min at 4°C and the pellet was resuspended in 10% glycerol, 10 mM Tris/HCl, 1 mM EDTA and 1 mM DTT, pH 7.5, and re-centrifuged at 100 000 *g* for 40 min at 4°C. The final pellet was resuspended in a small volume of the resuspension buffer and assayed for V-H$^+$-ATPase activity. V-H$^+$-ATPase reactions were started by the addition of 10 μg of protein in a total volume of 100 μl of reaction medium (50 mM Hepes, 100 mM KCl, 1 mM ATP and 2 mM $MgCl_2$, pH 7.5). All samples were also incubated in the presence of 1 μM bafilomycin A_1, a specific V-H$^+$-ATPase inhibitor. Only the bafilomycin-A_1-inhibited activity was considered. After 1 h at 28°C, release of P_i was monitored by the method of Lanzetta et al. (1979).

V-H$^+$-ATPase immunofluorescence

For V-H$^+$-ATPase localization, the samples were fixed in 4% paraformaldehyde diluted in PBS for 30 min and allowed to adhere to poly-L-lysine-coated glass slides. The samples were permeabilized for 3 min in 0.3% Triton X-100. Blocking was performed for 30 min in 50 mM NH_4Cl in PBS, followed by two 10 min washes in PBS containing 3% BSA. Monoclonal anti-(yeast V-H$^+$-ATPase, A subunit) antibody (Invitrogen) was diluted 1:100 in the same buffer and incubated with the samples for 1 h. After a series of wash steps, secondary antibodies (Alexa Fluor^{TM} 565 goat anti-mouse IgG; Invitrogen) were diluted in the same buffer (1:1000) and incubated with the samples for additional 1 h under gentle agitation. Samples were washed and observed using the microscope described above using filters with excitation at 480–500 nm and emission at 510–550 nm.

Western blot analysis

Protein (60 μg) from yolk organelles were subjected to 10% SDS/PAGE and the gel was electrotransferred on to a nitrocellulose membrane. The membrane was incubated in blocking buffer containing 10 mM Tris, 150 mM NaCl, 3% (w/v) BSA and 0.1% (v/v) Tween for 2 h. The membrane was then incubated for 3 h with the primary antibody (monoclonal antibody 8B1, against the A subunit of the yeast V-H$^+$-ATPase; Invitrogen), diluted 1:1000, followed by washings and incubation with goat anti-mouse antibodies conjugated to alkaline phosphatase (1:4000).

H$^+$ transport assays

ATP-driven H$^+$ uptake by the DVs was assayed by measuring changes in the absorbance of Acridine Orange at the wavelength pair 493–530 nm in an Olis-modified SLM-Aminco DW 2000 dual wavelength spectrophotometer (Palmgren, 1991; Scott et al, 1998). DVs (100–400 μg of protein) were resuspended in 2 ml of GluIM buffer in the presence of 3 μM Acridine Orange. ATP (1 mM), nigericin (5 μM) and NH_4Cl (20 mM) were added to the cuvette, as indicated in the Results section.

Acknowledgements

We thank the late Professor Arthur Kornberg for *E. coli* CA38 pTrcPPX1 and Adam Pyrzak for some preliminary work.

Funding

This work was supported by the Georgia Research Alliance/Barbara and Sanford Orkin Chair in Tropical and Emerging Global Diseases and Cellular Biology (to R.D.). I.B.R. and K.M. were supported in part by a training grant from the Ellison Medical Foundation to the Center for Tropical and Emerging Global Diseases. A.L. and P.I. were supported in part by the Department of Veterans Affairs, Veterans Health Administration, Office of Research and Development, Durham, NC, U.S.A., VAMC Biomedical Laboratory Research and Development and Pathology and Laboratory Medicine Service. I.B.R., K.M., E.A.M. and W.S. were supported in part by the Fundação de Amparo a Pesquisa do Estado de Rio de Janeiro (FAPERJ) and the Conselho Nacional de Pesquisas (CNPq, Brazil)

References

Abramov, A.Y., Fraley, C., Diao, C.T., Winkfein, R., Colicos, M.A., Duchen, M.R., French, R.J. and Pavlov, E. (2007) Targeted polyphosphatase expression alters mitochondrial metabolism and inhibits calcium-dependent cell death. Proc. Natl. Acad. Sci. U.S.A. **104**, 18091–18096

Burley, R.W. and Vadehra, D.V. (1989) The Avian Egg – Chemistry and Biology, John Wlley and Sons, New York

Castro, C.D., Meehan, A.J., Koretsky, A.P. and Domach, M.M. (1995) *In situ* ^{31}P nuclear magnetic resonance for observation of polyphosphate and catabolite responses of chemostat-cultivated *Saccharomyces cerevisiae* after alkalinization. Appl. Environ. Microbiol. **61**, 4448–4453

Castro, C.D., Koretsky, A.P. and Domach, M.M. (1999) NMR-observed phosphate trafficking and polyphosphate dynamics in wild-type and vph1-1 mutant *Saccharomyces cerevisae* in response to stresses. Biotechnol. Prog. **15**, 65–73

Consort Ribeiro, K., Benchimol, M. and Farina, M. (2001) Contribution of cryofixation and freeze-substitution to analytical microscopy: a study of *Tritrichomonas foetus* hydrogenosomes. Microsc. Res. Tech. **53**, 87–92

Docampo, R., de Souza, W., Miranda, K., Rohloff, P. and Moreno, S.N. (2005) Acidocalcisomes – conserved from bacteria to man. Nat. Rev. Microbiol. **3**, 251–261

Dyall, S.D. and Johnson, P.J. (2000) Origins of hydrogenosomes and mitochondria: evolution and organelle biogenesis. Curr. Opin. Microbiol. **3**, 404–411

Fang, J., Rohloff, P., Miranda, K. and Docampo, R. (2007) Ablation of a small transmembrane protein of *Trypanosoma brucei* (TbVTC1) involved in the synthesis of polyphosphate alters acidocalcisome biogenesis and function, and leads to a cytokinesis defect. Biochem. J. **407**, 161–170

Gomes, F.M., Ramos, I.B., Motta, L.M., Miranda, K., Santiago, M.F., de Souza, W. and Machado, E.A. (2008) Polyphosphate polymers during early embryogenesis of *Periplaneta americana*. J. Insect Physiol. **54**, 1459–1466

Han, K.Y., Hong, B.S., Yoon, Y.J., Yoon, C.M., Kim, Y.K., Kwon, Y.G. and Gho, Y.S. (2007) Polyphosphate blocks tumour metastasis via anti-angiogenic activity. Biochem. J. **406**, 49–55

Hernandez-Ruiz, L., Gonzalez-Garcia, I., Castro, C., Brieva, J.A. and Ruiz, F.A. (2006) Inorganic polyphosphate and specific induction of apoptosis in human plasma cells. Haematologica **91**, 1180–1186

Jiang, L., Phillips, T.E., Hamm, C.A., Drozdowicz, Y.M., Rea, P.A., Maeshima, M., Rogers, S.W. and Rogers, J.C. (2001) The protein storage vacuole: a unique compound organelle. J. Cell Biol. **155**, 991–1002

Kawazoe, Y., Shiba, T., Nakamura, R., Mizuno, A., Tsutsumi, K., Uematsu, T., Yamaoka, M., Shindoh, M. and Kohgo, T. (2004) Induction of calcification in MC3T3-E1 cells by inorganic polyphosphate. J. Dent. Res. **83**, 613–618

Komazaki, S., Takada, M. and Clark, N.B. (1993) Ultrastructural localization of calcium in the chick yolk sac membrane endodermal cells as revealed by cytochemistry and X-ray microanalysis. Anat. Embryol. **187**, 607–614

Kornberg, A. (1995) Inorganic polyphosphate: toward making a forgotten polymer unforgettable. J. Bacteriol. **177**, 491–496

Kornberg, A., Rao, N.N. and Ault-Riche, D. (1999) Inorganic polyphosphate: a molecule of many functions. Annu. Rev. Biochem. **68**, 89–125

Kulaev, I. and Kulakovskaya, T. (2000) Polyphosphate and phosphate pump. Annu. Rev. Microbiol. **54**, 709–734

Kumble, K.D. and Kornberg, A. (1995) Inorganic polyphosphate in mammalian cells and tissues. J. Biol. Chem. **270**, 5818–5822

Lanzetta, P.A., Alvarez, L.J., Reinach, P.S. and Candia, O.A. (1979) An improved assay for nanomole amounts of inorganic phosphate. Anal. Biochem. **100**, 95–97

LeFurgey, A., Davilla, S.D., Kopf, D.A., Sommer, J.R. and Ingram, P. (1992) Real-time quantitative elemental analysis and mapping: microchemical imaging in cell physiology. J. Microsc. 165, 191–223.

LeFurgey, A., Ingram, P and and Blum, J.J. (2001) Compartmental responses to acute stress in *Leishmania major* result in rapid loss of Na^+ and Cl^-. Comp. Biochem. Physiol. A Mol. Integr. Physiol. **128**, 385–394

LeFurgey, A., Gannon, M., Blum, J. and Ingram, P. (2005) *Leishmania donovani* amastigotes mobilize organic and inorganic osmolytes during regulatory volume decrease. J. Eukaryot. Microbiol. **52**, 277–289

Mann, K. and Mann, M. (2008) The chicken egg yolk plasma and granule proteomes. Proteomics **8**, 178–191

Morgan, A.J. and Galione, A. (2007) NAADP induces pH changes in the lumen of acidic Ca^{2+} stores. Biochem. J. **402**, 301–310

Motta, L.S., Ramos, I.B., Gomes, F.M., de Souza, W., Champagne, D.E., Santiago, M.F., Docampo, R., Miranda, K. and Machado, E.A. (2009) Proton-pyrophosphatase and polyphosphate in acidocalcisome-like vesicles from oocytes and eggs of *Periplaneta americana*. Insect Biochem. Mol. Biol. **39**, 198–206

Müller, F., Mutch, N.J., Schenk, W.A., Smith, S.A., Esterl, L., Spronk, H.M., Schmidbauer, S., Gahl, W.A., Morrissey, J.H. and and Renné, T. (2009) Platelet polyphosphates are proinflammatory and procoagulant mediators *in vivo*. Cell **139**, 1143–1156.

Nelson, N., Perzov, N., Cohen, A., Hagai, K., Padler, V. and Nelson, H. (2000) The cellular biology of proton-motive force generation by V-ATPases. J. Exp. Biol. **203**, 89–95

Palmgren, M.G. (1991) Acridine orange as a probe for measuring pH gradients across membranes: mechanism and limitations. Anal. Biochem. **192**, 316–321

Pick, U. and Weiss, M. (1991) Polyphosphate hydrolysis within acidic vacuoles in response to amine-induced alkaline stress in the halotolerant alga *Dunaliella salina*. Plant Physiol. **97**, 1234–1240

Pick, U., Zeelon, O. and Weiss, M. (1991) Amine accumulation in acidic vacuoles protects the halotolerant alga *Dunaliella salina* against alkaline stress. Plant Physiol. **97**, 1226–1233

Ruiz, F.A., Rodrigues, C.O. and Docampo, R. (2001a) Rapid changes in polyphosphate content within acidocalcisomes in response to cell growth, differentiation, and environmental stress in *Trypanosoma cruzi.* J. Biol. Chem. **276**, 26114–26121

Ruiz, F.A., Marchesini, N., Seufferheld, M., Govindjee, Docampo and R. (2001b) The polyphosphate bodies of *Chlamydomonas reinhardtii* possess a proton-pumping pyrophosphatase and are similar to acidocalcisomes. J. Biol. Chem. **276**, 46196–46203

Ruiz, F.A., Lea, C.R., Oldfield, E. and Docampo, R. (2004) Human platelet dense granules contain polyphosphate and are similar to acidocalcisomes of bacteria and unicellular eukaryotes. J. Biol. Chem. **279**, 44250–44257

Scott, D.A., de Souza, W., Benchimol, M., Zhong, L., Lu, H.G., Moreno, S.N. and Docampo, R. (1998) Presence of a plant-like proton-pumping pyrophosphatase in acidocalcisomes of *Trypanosoma cruzi*, J. Biol. Chem. 273, 22151–22158

Seufferheld, M., Vieira, M.C., Ruiz, F.A., Rodrigues, C.O., Moreno, S.N. and Docampo, R. (2003) Identification of organelles in bacteria similar to acidocalcisomes of unicellular eukaryotes. J. Biol. Chem. **278**, 29971–29978

Shiba, T., Nishimura, D., Kawazoe, Y., Onodera, Y., Tsutsumi, K., Nakamura, R. and Ohshiro, M. (2003) Modulation of mitogenic activity of fibroblast growth factors by inorganic polyphosphate. J. Biol. Chem. **278**, 26788–26792

Smith, S.A. and Morrissey, J.H. (2007) Sensitive fluorescence detection of polyphosphate in polyacrylamide gels using 4′,6-diamidino-2-phenylindole. Electrophoresis **28**, 3461–3465

Smith, S.A. and Morrissey, J.H. (2008) Polyphosphate enhances fibrin clot structure. Blood **112**, 2810–2816

Smith, S.A., Mutch, N.J., Baskar, D., Rohloff, P., Docampo, R. and Morrissey, J.H. (2006) Polyphosphate modulates blood coagulation and fibrinolysis. Proc. Natl. Acad. Sci. U.S.A. **103**, 903–908

Wang, L., Fraley, C.D., Faridi, J., Kornberg, A. and Roth, R.A. (2003) Inorganic polyphosphate stimulates mammalian TOR, a kinase involved in the proliferation of mammary cancer cells. Proc. Natl. Acad. Sci. U.S.A. **100**, 11249–11254

Weiss, M., Bental, M. and Pick, U. (1991) Hydrolysis of polyphosphates and permeability changes in response to osmotic shocks in cells of the halotolerant alga *Dunaliella*. Plant Physiol. **97**, 1241–1248

Wurst, H., Shiba, T. and Kornberg, A. (1995) The gene for a major exopolyphosphatase of *Saccharomyces cerevisiae*. J. Bacteriol. **177**, 898–906

Yang, Y.C., Bastos, M. and Chen, K.Y. (1993) Effects of osmotic stress and growth stage on cellular pH and polyphosphate metabolism in *Neurospora crassa* as studied by ^{31}P nuclear magnetic resonance spectroscopy. Biochim. Biophys. Acta **1179**, 141–147

Zakharian, E., Thyagarajan, B., French, R.J., Pavlov, E. and Rohacs, T. (2009) Inorganic polyphosphate modulates TRPM8 channels. PLoS One **4**, e5404

Zhang, H., Gomez-Garcia, M.R., Brown, M.R. and Kornberg, A. (2005) Inorganic polyphosphate in *Dictyostelium discoideum*: influence on development, sporulation, and predation. Proc. Natl. Acad. Sci. U.S.A. **102**, 2731–2735

Received 25 January 2010/27 February 2010; accepted 3 March 2010

Published as Immediate Publication 3 March 2010, doi:10.1042/BC20100011

© The Authors Journal compilation © 2010 Portland Press Limited

9- Discussão:

Apesar de serem organelas originalmente descritas e mais detalhadamente estudadas em protozoários, nos últimos anos a presença de acidocalcissomos tem sido identificada em uma grande variedade de microrganismos, sendo, por isso, vista como uma organela conservada ao longo da evolução (Docampo e cols., 2005). Apesar das crescentes observações sobre a presença de acidocalcissomos em diferentes organismos unicelulares, o único modelo em que estas organelas foram caracterizadas em um animal superior foi em plaquetas humanas, onde seu conteúdo de PoliP foi sugerido como modulador da cascata de coagulação sanguínea (Ruiz e cols., 2004). Nesta tese, organelas similares a acidocalcissomos foram identificadas e caracterizadas em sistemas de vitelo de ovos de diferentes animais: dois insetos, dois equinodermos e uma ave, caracterizando assim a primeira descrição de acidocalcissomos em modelos de animais superiores não mamíferos (invertebrados e vertebrados). Além disso, indícios da presença de acidocalcissomos já foram obtidos por nosso grupo em ovos de *zebra fish* e *Drosophila melanogaster* (dados não publicados), extendendo ainda mais a distribuição desta organela em sistemas de vitelo de diferentes filos.

Em geral, ovos são estruturas que estocam todo o material necessário para a formação dos tecidos do futuro embrião. Todo o seu conteúdo inicial passa por inúmeros processos, onde o pronúcleo se divide formando o embrião e o sistema de vitelo atua fornecendo elementos e moléculas fundamentais para que as células embrionárias possam crescer e se multiplicar. A presença de organelas similares a acidocalcissomos em sistemas de vitelo de diferentes animais ovíparos indica que esta organela pode ter funções semelhantes ou análogas nestes diferentes modelos durante a embriogênese.

Acidocalcissomos se caracterizam pelo acúmulo de alguns elementos inorgânicos e pela ausência ou baixíssima concentração de enxofre em seu lúmen. Enxofre é um elemento comumente utilizado como indicador do acúmulo de proteínas em diferentes estruturas, e sua ausência em acidocalcissomos indica que este compartimento não é especializado no estoque de proteínas, como seria de se esperar para um grânulo de vitelo típico. De fato, espectros de microanálise de raios-X feitos em vesículas maiores e menos eletrondensas de diferentes ovos evidenciaram o acúmulo de enxofre, carbono e oxigênio,

o que as caracteriza como grânulos especializados no acúmulo de proteínas. Desse modo, o estoque de elementos inorgânicos se mostra como uma característica marcante e única dos acidocalcissomos entre os diferentes organismos investigados nesta tese.

Sabe-se que elementos inorgânicos são fundamentais para o metabolismo celular, podendo fazer parte da estrutura de várias macromoléculas ou funcionando como co-fatores de diferentes enzimas (Schwartz e cols., 1994; Marin Briano e cols., 1995). Os elementos que compõem as células podem ser divididos em majoritários, traço ou microtraço, de acordo com a sua abundância nos organismos (Williams, 2006). É interessante notar que os elementos acumulados nos acidocalcissomos são elementos majoritários, sendo por isso requeridos em maior quantidade pelas células. A presença de uma organela com capacidade de acumular altas concentrações de fósforo, cálcio, potássio, sódio e magnésio em volumes relativamente pequenos, pode ser vista como uma estratégia evolutiva para o armazenamento de elementos inorgânicos para o embrião. Essa estratégia pode vir a ser especialmente importante nos ovos terrestres, que se caracterizam por ser um sistema fechado, sem contato ou capacidade de absorver moléculas do ambiente externo.

A presença de PoliP (que por ser um polímero aniônico é capaz de se ligar a cátions como Ca^{2+}, Mg^{2+} e K^{+}) no lúmen das organelas, possibilita o estoque de altas concentrações iônicas, sem os fortes efeitos osmóticos destas moléculas livres em solução (Kulaev e cols., 1999; Kornberg, 1999). Além disso, a dinâmica de hidrólise e polimerização de PoliP poderia funcionar como um gatilho para a liberação desses íons, e também para o fornecimento de Pi para as células. Em *T. cruzi*, já foi mostrado que o PoliP dos acidocalcissomos pode ser rapidamente degradado ou polimerizado, mediante diferentes estímulos, e que a degradação deste polímero está relacionada com a liberação de Ca^{2+} para o citoplasma (Ruiz e cols., 2001). Em sistemas de vitelo, mecanismos análogos a este poderiam acontecer, levando à degradação de PoliP e disponibilização de Pi, Ca^{2+}, Mg^{2+}, K^{+} e Na^{+} para a construção dos tecidos embrionários. A disponibilização de elementos para o embrião pode vir a se tornar uma função especialmente importante nos estágios mais tardios de embriogênese, onde a massa de células do embrião é maior, e as divisões celulares mais frequentes.

Apesar de serem capazes de estocar altas concentrações de elementos inorgânicos, os mecanismos pelos quais esses elementos seriam disponibilizados para o embrião, i.e. como estes íons são transportados do lúmen dos acidocalcissomos para as células embrionárias, ainda não são entendidos. A passagem de íons pela membrana dos acidocalcissomos nos sistemas de vitelo é provavelmente catalisada pelo acoplamento de bombas, trocadores e canais de membrana, assim como acontece em acidocalcissomos de protozoários (Docampo e cols., 2005). A natureza acídica ou capacidade de serem acidificados durante a embriogênse é uma característica que pode atuar dirigindo a força do gradiente de prótons, direcionando o transporte de trocadores do tipo Ca^{2+}/ nH^{+} ou Na^{+}/H^{+}. Assim, a acidificação ou alcalinização do compartimento, por ativação ou desativação das bombas, poderia funcionar como um mecanismo controlador da disponilização de determinados íons para o citoplasma, durante a embriogênese.

Sabe-se que o grau de acidificação de compartimentos intracelulares pode ser finamente regulado pelo balanço entre bombeamento ativo de prótons, vazamento de prótons pela membrana (*proton leak*) e transporte de contra-íons que podem balancear o gradiente elétrico, gerado pelas bombas (Demaurex, 2002). Dessa forma, em uma organela como o acidocalcissomo, onde o acúmulo de íons pode variar de acordo com a hidrólise de PoliP, outros fatores poderiam atuar diretamente na taxa de bombeamento de prótons pelas bombas. A capacidade de *proton leak* pela membrana ou a presença de trocadores capazes de gerar a entrada de Cl^{-} ou canais que permitam a saída passiva de K^{+}, por exemplo, poderiam influenciar a taxa de bombeamento de prótons pelas bombas, a assim controlar indiretamente a captação ou liberação de íons como o Ca^{2+}. Porém, em acidocalcissomos de sistemas de vitelo, as proteínas de membrana ainda não foram identificadas, sendo este o principal foco das perspectivas para a continuação deste estudo. A identificação de proteínas de membrana e observação dos seus efeitos sobre a embriogênese pode certamente nos prover indícios sobre as funções dos acidocalcissomos nestes modelos.

Uma outra possível função para os acidocalcissomos em sistemas de vitelo é sua participação em eventos de sinalização por liberação de Ca^{2+}. Ovos de equinodermos e vertebrados não mamíferos têm sido os principais modelos para o estudo de eventos globais e elementares de sinalização por liberação de Ca^{2+} (Whitaker, 2006) e, de fato,

estes foram os modelos inicias para os primeiros estudos sobre as liberações deste íon pelo RE (via $InsP_3R$ e RyR) e formação de ondas de Ca^{2+}. Um dos primeiros eventos da cascata de ativação dos ovócitos é a formação de ondas repetitivas de Ca^{2+}, que passam por toda a extensão dos ovos, sinalizando para que toda a estrutura se programe para o desenvolvimento inicial. Durante a embriogênese inicial, a principal questão sobre a sinalização por Ca^{2+} é o quanto este íon seria importante para as massivas divisões mitóticas do início da embriogênese. Em vários modelos já foi mostrado que o bloqueio da via de sinalização por fosfoinositídeos (que gera o $InsP_3$) leva à parada das divisões mitóticas (Becchetti e cols., 1997). Desde então, essa idéia vem sendo confirmada com experimentos mostrando injeções de agentes quelantes de Ca^{2+} e antagonistas para o $InsP_3R$ em vários modelos, e todos levam à parada das divisões nucleares (Whitaker, 2006). Além disso, os eventos de fusão entre diferentes grânulos de vitelo, que parecem ser importantes para a regulação da degradação do vitelo em insetos, também são dependentes de aumentos na concentração de Ca^{2+}.

Apesar do RE ser, obviamente, um elemento importante na sinalização por liberação de Ca^{2+} intracelular em ovócitos e ovos, nos últimos anos vem se mostrando também a importância de organelas acídicas que estocam cálcio na sinalização intracelular (recentemente revisado por Patel e Docampo, 2010). Tem se especulado que estas organelas podem fazer parte de pequenas liberações iniciais de Ca^{2+}, que por sua vez sinalizam por CICR (*calcium-induced calcium release*) para as liberações globais via $InsP_3R$ e RyR do RE. Desse modo, os acidocalcissomos poderiam fazer parte de diferentes eventos de sinalização por Ca^{2+} em ovócitos e ovos de diferentes modelos. Além disso, a presença de receptores para liberação de Ca^{2+} ativados por ligantes (como os TPCs ativados por NAADP, discutido abaixo) em acidocalcissomos ainda não foi devidamente investigada, e pode representar uma importante função para esta organela em diferentes modelos, até mesmo nos protozoários, que não apresentam um *pool* de cálcio sensível a $InsP_3$ (Moreno e cols., 1992), e tem seu maior estoque de cálcio nos acidocalcissomos (Docampo e cols., 2005).

Os acidocalcissomos descritos em sistemas de vitelo apresentam várias características similares entre si e típicas dessas organelas: 1) alta eletrondensidade; 2) acúmulo de elementos como fósforo, cálcio, magnésio, sódio e potássio; 3) acúmulo de

fósforo na forma de PoliP; e 4) natureza acídica, sendo capazes de acumular marcadores de ambientes ácidos como laranja de acridina. Porém, algumas variações foram encontradas entre os acidocalcissomos das diferentes espécies estudadas (tabela 1). Essas variações e suas possíveis funções em cada modelo serão discutidas abaixo, em seções separadas para cada espécie.

Tabela 1. Diferenças entre os acidocalcissomos em sistemas de vitelo de diferentes espécies.

Espécie	Traços de enxofre	PolyP	Ácidos desde o início da embriogênese	VH^+-PPase	Agrupados dentro de um compartimento	Tamanho (μm)
Periplaneta	Não	Sim	Não	Sim	Não	< 1,0
Rhodnius	Não	Sim	Não	Sim	Não	0,57 ± 0,21
Lytechinus	Sim	Sim	Sim	Não	Não	0,81 ± 0,23
						0,23 ± 0,12
Arbacia	Sim	Sim	Sim	Não	Não	0,43 ± 0,25
Gallus	Sim	Sim	Sim	Não	Sim	2,20 ± 0,36

Acidocalcissomos em ovos de insetos (*P. americana* e *R. prolixus*)

Até recentemente não existiam evidências para a existência de H^+-PPases vacuolares em células humanas, ou qualquer outra espécie do reino animal (McIntoshi e Vaidya, 2002). Em 2004, Motta e colaboradores descreveram a presença de atividade PPásica associada a membranas de vesículas de vitelo do inseto *Rhodnius prolixus*. Os extratos de vitelo também se mostraram imunoreativos a anticorpos anti VH^+-PPase de plantas (assim como acontece nos acidocalcissomos de protozoários), e a acidificação de compartimentos no vitelo, mediada a partir da adição de PPi, também foi detectada. Porém, apesar das crescentes evidências bioquímicas da presença desta enzima neste modelo, ainda não foi identificado em nenhuma espécie animal um gene análogo ao da VH^+-PPase de plantas ou protozoários.

Neste trabalho, a atividade PPásica detectada em ovos de *R. prolixus* e de outro inseto, *P. americana*, foi confirmada, e associada às organelas similares a acidocalcissomos. A presença de VH^+-PPases como marcador para acidocalcissomos em microorganismos é vastamente descrita (Rodrigues e cols., 1999; Ruiz e cols., 2001; Lemercier e cols., 2002, Miranda e cols., 2004) e, aparentemente, em insetos esta enzima também é acumulada nos acidocalcissomos de sitemas de vitelo. A atividade PPásica detectada nos sistemas de vitelo apresentou parâmetros cinéticos similares aos da enzima de protozoários e plantas, e foi enriquecida em frações de acidocalcissomos em *R. prolixus*. Além disso, em insetos, os mesmos anticorpos anti-VH^+-PPase de plantas que são imunoreativos para a enzima de protozóarios, se mostraram eficientes na detecção de uma banda de tamanho esperado (de 60-70 kDa) nos insetos.

Em tecidos com altas taxas proliferativas, como o desenvolvimento inicial embrionário, altos níveis de síntese de macromoléculas como ácidos nucleicos, lipídeos, etc, são observados (Gilbert, 2000). A síntese dessas macromoléculas requer a hidrólise de ATP, e, por consequência, PPi é formado como subproduto dessas reações. Assim, é provável que durante a fase inicial de desenvolvimento esta molécula se encontre em maior abundância no citoplasma dos ovos, e por isso, possa ser utilizada como um substrato de baixo custo energético para a promoção de bombeamento de prótons nos acidocalcissomos, paralelamente ao ATP utilizado pela H^+-ATPase vacuolar. A participação da VH^+-PPase na acidificação de compartimentos no vitelo pode representar uma nova forma de bombeamento de prótons em células animais, e pode vir a ser um modelo interessante para a compreensão do metabolismo energético em modelos de embriogênese.

Em *P. americana* e *R. prolixus*, as organelas similares aos acidocalcissomos não se encontram acidificadas no início da embriogênese, sugerindo que a ativação de uma bomba de prótons deva acontecer em algum momento da embriogênese inicial. Os mecanismos pelos quais estas organelas passam a ser acídicas (ativação de bombas de prótons, disponibilização de PPi, permeação de contra-íons, etc) seria um objeto de grande interesse para a compreensão dos mecanismos de disponibilização de moléculas fundamentais pelo sistema de vitelo. Além disso, em *R. prolixus*, já foi descrito que o PoliP pode inibir a atividade proteásica de uma catepsina-D e, por consequência a

degradação das proteínas de vitelo (Gomes e cols., 2010), caracterizando assim mais uma possível participação deste polímero nos processos de embriogênese.

O córtex de ovos é uma região especializada das células, na qual elementos de citoesqueleto, organelas e macromoléculas específicas se concentram e podem aderir à membrana plasmática. Em modelos não insetos, como equinodermos, moluscos, camundongo e *Xenopus laevis*, existem protocolos para isolamento subcelular do córtex de ovos (Terasaki e cols., 1991; Walker e cols., 1994; Alarcon and Elinson, 2001). Por outro lado, em insetos, até mesmo em *Drosophila*, a estrutura e funções do córtex dos ovos ainda são muito pouco investigadas (Sardet e cols., 2002). Em *R. prolixus* os acidocalcissomos foram localizados no córtex, sugerindo que em modelos de insetos esta região também pode ser especializada, contendo um grupo distinto de organelas e macromoléculas importantes para o desenvolvimento embrionário. A caracterização de novas organelas e da estrutura geral dessa região poderia contribuir para a compreensão da estrutura celular de sistemas de vitelo de ovos de insetos.

Ainda em *R. prolixus*, o fato da fração de acidocalcissomos isolados conter pelo menos ~ 24 % do total de cálcio detectado nos ovos indica que, pelo menos nesse modelo, esta organela é um dos principais compartimentos de estoque de cálcio do sistema. Por isso, a identificação de canais, trocadores e bombas de cálcio nessas organelas certamente nos ajudaria na investigação do papel dos acidocalcissomos neste modelo. Com este objetivo, atualmente estamos trabalhando na análise proteômica das proteínas de membrana extraídas da fração isolada de acidocalcissomos de *R. prolixus*. Uma questão que ainda se mantém em aberto é o quanto do cálcio nos acidocalcissomos estaria livre (Ca^{2+}), disponível para sinalização. Tendo em vista que uma quantidade considerável do PoliP detectado nos ovos também está estocada nos acidocalcissomos em ovos de dia 0, acreditamos que durante as etapas de embriogênese este polímero vai sendo degradado, disponibilizando o íon Ca^{2+} (entre outros) para ser transportado para o citoplasma, onde pode ser utilizado como mensageiro secundário para sinalização ou como elemento majoritário pelas celulas do embrião. Desse modo, uma das perspectivas desse projeto é fazer quantificações de elementos e PoliP nas organelas durante a embriogênese, e elucidar se os elementos inorgânicos dos acidocalcissomos de insetos são significativamente mobilizados durante a embriogênese incial.

Acidocalcissomos em ovos de equinodermos (*A. punctulata* e *L variegatus*)

Em equinodermos, a presença de organelas similares a acidocalcissomos foi caracterizada a partir de experimentos similares aos descritos para os insetos, principalmente a partir de microscopia eletrônica acoplada a microanálise de raios-X. Neste modelo, a presença de "grânulos vazios" distribuídos no citoplasma dos ovos (contendo um remanescente de conteúdo eletrondenso), vem sendo descrita desde o ínicio dos estudos de ultraestrutura em ovócitos e ovos de equinodermos (Epel e Carrol, 1975). Logo depois, a demonstração que este grânulos tinham uma natureza acídica foi feita por Lee e Epel (1983), porém, desde então, a participação dessas organelas nos eventos de ativação ou na embriogênese inicial não foi investigada. Nesse projeto, nós descrevemos que os "grânulos vazios" presentes em ovos não fertilizados de ouriço-do-mar correspondem a organelas similares a acidocalcissomos. A detecção de PoliP neste sistema foi feita utilizando ensaios enzimáticos, RMN e localização com DAPI e PPBD.

Apesar de serem organelas acídicas, eletrondensas e que acumulam grandes quantidades de elementos inorgânicos e PoliP, algumas características neste modelo se mostraram diferentes dos padrões observados para acidocalcissomos de insetos e microrganismos em geral (Docampo e cols., 2005). Ao contrário dos insetos, protozoários e plaquetas humanas, em ovos de ouriço não foi possível detectar atividade PPásica (hidrólise de PPi) em frações de membranas de diferentes materiais testados, inclusive na fração enriquecida em acidocalcissomos. Além disso, diferentes anticorpos anti-VH^{+}-PPase (dirigidos contra as sequências das enzimas de plantas e tripanosomatídeos) foram testados, e não houve imunoreatividade em nenhuma das preparações.

O tamanho dos acidocalcissomos de equinodermos também se mostrou bastante variável, diferente do observado em *R. prolixus* (no qual os acidocalcissomos têm uma média pouco variável de 0,57 ± 0,21 μm). Em *L. variegatus* os acidocalcissomos parecem corresponder a duas subpopulações de organelas, com médias de 0,81 ± 0,23 μm e 0,23 ± 0,12 μm. Em todo o caso, variações nos tamanhos de acidocalcissomos já foram observadas antes em tripanosomatídeos, onde há uma enorme diversidade entre o

tamanho das organelas em diferentes espécies, e até mesmo dentro de uma mesma espécie, o tamanho das organelas pode ser consideravelmente variável (Miranda e cols., 2004). Também diferentemente dos insetos, os acidocalcissomos de ouriço se localizam distribuídos no citoplasma, e não majoritarimente no córtex dos ovos como em *R. prolixus*. Esta diferença de localização pode ser reflexo do acúmulo de vitelo nestes diferentes modelos. Em ovos de inseto, o acúmulo de vitelo é tão grande que ao fim da vitelogênese os grânulos ocupam até 95 % do volume dos ovos, e durante esse processo especula-se que o vitelo empurre as outras organelas para a periferia dos ovos (Gilbert, 2000). Em equinodermos, o crescimento do ovócito não é tão exarcebado e, por isso, o deslocamento de organelas no citoplasma não é tão pronunciado.

Uma outra característica marcante dos acidocalcissomos de ouriço, única para todas as espécies estudadas, é a presença de traços consideráveis de enxofre no lúmen da organela em uma quantidade significativa de vesículas analisadas. Como discutido anteriormente, enxofre é um marcador para acúmulo de proteínas, e essa característica indica que em equinodermos os acidocalcissomos podem também estocar proteínas de reserva e enzimas, podendo participar de funcões mais abrangentes nestas células. De fato, em frações enriquecidas em acidocalcissomos de ouriços, nós pudemos facilmente detectar atividade PPásica solúvel e expolifosfatásica *in vitro*.

Apesar das diferenças em relação aos insetos e parasitos, ensaios de transporte de íons através da membrana dos acidocalcissomos de ouriço evidenciaram também várias características em comum aos acidocalcissomos de tripanosomatídeos. A organela é acidificada a partir da operação de uma ATPase vacuolar, sensível a bafilomicina A1. A alcalinização do compartimento, induzida pelo torcador K^+/H^+ nigericina, é associada à hidrólise de PoliP, como observado em *T. cruzi* (Ruiz e cols., 2001). Além disso, a presença de trocadores Ca^{2+}/H^+ e Na^+/H^+ foi detectada assim como em acidocalcissomos de *T. brucei, T. cruzi* e *L. donovani* (Vercesi e cols., 1994; Docampo e cols., 1995; Vercesi e Docampo, 1996, Vercesi e cols., 2000).

Ovos de equinodermos são vastamente utilizados como modelos para estudos de sinalização por Ca^{2+}, e a presença de vesículas acídicas fazendo parte desses processos, ao lado do RE, tem sido amplamente discutida (Patel e Docampo, 2010). Muitos desses estudos têm sido motivados em função da descoberta, em ouriços, de um novo

mensageiro secundário para liberação de Ca^{2+}, o NAADP. Há evidências que esse mensageiro tem como alvo um receptor em organelas com características lisossomais, que são capazes de estocar altas concentrações de Ca^{2+} (Yamasaki e cols., 2005; Galione e Ruas, 2005). Nesse contexto, em *L. variegatus,* nós investigamos também o perfil de liberação de Ca^{2+} via NAADP das frações de acidocalcissomos. Os resultados obtidos demonstraram que o sinal de Ca^{2+} liberado pelos acidocalcissomos não era enriquecido quando comparado com o sinal obtido de homogenatos totais. Além disso, não conseguimos detectar hidrólise de PoliP associada à saída de Ca^{2+} dos compartimentos, sugerindo, assim, que os acidocalcissomos não são as organelas alvo para o NAADP.

Por outro lado, apesar de não parecer ser a organela alvo para o NAADP, a liberação de Ca^{2+} dos acidocalcissomos pode ser induzida pela alcalinização da organela, dirigida pelos trocadores em determinadas condições. Por exemplo, durante a fertilização, a entrada de Na^{+} no citoplasma dos ovos, pela ativação de um trocador Na^{+}/H^{+} na membrana (Johnson e Epel, 1976), poderia induzir a alcalinização da organela (pelo trocador Na^{+}/H^{+}). Essa alcalinização pode indiretamente levar à liberação de Ca^{2+}, pelo acoplamento com o trocador Ca^{2+}/H^{+}. Dessa forma, os acidocalcissomos poderiam também fazer parte de eventos de sinalização por Ca^{2+}, ao lado do RE e de outras organelas com características lisossomais em ovos de ouriço. Além disso, a alcalinização da organela induzida pela entrada de Na^{+} nos ovos pode tambem estar associada à hidrólise de PoliP, disponibilizando assim Pi para a construção de moléculas como DNA e RNA durante as clivagens embrionárias iniciais.

Acidocalcissomos em ovos de galinha

Em ovos de galinha, a presença de acidocalcissomos foi também detectada a partir de técnicas de microscopia eletrônica. Burley e Vadehra, em 1989, já haviam descrito a presença de diferentes organelas e vesículas, observadas em microscopia de luz, no vitelo dos ovos (Figura 8). Estas vesículas receberam diferentes nomes, e uma delas, as chamadas “esferas de vitelo” já haviam sido observadas contendo pequenas vesículas em seu interior (Willems e Stockx, 1973a; 1973b). Neste trabalho, nós investigamos a natureza dessas organelas, e considerando suas características de

elementos, físicas e bioquímicas, as vesículas internas das "esferas de vitelo" foram caracterizadas como organelas similares a acidocalcissomos.

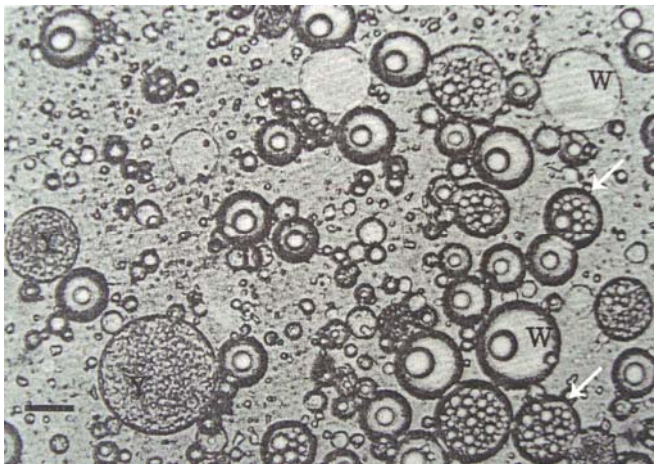

Figura 8: Organelas do vitelo de ovos de galinha observadas em 1989 por Burley e Vadehra. As setas brancas indicam as "esferas", como assim denominaram os autores, contendo vesículas menores no seu interior. Barra: 40 μm.
Imagem retirada de Burley e Vadehra, 1989. The avian egg. In: yolk structures. p 245.

Assim como os acidocalcissomos, as vesículas internas das esferas de vitelo são acídicas, eletrondensas e acumulam fósforo, cálcio, potássio, magnésio e sódio. Interessantemente, a presença de organelas similares a acidocalcissomos no interior de vesículas maiores já foi descrita em plantas (Jiang e cols., 2001; Docampo e cols., 2005). Em sementes, os vacúolos de estoque de proteínas contêm em seu interior uma organela conhecida como "globóide". Os globóides, assim como os acidocalcissomos, são acídicos, eletrondensos, acumulam elementos como fósforo, cálcio e potássio, e tem uma VH^+-PPase em sua membrana (Jiang e cols., 2001).

Experimentos de fracionamento subcelular nos permitiram obter uma fração com as vesículas internas enriquecidas, livres em suspensão. Assim como observado em acidocalcissomos de plaquetas humanas (Ruiz e cols., 2004), a atividade ATPásica foi detectada e enriquecida na fração de acidocalcissomos. Porém, a captação de prótons,

investigada pelo monitoramento da fluorescência da laranja de acridina, não pode ser observada. Esse tipo de padrão já foi descrito em acidocalcissomos de diferentes parasitos, após fracionamentos, e foi proposto que as subunidades desta proteína se perdem durante o procedimento, impedindo o bombeamento de prótons (Ruiz e cols., 2004; Docampo e cols., 2005). Além disso, assim como observado nos equinodermos, as preparações de ovos de galinha não apresentaram atividade PPásica e não eram imunoreativas a diferentes anticorpos anti-VH^{+}-PPase.

Uma característica marcante dos acidocalcissomos de ovos de galinha é que, em preparações de rotina para microscopia eletrônica de transmissão, a membrana das organelas não se encontra preservada. Até mesmo em amostras criofixadas sob alta pressão, as membranas das organelas não puderam ser observadas (dados não publicados). A ausência de membrana em diferentes organelas de vitelo (observadas em microscopia eletrônica), já havia sido descrita anteriormente por Burley e Vadehra (1989), e por isso, a presença, de fato, de membranas envoltórias em várias dessas estruturas ainda se encontra em aberto. Nos acidocalcissomos, a presença de membrana foi detectada a partir de experimentos de criofratura com as organelas isoladas, onde as faces P- e E- das membranas foram fraturadas, e seu padrão mais liso (i.e. com a presença de poucas partículas membranares quando comparadas com membranas fraturadas de outras organelas), foi observado. A ausência ou pouca frequência de proteínas na membrana dos acidocalcissomos pode ser o fator pelo qual a fixação química e a preparação de rotina não foram capazes de preservar a estrutura da membrana neste modelo. De qualquer forma, em nenhum outro modelo estudado, a natureza da membrana dos acidocalcissomos se mostrou tão distinta, sendo essa uma característica exclusiva das organelas dos ovos de galinha.

Um outro dado interessante é que os acidocalcissomos dos ovos de galinha são bem maiores do que os das outras espécies de sistemas de vitelo estudadas. As vesículas internas têm em média ~ 2,2 μm, enquanto que os acidocalcissomos de insetos e equinodermos ficam entre 0,2 e 1 μm. Além disso, apesar de não termos feito análises morfométricas reais (no vitelo inteiro, sem extrair as organelas), a frequência de esferas de vitelo, contendo um grupo de acidocalcissomos no seu interior, parece ser maior em grânulos extraídos de ovos de galinha (quando comparamos com os mesmos

experimentos feitos nos outros modelos). Assim, uma das perspectivas para esse projeto é investigar o volume que essas organelas ocupam no sistema de vitelo, e o quanto seu conteúdo poderia estar contribuindo para o estoque total de elementos nos ovo. De fato, tabelas nutricionais de ovos de galinha refletem consideravelmente o conteúdo de elementos encontrado nos acidocalcissomos (Burley e Vadehra, 1989).

Por fim, por ser um vertebrado, a formação dos tecidos durante a embriogênese neste modelo passa pela biogênese de ossos, o que certamente requer uma quantidade maior de fósforo e cálcio no sistema de vitelo. Apesar de algumas proteínas de vitelo nesses modelos serem altamente fosforiladas (fosvitinas) (Colman e cols., 1976; Fagotto e cols., 1994b; 1994b), ainda não se sabe se a hidrólise dessas proteínas, apenas, é capaz de prover todo o fósforo necessário para o crescimento embrionário. Assim, o envolvimento dos acidocalcissomos como fonte de fósforo e cálcio neste modelo pode vir a ser um objeto interessante de estudo.

10- Conclusões:

→ Sistemas de vitelo de ovos de *P. americana, R. prolixus, L. variegatus, A. punctulata* e *Gallus gallus* têm organelas similares a acidocalcissomos de eucariotos unicelulares;

→ Os acidocalcissomos de sistemas de vitelo acumulam elementos como fósforo, cálcio, magnésio, sódio e potássio;

→ Uma das formas de acúmulo de fósforo pelos acidocalcissomos de sistemas de vitelo é na forma de PoliP;

→ Os acidocalcsiomos de sistemas de vitelo são ácidos, ou podem se tornar acídicos durante a embriogênese;

→ Nos insetos, os acidocalcissomos apresentam atividade PPásica associada à membrana e imunoreatividade a anticorpos anti-VH^{+}-PPase, característica ausente nos acidocalcissomos de *Gallus gallus* e equinodermos.

→ Nos equinodermos, os acidocalcissomos podem liberar Ca^{2+}, mediante alcalinização da organela;

→ Nos ovos de galinha, os acidocalcissomos se encontram agrupados, no interior de vesículas maiores.

11- Referências Bibliográficas:

Aarhus, R., Graeff, R. M., Dickey, D. M., Walseth, T. F. and Lee, H. C. (1995). ADP-ribosyl cyclase and CD38 catalyze the synthesis of a calcium-mobilizing metabolite from NADP. *J Biol Chem* **270**, 30327-33.

Abreu, L. A., Valle, D., Manso, P. P., Facanha, A. R., Pelajo-Machado, M., Masuda, H., Masuda, A., Vaz, I., Jr., Lenzi, H., Oliveira, P. L. et al. (2004). Proteolytic activity of *Boophilus microplus* Yolk pro-Cathepsin D (BYC) is coincident with cortical acidification during embryogenesis. *Insect Biochem Mol Biol* **34**, 443-9.

Alarcon, V. B. and Elinson, R. P. (2001). RNA anchoring in the vegetal cortex of the *Xenopus* oocyte. *J Cell Sci* **114**, 1731-41.

Alberts, B., Johnson, A., Lewis, J., Raff, M., Roberts, K. and Walter, P. (2002). Molecular Biology of the Cell. New York: Garland science.

Bancroft, M. and Bellairs, R. (1976). The development of the notochord in the chick embryo, studied by scanning and transmission electron microscopy. *J Embryol Exp Morphol* **35**, 383-401.

Barnes, R. D. and Rupert, E. E. (1996). Zoologia dos Invertebrados: Roca.

Becchetti, A. and Whitaker, M. (1997). Lithium blocks cell cycle transitions in the first cell cycles of sea urchin embryos, an effect rescued by myo-inositol. *Development* **124**, 1099-107.

Bellairs, R. and Veini, M. (1980). An experimental analysis of somite segmentation in the chick embryo. *J Embryol Exp Morphol* **55**, 93-108.

Berridge, M. J. (1993). Cell signalling. A tale of two messengers. *Nature* **365**, 388-9.

Buning, J. (1994). The Insect Ovary: Chapman Hall.

Burley, R. W. and Vadehra, D. V. (1989). The avian egg. In egg yolk: Structure and properties. London: Blackwell publishing.

Calcraft, P. J., Ruas, M., Pan, Z., Cheng, X., Arredouani, A., Hao, X., Tang, J., Rietdorf, K., Teboul, L., Chuang, K. T. et al. (2009). NAADP mobilizes calcium from acidic organelles through two-pore channels. *Nature* **459**, 596-600.

Carafoli, E., Santella, L., Branca, D. and Brini, M. (2001). Generation, control, and processing of cellular calcium signals. *Crit Rev Biochem Mol Biol* **36**, 107-260.

Chestkov, V. V., Radko, S. P., Cho, M. S., Chrambach, A. and Vogel, S. S. (1998). Reconstitution of calcium-triggered membrane fusion using "reserve" granules. *J Biol Chem* **273**, 2445-51.

Cho, W. L., Tsao, S. M., Hays, A. R., Walter, R., Chen, J. S., Snigirevskaya, E. S. and Raikhel, A. S. (1999). Mosquito cathepsin B-like protease involved in embryonic degradation of vitellin is produced as a latent extraovarian precursor. *J Biol Chem* **274**, 13311-21.

Churchill, G. C., Okada, Y., Thomas, J. M., Genazzani, A. A., Patel, S. and Galione, A. (2002). NAADP mobilizes Ca($^{2+}$) from reserve granules, lysosome-related organelles, in sea urchin eggs. *Cell* **111**, 703-8.

Colman, A. and Gadian, D. G. (1976). 31P nuclear-magnetic-resonance studies on the developing embryos of *Xenopus laevis*. *Eur J Biochem* **61**, 387-96.

de Jesus, T. C., Tonelli, R. R., Nardelli, S. C., Augusto, L. D., Motta, M. C., Girard-Dias, W., Miranda, K., Ulrich, P., Jimenez, V., Barquilla, A. et al. Tor-like 1 kinase is involved in the control of polyphosphate levels and acidocalcisome maintenance in *Trypanosoma brucei*. *J Biol Chem*.

Demaurex, N. (2002). pH Homeostasis of Cellular Organelles. *News in Physiological Sciences* **17**.

Docampo, R., de Souza, W., Miranda, K., Rohloff, P. and Moreno, S. N. (2005). Acidocalcisomes - conserved from bacteria to man. *Nat Rev Microbiol* **3**, 251-61.

Docampo, R. and Moreno, S. N. (1999). Acidocalcisome: A novel Ca^{2+} storage compartment in trypanosomatids and apicomplexan parasites. *Parasitol Today* **15**, 443-8.

Docampo, R. and Moreno, S. N. (2001). The acidocalcisome. *Mol Biochem Parasitol* **114**, 151-9.

Docampo, R. and Moreno, S. N. (2008). The acidocalcisome as a target for chemotherapeutic agents in protozoan parasites. *Curr Pharm Des* **14**, 882-8.

Docampo, R., Scott, D. A., Vercesi, A. E. and Moreno, S. N. (1995). Intracellular Ca^{2+} storage in acidocalcisomes of *Trypanosoma cruzi*. *Biochem J* **310 (Pt 3)**, 1005-12.

Docampo, R., Ulrich, P. and Moreno, S. N. (2010) Evolution of acidocalcisomes and their role in polyphosphate storage and osmoregulation in eukaryotic microbes. *Philos Trans R Soc Lond B Biol Sci* **365**, 775-84.

Dvorak, J. A., Engel, J. C., Leapman, R. D., Swyt, C. R. and Pella, P. A. (1988). *Trypanosoma cruzi*: elemental composition heterogeneity of cloned stocks. *Mol Biochem Parasitol* **31**, 19-26.

Epel, D. and Carroll, E. J., Jr. (1975). Molecular mechanisms for prevention of polyspermy. *Res Reprod* **7**, 2-3.

Fagotto, F. (1990). Yolk degradation in tick eggs: II. Evidence that cathepsin L-like proteinase is stored as a latent, acid-activable proenzyme. *Arch Insect Biochem Physiol* **14**, 237-52.

Fagotto, F. (1991). Yolk degradation in tick eggs: III. Developmentally regulated acidification of yolk spheres. . *Develop. Growth and Differ.* **33**, 57-66.

Fagotto, F. (1995). Regulation of yolk degradation, or how to make sleepy lysosomes. *J Cell Sci* **108 (Pt 12)**, 3645-7.

Fagotto, F. and Maxfield, F. R. (1994a). Changes in yolk platelet pH during *Xenopus laevis* development correlate with yolk utilization. A quantitative confocal microscopy study. *J Cell Sci* **107 (Pt 12)**, 3325-37.

Fagotto, F. and Maxfield, F. R. (1994b). Yolk platelets in *Xenopus* oocytes maintain an acidic internal pH which may be essential for sodium accumulation. *J Cell Biol* **125**, 1047-56.

Fang, J., Rohloff, P., Miranda, K. and Docampo, R. (2007). Ablation of a small transmembrane protein of *Trypanosoma bruce*i (TbVTC1) involved in the synthesis of polyphosphate alters acidocalcisome biogenesis and function, and leads to a cytokinesis defect. *Biochem J* **407**, 161-70.

Fausto, A. M., Gambellini, G., Mazzini, M., Cecchettini, A., Masetti, M. and Giorgi, F. (2001). Yolk granules are differentially acidified during embryo development in the stick insect *Carausius morosus*. *Cell Tissue Res* **305**, 433-43.

Fialho, E., Nakamura, A., Juliano, L., Masuda, H. and Silva-Neto, M. A. (2005). Cathepsin D-mediated yolk protein degradation is blocked by acid phosphatase inhibitors. *Arch Biochem Biophys* **436**, 246-53.

Galione, A. and Ruas, M. (2005). NAADP receptors. *Cell Calcium* **38**, 273-80.

Gilbert, S. F. (2000). Developmental Biology. Sunderland: Sinauer Associates, Inc. .

Heifetz, Y., Yu, J. and Wolfner, M. F. (2001). Ovulation triggers activation of *Drosophila* oocytes. *Dev Biol* **234**, 416-24.

Jiang, L., Phillips, T. E., Hamm, C. A., Drozdowicz, Y. M., Rea, P. A., Maeshima, M., Rogers, S. W. and Rogers, J. C. (2001). The protein storage vacuole: a unique compound organelle. *J Cell Biol* **155**, 991-1002.

Johnson, J. D. and Epel, D. (1976). Intracellular pH and activation of sea urchin eggs after fertilisation. *Nature* **262**, 661-4.

Kornberg, A. (1999). Inorganic polyphosphate: a molecule of many functions. *Prog Mol Subcell Biol* **23**, 1-18.

Kulaev, I. and Kulakovskaya, T. (2000). Polyphosphate and phosphate pump. *Annu Rev Microbiol* **54**, 709-34.

Kulaev, I., Vagabov, V. and Kulakovskaya, T. (1999). New aspects of inorganic polyphosphate metabolism and function. *J Biosci Bioeng* **88**, 111-29.

Lee, H. C. and Epel, D. (1983). Changes in intracellular acidic compartments in sea urchin eggs after activation. *Dev Biol* **98**, 446-54.

LeFurgey, A., Ingram, P. and Blum, J. J. (1990). Elemental composition of polyphosphate-containing vacuoles and cytoplasm of *Leishmania major*. *Mol Biochem Parasitol* **40**, 77-86.

Lemercier, G., Dutoya, S., Luo, S., Ruiz, F. A., Rodrigues, C. O., Baltz, T., Docampo, R. and Bakalara, N. (2002). A vacuolar-type H+-pyrophosphatase governs maintenance of functional acidocalcisomes and growth of the insect and mammalian forms of *Trypanosoma brucei*. *J Biol Chem* **277**, 37369-76.

Lovell-Badge, R. H., Evans, M. J. and Bellairs, R. (1985). Protein synthetic patterns of tissues in the early chick embryo. *J Embryol Exp Morphol* **85**, 65-80.

Luo, S., Rohloff, P., Cox, J., Uyemura, S. A. and Docampo, R. (2004). Trypanosoma brucei plasma membrane-type $Ca^{(2+)}$-ATPase 1 (TbPMC1) and 2 (TbPMC2) genes encode functional $Ca^{(2+)}$-ATPases localized to the acidocalcisomes and plasma membrane, and essential for Ca(2+) homeostasis and growth. *J Biol Chem* **279**, 14427-39.

Mahowald, A. P., Goralski, T. J. and Caulton, J. H. (1983). *In vitro* activation of *Drosophila* eggs. *Dev Biol* **98**, 437-45.

Marchesini, N., Luo, S., Rodrigues, C. O., Moreno, S. N. and Docampo, R. (2000). Acidocalcisomes and a vacuolar H^+-pyrophosphatase in malaria parasites. *Biochem J* **347 Pt 1**, 243-53.

Marchesini, N., Ruiz, F. A., Vieira, M. and Docampo, R. (2002). Acidocalcisomes are functionally linked to the contractile vacuole of *Dictyostelium discoideum*. *J Biol Chem* **277**, 8146-53.

Marin Briano, M. V., Castillo Duran, C. and Uauy Dagach, R. (1995). Mineral balance during nutritional recuperation of infants with protein deficiency. *Arch Latinoam Nutr* **45**, 172-7.

McIntosh, M. T. and Vaidya, A. B. (2002). Vacuolar type H^+ pumping pyrophosphatases of parasitic protozoa. *Int J Parasitol* **32**, 1-14.

McNeil, P. L., Vogel, S. S., Miyake, K. and Terasaki, M. (2000). Patching plasma membrane disruptions with cytoplasmic membrane. *J Cell Sci* **113 (Pt 11)**, 1891-902.

Miranda, K., de Souza, W., Plattner, H., Hentschel, J., Kawazoe, U., Fang, J. and Moreno, S. N. (2008). Acidocalcisomes in Apicomplexan parasites. *Exp Parasitol* **118**, 2-9.

Miranda, K., Docampo, R., Grillo, O. and de Souza, W. (2004a). Acidocalcisomes of trypanosomatids have species-specific elemental composition. *Protist* **155**, 395-405.

Miranda, K., Docampo, R., Grillo, O., Franzen, A., Attias, M., Vercesi, A., Plattner, H., Hentschel, J. and de Souza, W. (2004b). Dynamics of polymorphism of acidocalcisomes in *Leishmania* parasites. *Histochem Cell Biol* **121**, 407-18.

Miranda, K., Rodrigues, C. O., Hentchel, J., Vercesi, A., Plattner, H., de Souza, W. and Docampo, R. (2004c). Acidocalcisomes of *Phytomonas francai* possess distinct morphological characteristics and contain iron. *Microsc Microanal* **10**, 647-55.

Moncayo, A. (2003). Chagas disease: current epidemiological trends after the interruption of vectorial and transfusional transmission in the Southern Cone countries. *Mem Inst Oswaldo Cruz* **98**, 577-91.

Montalvetti, A., Rohloff, P. and Docampo, R. (2004). A functional aquaporin co-localizes with the vacuolar proton pyrophosphatase to acidocalcisomes and the contractile vacuole complex of *Trypanosoma cruzi*. *J Biol Chem* **279**, 38673-82.

Moreno, S. N., Vercesi, A. E., Pignataro, O. P. and Docampo, R. (1992). Calcium homeostasis in *Trypanosoma cruzi* amastigotes: presence of inositol phosphates and lack of an inositol 1,4,5-trisphosphate-sensitive calcium pool. *Mol Biochem Parasitol* **52**, 251-61.

Moreno, S. N. and Zhong, L. (1996). Acidocalcisomes in *Toxoplasma gondii* tachyzoites. *Biochem J* **313 (Pt 2)**, 655-9.

Morgan, A. J. and Galione, A. (2007a). Fertilization and nicotinic acid adenine dinucleotide phosphate induce pH changes in acidic $Ca^{(2+)}$ stores in sea urchin eggs. *J Biol Chem* **282**, 37730-7.

Morgan, A. J. and Galione, A. (2007b). NAADP induces pH changes in the lumen of acidic Ca^{2+} stores. *Biochem J* **402**, 301-10.

Motta, L. S., da Silva, W. S., Oliveira, D. M., de Souza, W. and Machado, E. A. (2004). A new model for proton pumping in animal cells: the role of pyrophosphate. *Insect Biochem Mol Biol* **34**, 19-27.

Motta, L. S., Ramos, I. B., Gomes, F. M., de Souza, W., Champagne, D. E., Santiago, M. F., Docampo, R., Miranda, K. and Machado, E. A. (2009). Proton-pyrophosphatase and polyphosphate in acidocalcisome-like vesicles from oocytes and eggs of *Periplaneta americana*. *Insect Biochem Mol Biol* **39**, 198-206.

Oliveira, P. L., Petretski, M. D. A. and Masuda, H. (1989). Vitelling processing and degradation during embryogenesis of *Rhodnius prolixus*. *Insect Biochem*, 489-498.

Olivera, P. L., Gondim, K. C., Guedes, d. and Masuda, H. (1986). Uptake of Yolk Protein in *Rhodnius Prolixus*. *J. Insect Physiol.*, 859-866.

Page, A. W. and Orr-Weaver, T. L. (1997a). Activation of the meiotic divisions in *Drosophila* oocytes. *Dev Biol* **183**, 195-207.

Page, A. W. and Orr-Weaver, T. L. (1997b). Stopping and starting the meiotic cell cycle. *Curr Opin Genet Dev* **7**, 23-31.

Patel, S. and Docampo, R. Acidic calcium stores open for business: expanding the potential for intracellular Ca^{2+} signaling. *Trends Cell Biol* **20**, 277-86.

Paul, M., Johnson, J. D. and Epel, D. (1976). Fertilization acid of sea urchin eggs is not a consequence of cortical granule exocytosis. *J Exp Zool* **197**, 127-33.

Raikhel, A. S. and Dhadialla, T. S. (1992). Accumulation of yolk proteins in insect oocytes. *Annu Rev Entomol* **37**, 217-51.

Ramos, I. B., Miranda, K., de Souza, W. and Machado, E. A. (2006). Calcium-regulated fusion of yolk granules during early embryogenesis of *Periplaneta americana*. *Mol Reprod Dev* **73**, 1247-54.

Ramos, I. B., Miranda, K., de Souza, W., Oliveira, D. M., Lima, A. P., Sorgine, M. H. and Machado, E. A. (2007). Calcium-regulated fusion of yolk granules is important for yolk degradation during early embryogenesis of *Rhodnius prolixus* Stahl. *J Exp Biol* **210**, 138-48.

Ramos, I. B., Miranda, K., Pace, D. A., Verbist, K. C., Lin, F. Y., Zhang, Y., Oldfield, E., Machado, E. A., de Souza, W. and Docampo, R. (2010) Calcium and polyphosphate-containing acidic granules of sea urchin eggs are similar to acidocalcisomes but are not the targets for NAADP. *Biochem J*. accepted manuscript.

Ramos, I. B., Miranda, K., Ulrich, P., Ingram, P., LeFurgey, A., Machado, E. A., de Souza, W. and Docampo, R. (2010) Calcium- and polyphosphate-containing acidocalcisomes in chicken egg yolk. *Biol Cell* **102**, 421-34.

Ribolla, P. E., Bijovsky, A. T. and de Bianchi, A. G. (2001). Procathepsin and acid phosphatase are stored in *Musca domestica* yolk spheres. *J Insect Physiol* **47**, 225-232.

Rodrigues, C. O., Ruiz, F. A., Rohloff, P., Scott, D. A. and Moreno, S. N. (2002). Characterization of isolated acidocalcisomes from *Toxoplasma gondii* tachyzoites reveals a novel pool of hydrolyzable polyphosphate. *J Biol Chem* **277**, 48650-6.

Rodrigues, C. O., Scott, D. A. and Docampo, R. (1999a). Characterization of a vacuolar pyrophosphatase in *Trypanosoma brucei* and its localization to acidocalcisomes. *Mol Cell Biol* **19**, 7712-23.

Rodrigues, C. O., Scott, D. A. and Docampo, R. (1999b). Presence of a vacuolar H^+-pyrophosphatase in promastigotes of *Leishmania donovani* and its localization to a different compartment from the vacuolar H^+-ATPase. *Biochem J* **340 (Pt 3)**, 759-66.

Rohloff, P., Montalvetti, A. and Docampo, R. (2004). Acidocalcisomes and the contractile vacuole complex are involved in osmoregulation in *Trypanosoma cruzi*. *J Biol Chem* **279**, 52270-81.

Ruiz, F. A., Lea, C. R., Oldfield, E. and Docampo, R. (2004a). Human platelet dense granules contain polyphosphate and are similar to acidocalcisomes of bacteria and unicellular eukaryotes. *J Biol Chem* **279**, 44250-7.

Ruiz, F. A., Luo, S., Moreno, S. N. and Docampo, R. (2004b). Polyphosphate content and fine structure of acidocalcisomes of *Plasmodium falciparum*. *Microsc Microanal* **10**, 563-7.

Ruiz, F. A., Marchesini, N., Seufferheld, M., Govindjee and Docampo, R. (2001a). The polyphosphate bodies of *Chlamydomonas reinhardtii* possess a proton-pumping pyrophosphatase and are similar to acidocalcisomes. *J Biol Chem* **276**, 46196-203.

Ruiz, F. A., Rodrigues, C. O. and Docampo, R. (2001b). Rapid changes in polyphosphate content within acidocalcisomes in response to cell growth, differentiation, and environmental stress in *Trypanosoma cruzi*. *J Biol Chem* **276**, 26114-21.

Rust, M. K., Reierson, D. A. and Hansgen, K. H. (1991). Control of American cockroaches (Dictyoptera: Blattidae) in sewers. *J Med Entomol* **28**, 210-3.

Sagata, N. (1996). Meiotic metaphase arrest in animal oocytes: its mechanisms and biological significance. *Trends Cell Biol* **6**, 22-8.

Sardet, C. (1984). The ultrastructure of the sea urchin egg cortex isolated before and after fertilization. *Dev Biol* **105**, 196-210.

Sardet, C., Prodon, F., Dumollard, R., Chang, P. and Chenevert, J. (2002). Structure and function of the egg cortex from oogenesis through fertilization. *Dev Biol* **241**, 1-23.

Schier, A. F. (2007). The maternal-zygotic transition: death and birth of RNAs. *Science* **316**, 406-7.

Schwartz, L. H., Urban, T. and Hercberg, S. (1994). Antioxidant minerals and vitamins. Role in cancer prevention. *Presse Med* **23**, 1826-30.

Scott, D. A., de Souza, W., Benchimol, M., Zhong, L., Lu, H. G., Moreno, S. N. and Docampo, R. (1998). Presence of a plant-like proton-pumping pyrophosphatase in acidocalcisomes of *Trypanosoma cruzi*. *J Biol Chem* **273**, 22151-8.

Scott, D. A. and Docampo, R. (1998). Two types of H^+-ATPase are involved in the acidification of internal compartments in *Trypanosoma cruzi*. *Biochem J* **331 (Pt 2)**, 583-9.

Scott, D. A. and Docampo, R. (2000). Characterization of isolated acidocalcisomes of *Trypanosoma cruz*i. *J Biol Chem* **275**, 24215-21.

Scott, D. A., Docampo, R., Dvorak, J. A., Shi, S. and Leapman, R. D. (1997). In situ compositional analysis of acidocalcisomes in *Trypanosoma cruzi*. *J Biol Chem* **272**, 28020-9.

Seufferheld, M., Lea, C. R., Vieira, M., Oldfield, E. and Docampo, R. (2004). The $H^{(+)}$-pyrophosphatase of *Rhodospirillum rubrum* is predominantly located in polyphosphate-rich acidocalcisomes. *J Biol Chem* **279**, 51193-202.

Seufferheld, M., Vieira, M. C., Ruiz, F. A., Rodrigues, C. O., Moreno, S. N. and Docampo, R. (2003). Identification of organelles in bacteria similar to acidocalcisomes of unicellular eukaryotes. *J Biol Chem* **278**, 29971-8.

Slack, J. M. W. (2006). Essential developmental biology. London: Blackwell publishing.

Steinhardt, R., Zucker, R. and Schatten, G. (1977). Intracellular calcium release at fertilization in the sea urchin egg. *Dev Biol* **58**, 185-96.

TakahashiI, S. Y., Yamamoto, Y., Zhao, X., Watabe, S. (1996). *Bombyx* acid cysteine proteinase. *International Journal of Invertebrates Reproduction and Development* **30**, 265-281.

Terasaki, M., Henson, J., Begg, D., Kaminer, B. and Sardet, C. (1991). Characterization of sea urchin egg endoplasmic reticulum in cortical preparations. *Dev Biol* **148**, 398-401.

Unuma, T., Yamamoto, T., Akiyama, T., Shiraishi, M. and Ohta, H. (2003). Quantitative changes in yolk protein and other components in the ovary and testis of the sea urchin *Pseudocentrotus depressus*. *J Exp Biol* **206**, 365-72.

Urbina, J. A., Moreno, B., Vierkotter, S., Oldfield, E., Payares, G., Sanoja, C., Bailey, B. N., Yan, W., Scott, D. A., Moreno, S. N. et al. (1999). *Trypanosoma cruzi* contains major pyrophosphate stores, and its growth in vitro and in vivo is blocked by pyrophosphate analogs. *J Biol Chem* **274**, 33609-15.

Veini, M. and Bellairs, R. (1991). Early mesoderm differentiation in the chick embryo. *Anat Embryol (Berl)* **183**, 143-9.

Vercesi, A. E. and Docampo, R. (1996). Sodium-proton exchange stimulates Ca^{2+} release from acidocalcisomes of *Trypanosoma brucei*. *Biochem J* **315 (Pt 1)**, 265-70.

Vercesi, A. E., Grijalba, M. T. and Docampo, R. (1997). Inhibition of Ca^{2+} release from *Trypanosoma brucei* acidocalcisomes by 3,5-dibutyl-4-hydroxytoluene: role of the Na^{+}/H^{+} exchanger. *Biochem J* **328 (Pt 2)**, 479-82.

Vercesi, A. E., Moreno, S. N. and Docampo, R. (1994). Ca^{2+}/H^{+} exchange in acidic vacuoles of *Trypanosoma brucei*. *Biochem J* **304 (Pt 1)**, 227-33.

Vercesi, A. E., Rodrigues, C. O., Catisti, R. and Docampo, R. (2000). Presence of a $Na^{(+)}/H^{(+)}$ exchanger in acidocalcisomes of *Leishmania donovani* and their alkalization by anti-leishmanial drugs. *FEBS Lett* **473**, 203-6.

Vickerman, K. and Tetley, L. (1977). Recent ultrastructural studies on trypanosomes. *Ann Soc Belg Med Trop* **57**, 441-57.

Walker, C. W. U., T. McGinn, N.A. Harrington, L.M. Lesser, M.P. . (2001). Reproduction of sea urchins. In Edible sea urchins: Biology and Ecology. Elsevier Science.

Walker, G. R., Kane, R. and Burgess, D. R. (1994). Isolation and characterization of a sea urchin zygote cortex that supports in vitro contraction and reactivation of furrowing. *J Cell Sci* **107 (Pt 8)**, 2239-48.

Whitaker, M. (2006). Calcium at fertilization and in early development. *Physiol Rev* **86**, 25-88.

WHO. (2008). Report of the expert committee on the control of Chagas disease. In *Technical Report Series*, pp. 905, 85.

Willems, J. and Stockx, J. (1973a). Investigations on the structure of the yolk granules from the unfertilized hen's egg. *Arch Int Physiol Biochim* **81**, 989.

Willems, J. and Stockx, J. (1973b). Two varieties of granules in the yolk of the unfertilized hen's egg. *Arch Int Physiol Biochim* **81**, 988.

Williams, R. J. (2006). My past and a future role for inorganic biochemistry. *J Inorg Biochem* **100**, 1908-24

Yamahama, Y., Uto, N., Tamotsu, S., Miyata, T., Yamamoto, Y., Watabe, S. and Takahashi, S. Y. (2003). In vivo activation of pro-form Bombyx cysteine protease (BCP) in silkmoth eggs: localization of yolk proteins and BCP, and acidification of yolk granules. *J Insect Physiol* **49**, 131-40.

Yamasaki, M., Churchill, G. C. and Galione, A. (2005). Calcium signalling by nicotinic acid adenine dinucleotide phosphate (NAADP). *Febs J* **272**, 4598-606.

Yokota, Y. and Sappington, T. W. (2001). Vitellogen and Vitellogenin in echinoderms. . New Hampshire: Science publishers.

Livros Grátis

(http://www.livrosgratis.com.br)

Milhares de Livros para Download:

Baixar livros de Literatura
Baixar livros de Literatura de Cordel
Baixar livros de Literatura Infantil
Baixar livros de Matemática
Baixar livros de Medicina
Baixar livros de Medicina Veterinária
Baixar livros de Meio Ambiente
Baixar livros de Meteorologia
Baixar Monografias e TCC
Baixar livros Multidisciplinar
Baixar livros de Música
Baixar livros de Psicologia
Baixar livros de Química
Baixar livros de Saúde Coletiva
Baixar livros de Serviço Social
Baixar livros de Sociologia
Baixar livros de Teologia
Baixar livros de Trabalho
Baixar livros de Turismo